STABILIZATION OF DESIRED FLOW REGIMES

USING ACTIVE CONTROL

by

Heidi Sivertsen

A Thesis Submitted for the Degree of Dr. Ing.

Department of Chemical Engineering
Norwegian University of Science and Technology

Abstract

Ever since oil was discovered on the Norwegian continental shelf in the 1960s a lot of money and effort has been used in finding new technology that can increase production and recovery rates for the different fields. Today many fields are produced as satellite fields, where the production from several wells is transported via manifolds in long pipelines at the seabed leading to the receiving facilities. Here oil, water and gas are separated and further treated and transported along with the production from other wells and fields. The cost reduction when producing from satellite fields are off course enormous when compared to having separate production vessels for each well, but there are also some new challenges that arise.

Multiphase flow in pipelines and riser system is very complex and the behavior of the flow depends heavily on the flow regime. To be able to calculate important factors such as pressure drop and flow rates it is critical to know the flow regime in all parts of the system. The parameters that determine which flow regime will occur is also changing with time as the wells are getting more and more depleted at the end of their life-time. This means that the engineers must plan for different scenarios when designing the production and process system, depending on the age of the oil field.

Slugging is a flow regime that causes a lot of problems due to rapid changes in gas and liquid rates entering the separators and large variations in system pressure. The slugs can be formed in low-points in the topology of the pipelines. Riser slugging is one example of such, and can results in liquid slugs larger than the volume of the riser itself.

The pressures and pressure drop in the system are important factors when it comes to production and recovery rates of the system. Slugging can be avoided by increasing the pipeline pressure e.g. by choking back the production at the platform or increasing the separator pressure. The increase in pressure will force the flow into another and more desired flow regime without these large variations in flow rates. This, however, comes on the expense of production rate and recovery factor.

Another option is implementing equipment, such as slug-catchers, to handle the slug flow without the large impact on the down-stream facilities. The disadvantage is often huge implementation costs.

Simple automatic control systems can improve the production greatly without big cost due to expensive equipment. Simple PI controllers are already in use in some of the fields suffering from problems due to slugging in the pipeline, and the results have been very good. So far subsea sensors have been important for achieving good results. Such measurements are however not always available, the sensors might have failed due to old age and though surroundings or they might not have been installed in the first place. The task is then to find other control solutions using measurements that are available achieving the same good results.

For already existing systems encountering problems due to mature fields, new technology can be implemented in order to increase the production in the last years of the field's lifetime. A lot of money and effort are spent on research of new systems that can be implemented on the seabed and remove some of the problems due to multiphase flow in long pipelines. One example of such is the subsea separation and boosting station implemented on the Tordis field

in the autumn of 2007. The implementation of the subsea system is expected to increase the production from the Tordis field substantially.

This thesis describes simulations, analysis, lab experiments and results that have been performed in order to enhance the production from offshore oil and gas fields using automatic control. The first part of the thesis is based on applying different control solutions to riser slugging systems. These control structures only depend on topside sensors located on the platform; sensors that are much easier to implement, repair and replace should they stop working. Different solutions have been analysed using a relative simple Matlab-code earlier developed at our department. The analysis reveals that this is a very interesting control challenge. Results from tests performed both in a small-scale lab rig at our department and also at a medium-scale lab rig at Hydro's research center in Porsgrunn, Norway, are presented.

The second part of the thesis describes work done at StatoilHydro's research center in Trondheim, Norway, in the early stages of planning for the subsea system at Tordis. Different control strategies were tested in simulations using a combination of OLGA and Simulink simulators. This was done in order to discover new possibilities introduced by the subsea system. It was off course important to keep subsea separator properties such as pressure and level stable at all time for all the different scenarios that were tested. Results using different control structures are presented. The aim has been to; ensure equal production in each production pipeline, decrease well test time, avoid riser slugging and control the water cut in the flow entering the topside separators.

Acknowledgment

I consider myself very lucky to have been given the opportunity to work on this thesis. Having a background from mathematics and physics I was lacking a lot of knowledge regarding control theory and multiphase flow when I first started. Still, professor Sigurd Skogestad was willing to give me a chance based on my offshore field experience and my motivation to learn more about the offshore process industry from a more theoretical point of view. For this I am very grateful.

Being supervised by Sigurd Skogestad has been a great advantage for several reasons; his knowledge, enthusiasm, support and advices has pushed me all the way. Also, his close contact with the oil industry has given me the opportunity to work with people from the industry during my period at NTNU, which was very motivating.

Two of these contacts are Audun Faanes and John-Morten Godhavn from StatoilHydro's research center in Trondheim. After working for StatoilHydro on the Tordis project for some months, they gave me the opportunity to present the results in this thesis. I highly value their support and advices, not only regarding the Tordis project and the papers we submitted from this project, but also my thesis in general.

Vidar Alstad, former colleague at NTNU now working at StatoilHydro's research center in Porsgrunn, invited me to perform test on Hydros' lab rig in Porsgrunn. Both he and StatoilHydros' Kristin Hestetun stayed long hours with me at the lab so that I could get the results I needed. I am very greatful to them both, and also the technicians at the research center who worked hard to get the rig working satisfactory during the tests.

Espen Storkaas' model for riser slugging has been used a lot in this thesis. At the time I started working on my Ph.D., Espen was still working on his model in the office next to mine. He helped me getting to know the topic I was about to learn. He also helped me when I was struggling to use his model for the small-scale rigs.

Also other colleagues at NTNU made my stay there very enjoyable with their good spirit every day. They were always willing to give advises when I was stuck, usually in some kind of computer related problem. Especially Jørgen Bauck Jensen and Bjørn Tore Løvfall spend a lot of time helping me, and they never seemed unhappy to do it. I appreciate all the help I have gotten throughout the work on my thesis tremendously, without this help I would probably have used many days to fix some of the problems they so easily found solutions to.

I would also like to thank former Master students Ingvald Baardsen, Morten Søndrol, Håkon Olsen and Einar Hauge for the input they have put into this project.

I am very grateful to my family and my friends for being so supportive and encouraging. Also my boyfriend, Ketil Antonsen, deserves a great thanks for so patiently letting me have the living room to myself so many evenings as I was working on my thesis.

I would like to dedicate this thesis to the little angel growing inside of me as I am taking the last steps toward my Ph.D. degree.

Contents

Chapter 1

Introduction

1.1 Controlling the flow regime; anti-slug control

The behavior of multiphase flow in pipelines is of great concern in the offshore oil and gas industry, and a lot of time and effort have been spent studying this phenomena. The reason for this is that by doing relatively small changes in operating conditions, it is possible to change the flow behavior in the pipelines drastically. This has a huge influence on important factors such as productivity, maintenance and safety. Figure 1.1 shows different flow regimes that can develop in an upward pipeline.

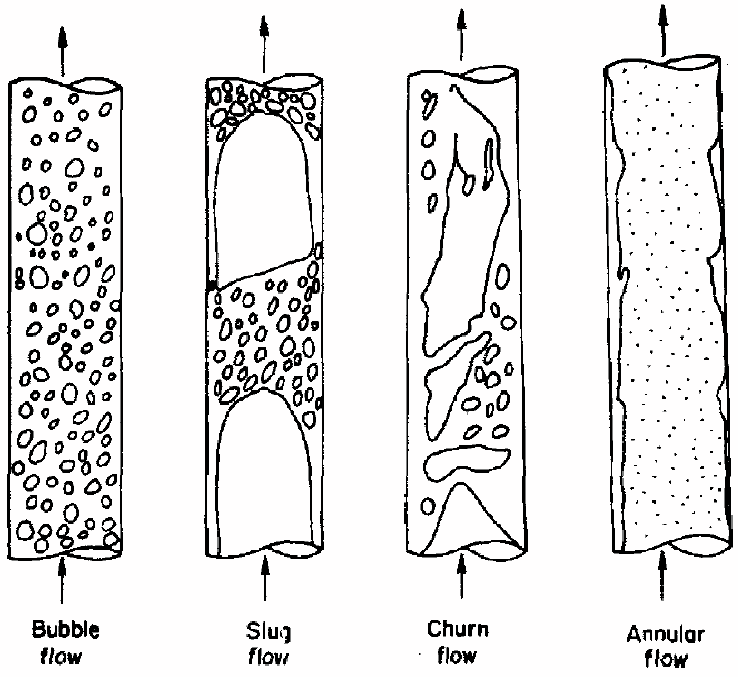

Figure 1.1: Vertical horizontal flow map of Taitel et al. (1980)

Some operating conditions lead to an undesirable flow regime that may cause severe

problems for the receiving facilities due to varying flow rates and pressure in the system. This usually happens in the end of the life cycle of a well, when flow rates are lower than the system was designed for. The rate and pressure variations are caused by a flow regime called slug flow. It is characterized by alternating bulks of liquid and gas in the pipeline.

Being able to avoid slug flow in the pipeline is of great economic interest. For this reason it is important to be able to predict the flow regime before production starts, so that the problems can be taken care of as soon as they arise. Traditionally flow maps as the one in Figure 1.2 have been produced as a tool to predict the flow regime that will develop in a pipeline (Taitel and Dukler (1976), Barnea (1987), Hewitt and Roberts (1969)). These maps show that the flow regime in a pipeline is highly dependent on the incoming superficial flow rates of gas (u_{GS}) and oil (u_{LS}).

Even though the system is designed to avoid such problems in the earlier years of production, the production rate is changed during the production lifetime and problems can arise later on. Note however that these flow maps represent the ”natural” flow regimes, observed when no automatic control is applied.

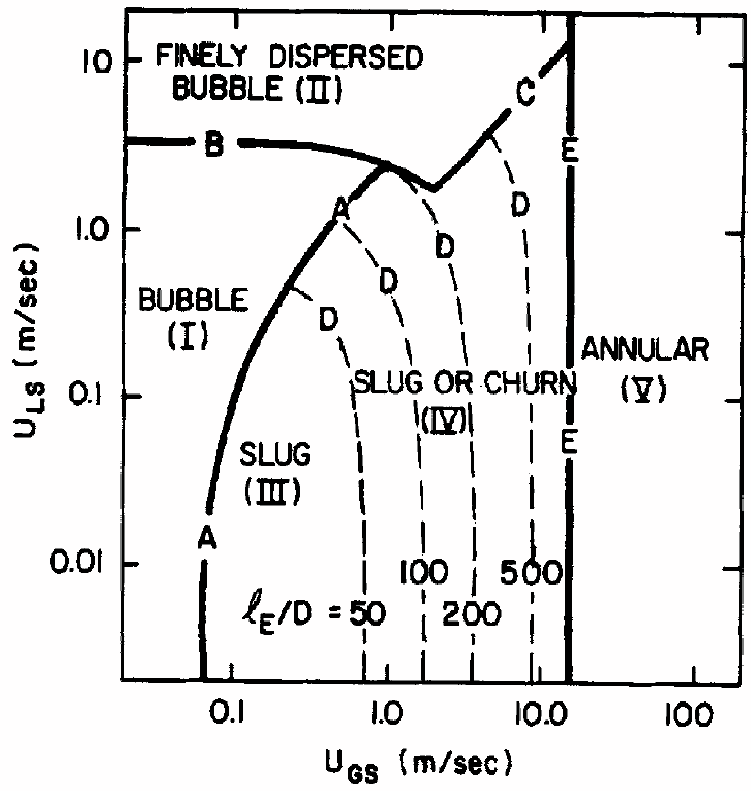

Figure 1.2: Flow pattern map for 25 mm diameter vertical tubes, air-water system (Taitel et al. (1980))

There exist different types of slugs, depending on how they are formed. They can be caused by hydro-dynamical effects or terrain effects. The slugs can also be formed due to transient effects related to pigging, start-up and blow-down and changes in pressure or flow

rates.

Hydrodynamic slugs are formed by liquid waves growing in the pipeline until the height of the waves is sufficient to completely fill the pipe. These slugs can melt together to form even larger slugs and occur over a wide range of flow conditions.

Terrain slugging is caused by low-points in the pipeline topography, causing the liquid to block the gas until the pressure in the compressed gas is large enough to overcome the hydrostatic head of the liquid. A long liquid slug is then pushed in front of the expanding gas upstream. One example of such a low-point is a subsea line with downwards inclination ending in a vertical riser to a platform. In some cases the entire riser can be filled with liquid until the pressure in the gas is large enough to overcome the hydrostatic pressure of the liquid-filled riser. Under such conditions a cyclic operation (limit cycle) is obtained. It is considered to consist of four steps (Schmidt et al. (1980), Taitel (1986)). These steps are illustrated in Figure 1.3. Liquid accumulates in the low point of the riser, blocking the gas (1). As more gas and liquid enters the system, the pressure will increase and the riser will be filled with liquid (2). After a while the amount of gas that is blocked will be large enough to blow the liquid out of the riser (3). After the blow-out, a new liquid slug will start to form in the low-point (4).

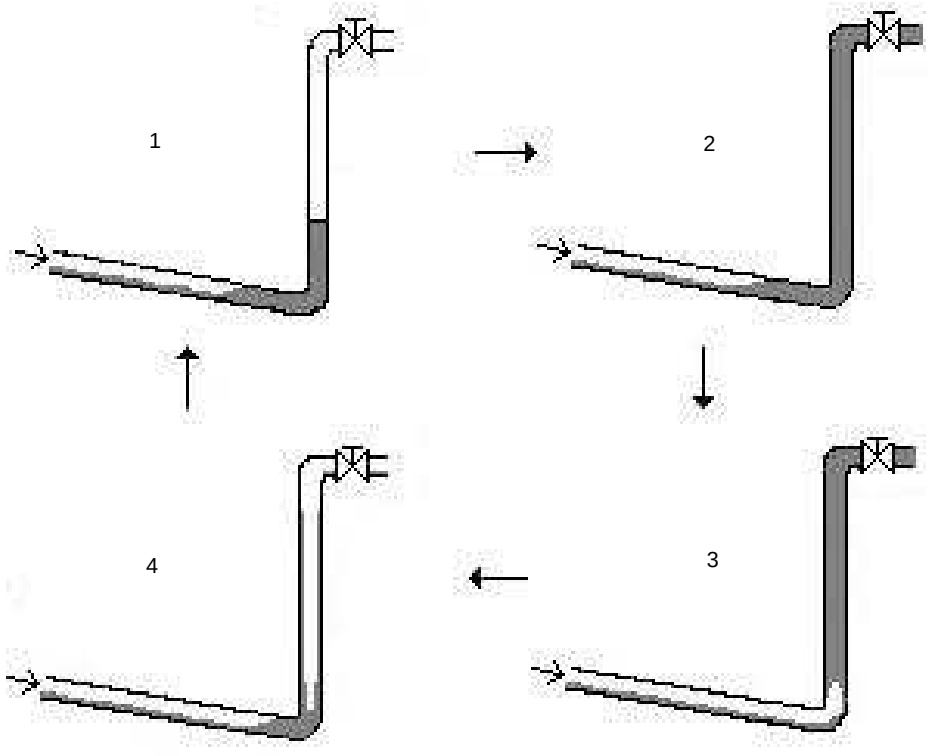

Figure 1.3: Illustration of the cyclic behavior (slug flow) in pipeline-riser systems

Terrain induced slugs can become hundreds of meters long, whereas hydrodynamic slugs are relatively shorter. This is also the reason why terrain slugging is often referred to as severe slugging.

Slug flow has a negative impact on the receiving facilities during offshore oil and gas production due to the large fluctuations in flow rates and pressure. Frequent problems are unwanted flaring and reduced operating capacity. The fluctuating pressure also leads to a lot of strain on other parts of the system, such as valves and bends. The burden on the topside separators and compressors can in some cases become so large that it leads to damages and plant shutdown, representing huge costs for the producing company. Being able to remove slugging has a great economic potential and this is why a lot of work and money has been spent on finding solutions to the problem.

It is possible to avoid or handle the slugs by changing the design of the system. Examples are; changing the pipeline topology, increasing the size of the separator, adding a slug catcher or installing gas lift. However, the implementation of this new equipment usually costs a lot of money.

Another option is changing the operating conditions by choking the topside valve (Sarica and Tengesdal (2000)). Also this comes with a drawback; the increased pressure in the pipeline leads to a reduced production rate and can lower the total recovery of the field that is being exploited.

In the last years there have been several studies on active control as a tool to ”stabilize” the flow and thereby avoiding the slug flow regime. Mathematically, the objective is to stabilize a flow region which otherwise would be unstable. A simple analogue is stabilization of a bicycle which would be unstable without control. Schmidt et al. (1979) was the first to successfully apply an automatic control system on a pipeline-riser system with a topside choke as actuator. Hedne and Linga (1990) showed that it was possible to control the flow using a PI controller and pressure sensors measuring the pressure difference over the riser. Lately different control strategies have also been implemented on production systems offshore with great success (Hollenberg et al. (1995), Courbot (1996), Havre et al. (2000), Skofteland and Godhavn (2003)).

Active control changes the boundaries of the flow map presented in Figure 1.2, so that it is possible to avoid the slug flow regime in an area where slug flow is predicted. This way it is possible to operate with the same average flow rates as before, but without the huge oscillations in flow rates and pressure. The advantages with using active control are large; it is much cheaper than implementing new equipment and it also removes the slug flow all together thereby removing the strain on the system. This way a lot of money can also be saved on maintenance. Also, it is possible to produce with larger flow rates than what would be possible by manually choking the topside valve.

Subsea measurements are usually included in the control structures that have been reported in the literature so far. Pressure measurements at the bottom of the riser or further upstream are examples of such measurements. When dealing with riser slugging, subsea measurements have proved to effectively stabilize the flow. When no subsea measurements are available, the task gets far more challenging.

Since subsea measurements are less reliable and much more costly to implement and maintain than measurements located topside, it is interesting to see if it is possible to control the flow using only topside measurements. Is it also possible to combine topside measurements in a way that improve the performance? And are the results comparable to the results obtained when using a controller based on subsea measurements?

Earlier studies on using only topside measurements are found in Godhavn, Fard and Fuchs (2005) where experiments where performed on a large rig and the flow was controlled using combinations of pressure and density measurements. This paper did however not compare the results found with what was obtainable using subsea measurements.

This thesis describes the study and results from both a small-scale and medium-scale lab rig, and compare the results from the two lab rigs to see how much the size of the system affect the result of the controllers that were tested.

The small-scale two-phase lab rig was build at the Department of Chemical Engineering at NTNU to test different riser slug control strategies without the huge costs involved in larger scale experiments. Earlier experiments on this small-scale rig had already shown that it was possible to stabilize the flow using a PI-controller with a pressure measurement located upstream the riser base as measurement (Sivertsen and Skogestad (2005)). The aim now was to control the flow using combinations of only topside measurements and to compare these results with results found when using upstream measurements.

A controllability analysis was performed in order to screen the different measurement candidates using a model developed by Storkaas et al. (2003). The analysis showed that it should be possible to control the flow using only topside measurements. The results from this analysis were then used as a background for the experiments performed in the lab.

Similar experiments were later performed on a *medium*-scale lab rig to investigate the effect the scale of the lab rig has on the quality of the controllers. The experiments were conducted at StatoilHydro Research Center in Porsgrunn. The facility was ideal for development and testing of new control solutions for anti-slug and separator control under realistic conditions. Figure 1.4 shows a photograph of the facility.

Several experiments were performed to test similar control configurations as was also tested on the NTNU small-scale lab rig. This was done in order to investigate whether different scales have an effect on the quality of the control structures. Having results from a larger rig could give an indication on whether the small-scale NTNU lab rig really was suitable as a tool for finding good control solutions to be used in larger scale facilities, such as a production platform.

The question was; could active control be used to stabilize the flow also for both rigs? In particular, it was interesting to see whether only topside measurements could be used to stabilize the flow.

1.2 Subsea water separation; the Tordis project

The second part of the thesis shows other areas of multiphase flow in oil production where automatic control can be implemented successfully in order to enhance production. This part of the thesis describes a study done in cooperation with StatoilHydro's research center in Trondheim, and was a part of project to increase the productivity of one of StatoilHydro's oil fields, Tordis. Also it was important for StatoilHydro to increase the competence and knowledge of the company on subsea installations.

The Tordis field operated by StatoilHydro has proved to be even more productive than anticipated when production began in 1994 (Godhavn, Strand and Skofteland (2005)). To

Figure 1.4: A birds-view perspective of the medium-scale riser rig at StatoilHydro Research Center in Porsgrunn

increase production and total recovery for the field in the last years of production, processing equipment is planned installed at the sea bed. This in order to separate produced water from the production stream, inject this water into a reservoir, and increase the production rate.

Subsea processing enables production from low-pressure reservoirs over long distances, and may increase the daily oil and gas production or even the total recovery from the reservoir. By injecting produced water into a reservoir, the water emission from topside to sea can be reduced, and the subsea transportation pipelines are better exploited. Compression and pumping enable a lower wellhead pressure, and hence an increased production. A general subsea production system with wells, manifold, subsea processing equipment, production pipelines and topside separators is shown in Figure 1.5.

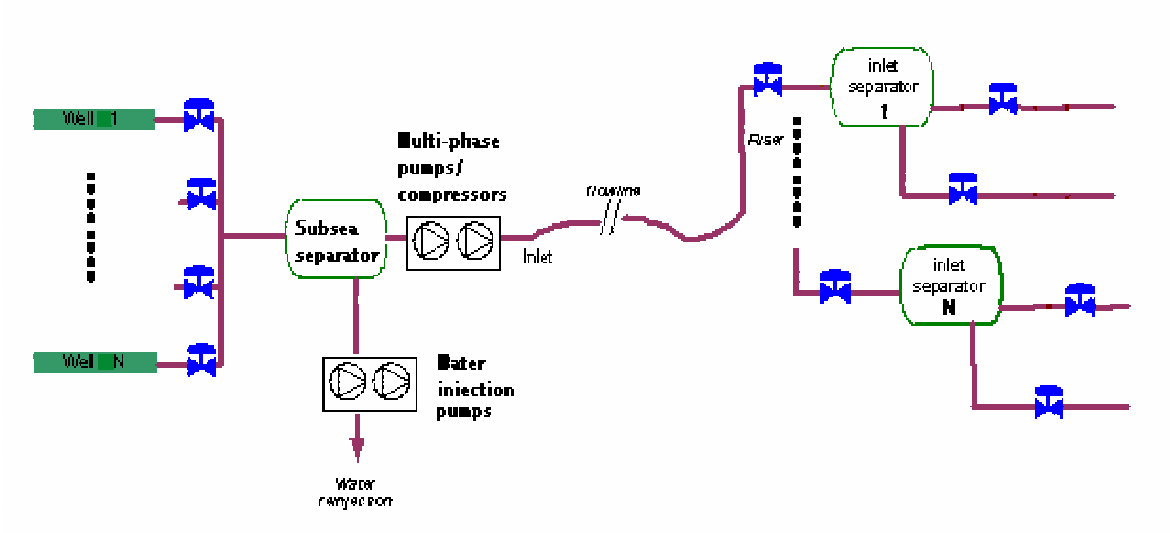

Figure 1.5: A production system including subsea processing equipment

Installation of subsea equipment leads to several challenges that need to be explored before the implementation. In the process of determining the control strategy and operation philosophy of the system, it is beneficial to perform dynamic simulations that capture the dynamical behavior adequately. Since the pressure, flow rates and composition of the flow vary with time, it is important to perform studies for several years throughout the life time of the field. The first question that needed answering was; which solutions are feasible and which one will solve the problems the best.

Having control of the subsea separator pressure and liquid levels are important as it determines the flow rates and compositions for the entire system. In Section 4, some solutions to achieve control of the separator will be presented. These control solutions are then expanded to achieve other benefits, such as faster well tests and control of the water rate that is transported with the oil and gas to the platform. Also slug control of the system, and a control system that ensures equal production in two riser downstream a split in the pipeline, will be presented in this section of the thesis.

The control solutions presented in this section are illustrated with dynamic simulations including all equipment from the wells to the two topside receiving separators at the Gullfaks

C platform. It is important to notice that these simulations were performed at a very early stage in the process of determining how to run the process, where the aim was to find feasible control solutions and not to find optimal control parameters. The controllers have therefore not been fine-tuned and simplified models for the equipment and pipelines have been used. This is also the reason why the absolute values for the different variables have been left out in this paper.

To simulate flow in the pipelines, OLGA 2000 dynamic multiphase simulator, provided by Scandpower Petroleum Technologies has been used. Most of the process equipment is simulated using Simulink. The OLGA - MATLAB toolbox enables the Simulink application to simulate multiphase flow in pipelines in OLGA together with additional process equipment and controllers modeled in Simulink. When combining these simulation tools, one needs to carefully consider which parts of the system to include in a simulation, and which assumptions can be made about the boundary conditions in each case.

Chapter 2

Anti-slug control applied to a small-scale rig

This section describes experiments performed on the small-scale lab rig, also called ”the Miniloop”, build at NTNU, Department of Chemical Engineering. Earlier experiments on this small-scale rig had shown that it was possible to stabilize the flow using a PI-controller with a pressure measurement located upstream the riser base as measurement (Sivertsen and Skogestad (2005)). Attempts to control the flow using only topside measurements had also been performed (Siversen and Skogestad (2005)).

During the experiments described in these articles, the slug flow behaved a bit different from that observed in larger facilities. Instead of severe slugs where the gas entered the riser, the gas was released as Taylor bubbles. As one Taylor bubble managed to enter the riser, several more would quickly follow as the pressure drop across the riser decreased. To get a slug flow pattern that was closer to severe slugs, the length of the riser and the size of the gas buffer tank was increased. After implementing this new equipment, the slug flow regime resembled more the severe slugs seen in larger rigs.

The aim now was to control the flow using only topside measurements and to compare these results with results found when using upstream measurements.

A controllability analysis was performed in order to screen the different measurement candidates using a model developed by Storkaas et al. (2003). The analysis showed that it should be possible to control the flow using only topside measurements. The results from this analysis were then used as a background for the experiments performed in the lab.

The experimental results were successful. They showed that it was possible to control the flow far better then predicted from the analysis and the results were in fact comparable with the results obtained when using a pressure measurement upstream the riser (subsea measurement). A paper with the results from this section is in the process of being published (Sivertsen, Storkaas and Skogestad (2008)).

2.1 Case description

2.1.1 Experimental setup

To test different control configurations, a small-scale two-phase flow loop with a pipeline-riser arrangement was build at the Department of Chemical Engineering at NTNU, Trondheim (Bårdsen (2003)). The flow consists of water and air, mixed together at the inlet of the system. Both the pipeline and the riser was made of a 20mm diameter transparent rubber hose, which makes it easy to change the shape of the pipeline system. A schematic diagram of the test facilities is shown in Figure 2.1.

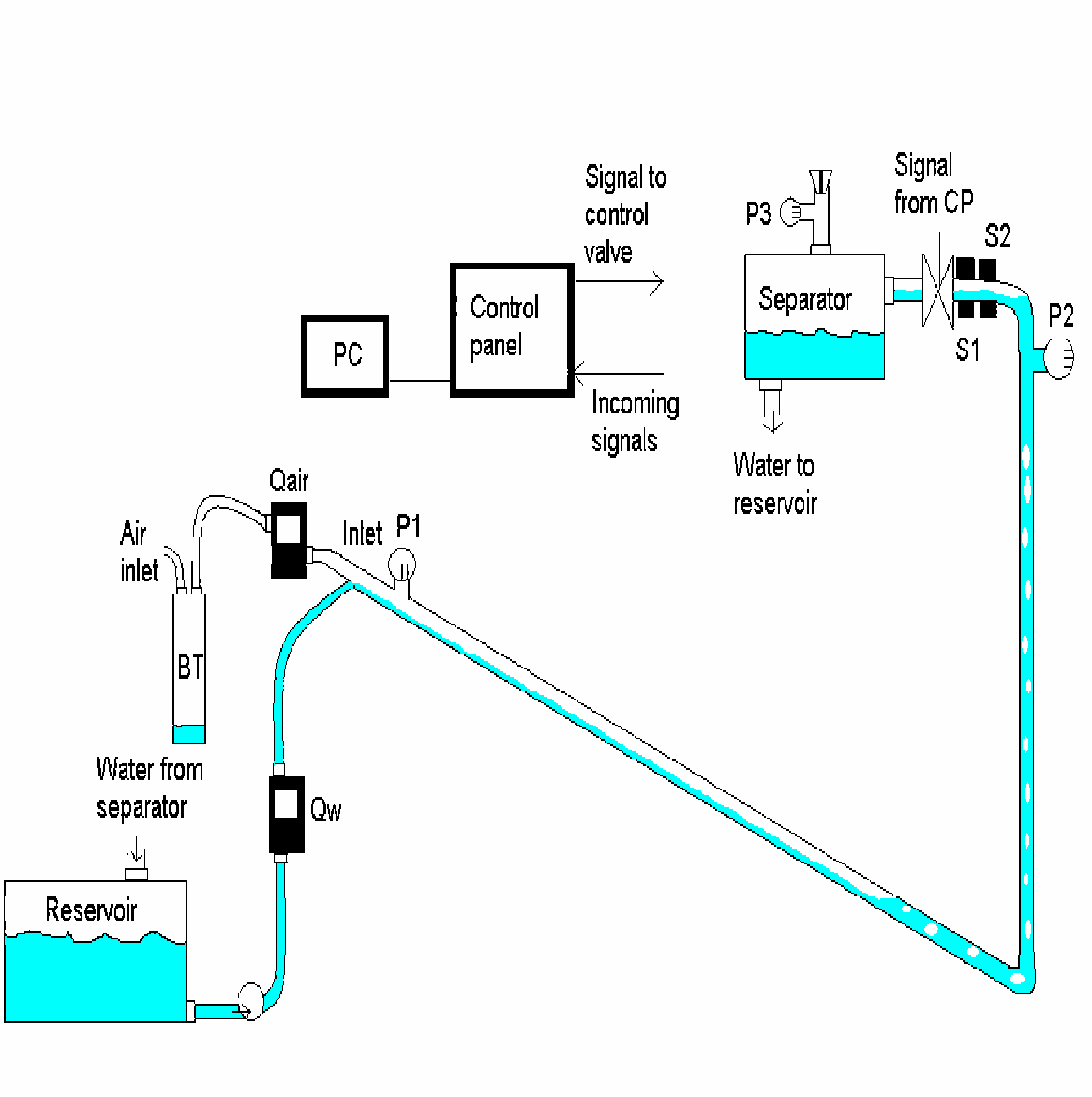

Figure 2.1: Experimental setup

From the inlet, which is the mixing point for the air and water, the flow is transported

trough a 3m long curved pipeline to the low-point at the bottom of the riser. Depending on different conditions such as water and air flow rates, slug flow may occur. At the top of the riser there is an acrylic tank which serves as a separator, leading the water to a reservoir while the air is let out through an open hole in the top. The separator is thus holding atmospheric pressure.

From the reservoir the water is pumped back into the system through the mixing point using a Grundfos UPS 25-120 180 pump with a lifting capacity of 12m. It is possible to adjust the power of the pump, thereby changing the pressure dependency of the inlet flow rate of the water. The pressure dependency during the experiments is discussed in Section 2.1.3. Periodic disturbances in the inlet flow rate of gas from the air supply system are also described in this section.

For slugging to appear there must be enough air in the system to blow the water out of the 2.7m long riser. This requires a certain amount of volume, which is accounted for by a 15 l acrylic buffer tank (BT) between the air supply and the inlet. The volume of the gas can be changed by partially filling this tank with water.

The inlet flow rates of gas (Q_{air}) and water (Q_w) determine whether we will have slug flow in open loop operation or not. The gas flow rate is measured at the inlet using a 2-10 l/min mass flow sensor from Cole-Parmer. The water flow rate was measured using a 2-60 l/min flow transmitter from Gemü. Typically inlet flow rates during an experiment are 5 l/min both for the gas and water.

Pressure sensors MPX5100DP from Motorola are located at the inlet (P_1) and topside (P_2). They measure the pressure difference between the atmospheric pressure and the pipeline pressure in the range 0-1 barg. Typically average values for the pressure during the experiments are approximately 0.2 barg at the inlet and 0.05 barg just upstream the topside control valve.

Two fiber optic sensors (S_1, S_2) from Omron are placed just upstream the control valve in order to measure the water content in the pipeline. Water in the pipeline will attenuate the laser beam and weaken the signal send to the control panel. The measurements from the fiber optic slug sensors needed some filtering because of spikes caused by reflections of the laser beam on the water/air interface (Figure 2.2). When correctly calibrated, the fiber optic sensors give a signal proportional to the amount of water the laser beam travels through in the pipeline and can be used to calculate the density ρ in the pipeline.

A pneumatic operated Gemü 554 angle seat globe valve with 20 mm inner diameter is installed at the top of the riser. A signal from the control panel sets the choke opening percentage of the valve. The valve responds well within a second to the incoming signal.

The control panel, consisting of Fieldpoint modules from National Instruments, converts the analog signals from the sensors into digital signals. The digital signals are then sent to a computer where they are continuously displayed and treated using Labview software. Depending on the control configuration, some of the measurements are used by the controller to set the choke opening for the control valve.

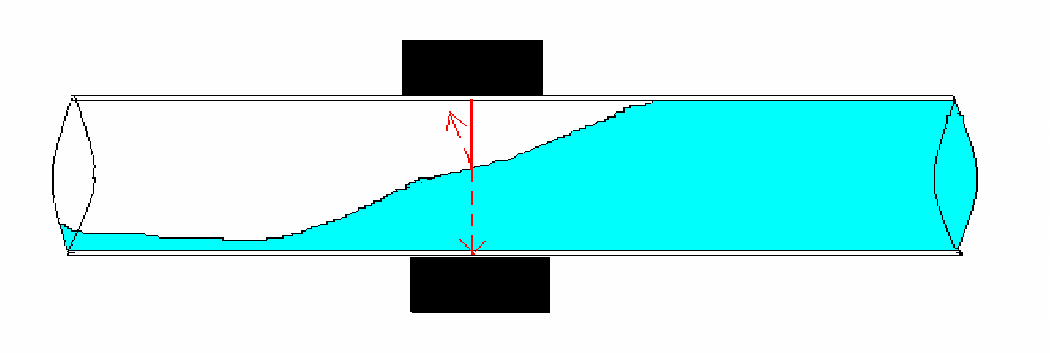

Figure 2.2: Reflection of light on water surface

2.1.2 Labview software

Labview from National Instruments was chosen as tool for acquiring, storing, displaying and analysing the data from the different sensors. Also, the valve opening of the topside valve was set from this program. The controllers was made using Labview PID controllers with features like integrator anti-windup and bump less controller output for PID gain changes.

Labview's PID Control Input Filter has been used to filter the noisy fiber optic signals. This is a fifth-order low-pass FIR (Finite Impulse Response) filter and the filter cut-off frequency is designed to be 1/10 of the sample frequency of the input value.

2.1.3 Disturbances

Two of the largest sources of disturbances during the experiments were the variations in the air and water inlet flow rates. The left plots in Figure 2.3 show how the air inlet rate Q_a is fluctuating with a period of approximately 200s between 5.5 and 5.9 l/min when the valve is 10% open and the flow is stable. These 200s fluctuations are caused by the on-off controller used for the pressurized air facility at the laboratory. The fluctuations in water rate Q_w are however quite small for this valve opening.

When the topside valve is fully open and the inlet pressure (P_1) starts to oscillate due to slug flow in the pipeline, larger fluctuations in the water flow was observed. The capacity of the water pump is pressure dependent, and oscillations in the inlet pressure cause the water rate to fluctuate between approximately 4.9 and 5.6 l/min as is seen from the right plots in Figure 2.3. The pressure oscillations also lead to oscillations in the air inlet flow rate, which come in addition to the 200s periodic fluctuations.

2.2 Controllability analysis and simulations

In order to have a starting point for the lab experiments, an analysis of the system has been performed. The analysis reveals some of the control limitations that can be expected using different measurements. Closed-loop simulations using these measurements are also described in this section.

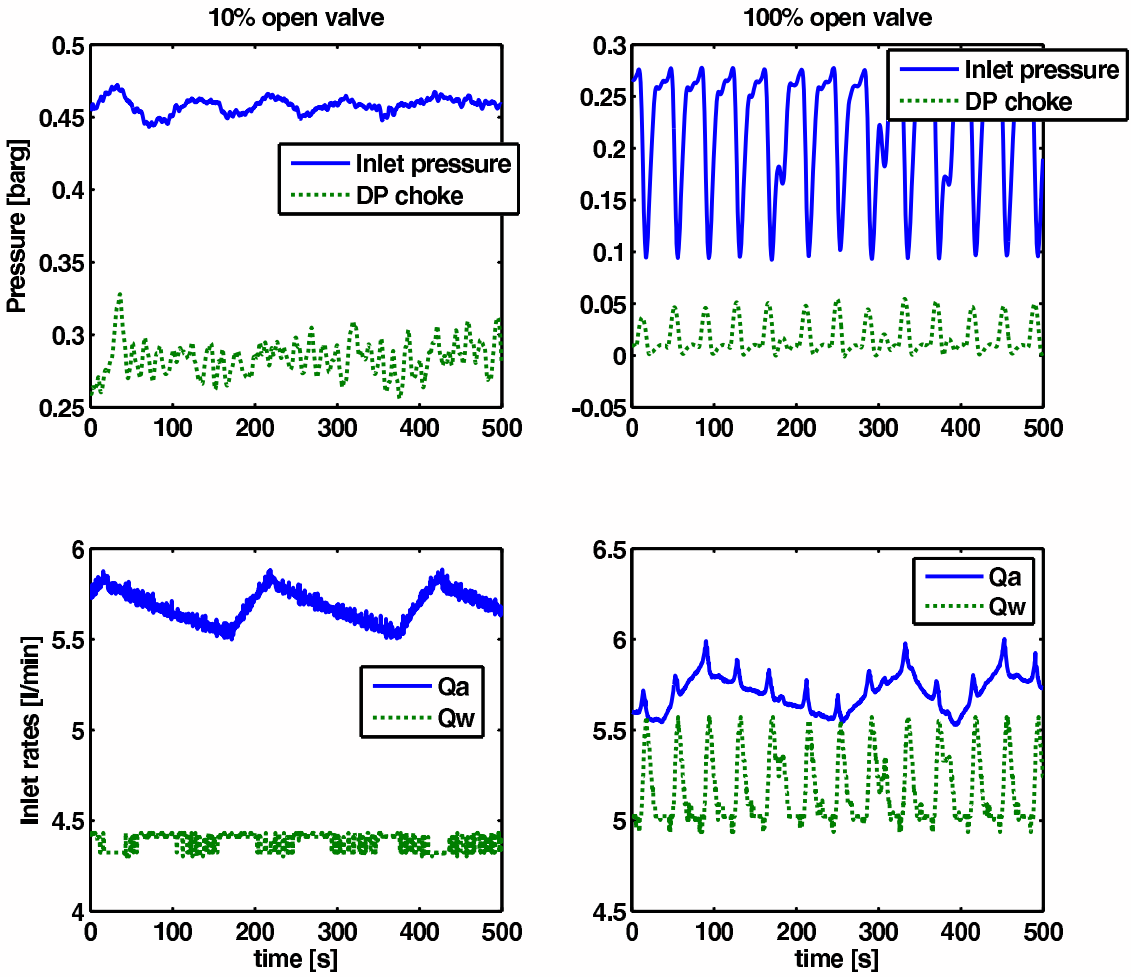

Figure 2.3: Disturbances in the inlet water flow rate (Qw) and air inlet rate (Qa)

2.2.1 Theoretical background

Given the feedback control structure shown in Figure 2.4, the measured output y is found by

$$y = G(s)u + G_d(s)d \tag{2.1}$$

u is the manipulated input, d is the disturbance to the system and n is measurement noise. G and G_d are the plant and disturbance models.

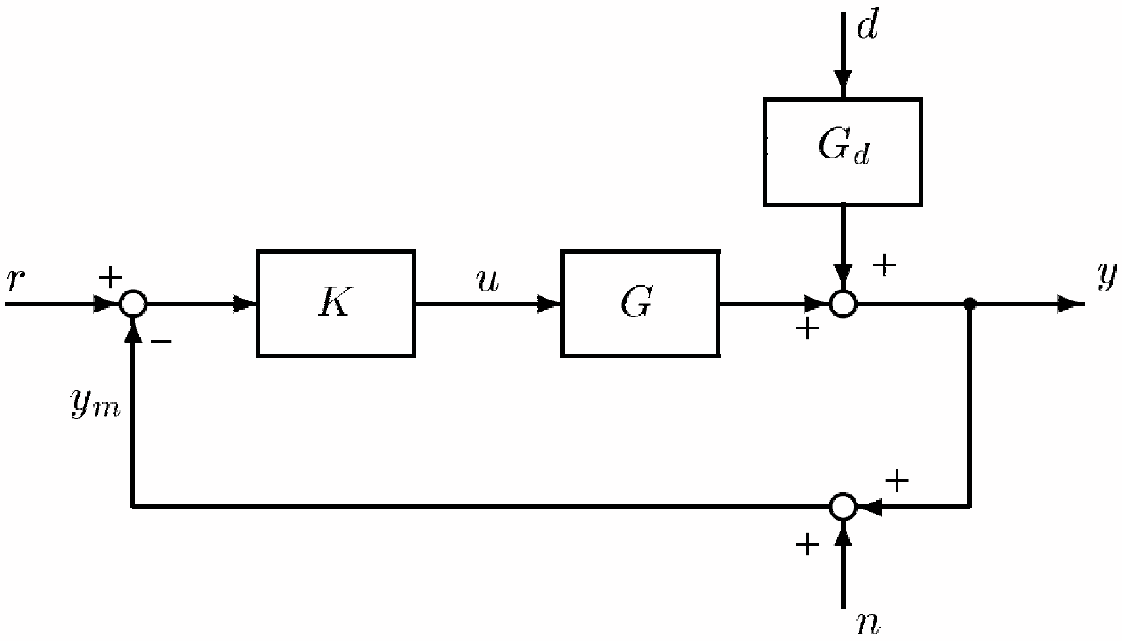

Figure 2.4: One degree-of-freedom negative feedback control structure (Skogestad and Postlethwaite (1996))

The location of RHP (Right Half Plane) poles and zeros in $G(s)$ impose bounds on the bandwidth of the system. These bounds can render it impossible to control the system when the RHP-poles and -zeros are located close to each other. Skogestad and Postlethwaite (1996) show that a pair of pure complex RHP-poles places a lower bound on the bandwidth of the closed loop system:

$$w_c > 1.15|p| \tag{2.2}$$

whereas a real RHP zeros imposes an *upper* bound

$$w_c < |z|/2 \tag{2.3}$$

For an imaginary RHP-zero the bound is

$$w_c < 0.86|z| \tag{2.4}$$

When comparing Equation (2.2) with (2.3) and (2.4), it is easy to see that if the RHP-zeros and -poles are located close to each other, bandwidth problems can occur. The closed-loop system can also be expressed as

$$y = Tr + SG_d d - Tn \tag{2.5}$$

Here $T = (I + L)^{-1}L$, $S = (I + L)^{-1}$ and $L = GK$. L is the loop transfer function, whereas S is called the classical sensitivity function and gives the sensitivity reduction introduced by the feedback loop. The input signal is

$$u = KSr - KSG_d d - KSn \tag{2.6}$$

and the control error $e = y - r$ is

$$e = -Sr + Sg_d d - Tn \tag{2.7}$$

From equations 2.5- 2.7 it is obvious that the magnitude for transfer functions S, T, SG, KS, KSG_d and SG_d give valuable information about the effect u, d and n have on the system. In order to keep the input usage u and control error e small, these closed-loop transfer functions need to be small. There are however some limitations on how small the peak values of these transfer functions can be. The locations of the RHP-zeros and -poles influence these bounds significantly.

Minimum peaks on S and T

Skogestad and Postlethwaite (1996) show that for each RHP-zero z of $G(s)$ the sensitivity function must satisfy Eq. (2.8) for closed-loop stability.

$$||S||_\infty \geq \prod_{i=1}^{N_p} \frac{|z + p_i|}{|z - p_i|} \tag{2.8}$$

Here $||S||_\infty$ denotes the maximum frequency response of S. This bound is tight for the case with a single RHP-zero and no time delay. Chen (2000) shows that the same bound is tight for T.

Minimum peaks on SG and SG_d

The transfer function SG is required to be small for robustness against pole uncertainty. Similar, SG_d needs to be small in order to reduce the effect of the input disturbances on the control error signal e. In Skogestad and Postlethwaite (1996) the following bounds are found for SG and SG_d

$$||SG||_\infty \geq |G_{ms}(z)| \prod_{i=1}^{N_p} \frac{|z + p_i|}{|z - p_i|} \tag{2.9}$$

$$||SG_d||_\infty \geq |G_{d,ms}(z)| \prod_{i=1}^{N_p} \frac{|z + p_i|}{|z - p_i|} \tag{2.10}$$

These bounds are valid for each RHP-zero of the system. Here G_{ms} and $G_{d,ms}$ are the "minimum, stable version" of G and G_d, with RHP poles and zeros mirrored into the LHP.

Minimum peaks on KS and KSG_d

The peak on the transfer function KS needs to be small to avoid large input signals in response to noise and disturbances, which could result in saturation. Havre and Skogestad (2002) derives the following bound on KS

$$||KS||_\infty \geq |G_s^{-1}(p)| \tag{2.11}$$

which is tight for plants with a single real RHP-pole p. Havre and Skogestad (2002) also finds

$$||KSG_d||_\infty \geq |G_s^{-1}(p)G_{d,ms}(p)| \tag{2.12}$$

When analyzing a plant, all of the closed-loop transfer functions should be considered.

2.2.2 Modelling

Storkaas et al. (2003) have developed a simplified model to describe the behavior of pipeline-riser slugging. One of the advantages of the model is that it is well suited for controller design and analysis. It consists of three states; the holdup of gas in the feed section (m_{G1}), the holdup of gas in the riser (m_{G2}), and the holdup of liquid (m_L). The model is illustrated in Figure 2.5.

Using this model we are able to predict the variation of system properties such as pressures, densities and phase fractions, and analyse the system around desired operation points. After entering the geometrical and flow data for the lab rig, the model was tuned as described in Storkaas et al. (2003) to fit the open loop behavior of the lab rig. The model data and tuning parameters are presented in Table 2.1.

A bifurcation diagram of the system is plotted in Figure 2.6. It was found by open-loop simulations at different valve openings and gives information about the valve opening for which the system goes unstable. Also the amplitude of the pressure oscillations for the inlet and topside pressure (P_1 and P_2) at each valve opening can be seen from the plot.

The upper line in the bifurcation plots shows the maximum pressure at a particular valve opening and the lower line shows the minimum pressure. The two lines meet at around 16% valve opening. This is the point with the highest valve opening which gives stable operation when no control is applied for this particular system. When Storkaas' model is properly tuned, the bifurcation point from the model will match the one from the experimental data. From the bifurcation diagram in Figure 2.6 it is seen that the tuned model values fit the results from the lab quite well. The dotted line in the middle shows the unstable steady-state solution. This is the desired operating line with closed-loop operation.

Figure 2.7 shows some of the simulations performed in order to find the bifurcation diagram. The plots show that the frequency predicted by the model is approximately 50% higher than the frequency of the slugs in the lab. In Figure 2.8 a root-locus diagram of the system is plotted. This plot shows how the poles cross into the RHP as the valve opening

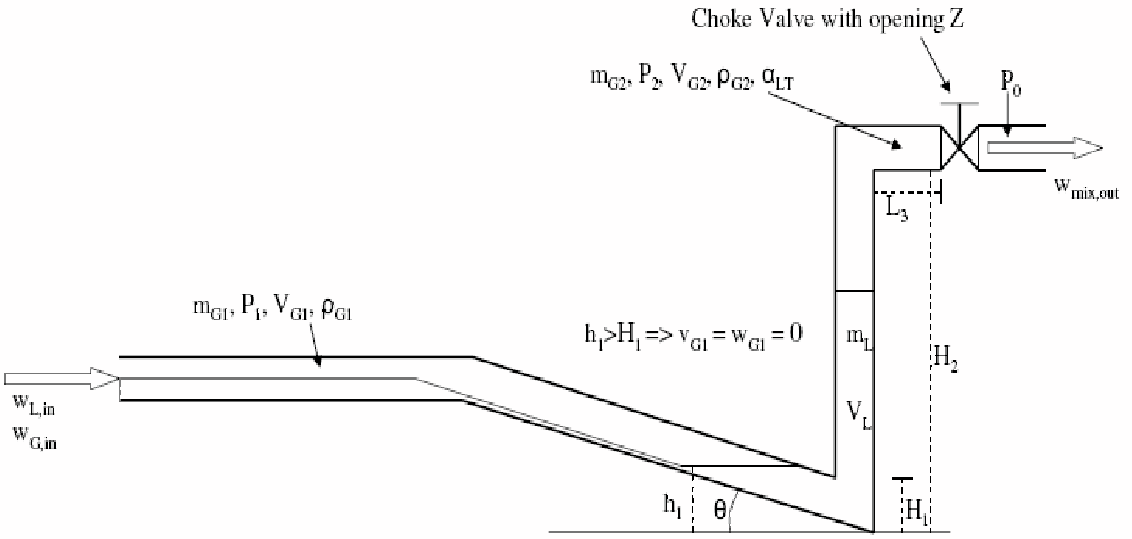

(a) Simplified representation of riser slugging

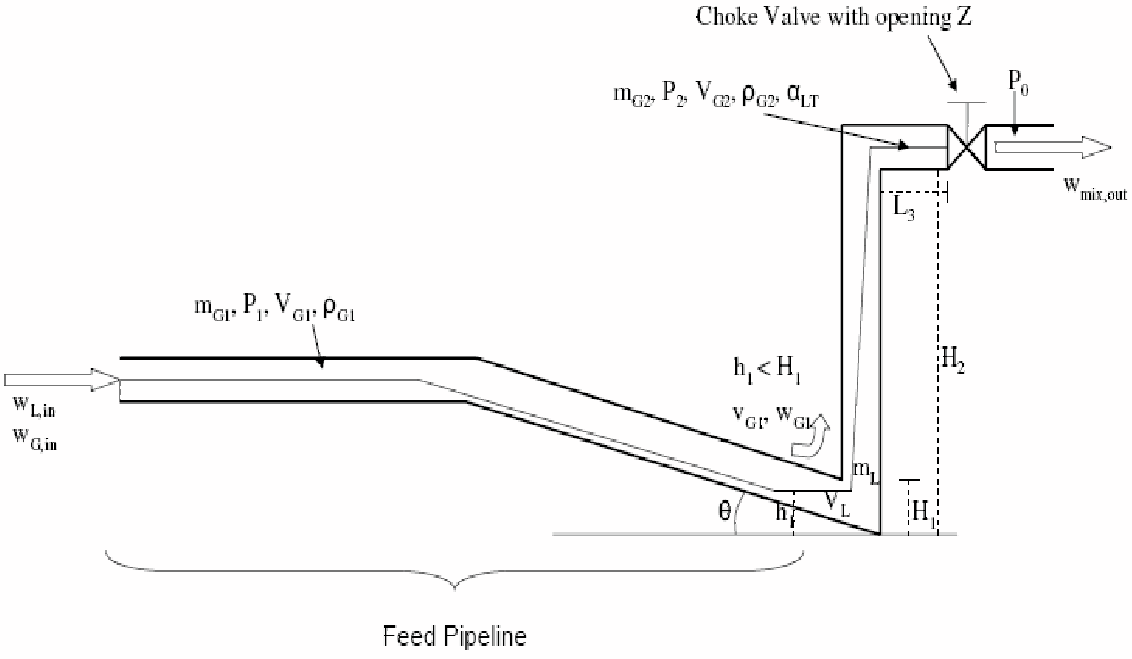

(b) Simplified representation of desired flow regime

Figure 2.5: Storkaas' pipeline-riser slug model (Storkaas et al. (2003))

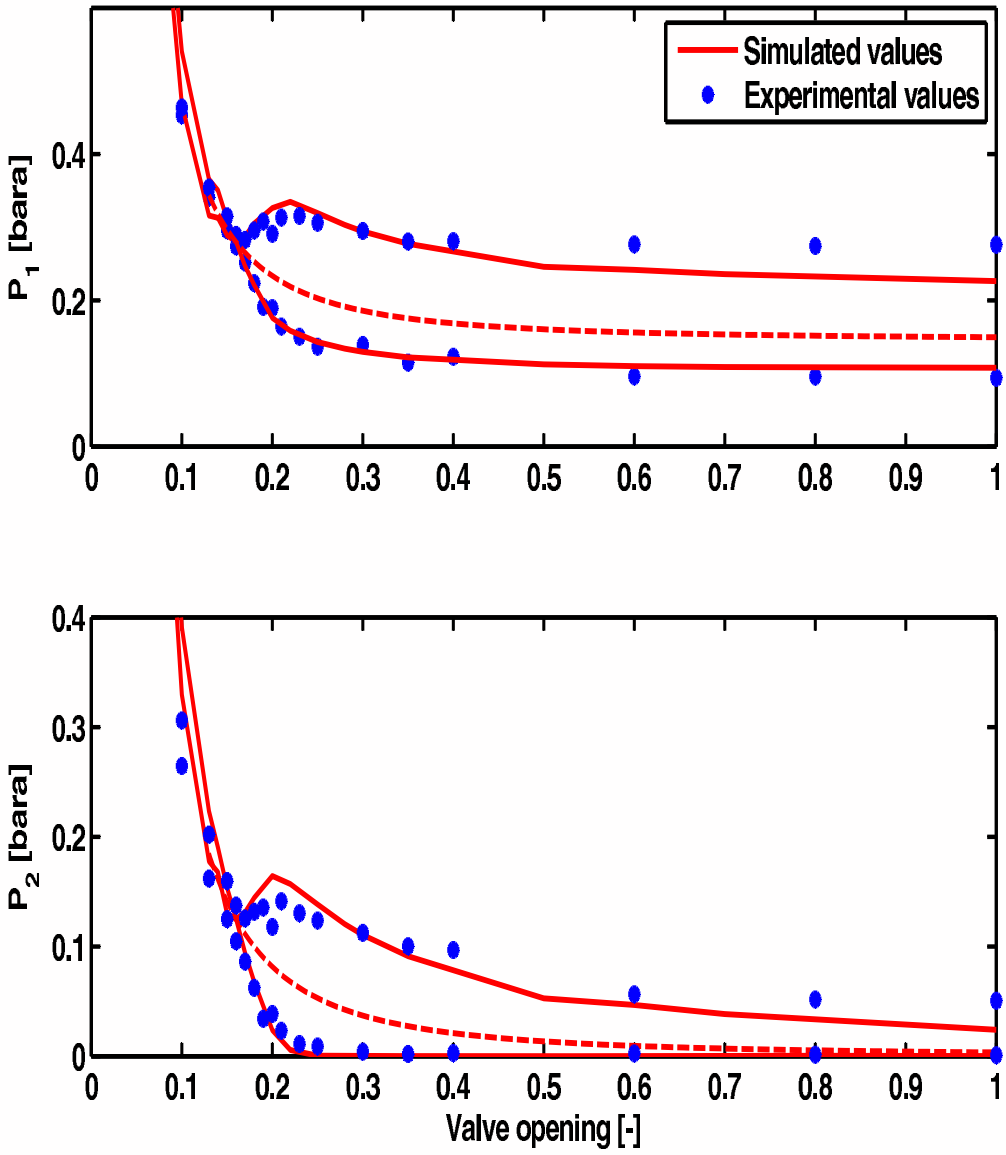

Figure 2.6: Bifurcation plot showing the open loop behavior of the system

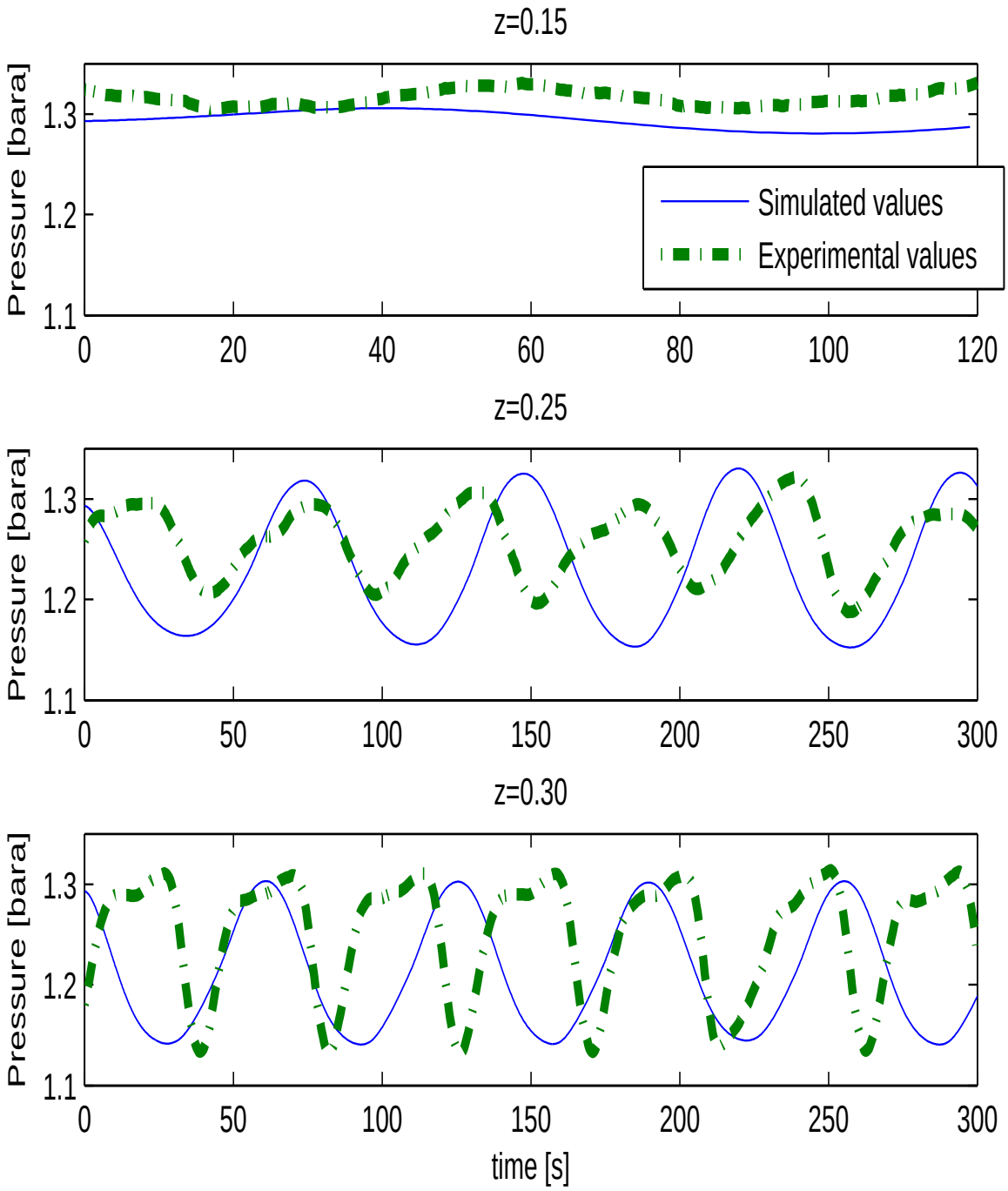

Figure 2.7: Open-loop behavior of inlet pressure P_1 for valve openings 15, 25 and 30%

Table 2.1: Model data parameters

Parameter	Symbol	Value
Inlet flow rate gas $[kg/s]$	$w_{G,in}$	$1.145e^{-4}$
Inlet flow rate water $[kg/s]$	$w_{L,in}$	0.090
Valve opening at bifurcation point [-]	z	0.16
Inlet pressure at bifurcation point $[barg]$	$P_{1,stasj}$	0.28
Topside pressure at bifurcation point $[barg]$	$P_{2,stasj}$	0.125
Separator pressure $[barg]$	P_0	0
Liquid level upstream low point at bifurcation point $[m]$	$h_{1,stasj}$	$9.75e^{-3}$
Upstream gas volume $[m^3]$	V_{G1}	$6.1e^{-3}$
Feed pipe inclination $[rad]$	θ	$1e^{-3}$
Riser height $[m]$	H_2	2.7
Length of horizontal top section $[m]$	L_3	0.2
Pipe radius $[m]$	r	0.01
Exponent in friction expression [-]	n	16
Choke valve constant $[m^{-2}]$	K_1	$2.23e^{-4}$
Internal gas flow constant [-]	K_2	0.193
Friction parameter $[s^2/m^2]$	K_3	$3.4e^3$

reaches 16% from below. This also confirms the results plotted in the bifurcation diagram in Figure 2.6.

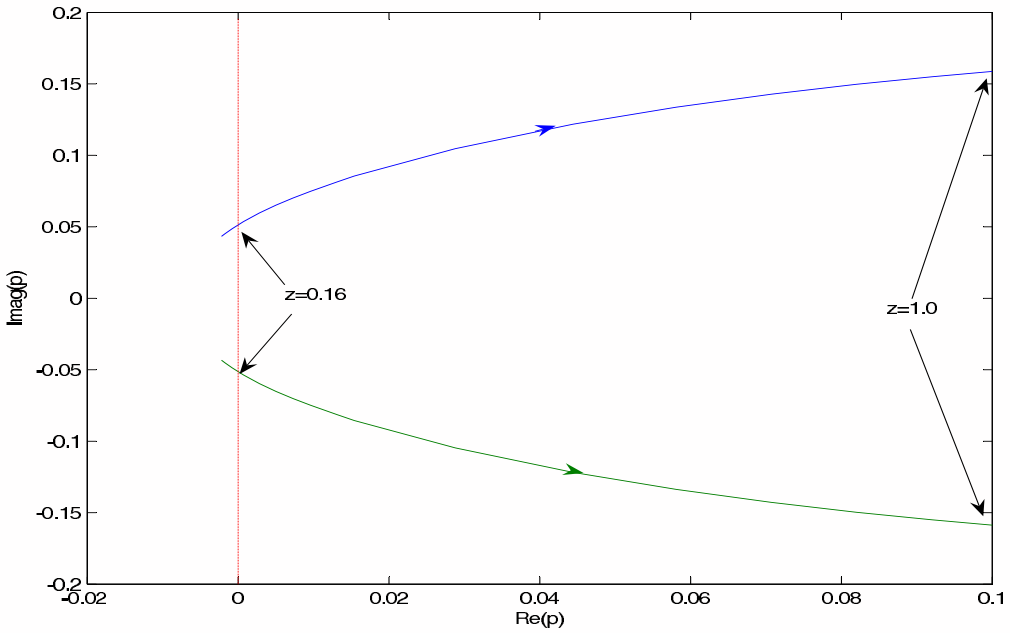

Figure 2.8: Root-locus plot showing the trajectories of the RHP open-loop poles when the valve opening varies from 0 (closed) to 1 (fully open)

2.2.3 Analysis

The model can now be used to explore different measurement alternatives for controlling the flow. The lab rig has four sensors as described in Section 2.1. There are two pressure sensors; one located at the inlet (P_1) and one located topside upstream the control valve (P_2). Also two fiber optic water hold-up measurements are located upstream the control valve. Using these measurements it is possible to estimate the density (ρ) and flow rates (F_Q, F_W) through the control valve. Figure 2.9 shows the different measurement candidates.

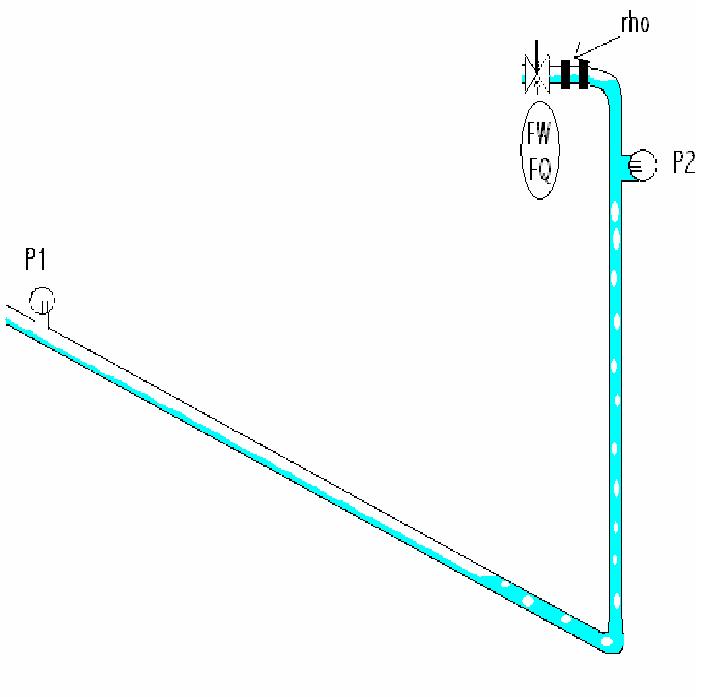

Figure 2.9: Measurement candidates for control

In Section 2.2.1 it was shown how the locations of the RHP poles and zeros had a big influence on the controllability of the system. By scaling the system and calculating the sensitivity peaks it is possible to get a picture of how well a controller can perform, using one of these measurements.

The process model G and disturbance model G_d were found from a linearization of Storkaas' model around two operation points. The model was then scaled as described in Skogestad and Postlethwaite (1996). The process variables were scaled with respect to the largest allowed control error and the disturbances were scaled with the largest variations in the inlet flow rates in the lab. The disturbances were assumed to be frequency independent. The input was scaled with the maximum allowed positive deviation in valve opening since the process gain is smaller for large valve openings. For measurements y = $[P_1; P_2; \rho; F_W; F_Q]$ the scaling matrix is De = diag[0.1 0.05 100 0.01 $1e^{-5}$ 0.1]. The scaling matrix for the outputs is Dd = diag [$1e^{-5}$ $1e^{-2}$]. This represents approximately 10% change in the inlet flow rates from the nominal values of $1.145e^{-4}$ kg/s (5.73 l/min) for gas and $90e^{-3}$ kg/s (5.4 l/min) for water. The input is scaled $Du = 1 - z_{nom}$ where z_{nom} is the nominal valve opening.

Tables 2.2 and 2.3 present the controllability data found. The location of the RHP poles and zeros are presented for valve openings 25 and 30 %, as well as stationary gain and lower bounds on the closed-loop transfer functions described in Section 2.2.1. The only two measurements of the ones considered in this analysis which introduces RHP-zeros into the system, are the topside density ρ and pressure P_2. The pole location is independent of the input and output (measurement), but the zeros may move. From the bifurcation plot in Figure 2.6 it is seen that both of these valve openings are inside the unstable area. This can also be seen from the RHP location of the poles.

Table 2.2: Control limitation data for valve opening 25%. Unstable poles at $p = 0.010 \pm 0.075i$.

Measurement	RHP zeros	Stationary gain	Minimum bounds				
		$\|G(0)\|$	$\|S\|$	$\|SG\|$	$\|KS\|$	$\|SG_d\|$	$\|KSG_d\|$
$P_1[bar]$	-	3.20	1.00	0.00	0.14	0.00	0.055
$P_2[bar]$	0.18±0.17i	5.97	1.13	1.59	0.091	0.085	0.055
$\rho[kg/m^3]$	0.032	0.70	1.20	4.62	0.048	0.31	0.056
$F_W[kg/s]$	-	0.00	1.00	0.00	0.015	1.00	0.055
$F_Q[m^3/s]$	-	2.59	1.00	0.00	0.015	0.00	0.055

Table 2.3: Control limitation data for valve opening 30%. Unstable poles at $p = 0.015 \pm 0.086i$

Measurement	RHP zeros	Stationary gain	Minimum bounds				
		$\|G(0)\|$	$\|S\|$	$\|SG\|$	$\|KS\|$	$\|SG_d\|$	$\|KSG_d\|$
$P_1[bar]$	-	1.85	1.00	0.00	0.34	0.00	0.086
$P_2[bar]$	0.18±0.17i	3.44	1.22	1.25	0.23	0.085	0.079
$\rho[kg/m^3]$	0.032	0.41	1.26	2.86	0.091	0.31	0.081
$F_W[kg/s]$	-	0.00	1.00	0.00	0.028	1.00	0.079
$F_Q[m^3/s]$	-	1.53	1.00	0.00	0.028	0.00	0.079

In Figure 2.10 the RHP poles and relevant RHP zeros are plotted together. The RHP zeros are in both cases located quite close to the RHP poles, which results in the high peaks especially for sensitivity function SG but also for S. From this we can expect problems when trying to stabilize the flow using these measurements as single measurements.

The stationary gain found when using the volumetric flow rate F_W is approximately zero, which can cause a lot of problems with steady state control of the system. Also the stationary gain for the plant using density ρ as measurement has a low stationary gain. The model is however based on constant inlet flow rates. The stationary gain for F_W predicted by the model is 0, which means that it is not possible to control the steady-state behavior of the system and the system will drift. Usually the inlet rates are pressure dependent, and the zeros for measurements F_Q and F_W would be expected to be located further away from the origin than indicated by Tables 2.2 and 2.3.

When comparing $|KS|$ and $|KSG_d|$ for the two valve openings, it is obvious that the peak values for these transfer functions increase with valve opening for all the measurement candidates, indicating that controlling around an operating point with a larger valve opening increases the effect disturbances and noise have on the input usage.

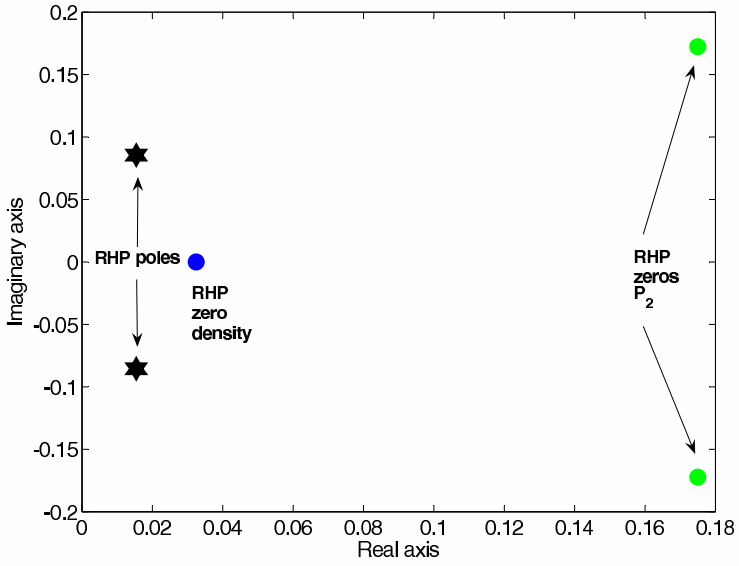

Figure 2.10: Plot-zero map for valve opening 30%

Figure 2.11 and 2.12 shows the Bode plots for the different plant models and disturbance models respectively. The models were found from a linearization of the model around valve opening 25%. For the volumetric flow rate measurement F_W, the value of the disturbance model G_dW is higher than plant model GW for low frequencies. For acceptable control we require $|G(jw)| > |Gd(jw)| - 1$ for frequencies where $|G_d| > 1$ (Skogestad and Postlethwaite (1996)). In this case both $|G_dW|$ and $|G_W|$ are close to zero, which means problems can occur for this measurement.

2.2.4 Simulations

Closed-loop simulations using Storkaas' model were performed in order to investigate the effect of the limitations found in the analysis. The measurements were used as single measurements in a feedback loop with a PI-controller. Figure 2.13 shows this control structure using the inlet pressure P_1 as measurement.

Figure 2.14 compares the simulation results using four different measurement candidates. The disturbances in inlet flow rates for the gas and water, as described in Section 2.1.3, are also included in these simulations. The only measurement that is not included is the topside pressure P_2, as the corresponding controller was not able to stabilize the flow.

At first, the controller is turned off and the system is left open-loop with a valve opening of 20% for approximately 5-10 min. From the bifurcation diagram in Figure 2.6 it was shown that the system goes unstable for valve openings larger than 16%. As expected, the pressure and flow rates start to oscillate due to the effects of slug flow.

When the controllers are activated, the control valve starts working as seen from the right plot in Figure 2.14. The aim of the simulation study is to see how far into the unstable region it is possible to control the flow with satisfactory performance. A larger valve opening gives

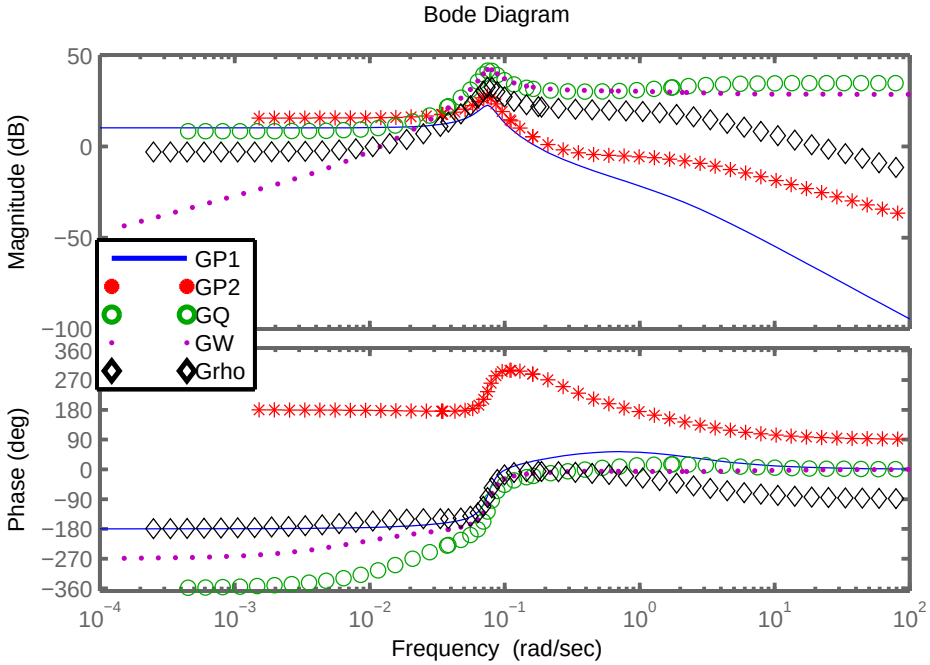

Figure 2.11: Bode plots for the plant models using different measurements

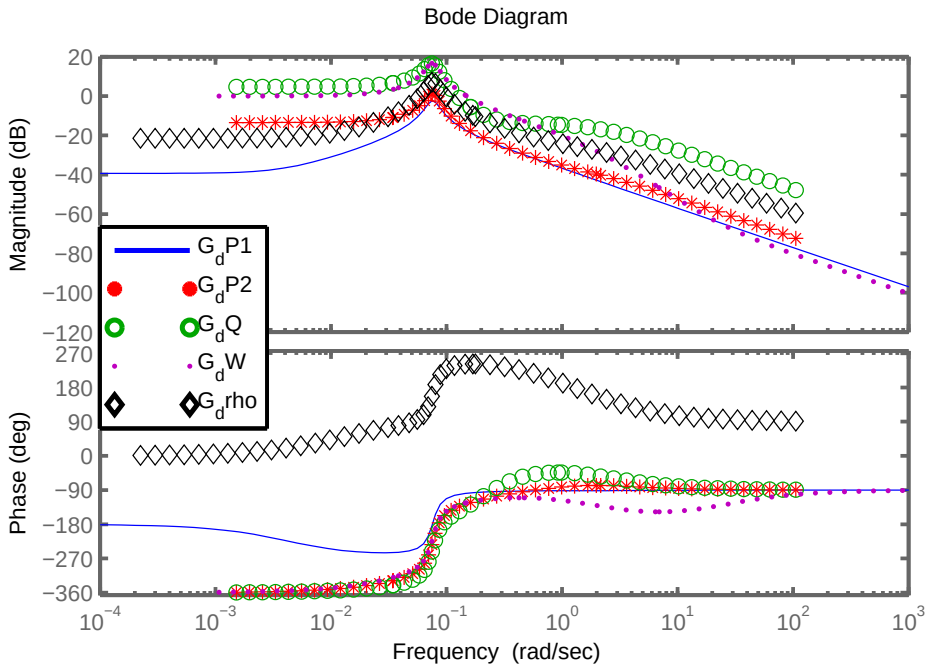

Figure 2.12: Bode plots for the disturbance models using different measurements

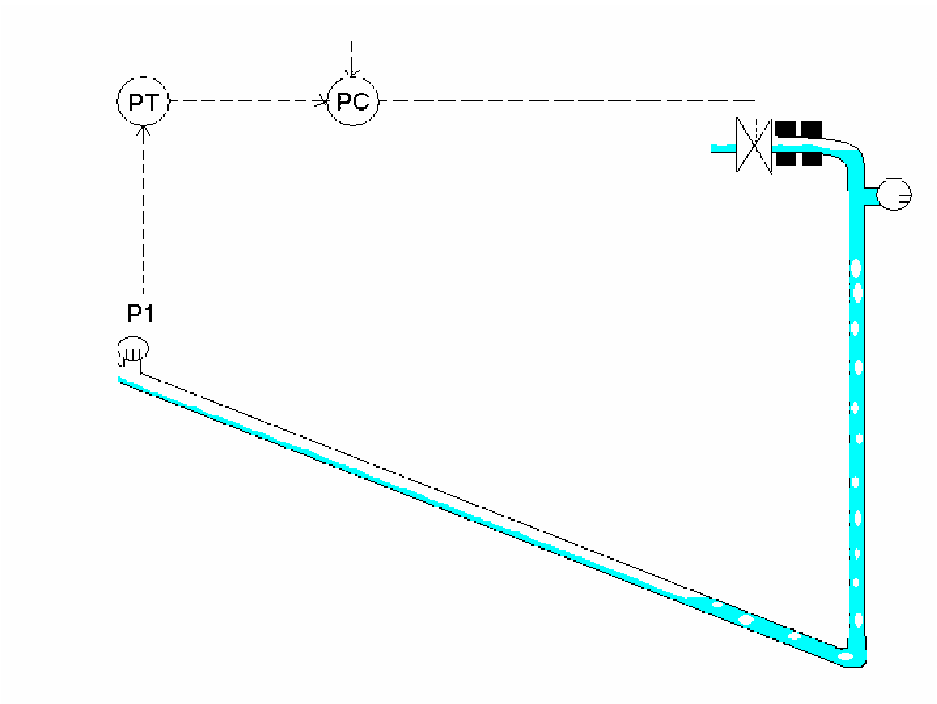

Figure 2.13: Feedback control using PI controller with inlet pressure P_1 as measurement

higher production with a given pressure dependent source.

As expected the measurement giving the best result was inlet pressure P_1. The upper left plot shows how the controller quickly stabilizes at the desired set point. The average valve opening is 25 %, which is far into the unstable region. After about 70 min the set point for the pressure is decreased, and the valve opening is now larger than 30%. Still the performance of the controller is good.

The figure also shows the results from controlling the flow using the topside volumetric flow rate F_Q, mass flow rate F_W and the density ρ. Not surprisingly the density measurement was not very well suited, as was expected from the analysis in Section 2.2.3. It was possible to control the flow using this measurement, but not at an average valve opening larger than 17-18 % which is just inside the unstable area. The benefits of using control are therefore negligible.

The relatively small oscillations seen in each plot has a period of 200s (3,3 min) and are caused by the periodic oscillations of the inlet air flow rate. The results using the topside pressure P_2 are not included in the figure. This is because it was not possible to stabilize the flow inside the unstable region using this measurement. Although the analysis suggested otherwise, the disturbances added in the simulations might have had a larger effect on this measurement than on the others.

Sometimes control configurations using *combinations* of measurements can improve the performance of a controller when compared with controllers using single measurements. This is why cascade controllers using different combinations of the topside measurements have been applied to the system. Figure 2.15 shows an example of such a control config-

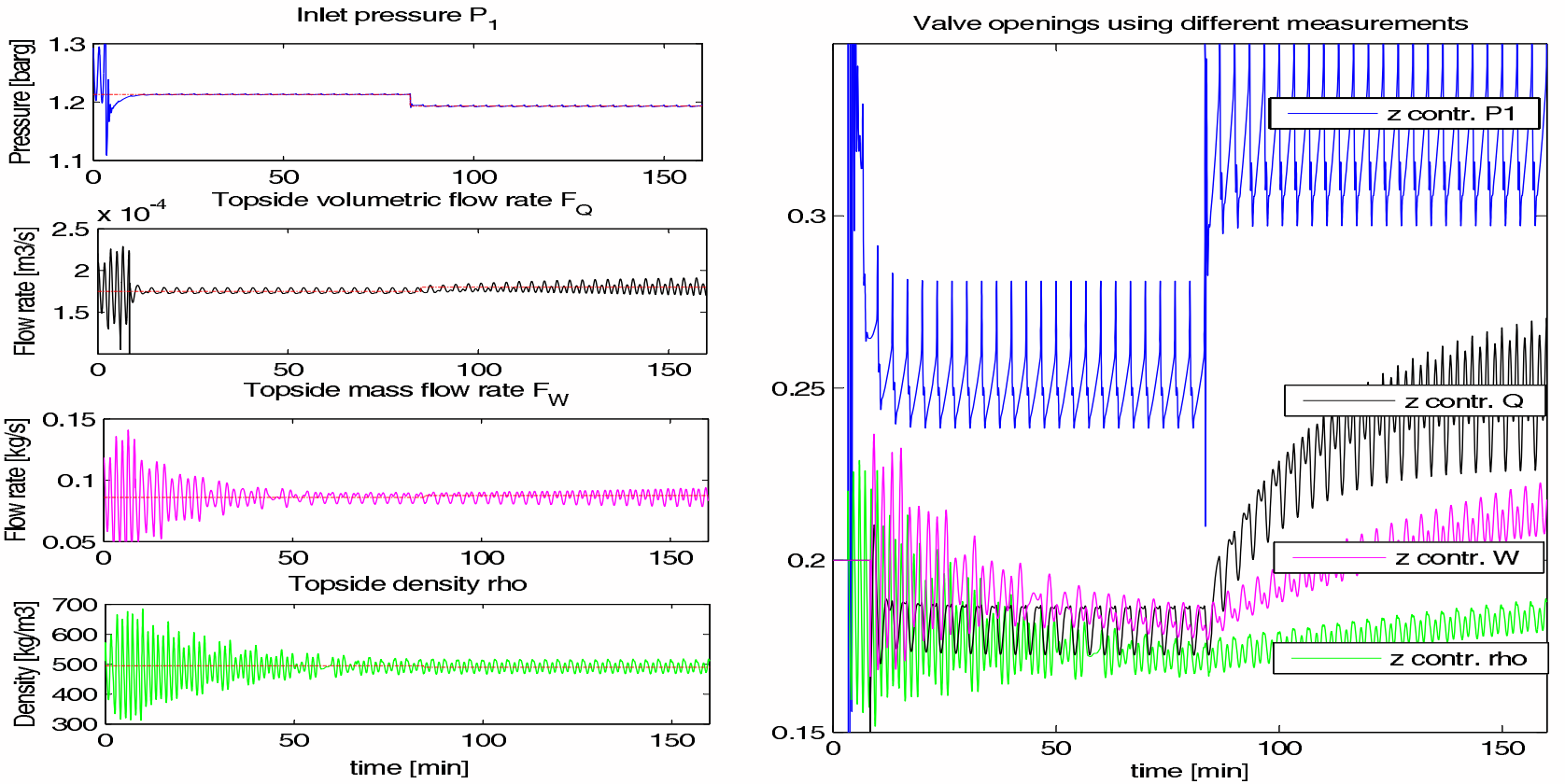

Figure 2.14: Simulations of stabilizing control using four alternative measurements (P_1, F_Q, F_W, ρ)

uration. The inner loop controls the topside density ρ, which by itself was not found to be well suited (Figure 3.10). In this case the set point for the density is set by an outer loop controlling the valve opening. This way drift due to the low stationary gain for ρ is avoided.

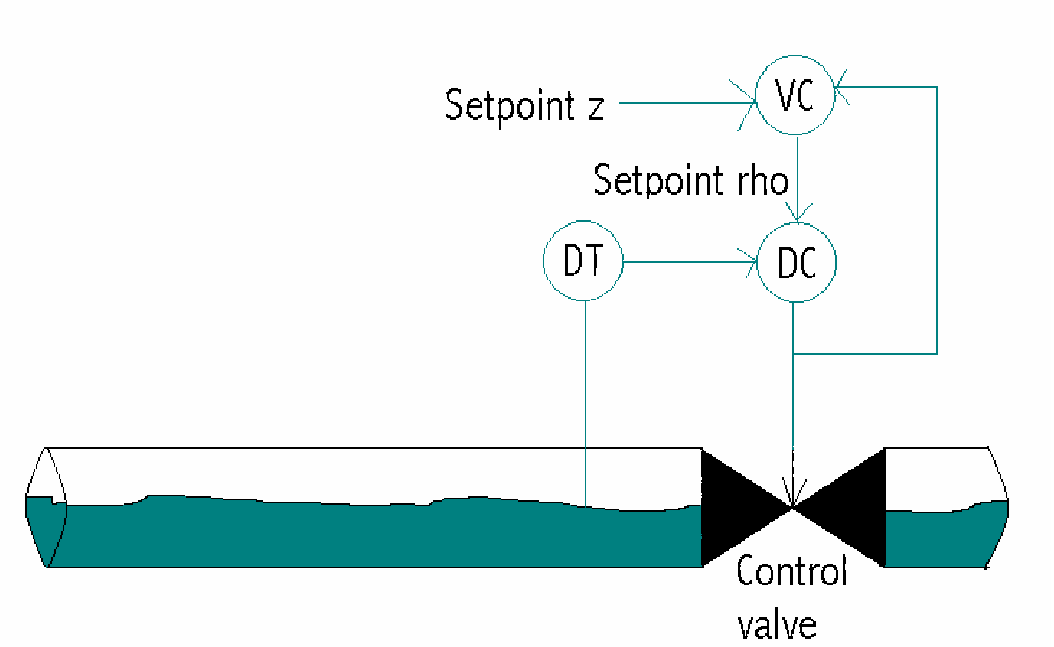

Figure 2.15: Cascade controller using measurements density ρ and valve opening z

The results from simulations using this control structure are plotted in Figure 2.16. The set point for the outer loop controller, controlling the valve opening, is increased from 17% to 18% after approximately 170 min. The flow then quickly becomes unstable, even though the valve opening is just inside the unstable region. Thus, there seems to be little benefit of the cascade as the results using this controller are approximately the same as when using the PI controller with density ρ.

Using one of the other measurements F_Q, F_W or P_1, in the inner loop instead might give better results as this measurement stabilizes the flow better than the density measurement ρ.

2.3 Experimental results

An attempt was made on controlling the flow using the fiber optic signal as measurement in the inner loop. The reason why flow measurements were not included in the experiments was because no direct measurements were available. One alternative would be to calculate the flow using the topside pressure measurement P_2, fiber optic signals S_1 and S_2 and the valve opening z. However, two-phase flow valve equations are empirical and also quite complicated, so it is reasonable to first use directly the measurements at hand.

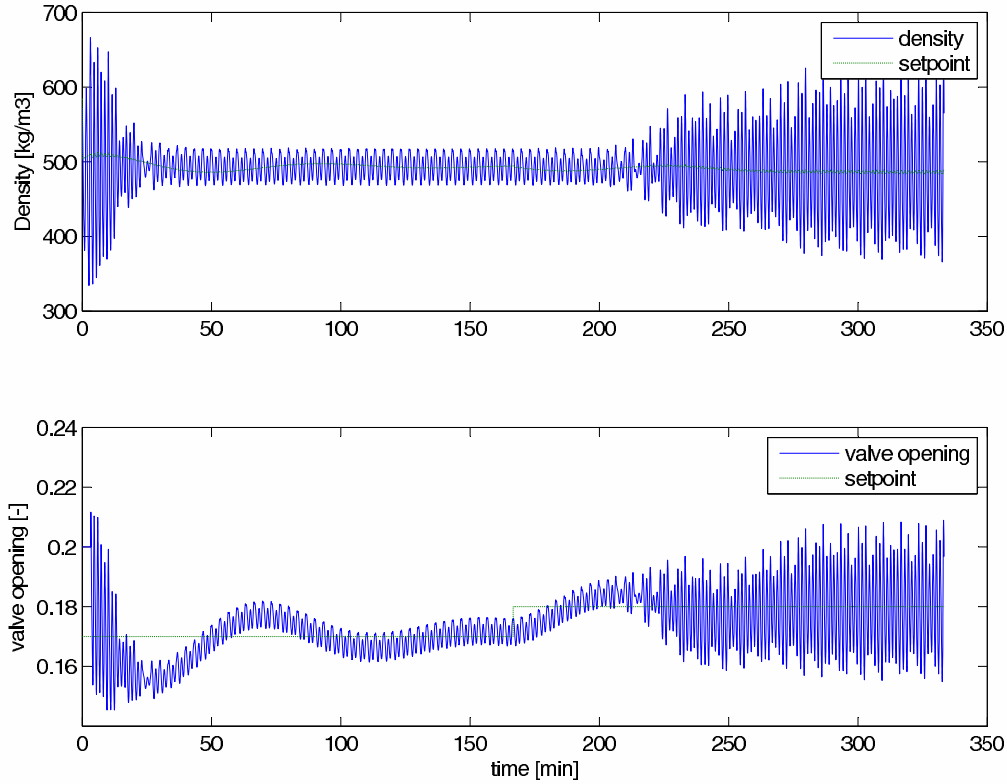

Figure 2.16: Simulation results using density ρ (inner loop) and valve opening z (outer cascade) as measured variables in a cascade control structure

Three different combinations of measurements were tested in a cascade control structure. In case (a), the inner controller controls the inlet pressure P_1 and the outer loop controls the valve opening z. Even though P_1 is not a topside measurement, the results using this controller serve as a basis to compare the other two with. The other two control structures use the fiber optic signal in the inner loop, and had either (b) the valve opening z or (c) the topside pressure P_2 as a measurement in the outer loop.

The experimental results in Figure 2.17 shows that stabilizing control was achieved for all three cases. First the system was left open-loop with a valve opening of 25%. Since this is well inside the unstable area, the pressures and density in the system is oscillating. After about 100s the controllers are activated, and in all three cases the controllers are able to control the flow. When the controllers are turned off after 500-600s, the flow quickly becomes unstable again. The thick lines indicated the set points for the different controllers. In plot a) and b) in Figure 2.17 the valve opening set point for the outer loop was 25% fully open, whereas for the experiment presented in plot c) the set point for the topside pressure P_2 in the outer loop was 0.056. Earlier experiments had shown that this lead to an average valve opening of about 25%.

From the analysis and simulations presented in Section 2.2, it is expected that the control

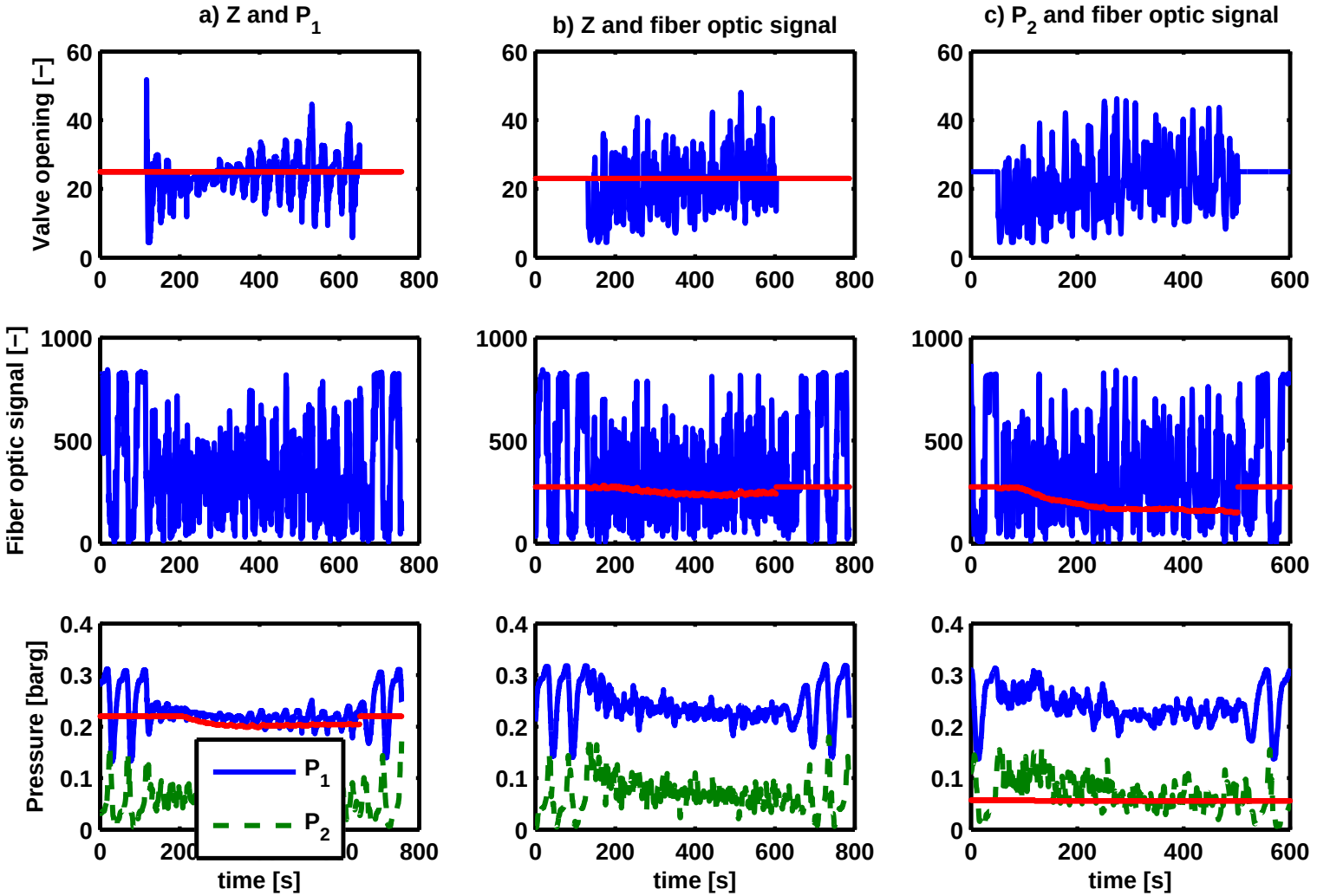

Figure 2.17: Experimental cascade control at a valve opening of approximately 25% using three control structures; (a) P_1 (inner loop) and z (outer) (b) Fiber optic signal (inner loop) and z (outer) (c) Fiber optic signal (inner loop) and P_2 (outer)

structure with the inlet pressure P_1 in the inner loop would perform best, as this measurement was by far the best suited for controlling the flow as seen both from simulations and control limitations for each measurement candidate. Also, the fiber optic signal at the laboratory is extremely noisy as the plots in Figure 2.17 show. Despite this, when looking at the experimental results, the differences are less obvious. In fact, using the fiber optic signal as the inner measurement works quite well, contradicting the results from the analysis in Section 2.2.

The main reason for adding the outer loop is to avoid drift in the inner loop caused by the low steady state gain shown in Tables 2.2 and 2.3. Since the results from the experiments using a cascade configuration by far outperform the results from the simulations, it was reason to question the values given by the model. This is why an attempt was made to see whether it was possible to control the flow using the fiber optic signal as *only* measurement for control. Figure 2.18 shows the results using this PI controller and the fiber optic measurement.

Also now the controller manages to stabilize the system. The system does not seem to drift, which means that the steady state gain from valve position to density is not too small for stabilizing the flow. Controlling the system at a larger average valve opening led to reduced performance and the flow either became unstable or the controller did not manage to satisfactory keep the measurements at the desired set points (large fluctuations).

In general, as the analysis showed, the control task gets harder as the valve opening increases. This is due to the fact that the gain is reduced as the valve opening increases. By gradually increasing the average valve opening, either by increasing the set point for valve opening in the outer loop or, for case c) in Figure 2.17, reducing the set point for the fiber optic measurement, the effect of this increase in valve opening was seen.

Some results are plotted in Appendix A for the three cascade structures a), b) and c) in Figure 2.17. Here it is seen that the effect of increasing the average valve opening from approximately 24% to 32% using P_1 as the inner measurement leads to increasingly larger fluctuations around the set points. The same experiments were performed using the fiber optic signal as measurement in the inner loop with b) z and c) P_2 in the outer loop. As expected, the system eventually goes unstable as the valve opening is increased. The average valve opening for which the system goes unstable using these controllers were approximately b) 26% and c) 29%.

2.4 Discussion

When comparing different controllers, the tuning of the parameters has a high influence on the results. None of the controllers described in these experiments have been fine-tuned and the results might be improved further with some more work. This is why the maximum average valve opening for which the controllers stabilize the flow, presented in Section 2.3, might be increased with proper tuning. However, from the results it seems obvious that all three controllers perform well up to approximately 25% valve opening and that as the valve opening moves towards an average value of 30% the controller performance decreases for all the controllers.

The timing for when the controller was activated seemed to have an effect in how quickly

the controller managed to control the flow. Activating the controller at a pressure peak in the system was most advantageous.

It is important to note that the model used for the analysis is a very simplified model. It was used merely as a tool to see which problems might occur in the lab, and the underlying reasons for the problems. When comparing the experimental results with analysis and simulations using Storkaas' model prior to the experiments, it was clear that the experimental results were far better in terms of stabilization than the model predicted when using the density/fiber optic signal as measurement.

An attempt was made to model the small-scale rig using multiphase simulator OLGA

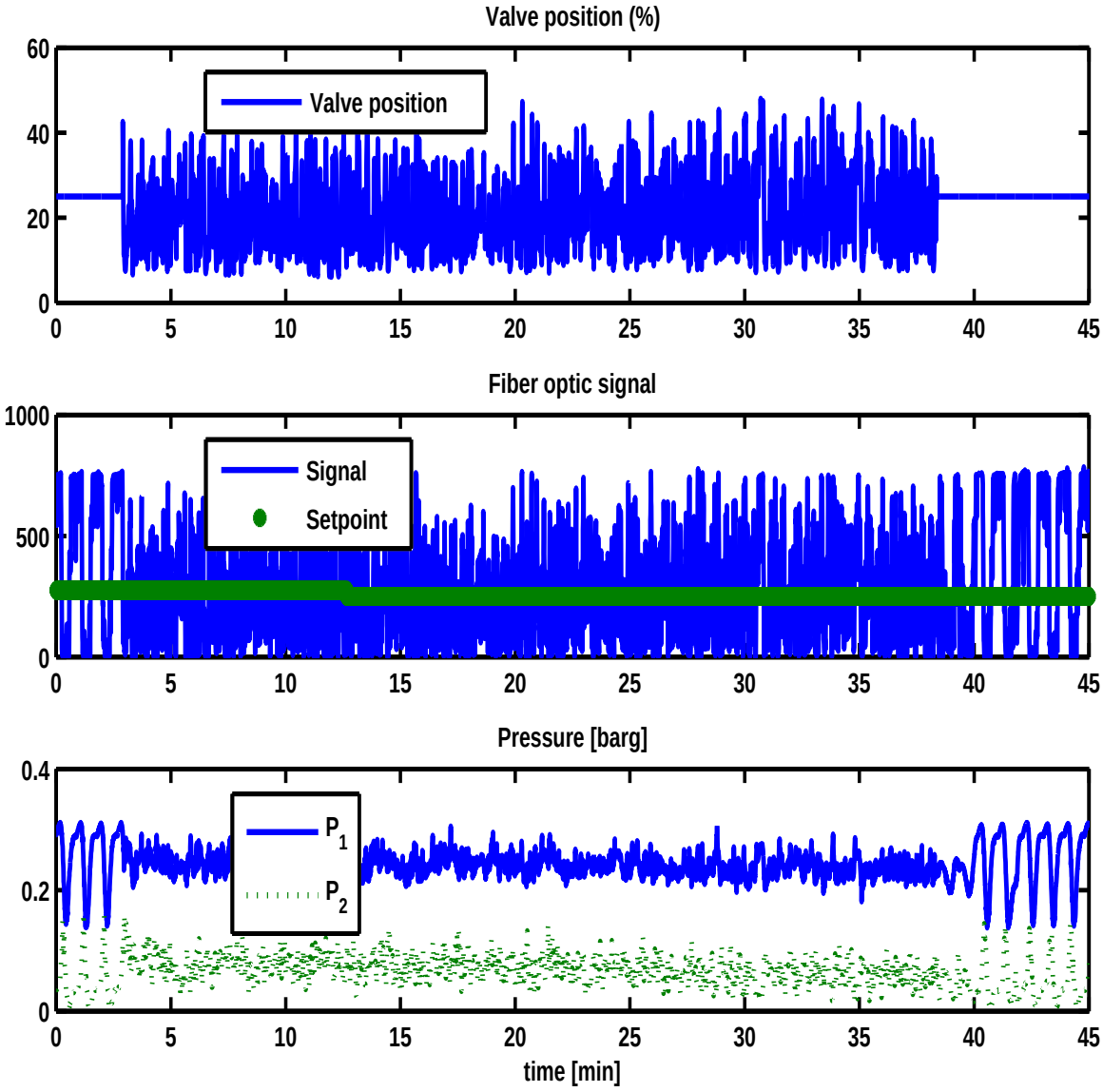

Figure 2.18: Experimental results using a PI controller with fiber optic signal as single measurement (no outer loop added)

from Scandpower Petroleum Technologies. However, the simulations seemed to fail due to numerical errors, which could be caused by the small scale nature of the rig.

Even though results using only a PI controller and a single topside fiber optic measurement seemed to work very well, without the expected steady state drift, there are other advantages in adding an outer loop. One example of such is that it may be more intuitive to understand what is going on with the plant when adjusting the set point for the valve opening rather than the set point for the topside density or flow rates.

The experiments were conducted on a small-scale rig with only 20mm inner diameter pipeline. Whether or not the results can be directly applied to larger test facilities is further investigated in Section 3.

2.5 Conclusion

This section of the thesis presents results from a small-scale riser laboratory rig where the aim was to control the flow using only topside measurements and thereby avoiding slug flow in the pipeline.

The results were good in the sense that it was possible to control the flow with good performance far into the unstable region. In order to avoid the slug merely by choking the topside valve it would be necessary to operate with a valve opening of 15%, whereas by using automatic control it was possible to control the flow with an average valve opening of 25%, despite very noisy measurements. This makes it possible to produce with a larger production rate and increase the total recovery from the producing oil field.

Chapter 3

Anti-slug control applied to a medium-scale rig

In Section 2, results from a small-scale lab rig build at the Department of Chemical Engineering, NTNU showed that, despite noisy measurements, it is still possible to stabilize the flow in an unstable area using only topside measurements. The question to be answered now is; do these results also apply for larger riser-systems?

In this section, we look at some results obtained from a 10m high, 3" diameter *medium*-scale test rig located at StatoilHydro's Research Center in Porsgrunn, Norway. Several cascade control structures are tested and compared; both with each other and the results obtained from the small-scale NTNU loop. The rig was also modeled and analysed using the simple three-state model described in Section 2.

The new experiments were successful and confirmed the results achieved using the small-scale rig. This suggests that the small-scale lab loop can be used as a tool to predict possible useful control strategies for the riser slug problem. A paper with the results from this section is in the process of being published (Sivertsen, Alstad and Skogestad (2008)).

3.1 Experimental setup

During the experiments the flow consisted of water and air. The pipe diameter is 3" (7.6 cm) and the height of the riser is approximately 10 m. The inflow rates of gas and water is pressure dependent. Water inlet rate during the experiments was 7-8 m^3/h while the air inflow rate fluctuated between 8 to 11 m^3/h. Figure 3.1 show a schematic overview of the layout and available instrumentation.

The loop includes an approximately 4 m long section where gas, oil and water are introduced through different inlets. This "well section" consists of annulus and tubing, a 15.2 cm outer pipe and a 7.6 cm inner tubing with perforations.

The pipe section consist partly of flexible tubing, hence it is possibly to vary the geometry of the piping. This way the inclination of the riser and other parts of the pipe can be adjusted to achieve the desired geometry.

The pipeline geometry during the experiments was chosen to give terrain-induced slug-

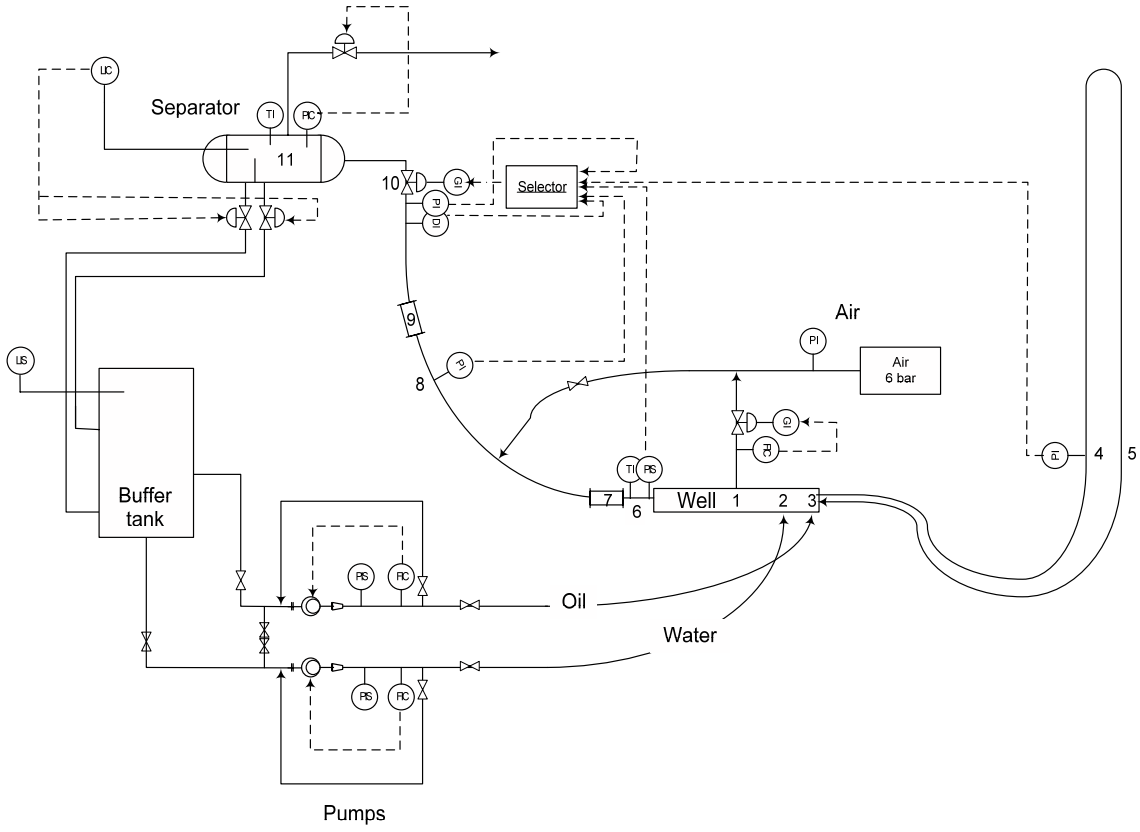

Figure 3.1: Schematic overview of the layout and available instrumentation

ging. A more detailed schematic of the geometry used in the experiments is shown in Figure 3.2. The numbers indicate the location of feeding inlets and important instrumentation.

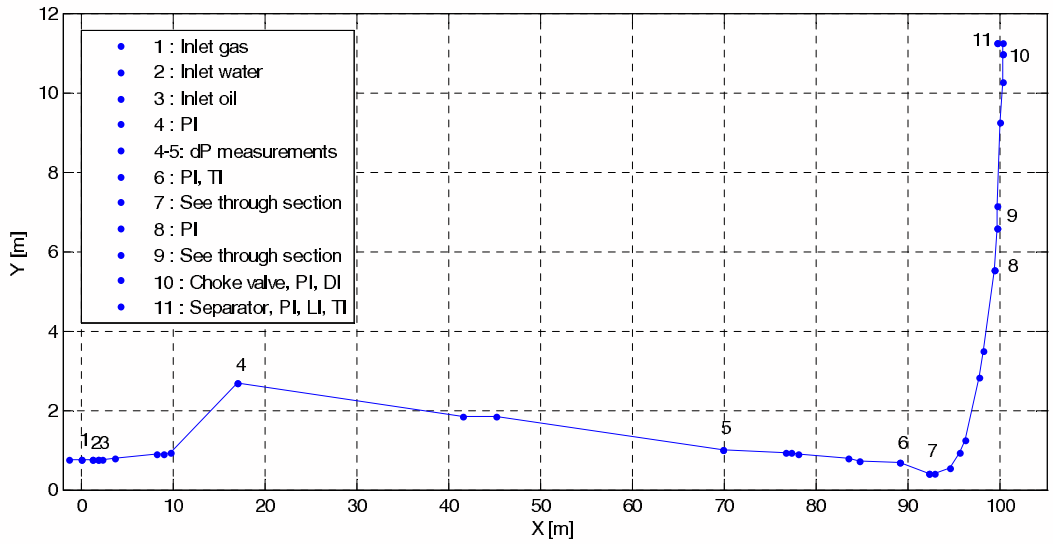

Figure 3.2: Schematic of the geometry of the riser-system

The numbers 1, 2 and 3 indicate the air, water and oil inlets respectively. Downstream this section the pipeline is close to horizontal for about 10 m. An approximately 7 m, 35° inclined section then follows. A pressure measurement (P_1) is implemented at the end of this section (4). The next 60 m section has a 1.8° declination, followed by an approximately 20 m horizontal section with a pressure and temperature measurement at the end (6). A 10 m long vertical riser then follows a low point in the geometry (7). The low-point contains a see-trough section, which makes it possible to determine visually the flow regime in this section. At the top of the riser, a production choke (10) and separator (11) are located. There is also a pressure measurement (8) and a see-through section (9) located half-way up the riser. Upstream the production choke a pressure measurement (P_2) and a gamma densiometer are implemented.

The water and oil outlets from the separator are returned to a large 10 m^3 buffer tank. The oil and water feed are pumped from this buffer tank back to the respective phase inlets in the well section using two displacement pumps. Before entering the well section, the feed flow rate and density of each phase are measured.

3.1.1 Gas feed

The compressed air is supplied from the local air supply net. The supplied air holds a pressure of approximately 7 bara. An automatic control valve controls the feed flow rate of compressed air to the well section. During experiments the feed flow of air is normally in the range 15 to 50 kg/h.

The mass flow and the density of the compressed air are measured using a Coriolis type mass flow meter.

3.1.2 Water feed

A displacement pump controls the feed flow rate of water. The power is either set directly by the operator, or given as output from a feedback controller using the volumetric flow rate as measurement. The pressure and single-phase flow rates are measured downstream the pumps, using a differential pressure volumetric flow meter (Pivot tube) for the air and a Coriolis type mass flow for the water.

3.1.3 Separator

The three-phase separator located at the top of the riser has a volume of approximately 1.5 m^3. A 53 cm high weir plate separates the oil and water outlets. The separator is equipped with a pressure measurement and measurements of the oil and water levels. No oil was added to the flow during the experiments presented in this thesis.

3.1.4 Control choke valve

The control choke valve is a vertically positioned valve located at the top of the riser. The valve is equipped with a Profibus-PA Positioner, which returns the actual valve position to the control system.

Choke valve characteristics

Several flow experiments had been performed in order to find the single- and two-phase (water/air) valve characteristics:

$$Q = \overbrace{C_v f(z)}^{K(z)} \sqrt{\frac{\Delta P}{\rho}} \tag{3.1}$$

C_v is the valve constant and $f(z)$ is the characteristics of the valve. ΔP is the pressure drop across the valve and ρ is the density of the fluid. For valve openings less than 50% and 60% for single-phase and two-phase flow respectively, the characteristics were found to be close to linear. Thus, Equation (3.1) can be written

$$Q/C_v = z\sqrt{\frac{\Delta P}{\rho}} \tag{3.2}$$

Values for Q/C_v can be calculated from given values for valve opening z, measured pressure drop across the valve ΔP and measured density ρ.

3.1.5 Instrumentation

A number of automatic control valves are installed. This includes the production choke valve, the valves controlling gas, water and oil outlet from the separator and the feed flow of air to the well section. These valves can be operated either in manual mode or in automatic mode where valve openings are given as output from PID feedback controllers. The rig is controlled from a control room located close to the rig.

3.2 Controllability analysis

3.2.1 Modelling

In Section 2, it was shown how an analysis of a model describing a *small*-scale lab-rig did reveal fundamental control limitations depending on which measurements that were used for control. This was found using a simplified model (Storkaas et al. (2003)). One of the advantages of this simple model is that it is well suited for controller design and analysis. It consists of three states; the holdup of gas in the feed section (m_{G1}) and in the riser (m_{G2}), and the holdup of liquid (m_L). The model is illustrated in Figure 2.5.

The same model was used to predict the behavior for the medium-scale lab rig used in this study. Using this model the system was analysed in the same way as in Section 2. Both open- and closed loop simulations were performed.

Table 3.1: Model data parameters

Parameter	Symbol	Value
Inlet flow rate gas [kg/s]	$w_{G,in}$	0.0075
Inlet flow rate water [kg/s]	$w_{L,in}$	1.644
Valve opening at bifurction point [-]	z	0.12
Inlet pressure at bifurcation point [$barg$]	$P_{1,stasj}$	0.9
Topside pressure at bifurcation point [$barg$]	$P_{2,stasj}$	0.3
Separator pressure [$barg$]	P_0	0
Liquid level upstream low point at bifurcation point [m]	$h_{1,stasj}$	0.05
Upstream gas volume [m^3]	V_{G1}	0.2654
Feed pipe inclination [rad]	θ	0.05
Riser height [m]	H_2	10
Length of horizontal top section [m]	L_3	0.1
Pipe radius [m]	r	0.0381
Exponent in friction expression [-]	n	2.15
Choke valve constant [m^{-2}]	K_1	0.0042
Internal gas flow constant [-]	K_2	1.83
Friction parameter [s^2/m^2]	K_3	72.37

After entering the geometrical and flow data for the lab rig, the model was tuned as described in Storkaas et al. (2003) to fit the open loop behavior of the lab rig. The model data and tuning parameters are presented in Table 3.1. After inserting new system parameters

and re-tuning the model, the open-loop data found using the model fitted the experimental results quite well as shown by the bifurcation plot in Figure 3.3.

The bifurcation diagram gives information about the valve opening for which the flow becomes unstable and shows the amplitude of the pressure oscillations for the inlet and topside pressures (P_1 and P_2). The upper lines in the bifurcation plot show the maximum pressure at a particular valve opening and the lower line shows the minimum pressure. The lines meet at the "bifurcation point" when the valve opening is approximately 12%. This is the point where transition to slug flow occurs naturally and this is the highest valve opening which gives "non-slug" behaviour in open-loop operation, without control. The dotted line in the middle shows the unstable "non-slug" solution predicted by the model. This is the desired operating line with closed-loop operation.

The bifurcation plot was obtained by open-loop simulations of the system at different valve openings. Some of these results are plotted in Figure 3.4 together with experimental results. The model fit the experimental data quite well, in terms of both amplitude and frequency of the oscillations. Note that a shift in time does not matter. The match between simulated and experimental results is especially very good for a valve opening of 14.9%.

In Figure 3.5 a root-locus diagram of the system is plotted. This shows how the poles, computed eigenvalues from the model, cross into the RHP as the valve opening reaches 12% from below. This confirms what was seen in the bifurcation diagram.

3.2.2 Analysis

The model can now be used to explore different measurement alternatives for controlling the flow. The following measurements were analysed in this study; inlet pressure P_1, pressure upstream production choke P_2, density ρ, mass flow rate F_W and volumetric flow rate F_Q through the topside choke. Figure 2.9 shows the different measurement candidates.

In Section 2 it was shown how the RHP poles and zeros and their locations compared to each other in the imaginary plane had a large influence on the controllability of the system. By scaling the system and calculating the sensitivity peaks, it is possible to get a picture of the challenges in terms of stabilizing the system.

The process model G and disturbance model G_d were found by linearizing Storkaas' model at two operation points (z = 0.15 and z = 0.2). The process variables were scaled with respect to the largest allowed control error and the disturbances were scaled with the largest variations in the inlet flow rates in the lab, as described in Skogestad and Postlethwaite (1996). The disturbances were assumed to be frequency independent. The input was scaled with the maximum allowed positive deviation in valve opening since the process gain is smaller for large valve openings. For measurements y=[P_1 P_2 ρ F_W F_Q], the scaling matrix is De=diag[0.1bar 0.1bar 50kg/m^3 0.2kg/s $1e^{-3}m^3/s$]. The scaling matrix for the disturbances d=[m_G and m_L] is Dd= diag [$2e^{-3}$kg/s 0.2kg/s]. The nominal values are 0.0075 kg/s for the gas and 1.64 kg/s for the water rate. The input is scaled $Du = 1 - z_{nom}$ where z_{nom} is the nominal valve opening.

Tables 3.2 and 3.3 summarize the results of the analysis. The locations of the RHP poles and zeros are presented for valve openings 15 and 20%, as well as stationary gain and lower bounds on the closed-loop transfer functions described Section 2. The pole location

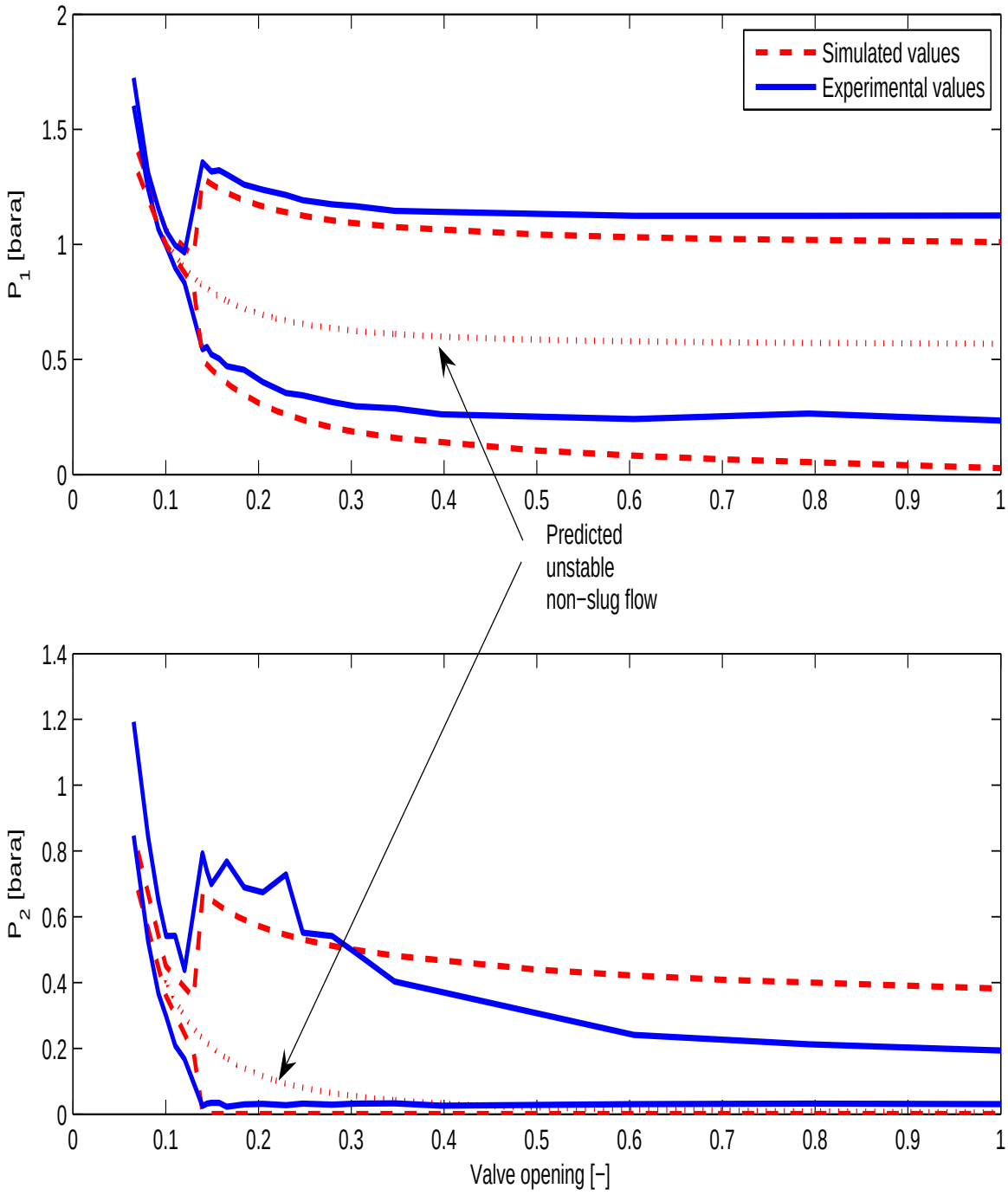

Figure 3.3: Bifurcation plot for the medium scale rig: Pressures at inlet (P_1) and topside (P_2) as function of choke valve opening z

is independent of the input and output (measurement), but the zeros may move. From the bifurcation plot in Figure 3.3, it is seen that both of these valve openings are inside the unstable area. This can also be seen from the RHP location of the poles.

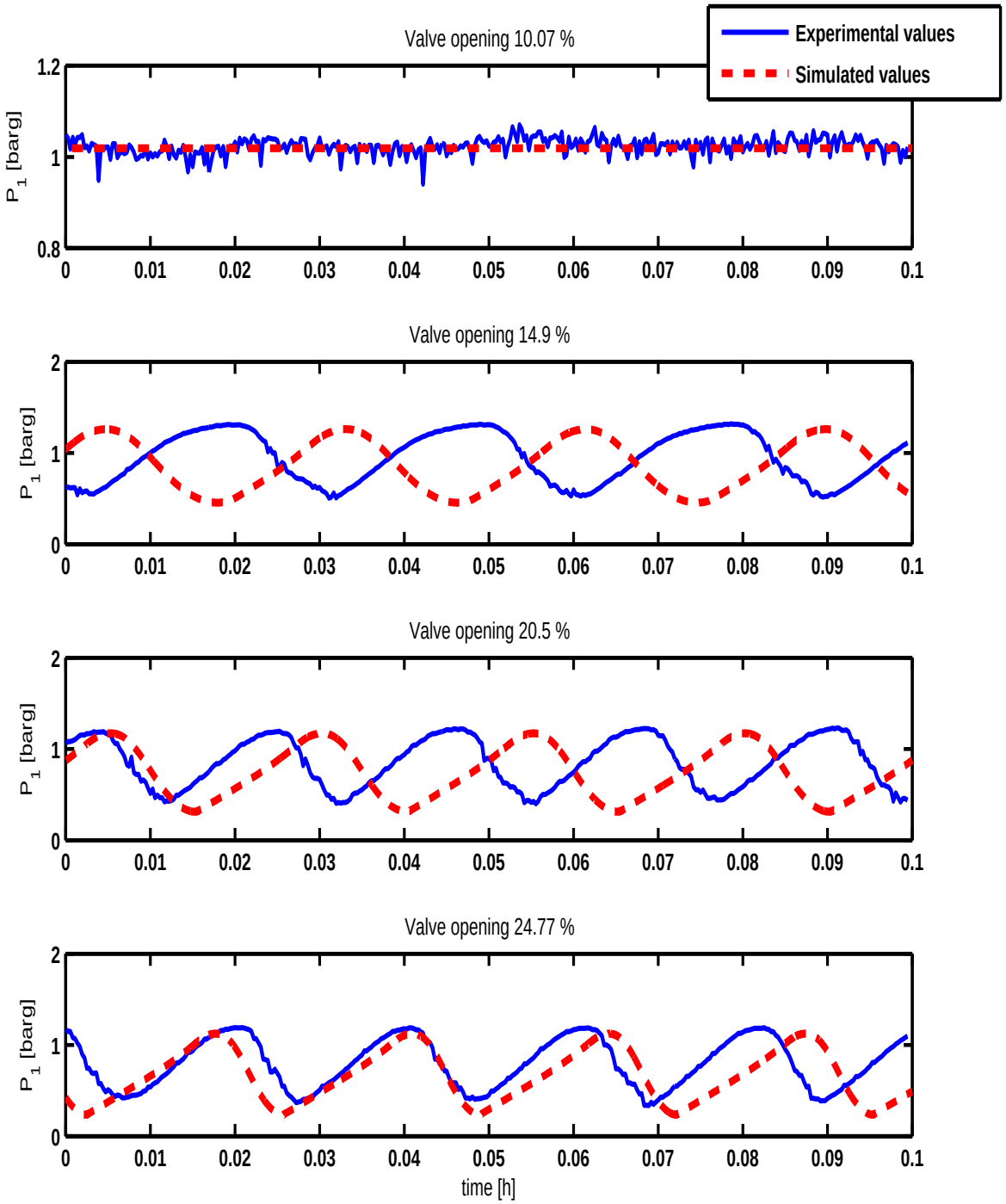

Figure 3.4: Open loop data for valve openings 10, 15, 20 and 25%.

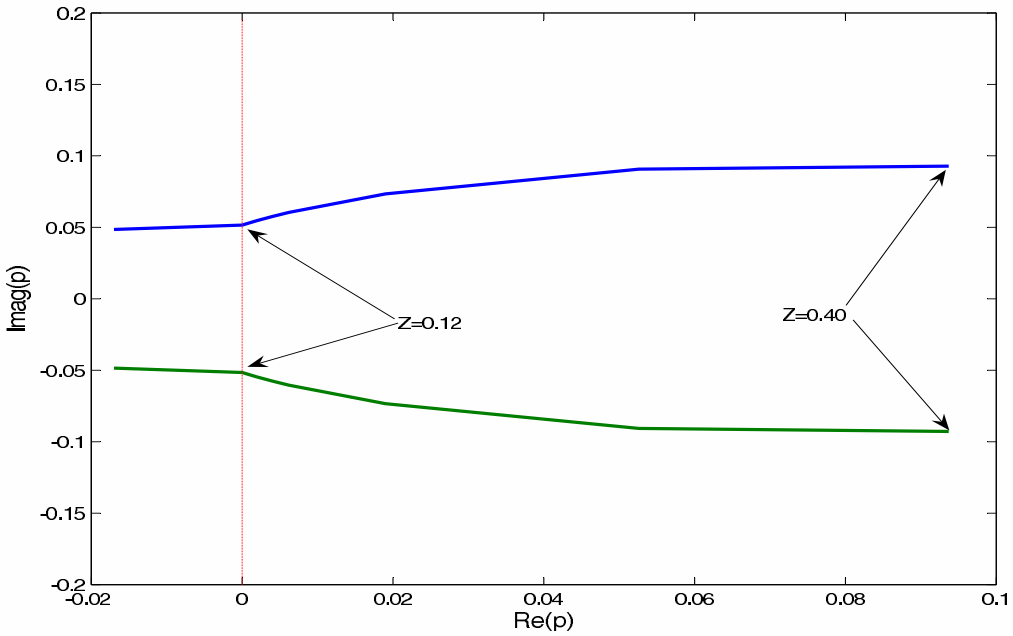

Figure 3.5: Root-locus plot showing the trajectories of the RHP open-loop poles when the valve opening varies from 0 (closed) to 0.4

The only two measurements of the ones considered in this analysis which introduces RHP-zeros into the system, are the topside density ρ and pressure P_2. The RHP zeros are in both cases located quite close to the RHP poles, which results in the high peaks especially for sensitivity function SG but also for S. In Figure 3.6 the RHP poles and relevant RHP zeros are plotted together. This plot shows that we can expect problems when trying to stabilize the flow using these measurements as controlled variables.

The model is based on constant inlet flow rates. The stationary gain for F_W predicted by the model is 0, which means that it is not possible to control the steady-state behavior of the system and the system will drift. Usually the inlet rates are pressure dependent, and the zeros for measurements F_Q and F_W would be expected to be located further away from the origin than indicated by Tables 3.2 and 3.3.

Figure 3.7 and 3.8 shows the Bode plots for the different plant models and disturbance models respectively. The models were found from a linearization of the model around valve opening 15%. As in Section 2, the Bode plots show that for the mass flow rate measurement F_W, the low frequency value of the disturbance model $|G_dW|$ is higher than plant model $|GW|$. For acceptable control we require $|G(jw)| > |G_d(jw)| - 1$ for frequencies where $|G_d| > 1$ (Skogestad and Postlethwaite (1996)). In this case $|G_d(0)|$ is 1.01 and G_W is close to zero, which means problems can occur for this measurement.

Table 3.2: Control limitation data for valve opening 15%. Unstable poles at $p = 0.0062 \pm 0.060i$.

Measurement	RHP zeros	Stationary gain	Minimum bounds				
		$\|G(0)\|$	$\|S\|$	$\|SG\|$	$\|KS\|$	$\|SG_d\|$	$\|KSG_d\|$
$P_1[bar]$	-	22.9	1.00	0.00	0.016	0.00	0.042
$P_2[bar]$	1.00, 0.09	20.5	1.21	15.6	0.017	0.54	0.040
$\rho[kg/m^3]$	0.051	33.1	1.22	33.4	0.011	1.02	0.042
$F_W[kg/s]$	-	0.00	1.00	0.00	0.006	0.00	0.042
$F_Q[m^3/s]$	-	8.3	1.00	0.00	0.013	1.02	0.040

Table 3.3: Control limitation data for valve opening 20%. Unstable poles at $p = 0.019 \pm 0.073i$

Measurement	RHP zeros	Stationary gain	Minimum bounds				
		$\|G(0)\|$	$\|S\|$	$\|SG\|$	$\|KS\|$	$\|SG_d\|$	$\|KSG_d\|$
$P_1[bar]$	-	10.1	1.00	0.00	0.082	0.00	0.090
$P_2[bar]$	1.08, 0.089	8.94	1.66	10.7	0.10	0.55	0.070
$\rho[kg/m^3]$	0.050	2.87	1.60	19.6	0.048	1.27	0.080
$F_W[kg/s]$	-	0.00	1.00	0.00	0.021	0.00	0.070
$F_Q[m^3/s]$	-	4.16	1.00	0.00	0.047	0.00	0.070

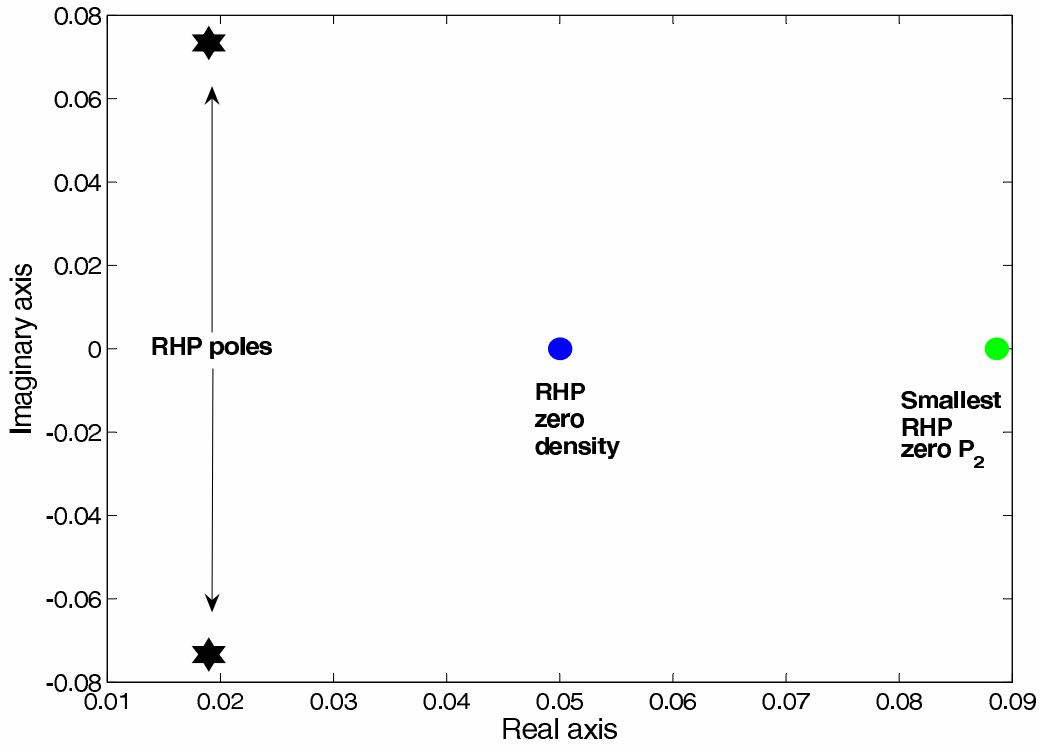

Figure 3.6: Plot-zero map for valve opening 20%

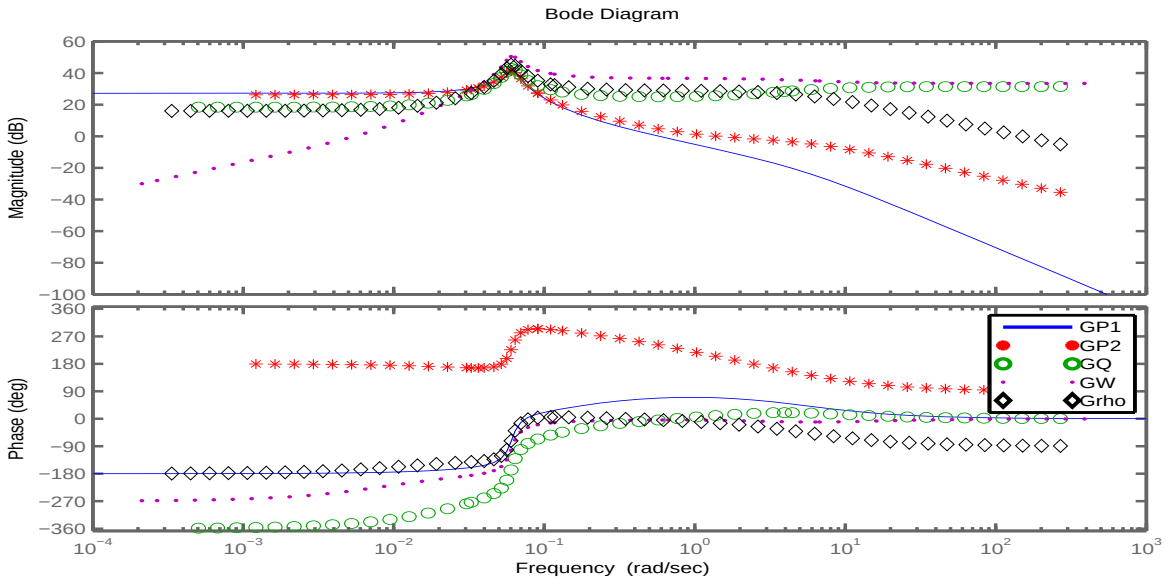

Figure 3.7: Bode plots for the plant models using different measurements

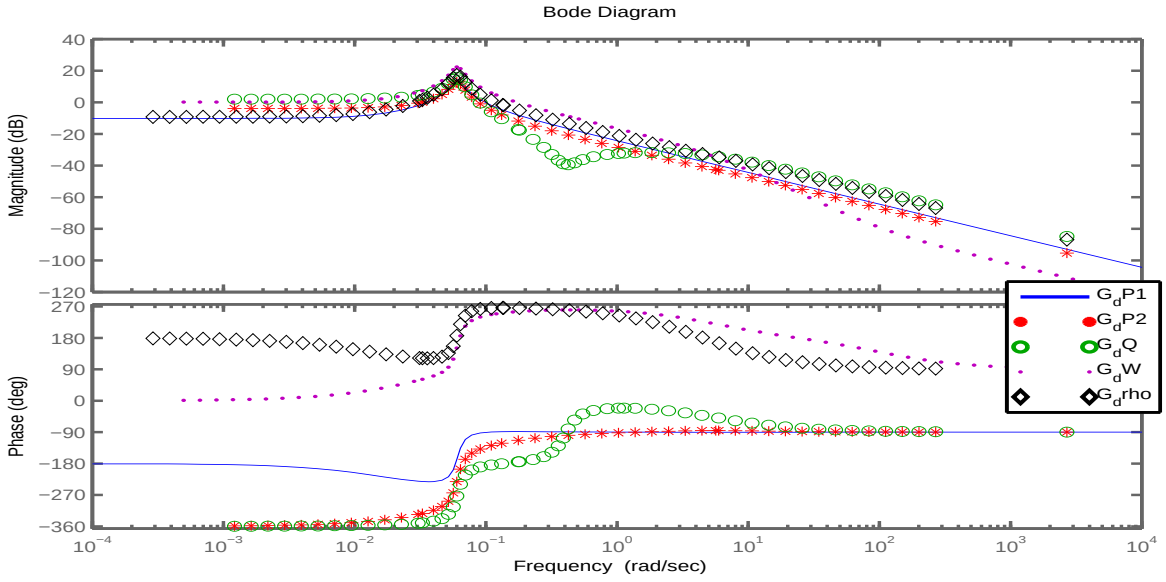

Figure 3.8: Bode plots for the disturbance models using different measurements

3.2.3 Simulations

Closed-loop simulations were performed in order to investigate the effect of the limitations found in the analysis. The measurements were used as single measurements in a feedback loop with a PI-controller. Figure 3.9 shows this control structure using the inlet pressure P_1 as measurement.

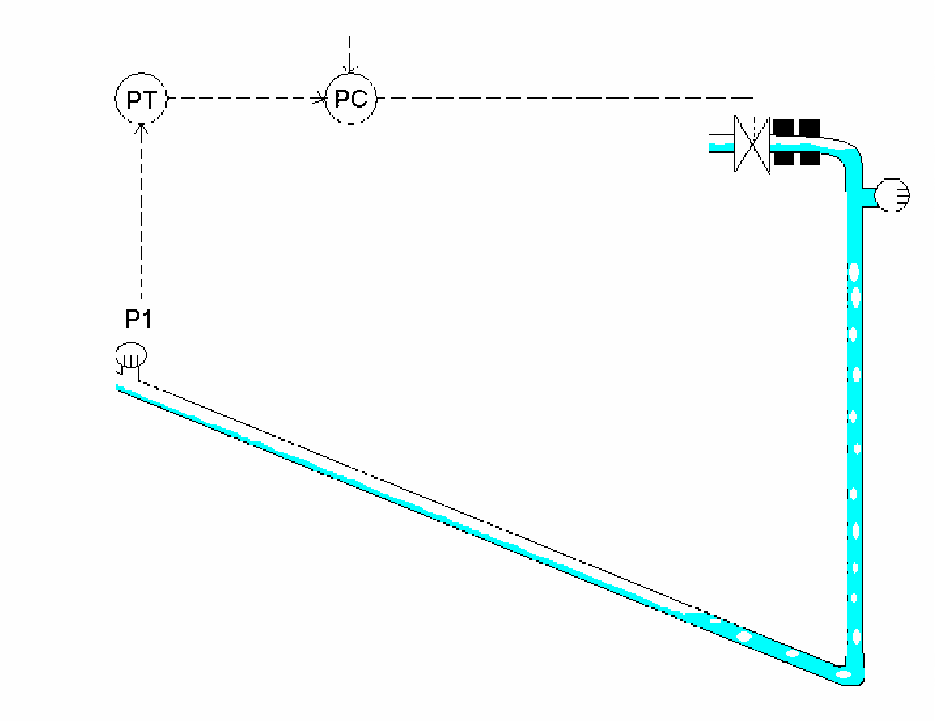

Figure 3.9: Feedback control using PI controller with inlet pressure P_1 as measurement

Figure 3.10 compares the simulation results obtained using four different measurement candidates. Disturbances in inlet flow rates for the gas and water are not included in the simulations. The results could for this reason differ somewhat from the results obtained in Section 2. Despite this, the results were quite similar. Results using the topside pressure P_2 are not included in the plot, as the corresponding controller was not able to stabilize the flow.

At first, the controllers are turned off and the system is left open loop for approximately three and a half minute with a valve opening of 20%. From the bifurcation diagram in Figure 3.3 it was shown that the system goes unstable for valve openings larger than 12%. As expected the system oscillates due to the presence of slug flow.

When the controllers are activated, the control valves start working as seen from the right plot in Figure 3.10. After about 80 minutes the set points are changed for all the controllers, bringing the flow further into the unstable region. The aim of the simulation study is to be able to control the flow with satisfactory performance as far into the unstable region as possible, which means with as high average valve opening as possible.

As in Section 2, the controllers giving the best results were the ones using inlet pressure P_1 and volumetric flow rate F_Q as measurements. However, this time the flow controller F_Q

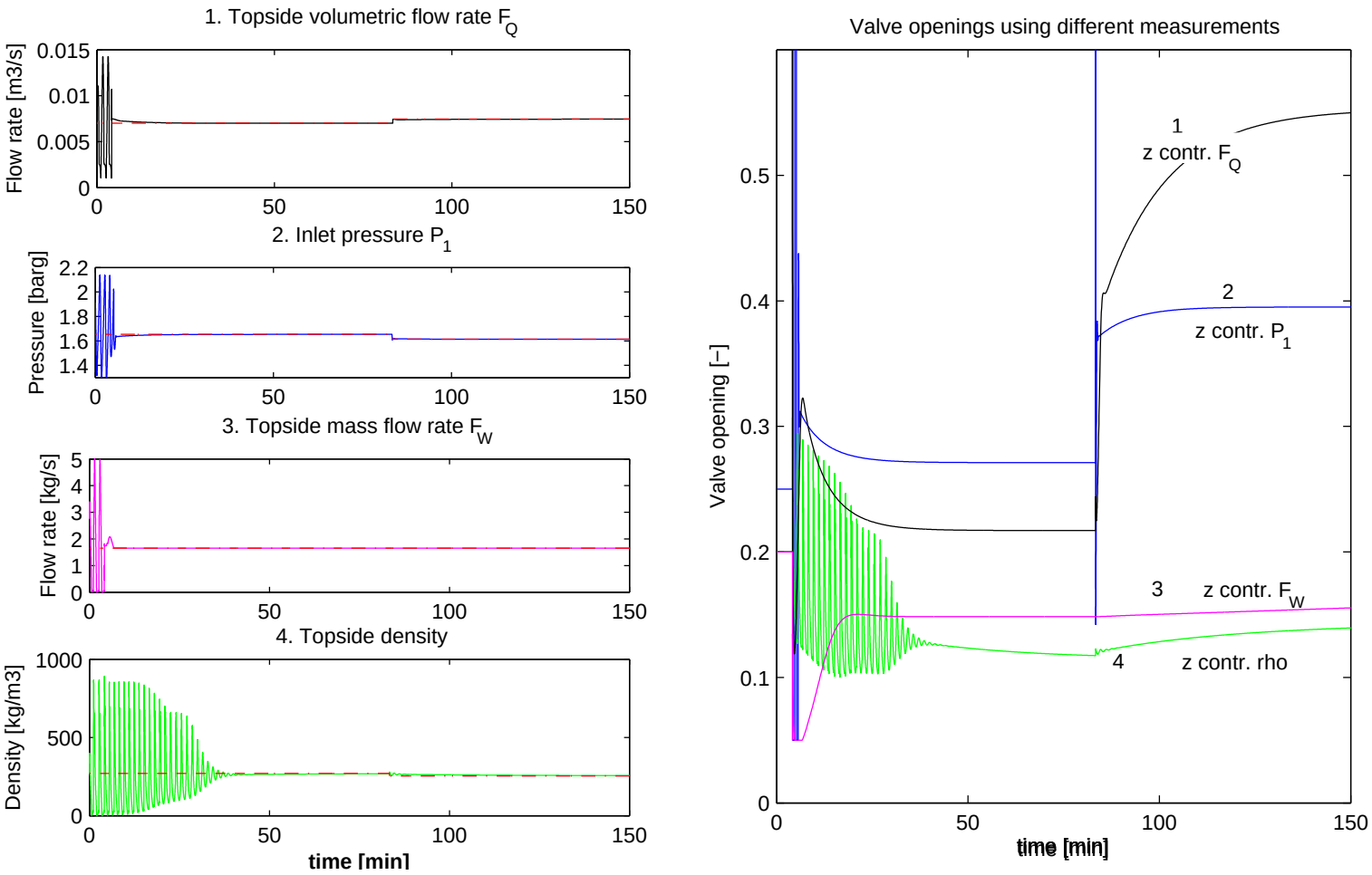

Figure 3.10: Stabilizing slug flow using the choke valve (z); PI control with four alternative measurements

outperformed the pressure controller, being able to stabilize the flow with an average valve opening of impressing 55%. Based on earlier knowledge of slug control and experimental results; these results are too good to be true, and might come from the fact that no disturbances in the inlet flow rates were added in the simulations this time.

The results using the density and mass flow controller were quite similar to those obtained for the small scale lab rig in Section 2. It was possible to control the flow in the unstable region, but the controllers were slow and did not manage to stabilize the flow very far into the unstable region.

3.3 Experimental results

The analysis in Section 3.2.2 showed that both the inlet pressure, P_1, and the scaled topside volumetric flow rate, F_Q, were suitable for stabilizing the flow. The results using the topside density ρ were not as good as for P_1 and F_Q, but still it was possible to control the flow using also this measurement.

Looking at Table 3.3 it is clear that except for the mass flow measurement F_W with zero steady-state gain, ρ is the measurement having the lowest steady-state gain at valve opening 20%. This explains why the controller does not seem to be able to keep the flow stable at the set point after the flow has been stabilized. Also for the volumetric flow rate measurement F_Q the steady-state gain is quite low for valve opening 20%. We might expect the same problems using this measurement as the single measurement.

Control configurations using combinations of measurements can improve the performance of a controller when compared to controllers using single measurements. In order to avoid the drift problem, different cascade controllers were tested experimentally. Six cascade controllers with different measurement combinations were tested;
(a) z (outer) and P_1 (inner)
(b) P_2 (outer) and P_1 (inner)
(c) z (outer) and ρ (inner)
(d) P_2 (outer) and ρ (inner)
(e) z (outer) and F_Q (inner)
(f) P_2 (outer) and F_Q (inner).

The measurements were combined in a cascade control configuration, where the set point for the inner controller is adjusted by the outer loop to prevent the inner controller from drifting. This way ρ and F_Q can be used as measurement in an inner loop, even though the controller based solely on one of these measurements suffer from the drift problem. The volumetric flow measurement used during the experiments was scaled with respect to the choke valve constant C_v.

Topside measurements are often noisy, and so also in this case. For this reason the density measurement signal was filtered using a first-order low-pass filter with a time constant of $4s$.

Additional experiments were performed using the inlet pressure P_1 as measurement for the inner loop. Although P_1 is not a topside measurement, and often not available in many real subsea applications, it was included to serve as a comparison for the other controllers. As outer measurements, the pressure drop across the control valve P_2 and topside choke

valve opening z were used.

Figure 3.11 shows a sketch of a cascade control structure for alternative (d) and Figures 3.12-3.14 shows the experimental results for all six alternatives. The left plot shows the results when valve opening z is used as outer loop measurement. In the right plot the topside pressure P_2 is used as outer measurement.

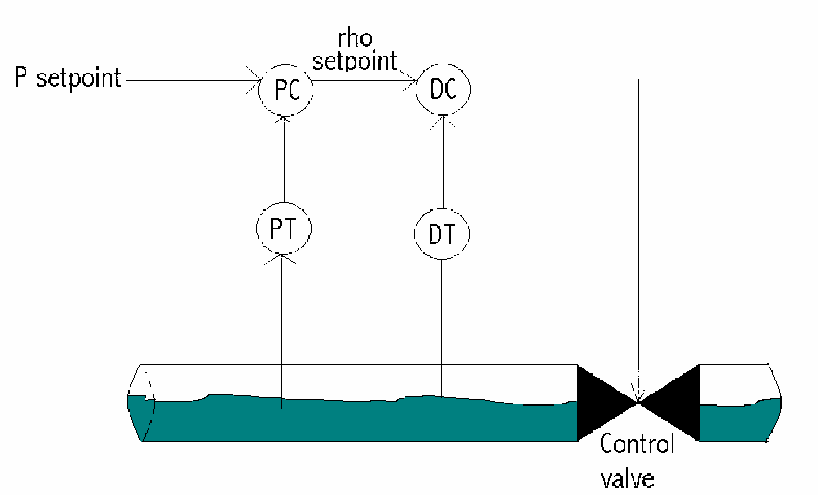

Figure 3.11: Cascade control with measurements density ρ (inner loop) and pressure drop across topside valve P_2 (outer loop)

During the experiments, the operation is gradually moved further into the unstable region by changing the set point in the outer loop (increasing z_S and decreasing $P_{2,S}$). The valve opening for which the flow can no longer be stabilized gives a measure on the performance of each controller. Note that being able to increase the mean valve opening and at the same time keep the flow stable has large economic advantages. This is because producing at a higher valve opening implies less friction loss and increased production.

The results using all of the controllers were very good, and they all managed to stabilize the flow far into the unstable region. The upper plot in each of the sub figures shows how the valve opening is increased during the experiments.

Table 3.4 compare the average values the last 12 min before the controllers go unstable. As mentioned, the mean valve opening gives a good indication of the quality of the controller. See also Figure B.1 in Appendix B which shows detailed plots for all the controllers the last 12 minutes before instability.

Based on the results, we conclude that using P_2 in the outer loop and either P_1 or F_Q in the inner loop is the best choice with average maximum valve openings 23.8% and 23.9% respectively. The third best choice is using z in the outer loop and F_Q in the inner loop (22.8%).

The controllers were not fine-tuned and the results might for this reason be influenced somewhat by the quality of the tuning. Still, the results showed that it was possible to stabi-

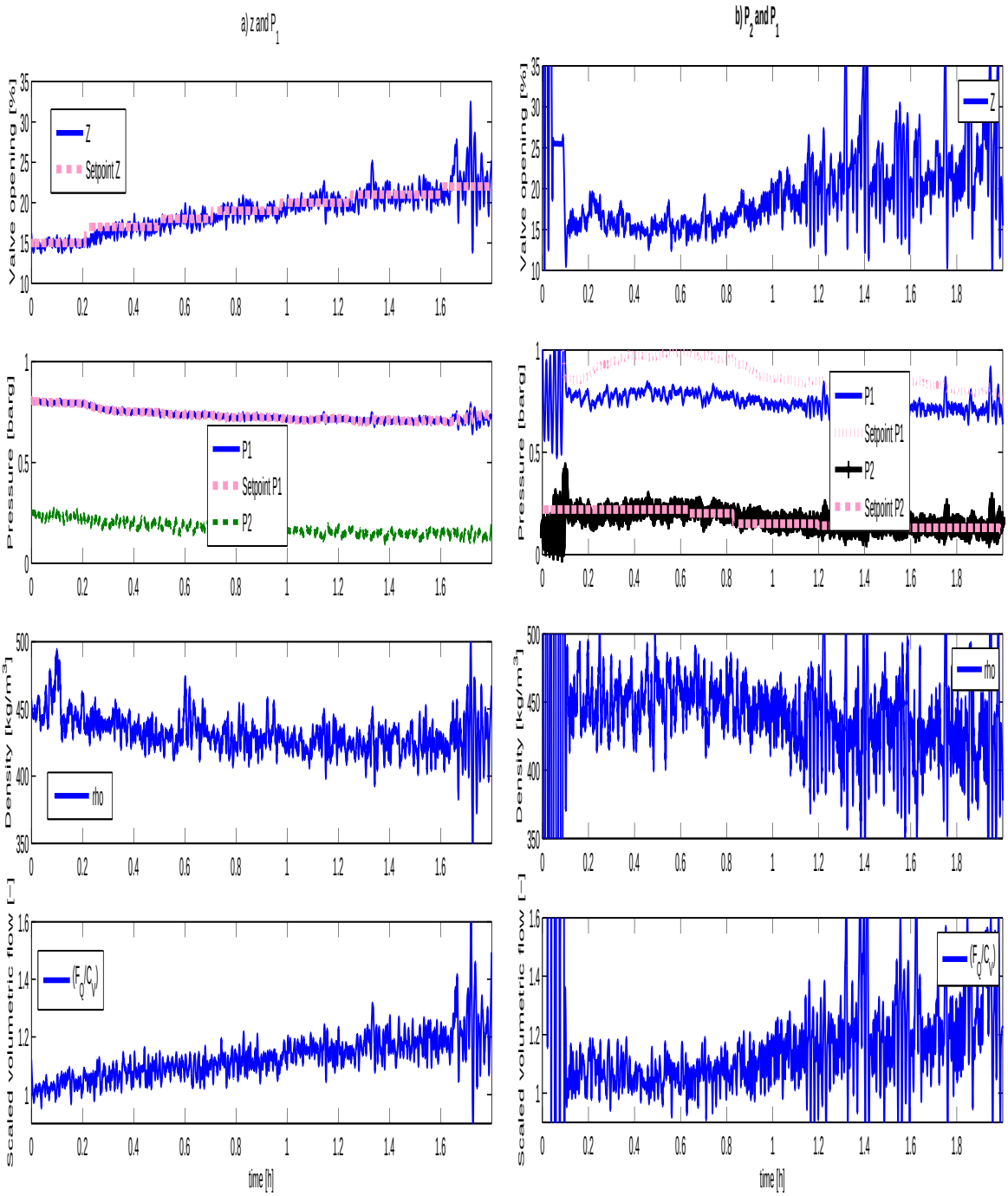

Figure 3.12: Experimental results using P_1 in the inner loop and a) z and b) P_2 in the outer loop

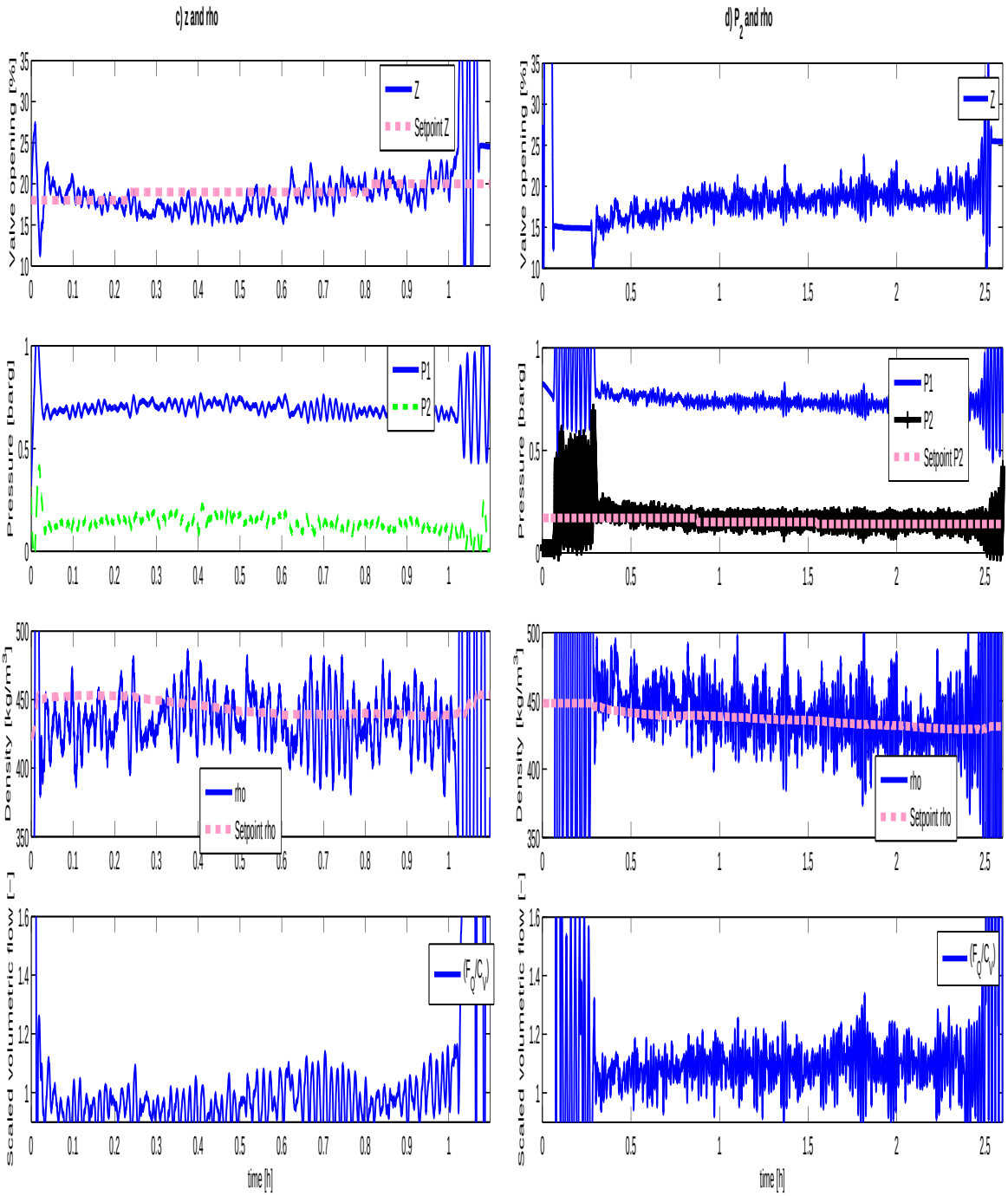

Figure 3.13: Experimental results using ρ in the inner loop and c) z and d) P_2 in the outer loop

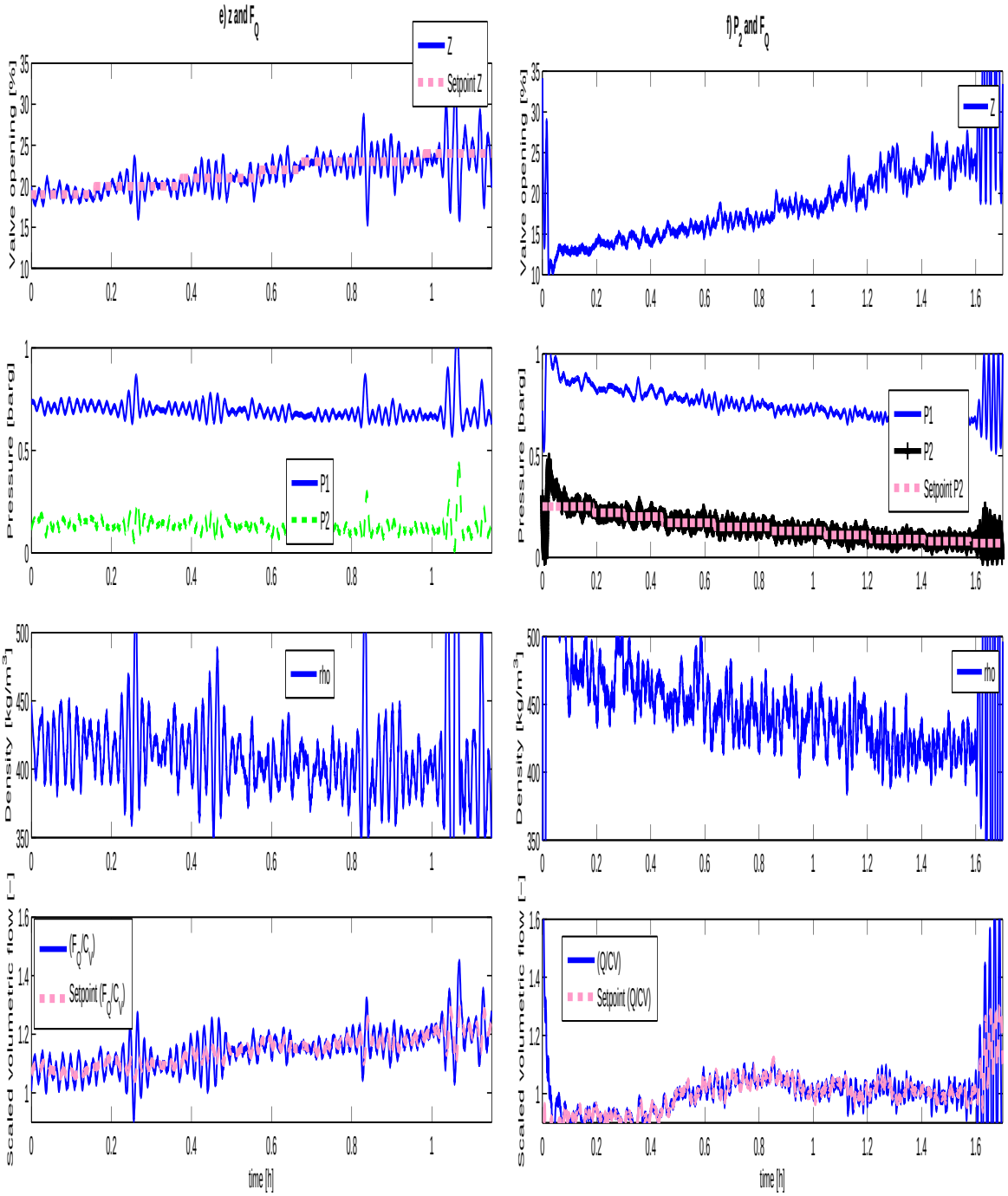

Figure 3.14: Experimental results using F_Q/C_v in the inner loop and e) z and f) P_2 in the outer loop

Table 3.4: Mean values just before instability using different cascade controllers, based on data plotted in Figure B.1 (Appendix B)

Outer loop	z			P_2		
Inner loop	P_1	ρ	F_Q/C_v	P_1	ρ	F_Q/C_v
$P_1[barg]$	0.71	0.68	0.68	0.72	0.72	0.67
$P_2[barg]$	0.146	0.123	0.119	0.132	0.142	0.079
$\rho[kg/m^3]$	425	433	403	424	433	417
$Q/C_v[-]$	1.18	0.98	1.18	1.28	1.0943	0.997
$z[\%]$	20.9	19.5	22.8	23.8	19.3	23.9
$F_w[kg/h]$	7.24	7.55	7.6	7.54	7.60	7.55
$F_Q[m^3/h]$	7.53	10.07	9.2	8.17	8.56	11.05
$Figure$	B.1(a)	B.1(b)	B.1(c)	B.1(d)	B.1(e)	B.1(f)

lize the flow very well using only topside measurements and that these results are comparable with the results found when including subsea measurement P_1 as one of the measurements.

3.4 Discussion

It is important to note that Storkaas' model used to analyze the system is a very simplified model, and it was used merely as a tool to see which problems might occur in the lab, and the underlying reasons for the problems. When comparing the experimental results with analysis and simulations using Storkaas' model prior to the experiments, it was clear that the experimental results were far better than the model predicted when using the density as measurement. The model is however not very detailed, and it is merely used as a tool to understand the underlying dynamics of the problem.

The pressure dependency of the inflow rates of gas and water was not included, and the effect of this dependency probably helps to stabilize the flow since the inlet rates are decreased as more water accumulates in the riser.

During the experiments the timing for when the controller is activated (where in the slug-cycle) was very important for the controller's ability to stabilize the flow. When the controller was activated just after the inlet pressure had peaked, the controller managed to stabilize the flow quite easily. If the controller was activated at some other time, usually the controller did not manage to stabilize the flow at all.

Also, the tuning of the controllers has a big influence on the results. Even better results might be achieved with other types of controllers or better tuning. This is also why it is not possible to make a clear recommendation of which combination of measurements is best. The study does however show that all the combinations tested in this study, stabilize the flow quite well.

3.5 Conclusion

This section has presented results from a medium-scale riser rig where the aim was to control the flow using only topside measurements. The results show that it was possible to stabilize the flow using different combinations of topside measurements. Table 3.4 shows the different controller results compared to each other. The best results were achieved with the scaled volumetric flow rate F_Q/C_v as the inner measurement, although this result may be dependent on the tuning of the controllers. All of the controllers managed to stabilize the flow well, increasing the maximum valve opening from 12% without control to more than 20% with control.

When comparing the results with similar experiments performed on a small-scale riser rig build at our department, Section 2, the results using different control configurations are quite similar. This suggests that the small-scale riser rig might be suitable for testing different control strategies prior to more costly and time-consuming tests on larger rigs.

Chapter 4

Control challenges and solutions for a subsea separation and boosting station

4.1 Introduction

The Tordis field operated by StatoilHydro has proved to be even more productive than anticipated when production began in 1994 (Godhavn, Strand and Skofteland (2005)). To increase production and total recovery for the field in its last years of production, processing equipment is planned installed at the sea bed. This is to separate produced water from the production stream and inject it into a reservoir, with the aim to increase the production rate and recovery from of the field.

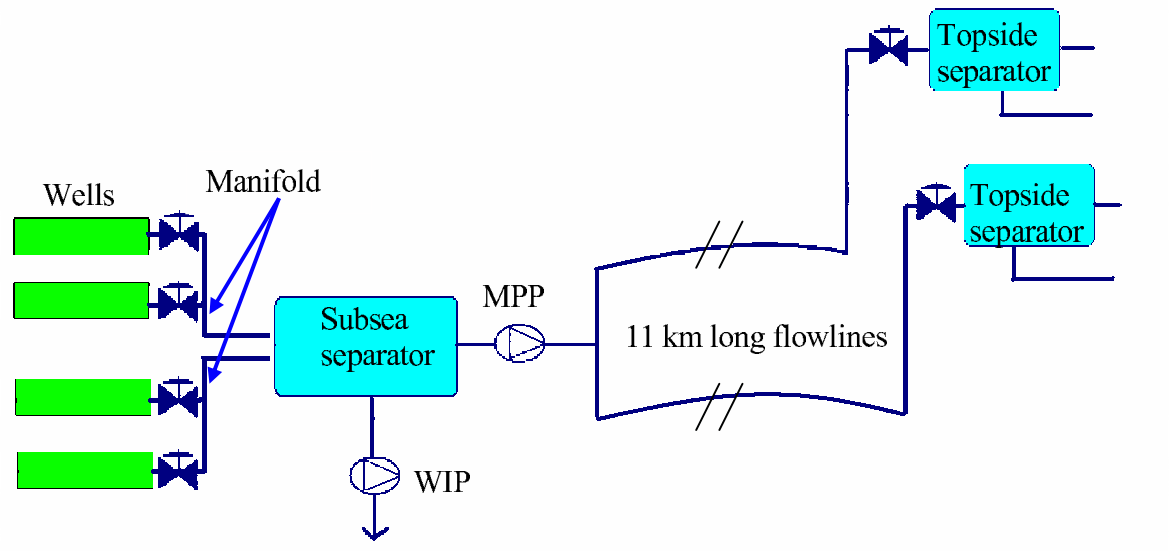

Figure 4.1: Subsea processing equipment planned at the Tordis field

Subsea processing enables production from low-pressure reservoirs over long distances, and may increase the daily oil and gas production and also the total recovery from the reser-

voir. By injecting produced water into a reservoir, the water emission from topside to sea can be reduced, and the subsea transportation pipelines are better exploited. Compression and pumping enable a lower wellhead pressure, and hence an increased production.

However, the installation of new subsea equipment leads to several new challenges, also related to process control. There can be several ways to solve these problems, so the first question that needed answering was; which solutions are feasible and which one will solve the problems the best.

In the process of determining the control strategy and operation philosophy of the system, it is beneficial to perform dynamic simulations that capture the dynamical behavior adequately. Since the pressure, flow rates and composition of the flow vary with time, it is important to perform studies for several years throughout the life time of the field.

Control of the subsea separator pressure and liquid levels are important as it determines the flow rates and compositions for the entire system. In Section 4.4, some solutions to achieve control of the separator will be presented. These control solutions are then expanded to achieve other benefits, such as faster well tests and control of the water rate that is transported with the oil and gas to the platform.

Under certain conditions a flow regime called riser slugging can develop in the pipelines, which is undesirable because it can introduce large pressure oscillations in the system. In the end of Section 4.4 it will be shown that this problem can be solved using feedback control.

The control solutions presented in section 4.4 have also been published in Sivertsen et al. (2006). They are illustrated with dynamic simulations including all equipment from the wells to the two topside receiving separators at the Gullfaks C platform (Figure 4.1). In this figure, MPP and WIP are multiphase pump and water injection pump respectively.

It is important to notice that these simulations were performed at a very early stage in the process of determining how to run the process, where the aim was to find feasible control solutions and not to find optimal control parameters. The controllers have therefore not been fine-tuned and simplified models for the equipment and pipelines have been used. This is also the reason why the absolute values for the different variables have been left out in this section of the thesis.

Section 4.4.4 has not previous been published. Due to a tight time schedule, a planned paper from these simulations was not realized. However, the problem is quite interesting and the results using automatic control was good. This is why a presentation of this work has been included in the thesis.

To simulate flow in pipelines, the OLGA 2000 dynamic multiphase simulator provided by Scandpower Petroleum Technologies has been used. Most of the process equipment is simulated using Simulink. The OLGA - MATLAB toolbox enables the Simulink application to simulate multiphase flow in pipelines in OLGA and link it with additional process equipment and controllers modeled in Simulink.

When combining these simulation tools, one needs in each case to carefully consider which parts of the system to include in a simulation, and which assumptions can be made about the boundary conditions. The simulation strategies are described more thoroughly in Section 4.3. The results from this section has also been presented in Sivertsen et al. (2005).

4.2 Subsea processing equipment

Oil, gas and water are transported from the manifold to the subsea separator through two pipelines (Figure 4.1). From the separator some of the water is to be injected into a disposal reservoir. The remaining water will be transported along with the oil and gas through two pipelines into each topside separator at the Gullfaks C platform. A multiphase boosting pump (MPP) will be installed downstream the separator.

4.2.1 Wells

There are eight wells producing oil, water and gas to the Gullfaks C platform. The flows from the wells are merged at the manifold. Two short pipelines, each receiving the production from four wells, transport the fluid to the subsea separator.

4.2.2 Pipelines

To simulate the pipelines between the wells, the subsea separator and the topside separators, OLGA 2000 have been used. OLGA 2000 is a commercially available dynamic multiphase flow simulator. In our study, OLGA has been linked to Simulink.

4.2.3 Subsea Separator

The subsea separator is illustrated in Figure 4.2. In the separator the water, oil and gas separate due to gravity. The water, which is heaviest, sinks to the bottom. Most of the water is to be injected into a disposal reservoir through an outlet in the bottom of the separator. It is important that no oil enters this reservoir. The rest of the water is transported to the platform along with the gas and oil.

The levels of water and oil are determined by the inlet and outlet flow rates. The multiphase pump and the water pump speed will therefore influence these levels. The rest of the separator is filled with gas.

The separator is simulated using a simple Simulink model. It computes the separator pressure, density, composition and levels. It is assumed that the pressure is independent of height, that is: the pressure at the bottom is the same as in the gas layer at the top of the separator. The composition of the stream going to the platform is determined by the water and oil levels. If the level of the water is below the outlet leading topside, no water will be transported topside. The same goes for the oil level, which depends both on the oil and water layer thickness. As already mentioned, the flow rate will be determined by the multiphase pump speed and the pressure in the separator and the pipelines.

4.2.4 Pumps

Multiphase pump (MPP). To be able to operate the subsea separator at a low pressure despite the friction loss caused by the 11 km long pipelines to the Gullfaks C platform, pumps or compressors are planned installed.

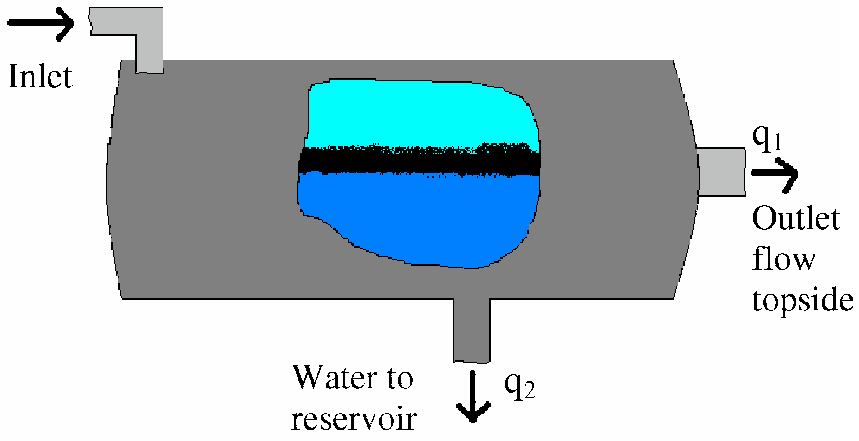

Figure 4.2: Subsea separator

To control the separator pressure by adjusting the pump speed and thereby the flow rate to topside, q_1, a multiphase boosting pump will be installed downstream the subsea separator.

Water pump (WIP). There is also a need for a water pump to pump the water into the disposal reservoir, holding a higher pressure than the subsea separator.

The water rate through the water pump, q_2, depends on the pressure difference between the reservoir and the subsea separator, and also the pump speed.

Pump speed and pressure drop over the *multiphase* pump will in the same way determine the topside production rates, but composition and density of the flow will also influence these flow rates.

4.2.5 Choke valves

There are choke valves for each of the eight wells, which make it possible to adjust the flow from each well independently. These choke valves can be used for well tests, where one well after another is shut down.

At the top of each riser there are topside production choke valve. They make it possible to control the flow transported into each of the topside separators, and can be adjusted manually or by a controller.

4.2.6 Measurements

Several measurements will be available, monitoring pressure, density, flow rates and other values which are necessary for controlling the different parts of the system. Measurements used directly for control are the manifold pressure, the subsea separator pressure and water level, pressure drop and density over topside production chokes, water rate out of topside separators and the pressure downstream the multiphase subsea pump. The pressure drop

and density across the topside chokes are used to calculate the flow rate through the topside chokes as there are no flow measurements available.

4.3 Simulation strategies

The focus of this section is to demonstrate different ways of combining OLGA 2000 and Simulink, and how to divide the overall process model into sub-models in order to study local phenomena.

4.3.1 Integration of OLGA 2000 and Simulink

Using the OLGA - MATLAB toolbox it is possible to run OLGA simulations from a Simulink environment. The Simulink OLGA encapsulation enables the Simulink application to simulate multiphase flow in pipelines in OLGA 2000 together with additional process equipment. The communication between OLGA and Simulink is synchronous, which means that when the interface has sent a message to OLGA 2000, it waits until a response has been received before returning to Matlab.

From the OLGA block it is possible to get all the information about the flow and the equipment that is modeled in OLGA, into Simulink. In Simulink the information can be displayed and stored during the simulation. The values of the OLGA variables can this way be used for process equipment modeled in Simulink, such as controllers and separators. The outputs generated from the Simulink process equipment, such as separator pressure, are then sent back to OLGA and used as inputs for the OLGA calculations in the next time step.

Using OLGA 2000 to run all the simulations is also an option, as it is possible to include separators, controllers and other equipment in the models. There are, however, some advantages of combining OLGA 2000 with Simulink. Sometimes it is desired to use other models for process equipment than the ones provided by OLGA, e.g. separators and controllers. It is particularly easy to implement these in Matlab/Simulink.

For the simulations performed during the study of our system, combinations of these methods have been used. To save computing time, and also to avoid some of the numerical problems that can occur during large simulations, parts of the system have been left out during some of the simulations. When doing this, it is important that the boundary conditions are well taken care of. Sometimes assuming constant values at the boundaries can be justified, but it is not always the case.

The calculations made by Simulink requires a very small percentage of the simulation time compared to the OLGA calculations. When sending inputs to OLGA, such as changes in boundary conditions or flow rates, the OLGA simulation time might increase. If these inputs are not essential for the results, it might be an idea to keep some of these inputs constant to reduce the time of the simulation.

Figure 4.3 shows the different ways to divide the system in our case. The wells and the pipelines into the subsea separators are modeled in OLGA, while the subsea separator and pumps are modeled in Simulink. The pipelines from the multiphase pump to topside are

modeled in OLGA, and the topside separators are modeled in Simulink. All the controllers have also been modeled in Simulink.

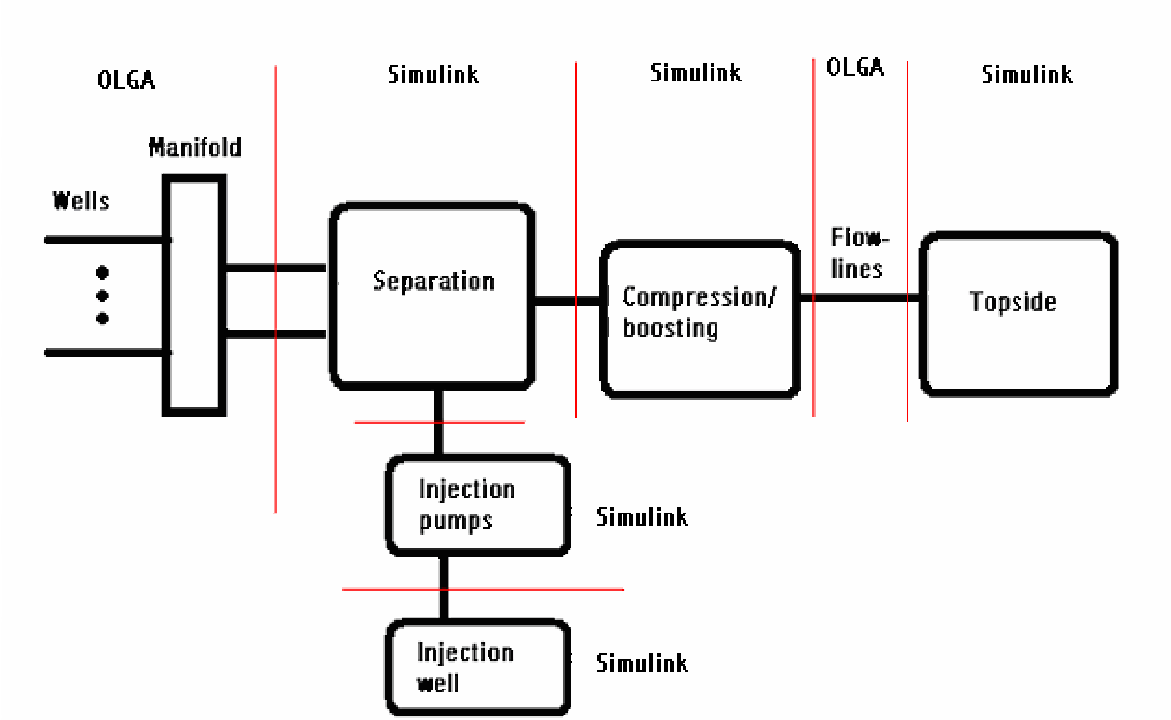

Figure 4.3: The subsystems of a general subsea processing system

To see how different parts of the total system can be run separately, some of the simulations that have been made will be presented. These simulations were performed during an early stage of the decision process on how to run the subsea system, so not all of this equipment or control structures will be used later on. However, they are included to show some of the considerations that where made when combining OLGA and Simulink.

4.3.2 Sequential simulations

One obvious possible way of doing the simulations, would be to run the different parts simulated in OLGA 2000 and Simulink separately. Then the time series obtained from one part could be used as input to a downstream simulation. The advantage of using such a method is that the simulations would in many cases require less time, and the programming would also be easier. The disadvantage is that this method does not capture the interactions between the different parts of the system, which can change the way the system behaves significantly. For example, the flow rates from one unit can be applied as input to the downstream unit. The sequential simulation will be appropriate if these flow rates are independent of the downstream pressure.

In Storkaas and Godhavn (May 2005) OLGA 2000 simulations were run with a controller implemented in Simulink. The resulting outflow from OLGA was later used as varying

inflow into an advanced topside simulator (ASSET from Kongsberg Maritime) to see how the topside facilities would handle the flow variations.

4.3.3 Integrated simulation of wells and subsea separator

The well and subsea separator simulations are important for studying the separator states during periods with varying well rates and pressure. Figure 4.4 shows a possible configuration in Simulink. Values for the flow rates of oil, water and gas are sent from the OLGA block to Simulink along with the pressure at the manifold. The flow rates are sent to the model of the subsea separator, while the inlet pressure is needed for the controller. The separator pressure is used by both the controller and as boundary condition for the OLGA block.

The choke opening percentage for the subsea chokes, set by Simulink, are also inputs for the OLGA block. If variations in separator pressure can be neglected by the OLGA model, computational speed can be increased by running the simulations with a constant downstream pressure input to the OLGA block.

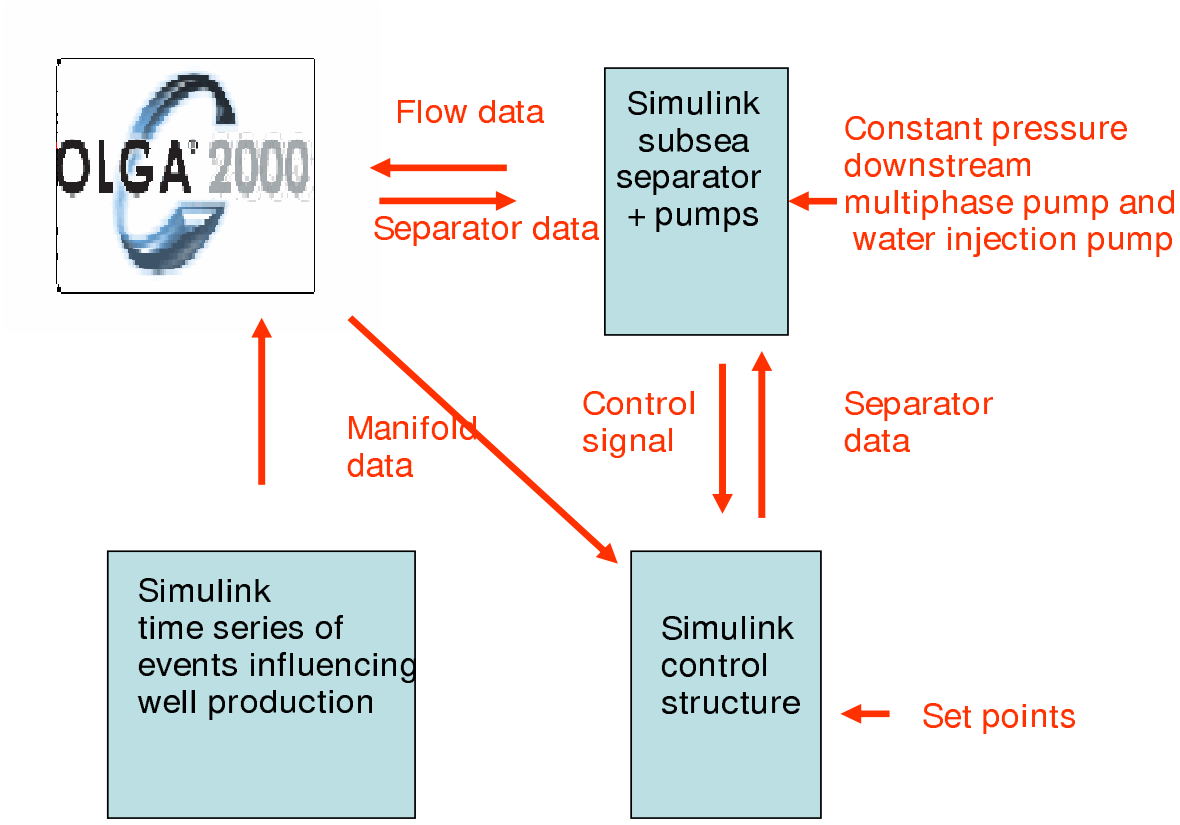

Figure 4.4: Simulation of wells and subsea separator

The downstream equipment is not included in the simulations, so assumptions have to be made about the boundary conditions. In these simulations we have assumed a constant pressure downstream the multiphase pump. This assumption was based on the fact that

this pressure, as shown later, will most likely be controlled using other controllers and not allowed to vary very much.

One example of a simulation that uses this set-up is presented in Section 4.4.2.

4.3.4 Integrated simulation of subsea separator, flow lines and topside separator

Simulations that include all equipment from the subsea separator to the topside separators can be used to see how changes in the subsea separator conditions influence the topside facilities and vice versa. The simulation includes the subsea separator, the multiphase pump, the water injection pump, the pipelines to topside and the topside separators. Figure 4.5 shows how this was done in Simulink. Constant flow of oil, gas and water into the subsea separator was assumed. The reason why the wells were not included in the simulations, is that including them would lead to a very long simulation time. One example of such a simulation is given in Section 4.4.1.

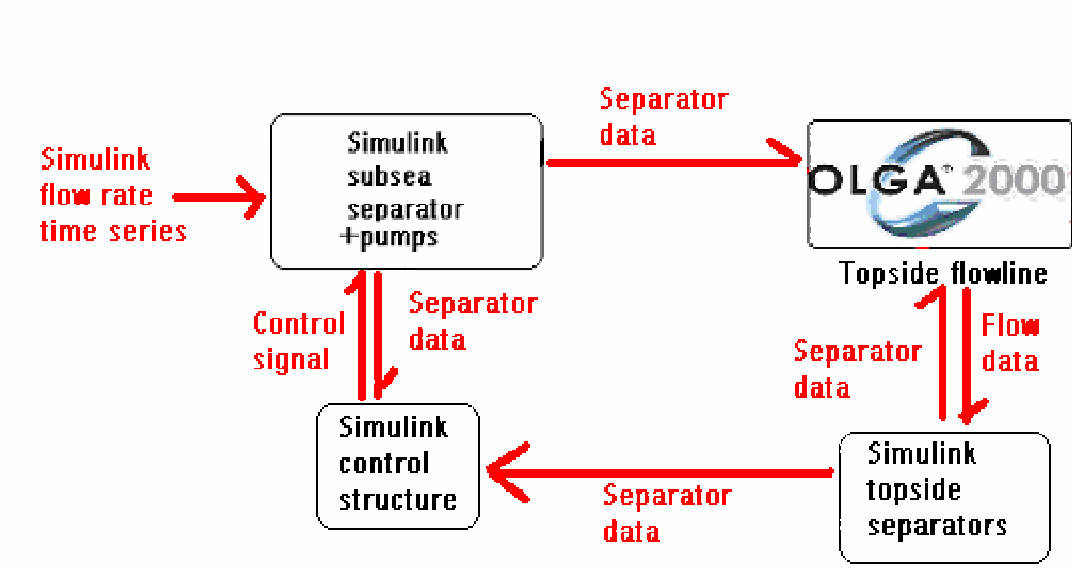

Figure 4.5: Simulation of subsea separator and topside pipelines

The pressure difference over the subsea chokes located downstream each well is quite large, so minor downstream pressure variations will not influence the flow rates very much. This pressure is not expected to differ dramatically, since the pressure in the subsea separator is held constant using controllers. Assuming constant flow rates into the separator is therefore justified.

It is also assumed that the equipment located downstream the topside separators are able to handle the flow rates from each separator. These flow rates are determined by controllers designed to keep the separator levels and pressure constant.

The flow rates of oil, gas and water out of the subsea separator are inputs to the OLGA block simulating the topside pipelines. These are obtained from the subsea separator model.

Outputs from the OLGA model are the flow rates trough the topside chokes and the inlet pressure downstream the multiphase pump. The flow rates are sent to the models for the topside separators while the inlet pressure is used by a slug controller not shown in the figure. From the subsea separator model we also get the water level and pressure, needed for the controller and the model for the water injection pump.

4.3.5 Flow line simulations

Figure 4.6 shows the Simulink model for the topside pipeline, topside choke and controllers. This configuration has been used for testing a slug controller (see Section 4.4.3). From the OLGA block the inlet pressure of the pipeline is sent as input to the Simulink model of the controller. The controller calculates new topside choke openings that are sent as inputs back to the OLGA model.

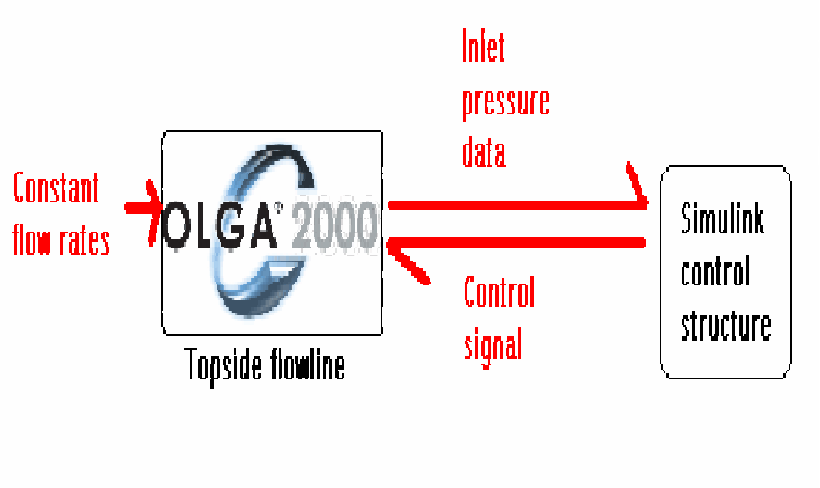

Figure 4.6: Slug control simulation setup

In this simulation it is assumed constant flow rates of oil, water and gas from the multiphase pump. In this way, the effect of pressure variations at the inlet of the pipelines on the flow rates upstream will not be modeled. When the slug controller is active this pressure will be fairly constant during normal operation.

4.4 Control solutions and results

Several dynamic simulations were performed to test different control strategies for the system, and some of these will be presented here. The results will be used in the design of the control system and this way serve as a basis for further studies. The solutions presented here might therefore not be the ones implemented in practice.

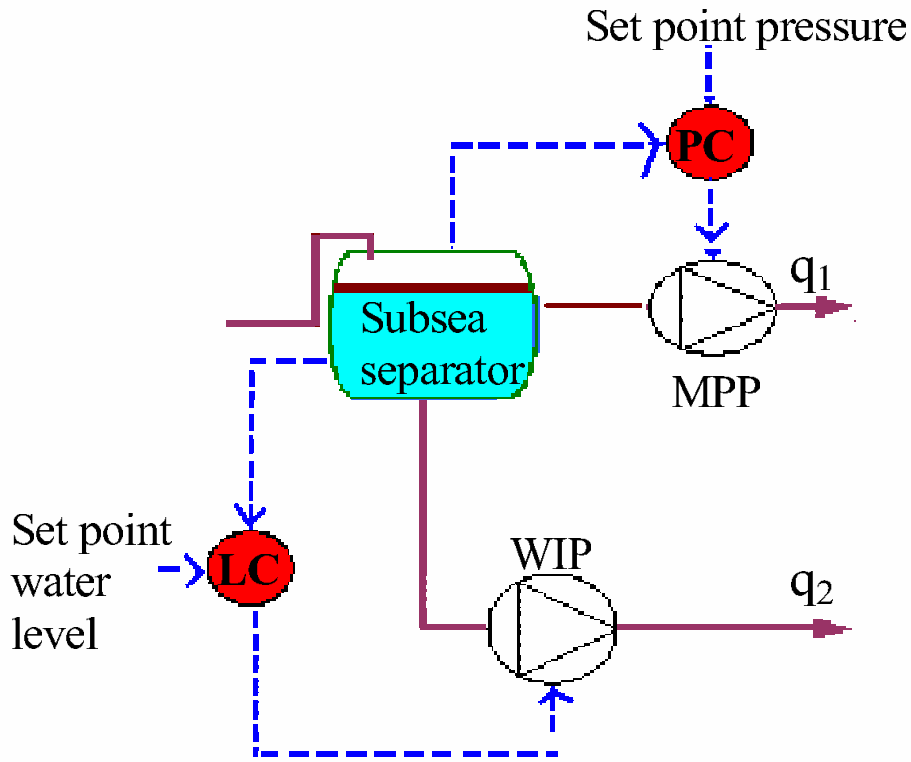

Figure 4.7: PI control of subsea separator pressure and water level

4.4.1 Control of subsea separator pressure and levels

Decentralized PI control of subsea separator pressure and water level

To keep the oil contents in the injected water below a given limit, it is important to control the separator water level. By increasing the flow rate of the water injected into the disposal reservoir, the water level will decrease. The flow rate through the water injection pump depends on the pressure difference across the pump and the pump speed. The speed of the pump can be set by a controller.

It is also important to control the separator pressure as this pressure will affect the wells and their production. The separator pressure can be controlled by changing the total flow rate to topside, which again is influenced by the speed of the multiphase pump. During the simulations this flow rate was set by the controller directly. The reason for this is that there was no model of the multiphase pump available at the time of the simulations.

Even though there are quite strong interactions between the level and pressure control, as will be shown, simple PI controllers were used to study how well the separator could be controlled. This is illustrated in Figure 4.7.

Figure 4.8 shows the results from a simulation where the input rates of water, gas and oil are reduced by 50% after 30 min. The pressure drops as the flow rates are reduced, but after about 15 min the pressure is back to normal due to the controller action.

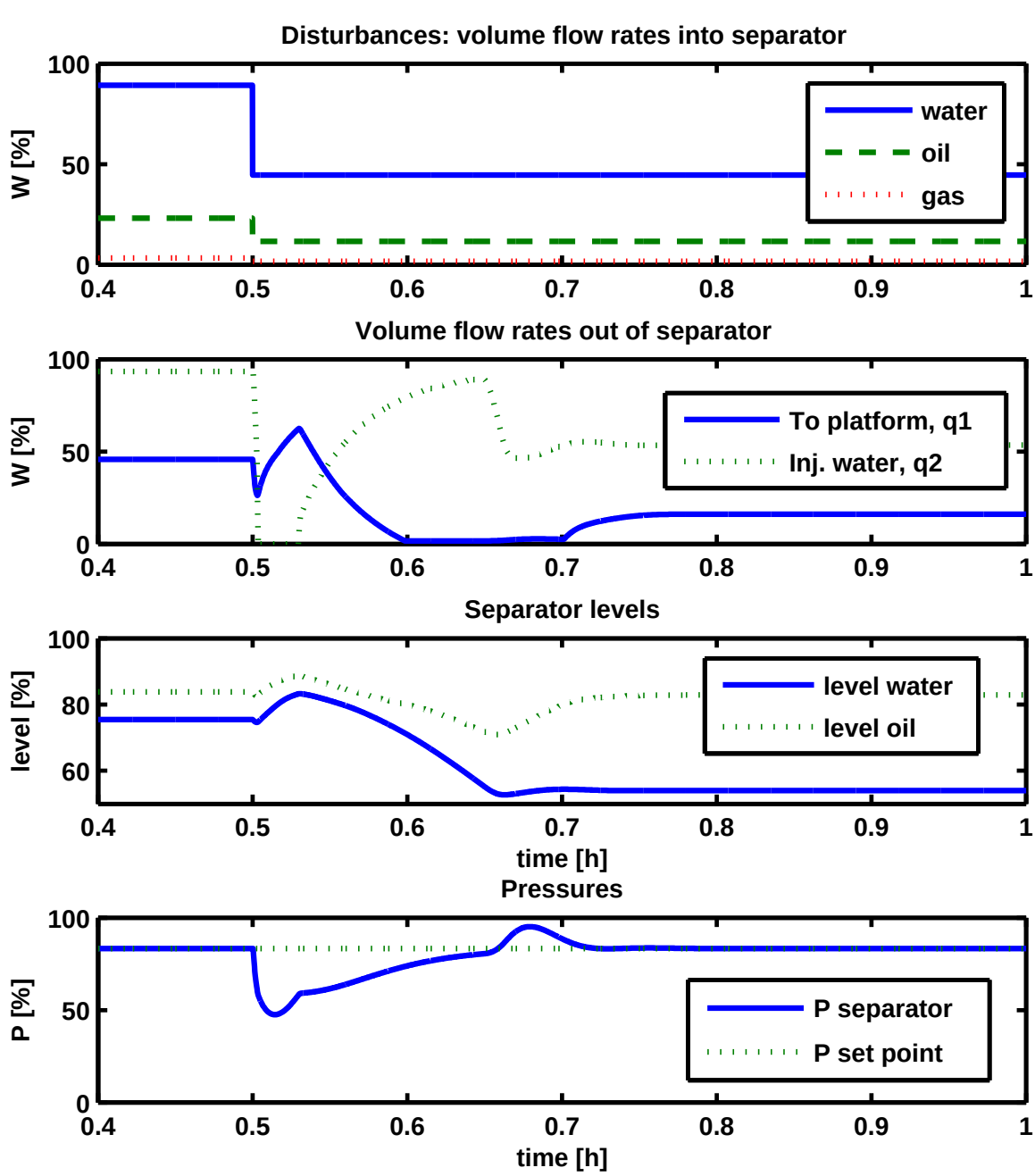

Figure 4.8: Results using PI controllers to control subsea separator pressure and water level

What might seem surprising is that the water and liquid level start to increase at the time the inlet rates are reduced, before they decrease and end up at lower levels than they initially had. The reason for this is that the separator pressure and water level affect each other. When the separator pressure decreases due to the reduced inlet flow rates, it makes it harder for the water pump to inject water into the reservoir. Because of this, the water rate injected to the reservoir, q_2, temporarily goes down to zero, explaining the increase in levels.

In practice, a zero flow rate will cause problems for the water pump, but better tuning

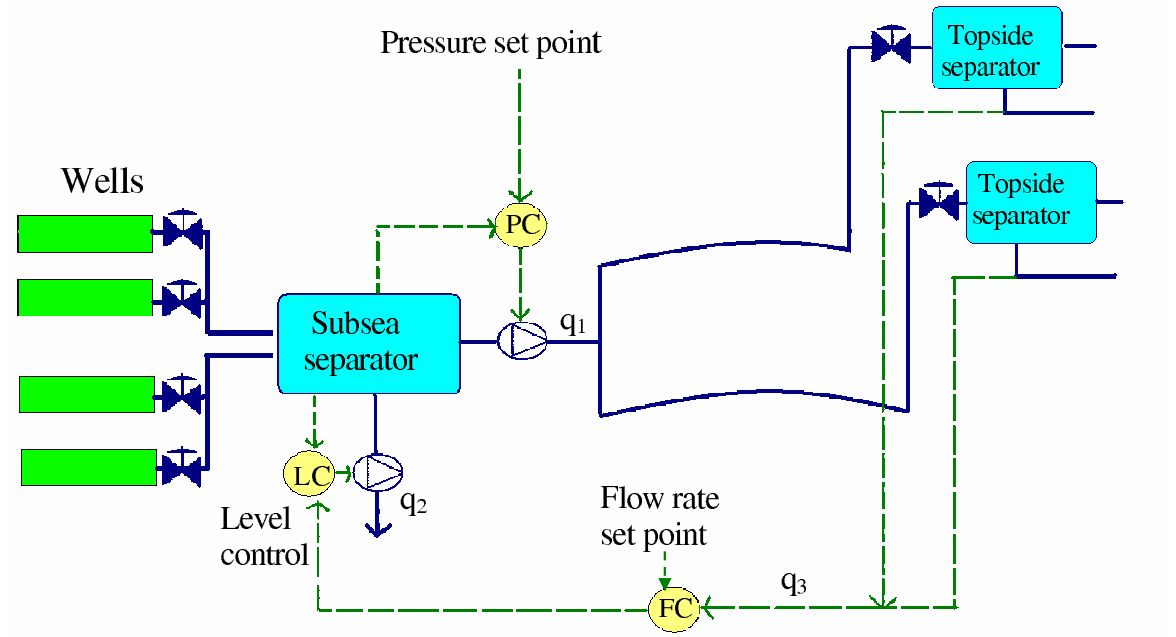

Figure 4.9: Cascade control of subsea separator water level and water rate topside

of the controller or other control configurations will remove this problem. Another way of avoiding this problem could be to use some other control configuration, e.g. a cascade controller where the inner loop controls the flow rate through the water pump and the outer loop controls the water level in the separator.

Cascade control : Control of water rate to topside

The gas and oil to the Gullfaks C platform (q_1) may still contain some water which needs to be handled topside. Since the downstream process can only handle limited amount of water, good control of this water rate is desired.

By changing the water level in the subsea separator it is possible to control this water rate. Figure 4.9 shows one way of doing this. It is an extension of the control structure presented in 4.4.1. An increased water level will lead to increased water rate topside (see Figure 4.2). A cascade configuration using the water rate out of the topside separator, q_3, in a slow outer loop and the water level in the inner loop, was developed to handle this.

Figure 4.10 shows the results from a simulation where the inlet flow rates are reduced by 50% after 1h. The set-point for the water level controller is increased when less water is transported topside due to reduced inlet rates.

After about 5 hours the water flow rate is back at its set-point, even though the flow rates into the subsea separator have been reduced substantially.

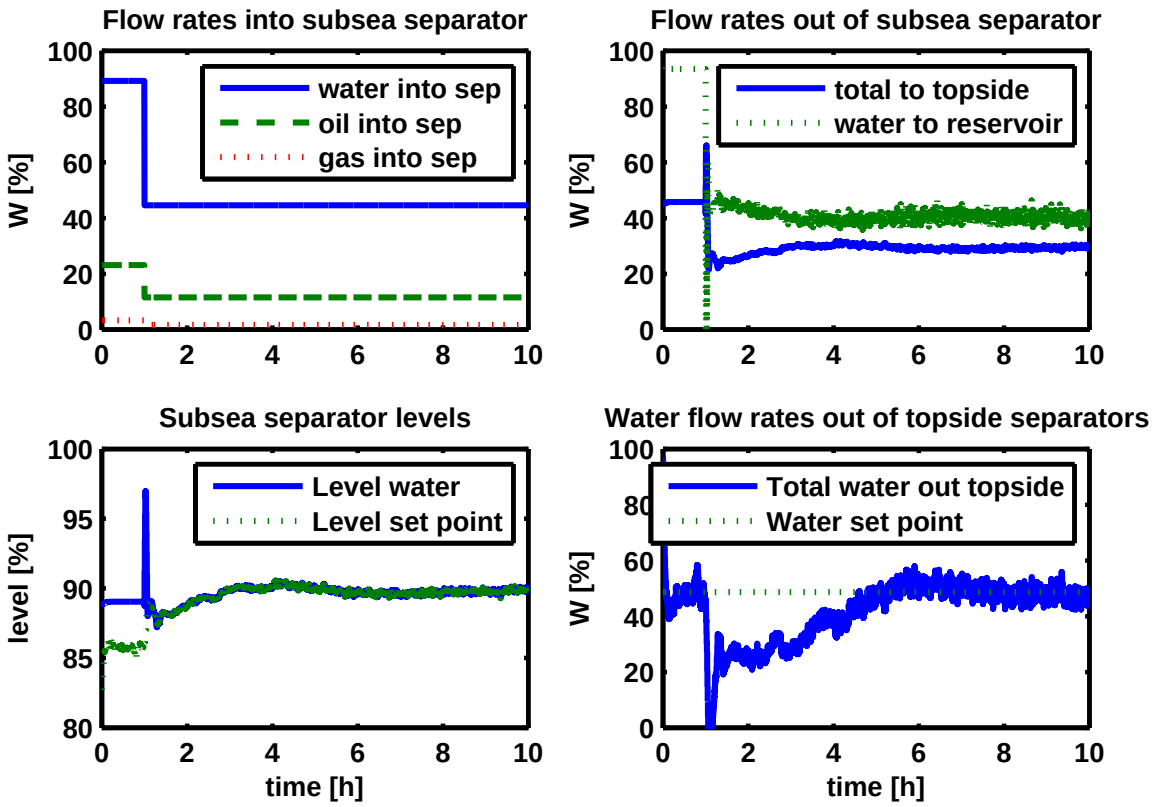

Figure 4.10: Results using a cascade controller to control subsea separator water level and water rate topside

4.4.2 Well head pressure control

During a well test, one well after the other is shut down in order to determine the production rate from each individual well (deduction principle for tie-ins). Performing well tests is costly, as the production is reduced while the well test lasts. Being able to reduce the duration of a test has a large economic potential. Using active control might reduce the time needed to perform a well test.

When a well is shut down, the pressure drop in the pipeline will decrease due to the reduced flow rate in the pipe. This way the other wells will produce more, leading to a wrong estimate of the production from the well that is closed. Therefore, during well testing, the pressure at the *manifold* is kept constant rather than the subsea separator pressure which is normally controlled (Figure 4.7). There is actually a need for the subsea separator pressure to *increase* during a well test. The alternative would be to reduce the well choke openings accordingly.

There are several ways to do this. One possible alternative (alternative 1) is a cascade control configuration. The outer loop controls the manifold pressure where the set-point is the initial pressure before the well test. The inner loop controls the subsea separator pressure. This way the set-point for the subsea separator pressure will automatically increase for every well that is shut down. The cascade control configuration is illustrated in Figure 4.11.

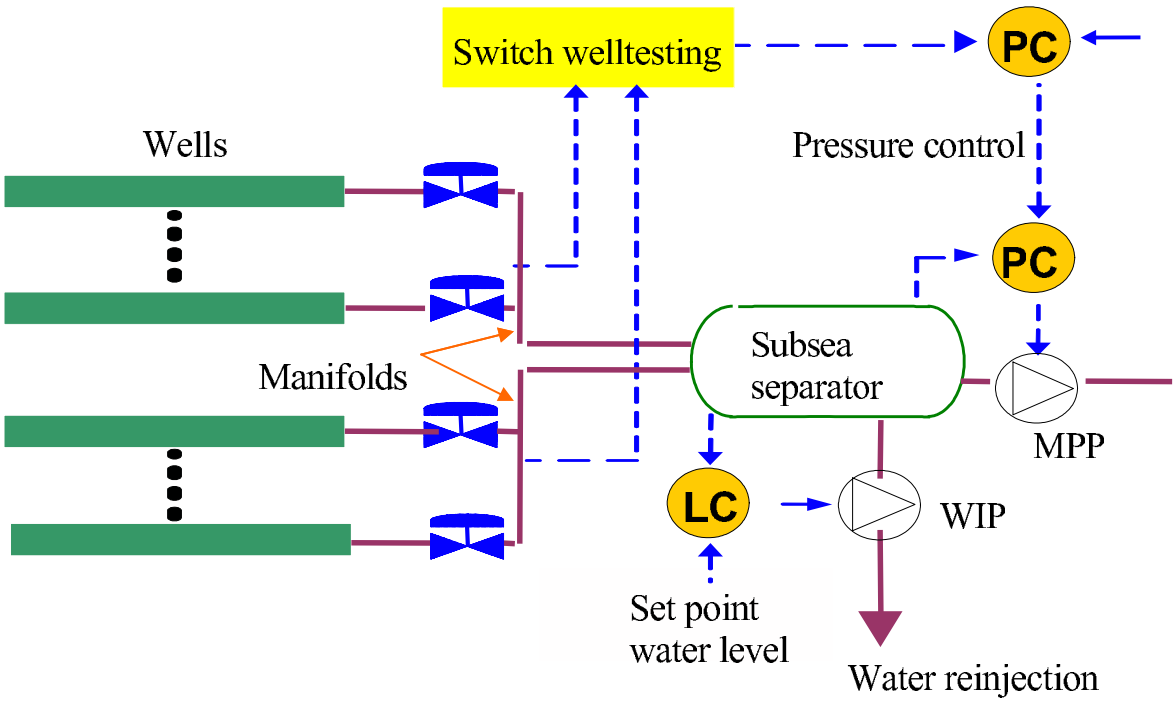

Figure 4.11: Welltest using cascade configuration (alternative 1)

Using the cascade controller for the well test, it was possible to bring the manifold pressure back to its original value. Figure 4.12 shows the results when three of the wells are shut down one after another. The plot at the bottom shows how the subsea separator pressure increases to counteract the effect of the reduced pressure loss in the pipelines upstream the separator.

Another way of controlling the manifold pressure (alternative 2), is to estimate how much the manifold pressure will drop when a well is shut down, and then increase the set-point for the subsea separator pressure accordingly. This way the simple pressure PI controller described in Section 4.4.1 can be used, as long as steps in the set-point are introduced. It is important to get good estimates of how much the separator pressure need to increase in order to use this method. Results from simulations show that it is possible to reduce the time before the manifold pressure reaches its initial value to less than 15 min. This is illustrated in Figure 4.13.

The results from the simulations show how long it takes for the manifold pressure to retain its initial value after a well is shut down. This information can be used to predict the duration of a well test.

4.4.3 Slugging

Riser slugging is a well known problem offshore, where alternating bulks of liquid and gas enter the receiving facilities and cause problems due to pressure and separator level oscillations. The results are poor separation and wear on the equipment.

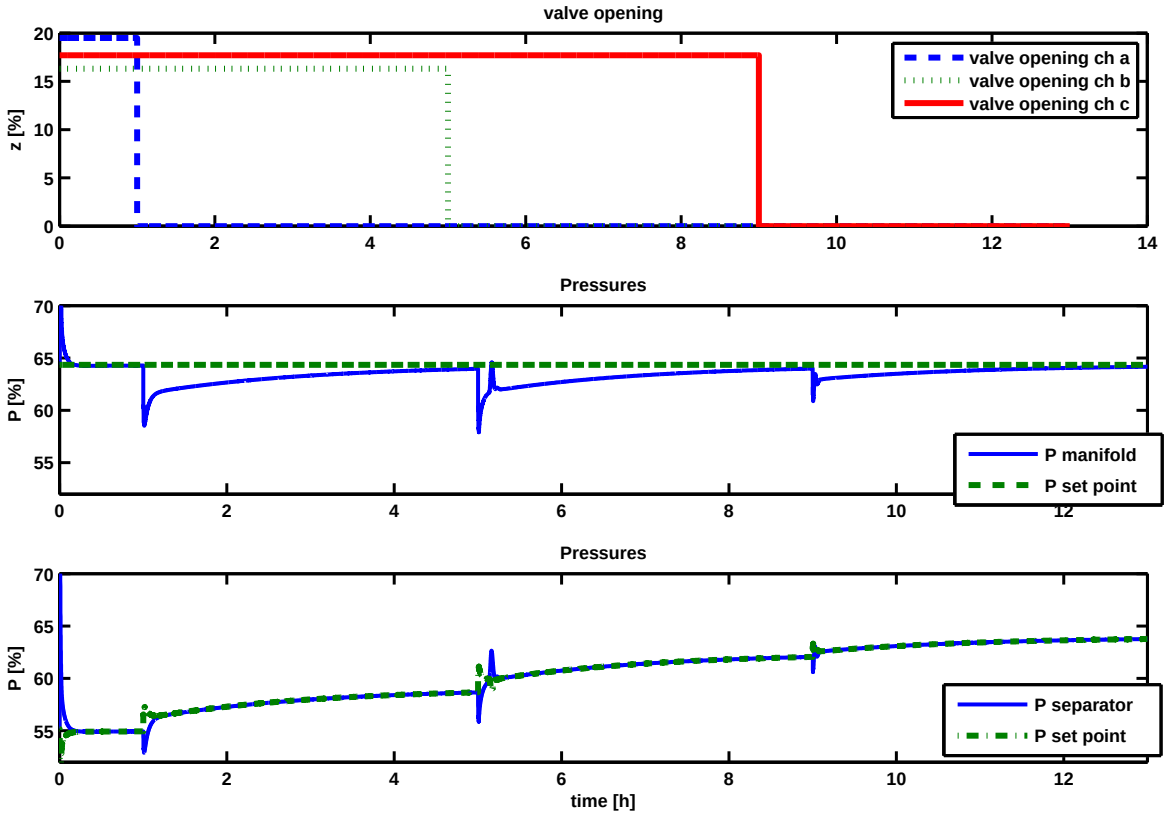

Figure 4.12: Welltest results (alternative 1)

There are several ways to deal with the problem, but using active control has in the last years been the preferred way to avoid riser slugging, Courbot (1996), Havre et al. (2000), Hedne and Linga (1990), Skofteland and Godhavn (2003). Today a combination of active slug control and model predictive control (MPC) is used at Gullfaks C (Godhavn, Strand and Skofteland (2005)).

A simple PI controller using the pressure upstream the flow-line ending in the riser and a control valve at the top of the riser has proved to be effective, as was seen is Chapters 2 and 3. Without control, this pressure oscillates strongly during slugging. With control, the flow is forced into another flow regime. Storkaas (2005) used control theory to prove that using the upstream pressure, it is possible to stabilize the flow and also to achieve good performance. This control configuration is illustrated in Figure 4.14.

Results from a simulation with the slug controller are shown in Figure 4.15. During the first 4 hours the controller is inactive, resulting in slugging in the pipeline and the pressure variations shown in the upper plot. When the controller starts working, the pressure stabilizes at the desired set-point.

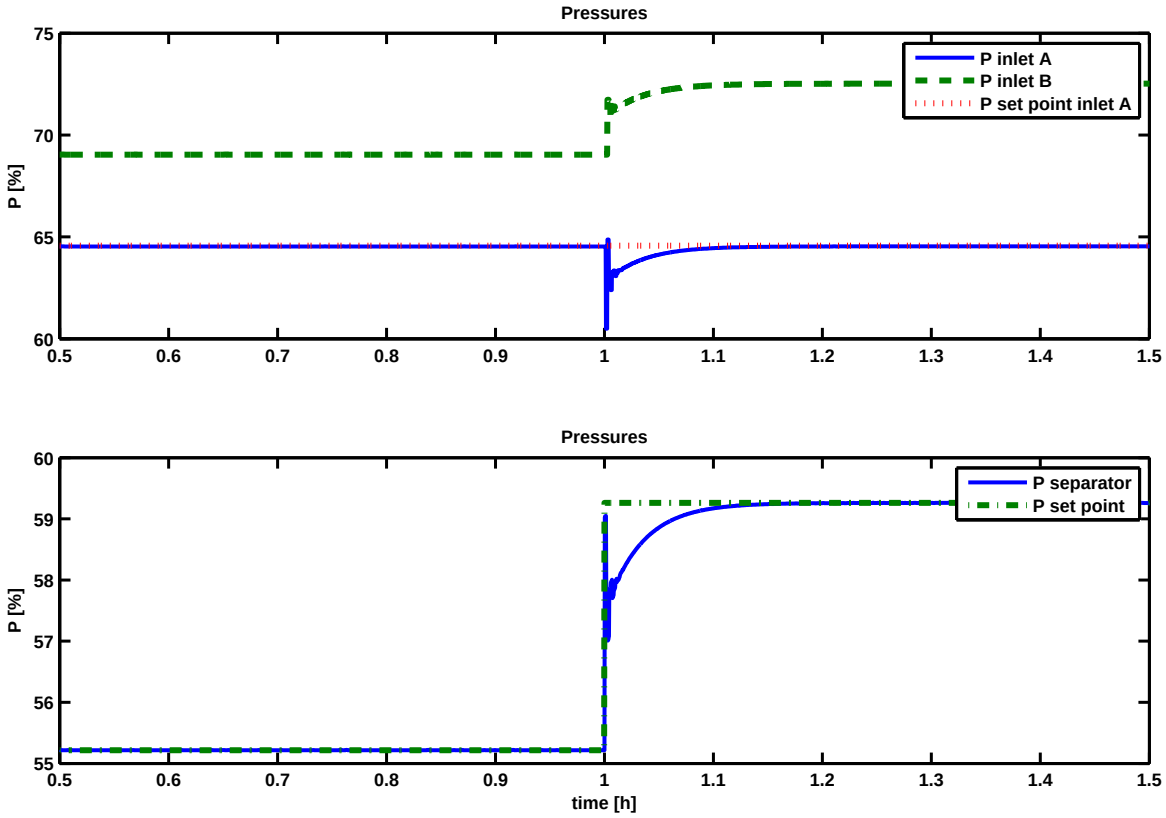

Figure 4.13: Welltest results using a PI controller with set point changes (alternative 2)

4.4.4 Controlling the split of the flow into two flow lines

Splitting multiphase flow into two streams may cause serious problems in terms of flow variations and instability (Spacey et al. (2000), Tshuva et al. (1999), Taitel et al. (2003), Minzer et al. (2004).

Downstream the multiphase boosting pump the pipe is split into two 11 km long pipelines transporting fluid to each topside separator at the Gullfaks C platform. The problem is that flow rates in the two pipelines are not necessarily similar, even though the geometry and pressure at both ends of the pipelines are the same. Some simulations showed that for certain conditions, almost all of the flow was produced through just one of the pipelines. The riser connected to the other pipeline was then filled with liquid.

The reason for this uneven distribution can be found from a plot of the pressure drop over the pipeline versus the fluid flow rate for the system. This is illustrated in Figure 4.16.

At low flow rates the pressure drop has a negative slope. The flow is gravity dominated, meaning that the slip between the phases changes with flow rate. Thus, as the flow rate gets reduced more liquid will accumulate in the riser, resulting in a larger hydrostatic pressure drop over the riser. This is also the region where slugging is most likely to occur.

Increasing the flow rate will lead to a positive slope for the curve. Less liqiud is accumulated, so the pressure drop due to gravity decreases. However, in this region friction forces have a larger effect on the pressure drop. Thus, as the flow rate increases the pressure loss

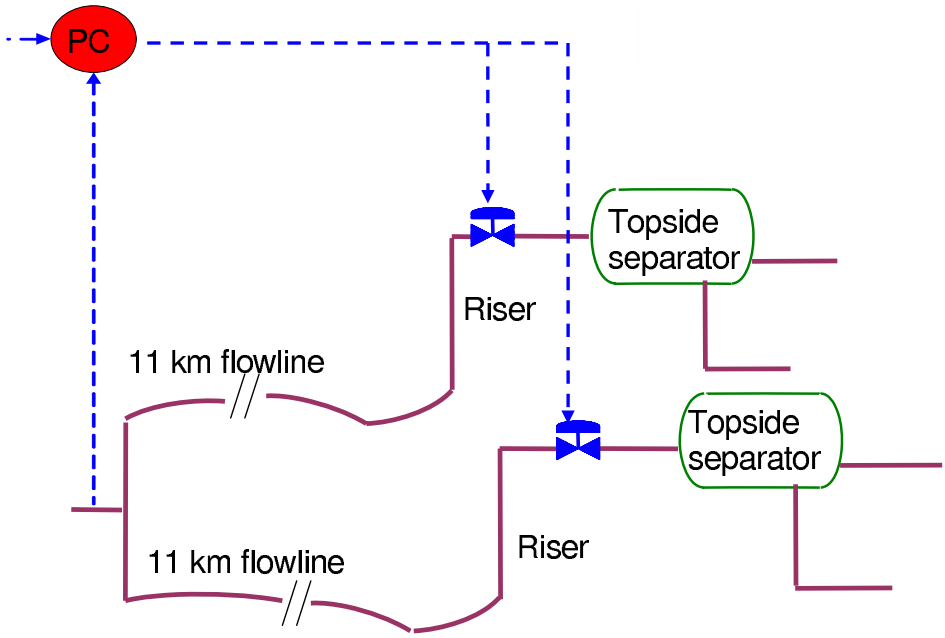

Figure 4.14: Slug control applied to Tordis

due to friction will increase.

Because of this, two different flow rates can result in the same pressure drop in the pipeline, which explains why a split into two similar pipelines can result in almost all of the fluid being transported through only one of the pipelines. The riser in the other pipeline fills up with liquid and has minimal fluid transportation.

Simulations show that this could be a possible scenario also for the Tordis field. In order to handle this problem, flow controllers at the top of the riser were tested through simulations. In these simulations the flow rate through the topside control choke was estimated using a simplified flow equation for mass flow through a choke.

$$W = z * k * \sqrt{\Delta P * \rho} \tag{4.1}$$

The pressure drop over the topside choke, ΔP, and the density upstream the choke, ρ, are assumed known from measurements. The valve coefficient, k, is estimated. z is the valve opening.

Because of the possibility of slugging in the two risers, simulations using a cascade control configuration have been performed. The outer loop then controls the inlet pressure for the pipelines, whereas the inner loops control the flow rates through the topside chokes. To make sure that this outer controller does not give a too large set-point to the inner flow controllers, the set-point has an upper limit of 0.7 times the total flow rate into the system. If the flow rate through one of the topside chokes is larger than the set-point, the choke will close, forcing more fluid to enter the other pipeline where the choke opening is larger. This control structure is illustrated in Figure 4.17.

Results from simulations using this controller are plotted in Figure 4.18. The controller is activated after six hours, where the flow rates estimates through the topside choke differ

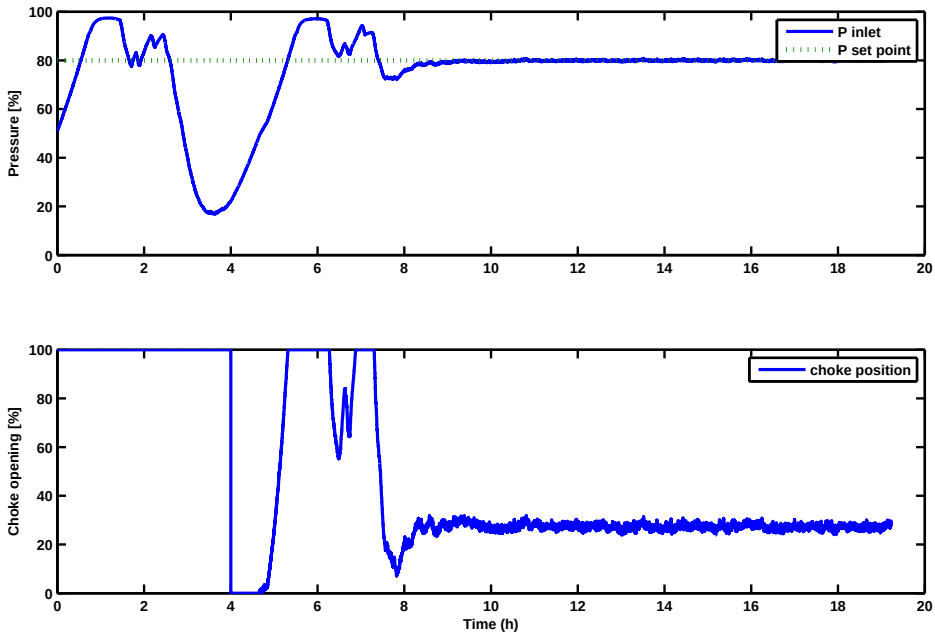

Figure 4.15: Slug control results

with a factor of about two. As the figure shows, the pressure at the riser-base in pipeline A is almost the same as the pressure downstream the multiphase pump, 11 km away. The reason for this is that the flow rate in this case is so low that the friction loss is almost negligible for

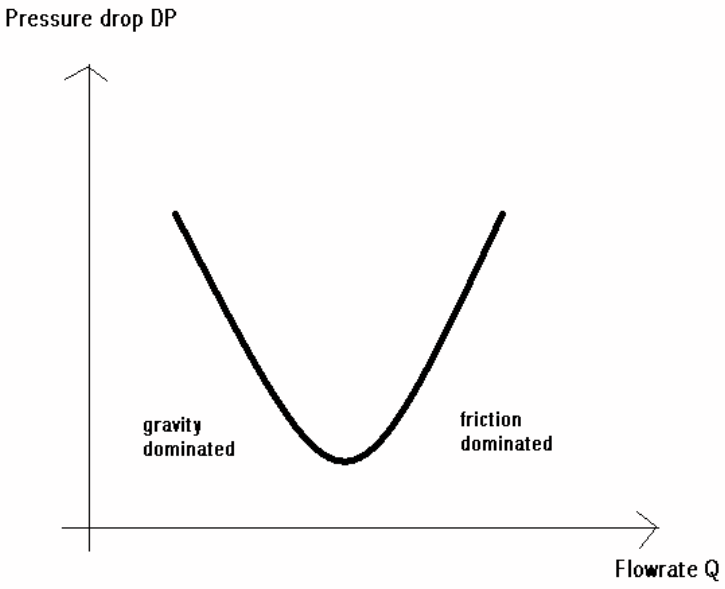

Figure 4.16: Pressure drop over flow-line as function of flow rate

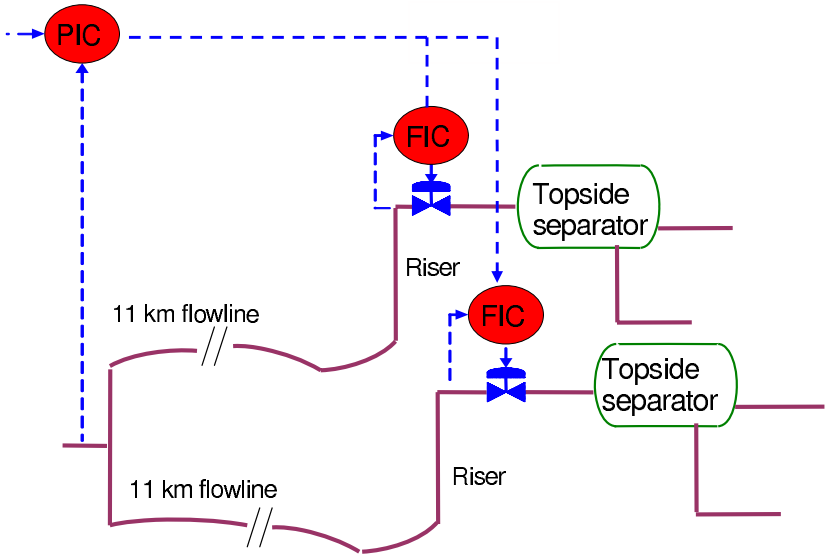

Figure 4.17: Control configuration to handle uneven flow in pipelines with common inlet

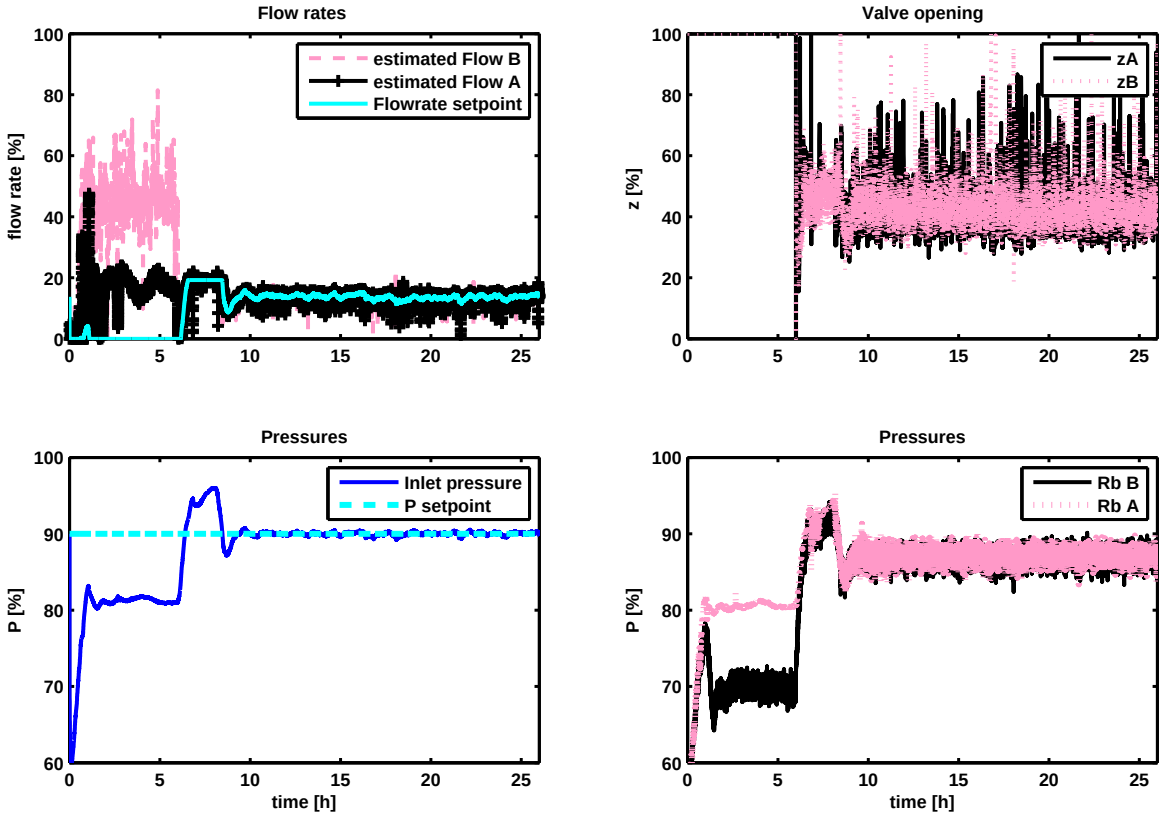

Figure 4.18: Split control results

this pipeline. The pressure loss for pipeline A comes from the fact that the riser is filled with liquid and therefore has a much larger gravity loss than the riser in pipeline B. For pipeline B, however, the friction loss is much greater due to the larger flow rate.

The controller almost immediately even outs the flow rate differences for the two pipelines as can be seen both from the flow rate plots and the pressure plots.

4.5 Discussion

This section has shown some possible control strategies for a subsea separation and boosting station planned for the Tordis oil field.

The simulations have been performed at a very early stage, before the final decisions about equipment and operation have been made. Because of this, simplified models of the pipelines and equipment was used. Also, the controllers have not been fine-tuned to get the best results at this stage. The results from this study will therefore differ from the final results. The simulations can, however, be used as a basis for later studies.

Examples of what better designed controllers can accomplish are; decreasing the time of the welltest (Figure 4.12) and removing the effect that leads to the topside choke saturating in the first 4 hours of slug control (Figure 4.15).

There are also other dynamic process simulators that are commercially available and may be combined with OLGA 2000 for pipeline simulations.

D-SPICE is a dynamic simulator provided by Fantoft Process Technologies. The simulator contains a module, the OLGA 2000 Interface (OLGAIF), that can be used to run an OLGA simulation as an integrated part of a D-SPICE model. Similar possibilities exists also for ASSET from Kongsberg Maritime and HYSYS from Aspentech.

4.6 Conclusion

The implementation of new subsea processing equipment to improve the productivity for a subsea oilfield is expected to introduce several new challenges regarding operation and process control that need to be addressed before the start-up. This section of the thesis presents some results from dynamic simulations performed in order to investigate how the use of automatic control might solve these challenges. For the different scenarios presented here, automatic control shows good results.

Using a combination of OLGA 2000 and Simulink simulator tools, it has been possible to study and plan for the implementation of the subsea station. Depending on the problem at hand, local sub-models have been combined in different ways to save simulation time without introducing too large errors due to simplifications. Doing so requires a careful consideration of all assumptions for the boundary conditions.

The simulations presented in this section was meant as a basis for later studies. It was important to capture the interactions between the different subsystems.

Examples of what better suited controllers can accomplish are; decreasing the time of well tests (Figure 4.12) and removing the effect that leads to the topside choke saturating in the first 4 hours of slug control (Figure 4.15).

Chapter 5

Conclusions and further work

5.1 Conclusions

5.1.1 Anti-slug analysis' and experiments

In Section 2 and 3 analysis' and experimental results from a small-scale and a medium-scale riser-rigs were presented. The rigs were used to see whether it was possible to control the flow, avoiding unwanted slug flow in the riser, using only topside measurements.

The first experiments were conducted on the small-scale lab rig at NTNU. An analysis of the system was presented, which showed that using topside measurements of density, pressure, and flow rates would be difficult and not at all comparable with using inlet pressure as measurement. Offshore, the inlet pressure located on the sea bed is often not available. That is why control configurations using *combinations* of topside measurements were sought.

Since there were no good measurements of the flow rates or density topside, a fiber optic signal used for determining the hold up of water in the flow line was used as measurement. The measurement suffered from a lot of noise, coming from the fact that every time a bubble passed the laser beam of the sensor, a spike occurred in the signal. Regardless of this; the results were in fact quite good. Cascade control configurations with the fiber optic signal in the inner loop, and z or P_2 in the outer loop both managed to control the flow far into the unstable region.

An attempt was made to stabilize the flow using only the fiber optic signal in a PID controller. Despite the fact that the analysis had shown that the topside measurements were difficult to use, and also the fact that this single measurement was extremely noisy, the controller actually managed to control the flow.

After performing these small-scale experiments the natural thing to ask was; would these result also apply for larger rigs? An opportunity to test this came when StatoilHydro offered to let us do some tests on their test rig at Porsgrunn Research Center.

An analysis of this medium-scale rig indicated the same problems as for the smaller rig, but simulations showed that using volumetric flow rate as topside measurements would lead to amazing good results. However, there were good reasons to doubt these results as no disturbances in inlet flow rates was added in the simulations. In reality, the inlet rates had a substantial pressure dependency.

First, an attempt was made to see if it was possible to control the flow using only a density measurement. Even though the controller quickly stabilized the flow, it eventually became unstable while the controller was still working. This could be explained by the analysis, which showed a to low steady state gain for this measurement. This would lead to the controller drifting of from the set point, as was seen in the experiments.

Six cascade controllers were tested, using inlet pressure, topside density and topside flow rate as inner measurement and topside choke opening and pressure as outer measurement. They all worked quite well, managing to control the flow at a far larger valve opening than would normally lead to slug flow.

Based on these results it is naturally to conclude that more test on even bigger rigs should be conducted, and eventually also test these controllers offshore so that they can be used on fields were subsea measurements are not easily accessible.

5.1.2 Subsea separation; the Tordis project

In section 4 the simulation study of different control structures used to control a subsea separation and boosting station was described. The subsea station is the first of its kind in full scale, and it is going to increase the recovery of Tordis substantially.

Several control structures were investigated and simulated, and four of these have been presented in this thesis. The most important task of the study was to make sure that it was possible to have control of the separator pressure and water and oil levels.

However, the new system also offered some new and interesting opportunities. By adjusting the speed of the multiphase pump and the water pump, it was possible to control the fraction of water transported with the oil and gas to the topside facilities instead of being injected into the disposal reservoir.

Also presented in this section was a study on adjusting the separator pressure to keep the manifold pressure stable during well tests. A section on how the production split into two pipelines ending into two topside separators was included in the end. When the studies showed that the production did not split evenly into the two pipelines, a controller easily solved the problem.

5.2 Further work

5.2.1 Anti-slug analysis' and experiments

From the anti-slug control experiments one naturally wonder how the results would be one even larger test rigs as the one at Tiller, Trondheim. Also an attempt to implement this offshore would be very interesting.

Before testing these control structures at larger rigs, further testing on the lab rig at NTNU could give valuable information. Conducting the experiments with different kind of disturbances is one example of such, giving an indication about how robust the controllers are towards different kind of disturbances, e.g. fluctuating separator pressure.

Also; tuning of the controllers or using other control configurations could to increase the quality of the controllers. Other control configurations based on optimization on models might also improve the quality of the controllers. One example would be H_{inf} controllers.

Using other measurements than the ones presented in this thesis, as measured variable in the control configurations, might give better results. Analysing such measurements could give a hint about what problems to expect in the lab.

Both in the small- and medium scale experiments, it was clear that the timing for when the controllers were activated actually was essential to whether the controller managed to control the flow or not. Further investigations on the reasons behind this, and what the optimal time for activating the controller is, would be interesting.

5.2.2 Subsea separation; the Tordis project

The new subsea station offers a lot of new opportunities whith respect to controlling the flow and the pressure in the pipelines toward the Gullfaks C platform. When the papers Section 4 is based upon were published, it still was not for certain that the subsea separator would be implemented. After thorough studies, StatoilHydro finally decided to go for the solution, and it became one of the projects with highest profile in the company. One of the reasons for this was the fact that subsea processing is a new area in the oil business, and StatoilHydro wanted to increase their knowledge in this area.

The production from Tordis was routed through the subsea separator for the first time in December 2007. The subsea separator itself seem to be a success, however problems with the injection well has led to the injection being stopped for the time being.

Bibliography

Bårdsen, I. (2003), 'Slug regulering i tofase strømning - eksperimentell verifikasjon', Project report, Norwegian University of Science and Technology.

Barnea, D. (1987), 'A unified model for predicting flow pattern transitions for the whole range of pipe inclinations', *Int. J. Multiphase Flow* **13**, 1–12.

Chen, J. (2000), 'Logarithmic integrals, interpolation bounds and performance limitations in MIMO feedback systems', *IEEE Transactions on Automatic Control* **AC-45**(6), 1098–1115.

Courbot, A. (1996), 'Prevention of severe slugging in the Dunbar 16" multiphase pipeline', *Offshore Technology Conference, May 6-9, Houston, Texas* .

Godhavn, J., Fard, M. and Fuchs, P. (2005), 'New slug control strategies, tuning rules and experimental results', *Journal of Process Control* **15**(15), 547–577.

Godhavn, J.-M., Strand, S. and Skofteland, G. (2005), 'Increased oil production by advanced control of receiving facilities', *IFAC world congress, Prague, Czech Republic* .

Havre, K. and Skogestad, S. (2002), 'Achievable performance of multivariable systems with unstable zeros and poles', *International Journal of Control* **74**, 1131–1139.

Havre, K., Stornes, K. O. and Stray, H. (2000), 'Taming slug flow in pipelines', *ABB review* **4**(4), 55–63.

Hedne, P. and Linga, H. (1990), 'Supression of terrain slugging with automatic and manual riser choking', *Advances in Gas-Liquid Flows* pp. 453–469.

Hewitt, G. and Roberts, D. (1969), Studies of two-phase flow patterns by simultaneous x-ray and flash photography, Technical report, UKAEA Report AERE M-2159.

Hollenberg, J., de Wolf, S. and Meiring, W. (1995), 'A method to supress severe slugging in flow line riser systems', *Proc. 7th Int. Conf. on Multiphase Technology Conference* .

Minzer, U., Barnea, D. and Taitel, Y. (2004), 'Evaporation in parallel pipes - splitting characteristics', *Int. J. of Multiphase flow* **30**, 763–777.

Sarica, C. and Tengesdal, J. (2000), 'A new teqnique to eliminate severe slugging in pipeline/riser systems', *SPE Annual Technical Conference and Exhibition,Dallas, Texas* pp. pp. 1–9. SPE 63185.

Schmidt, Z., Brill, J. and Beggs, H. (1980), 'Experimental study of severe slugging in a two-phase pipeline-riser system', *Soc. Pet. Eng. J.* pp. 407–414. SPE 8306.

Schmidt, Z., Brill, J. and Beggs, H. D. (1979), 'Choking can eliminate severe pipeline slugging', *Oil & Gas Journal* (12), 230–238.

Siversen, H. and Skogestad, S. (2005), 'Cascade control experiments of riser slug flow using topside measurements', *16th IFAC world congress, Prague* .

Sivertsen, H., Alstad, V. and Skogestad, S. (2008), Medium-scale experiments on stabilizing riser slug flow, To be published.

Sivertsen, H., Godhavn, J.-M., Faanes, A. and Skogestad, S. (2005), 'Dynamic study of a subsea processing system', *Scandinavian Conference on Simulation and Modeling, Trondheim* .

Sivertsen, H., Godhavn, J.-M., Faanes, A. and Skogestad, S. (2006), 'Control solutions for subsea processing and multiphase transport', *ADCHEM, Gremado Brazil April* .

Sivertsen, H. and Skogestad, S. (2005), 'Anti-slug control experiments on a small scale two-phase loop', *ESCAPE'15, Barcelona, Spain* .

Sivertsen, H., Storkaas, E. and Skogestad, S. (2008), Small-scale experiments on stabilizing riser slug flow, To be published.

Skofteland, G. and Godhavn, J. (2003), 'Suppression of slugs in multiphase flow lines by active use of topside choke - field experience and experimental results', *Multiphase '03, San Remo, Italy* .

Skogestad, S. and Postlethwaite, I. (1996), *Multivariable feedback control*, John Wiley & sons.

Spacey, T., Azzopardi, B. and Conte, G. (2000), 'The split of annular two-phase flow at a small diameter t-junction', *Int. J. of Multiphase flow at a small diameter T-junction* **26**, 845–856.

Storkaas, E. (2005), Stabilizing control and controllability: Control solutions to avoid slug flow in pipeline-riser systems, PhD thesis, Norwegian University of Science and Technology.

Storkaas, E. and Godhavn, J. (May 2005), 'Extended slug control for pipeline-riser systems', *Multiphase production technology '05, Barcelona, Spain* .

Storkaas, E., Skogestad, S. and Godhavn, J. (2003), 'A low-dimentional model of severe slugging for controller design and analysis', *Multiphase '03, San Remo, Italy* .

Taitel, Y. (1986), 'Stability of severe slugging', *Int. J. Multiphase Flow* **12**(2), 203–217.

Taitel, Y., Barnea, D. and Dukler, A. (1980), 'Modeling flow pattern transitions for steady upward gas-liquid flow in vertical tubes', *AIChE Journal* **26**, 345–354.

Taitel, Y. and Dukler, A. (1976), 'A model for predicting flow regime transitions in horizontal and near-horizontal gas-liquid flow', *AIChE Journal* **22**, 47–55.

Taitel, Y., Pustylnik, L., Tshuva, M. and Barnea, D. (2003), 'Flow distibution of gas and liquid in parallel pipes', *Int. J. of Multiphase flow* **29**, 1193–1202.

Tshuva, M., Barnea, D. and Taitel, Y. (1999), 'Two-phase flow in inclined parallel pipes', *Int. J. of Multiphase Flow* **25**, 1491–1503.

Appendix A

Experimental data small-scale loop

A.1 Control quality during cascade control experiments

Several experiments were conducted in Section 2 in order to compare the quality of the controllers tested. Some of the results are presented here.

A.1.1 Controlling valve position and inlet pressure

Table A.1 shows the average values during the experiments. The experimental results are plotted in Figures A.1-A.9.

Table A.1: Results using valve position and inlet pressure for control measurements

	Average values				
Setpoint	z	P_1	P_2	ρ	Fw
24	24.19	0.2201	0.0550	288	5.168
25	25.26	0.2190	0.0519	302	5.174
26	26.86	0.2189	0.0500	323	5.171
27	27.69	0.2189	0.0488	388	5.174
28	29.20	0.2169	0.0459	351	5.184
29	29.62	0.2169	0.0452	371	5.190
30	30.87	0.2154	0.0522	367	5.200
31	32.19	0.2171	0.0425	391	5.200
32	34.00	0.2162	0.0399	397	5.200

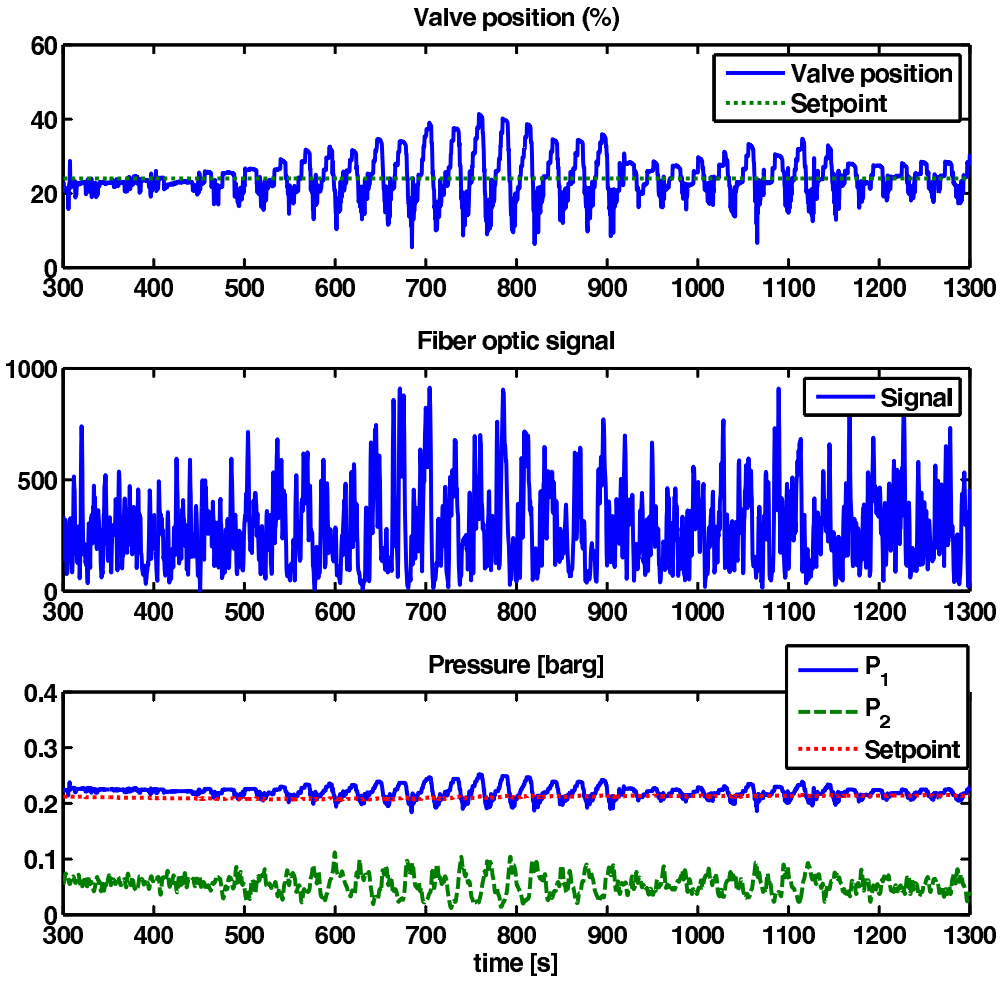

Figure A.1: Control quality when setpoint outer loop is 24%

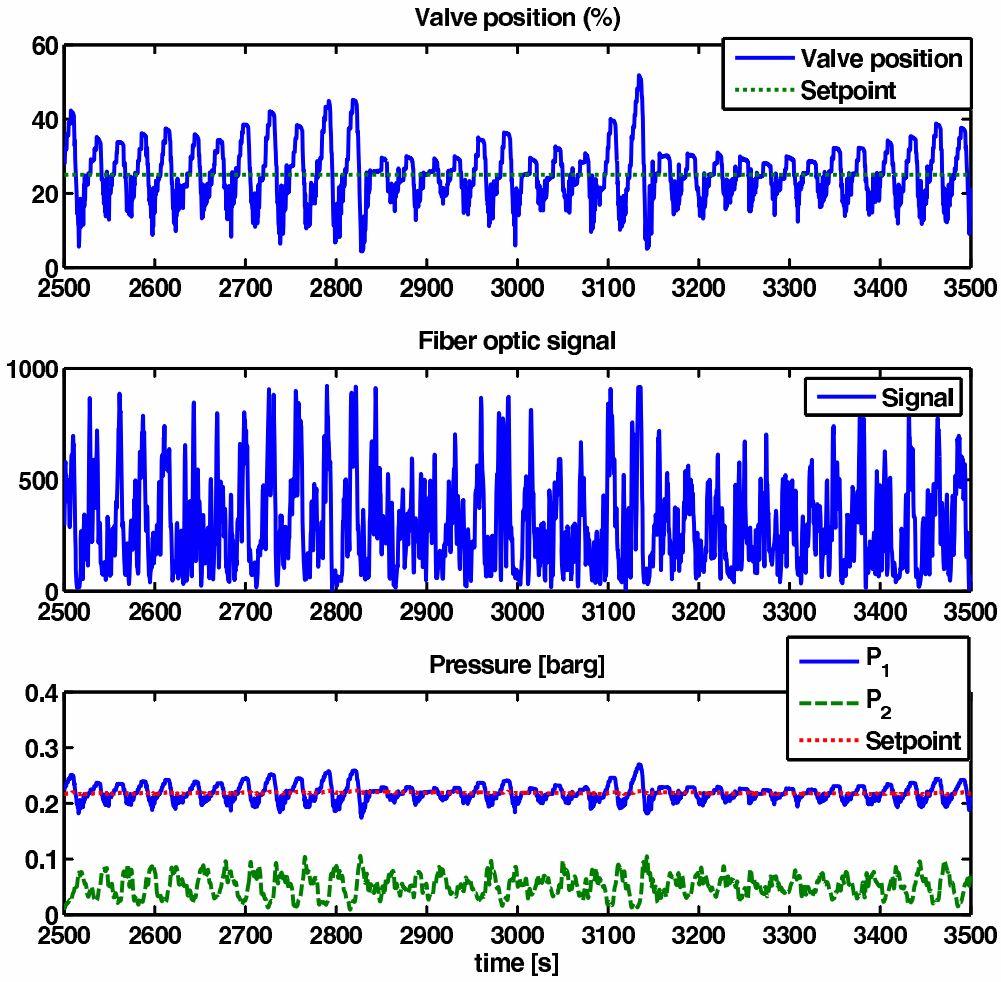

Figure A.2: Control quality when setpoint outer loop is 25%

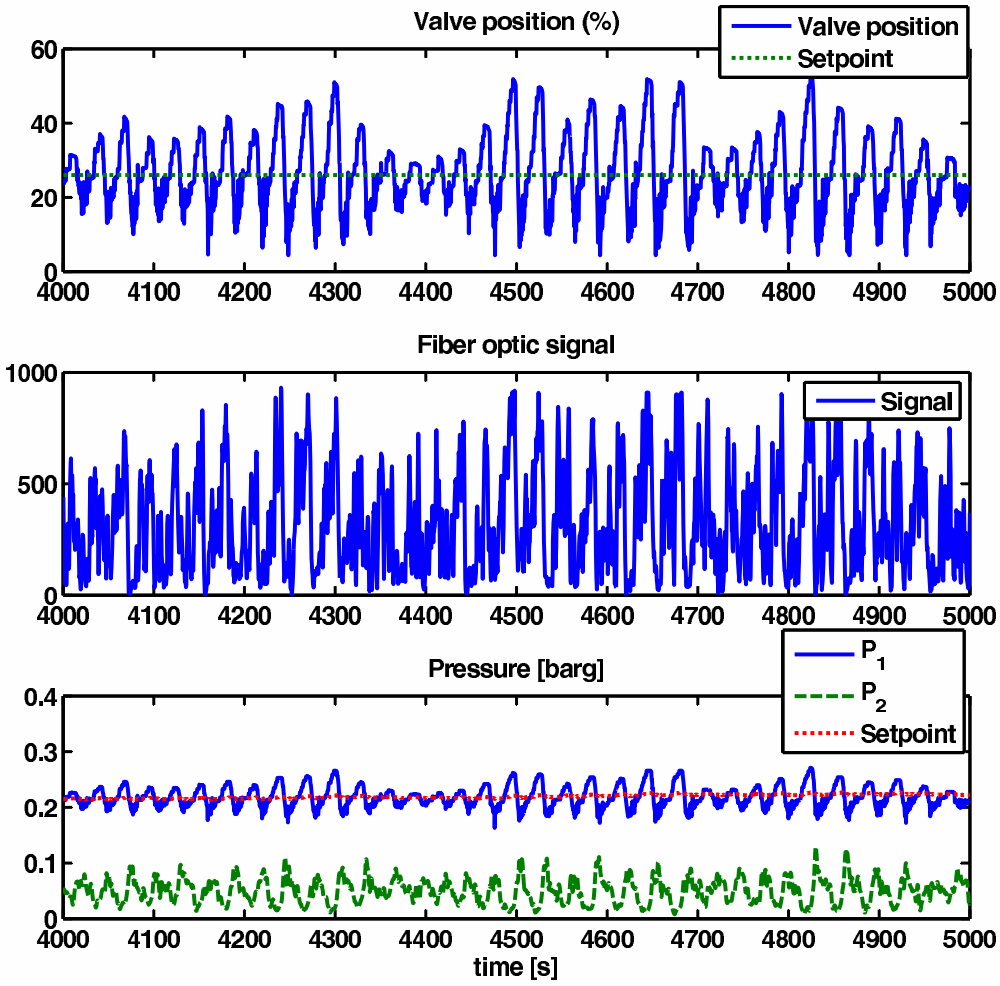

Figure A.3: Control quality when setpoint outer loop is 26%

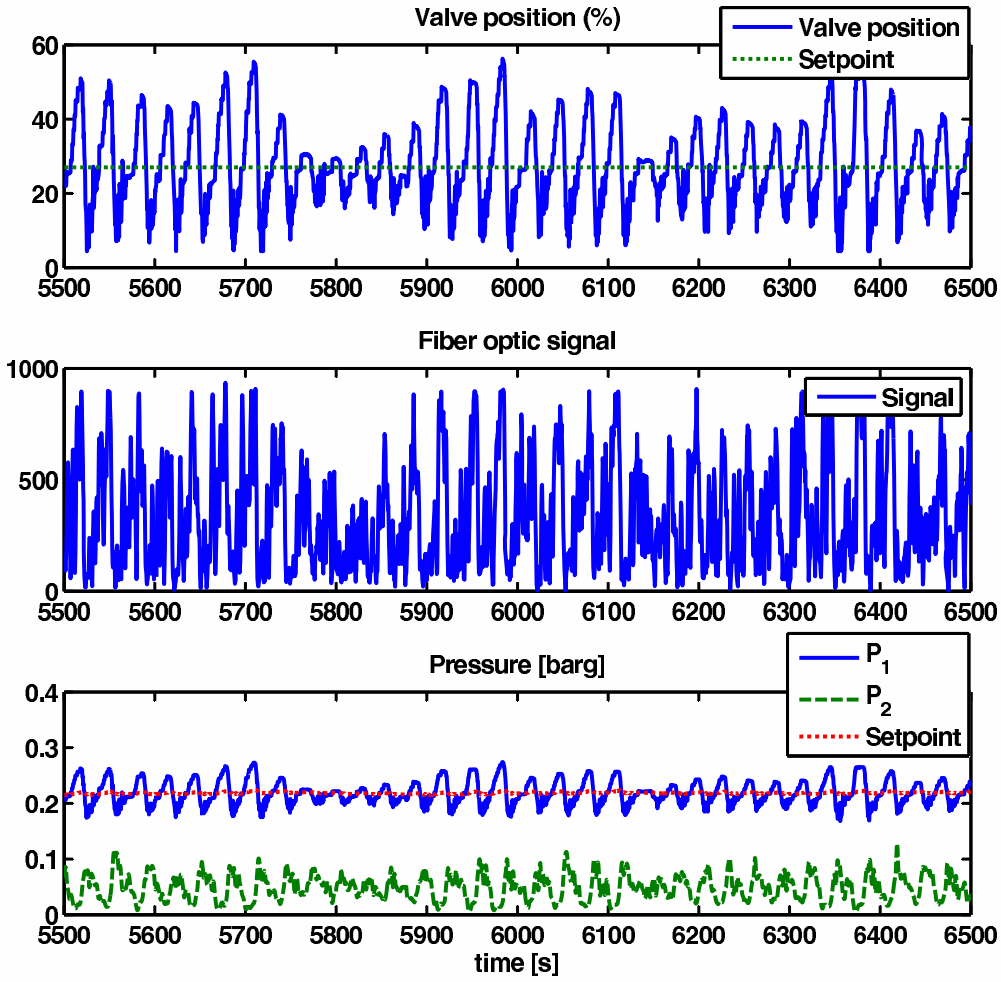

Figure A.4: Control quality when setpoint outer loop is 27%

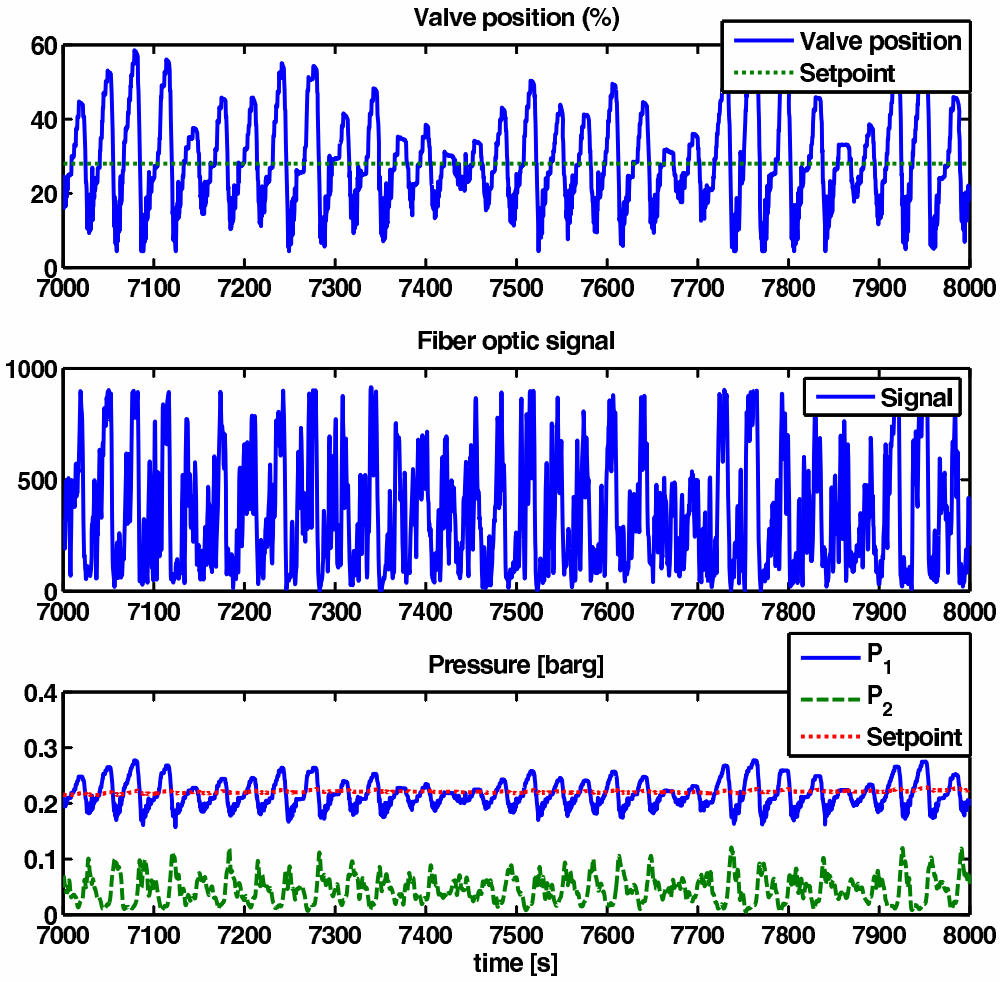

Figure A.5: Control quality when setpoint outer loop is 28%

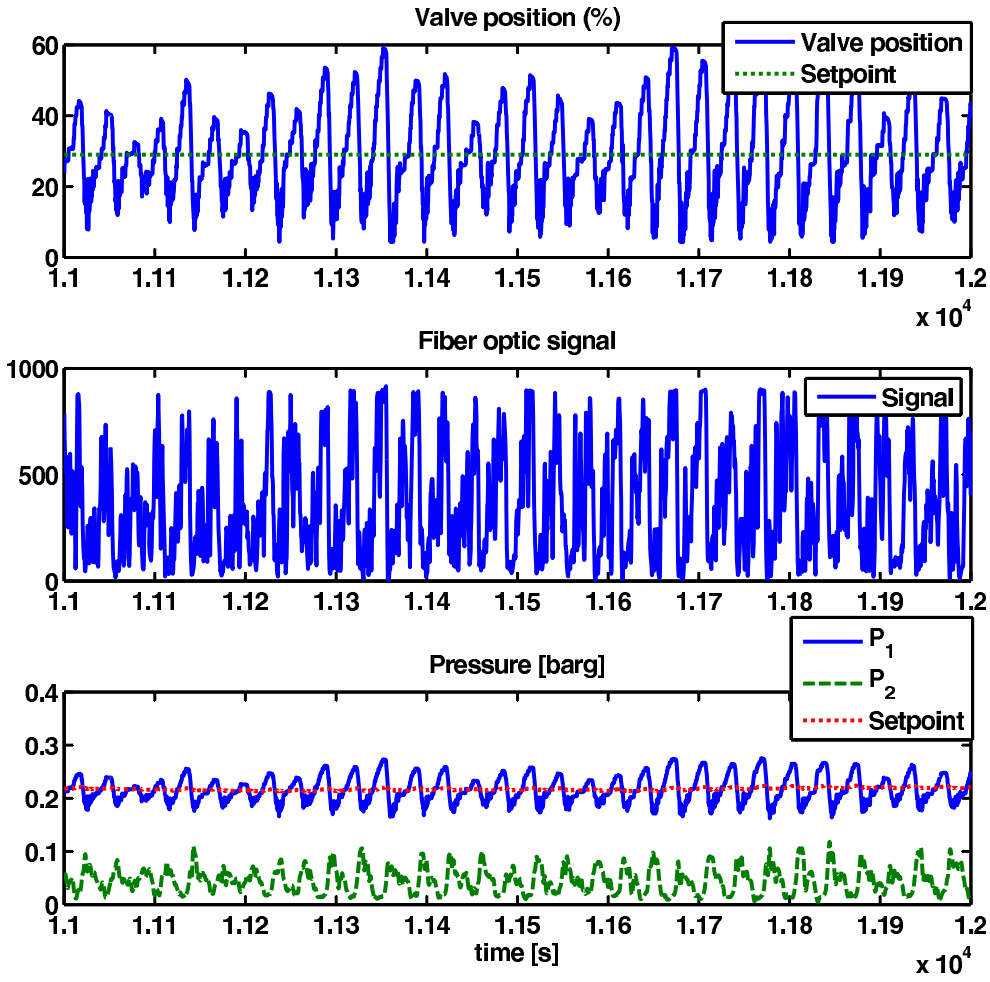

Figure A.6: Control quality when setpoint outer loop is 29%

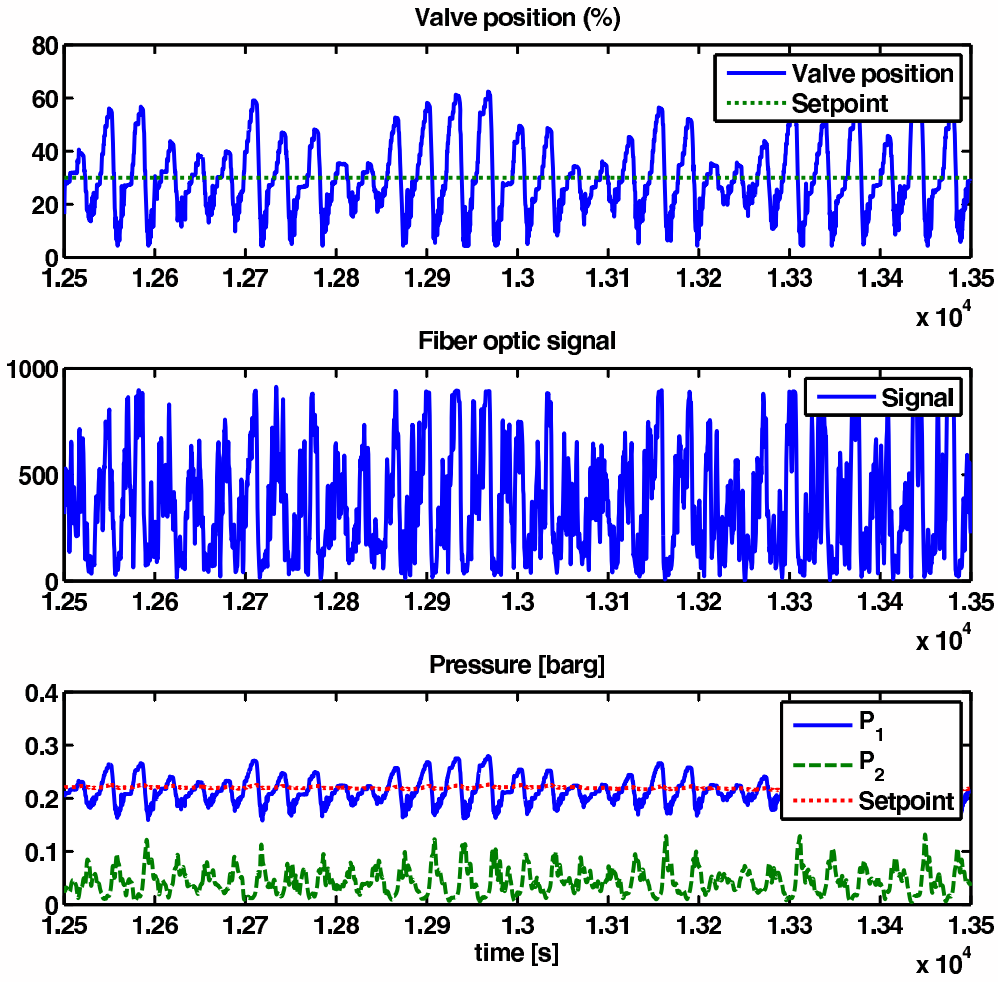

Figure A.7: Control quality when setpoint outer loop is 30%

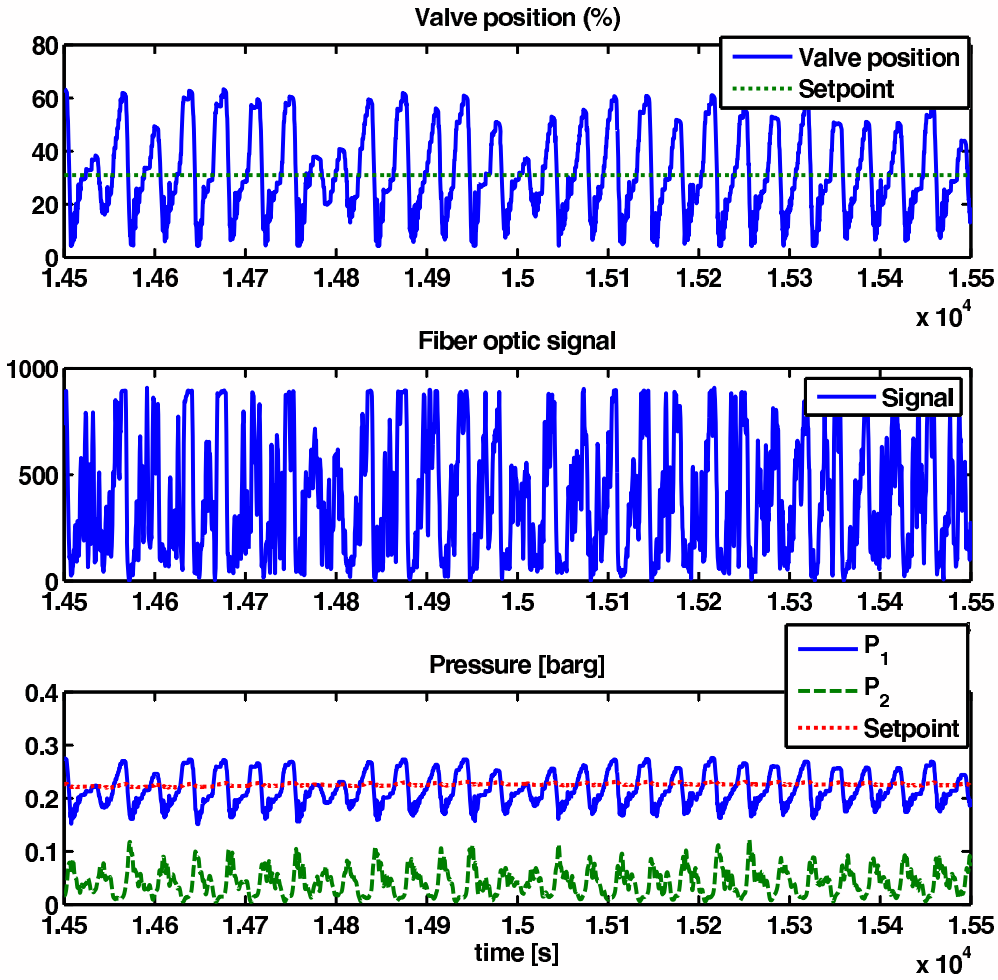

Figure A.8: Control quality when setpoint outer loop is 31%

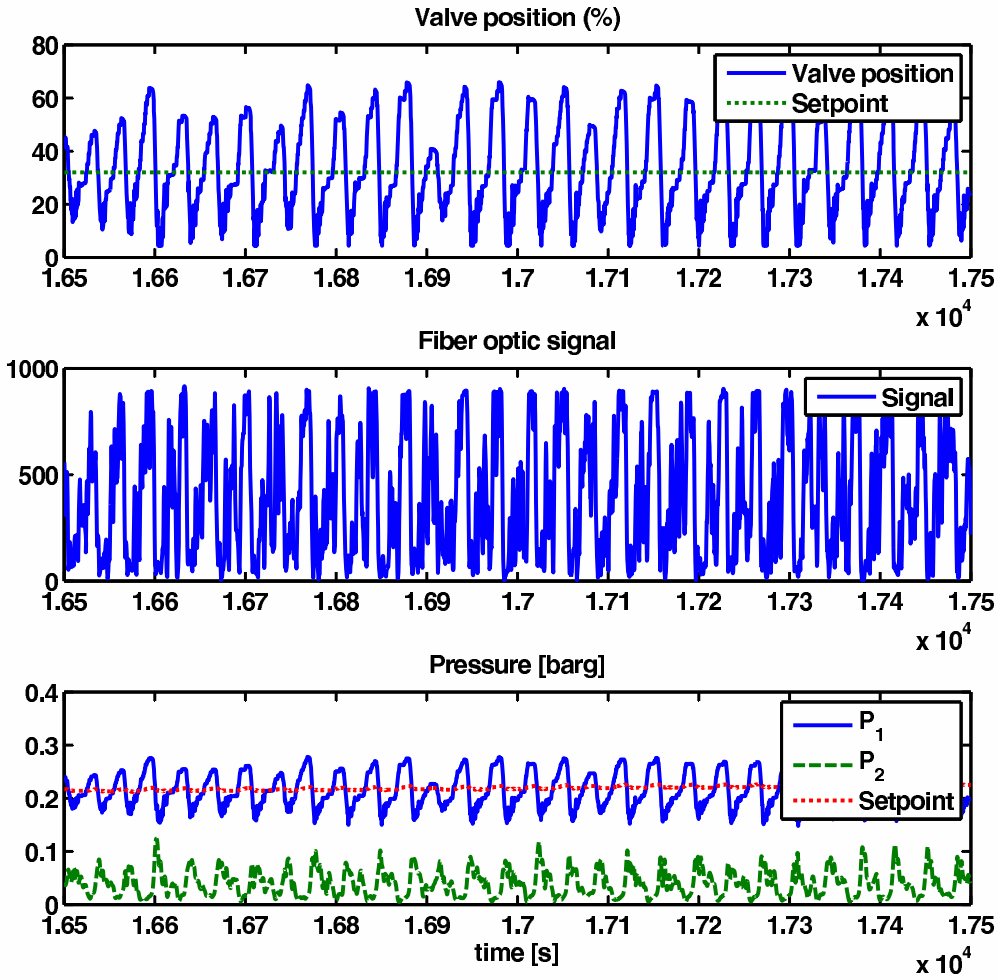

Figure A.9: Control quality when setpoint outer loop is 32%

A.1.2 Controlling valve position and fiber optic signal

Table A.2 shows the average values during the experiments. The experimental results are plotted in Figures A.10-A.11.

Table A.2: Results using valve position and inlet pressure for control measurements

	Average values				
Setpoint	z	P_1	P_2	ρ	Fw
25	24.97	0.2219	0.0566	283	5.230
26	25.95	0.2195	0.0532	277	5.238

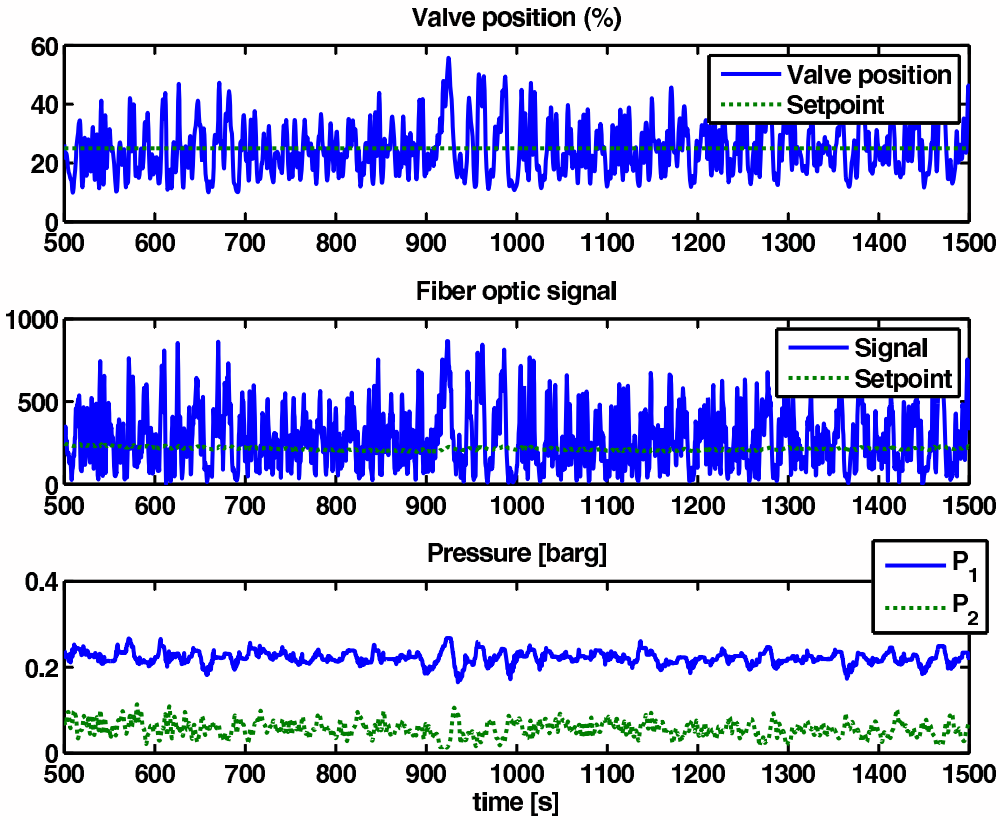

Figure A.10: Control quality when setpoint outer loop is 25%

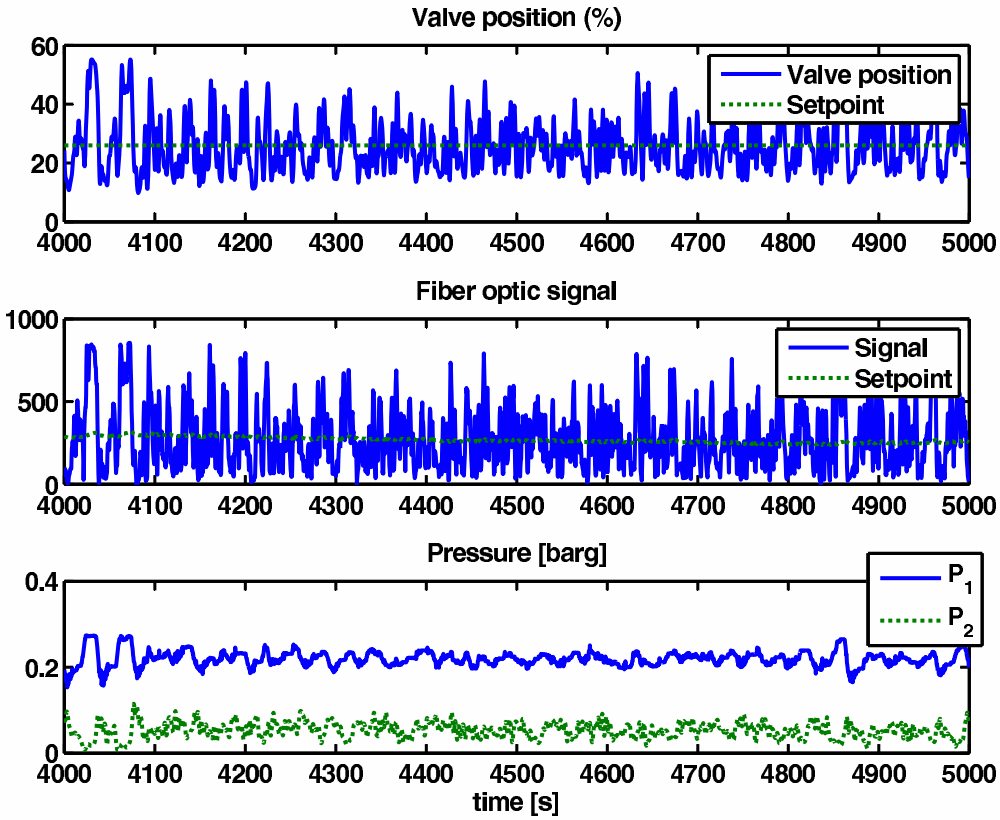

Figure A.11: Control quality when setpoint outer loop is 26%

A.1.3 Controlling topside pressure and fiber optic signal

Table A.3 shows the average values during the experiments. The experimental results are plotted in Figures A.12-A.16.

Table A.3: Results using valve position and topside density for control measurements

	Average values				
Setpoint	z	P_1	P_2	ρ	Fw
0.057	24.66	0.2192	0.0574	284	5.177
0.055	25.25	0.2178	0.0548	295	5.186
0.052	26.22	0.2167	0.0516	289	5.205!
0.050	27.46	0.2153	0.0496	300	5.198
0.048	29.26	0.2179	0.04555	323	5.173!

Figures showing the behavior when increasing the setpoint for the outer loop:

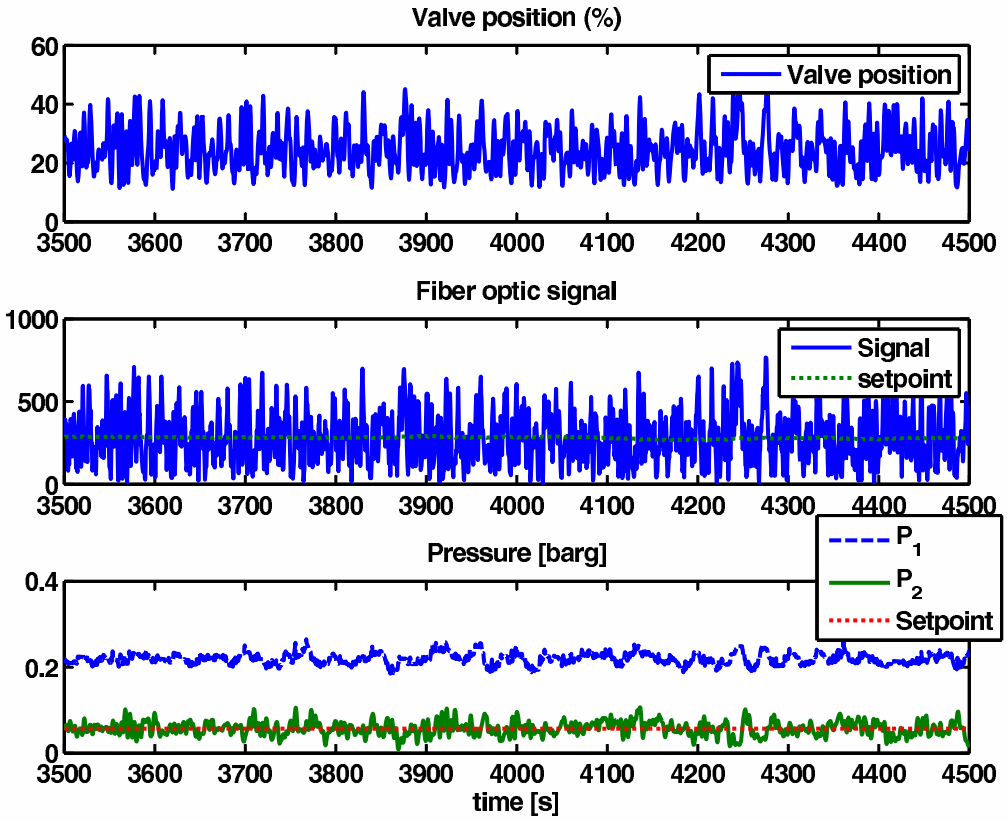

Figure A.12: Control quality when setpoint outer loop is 0.057%

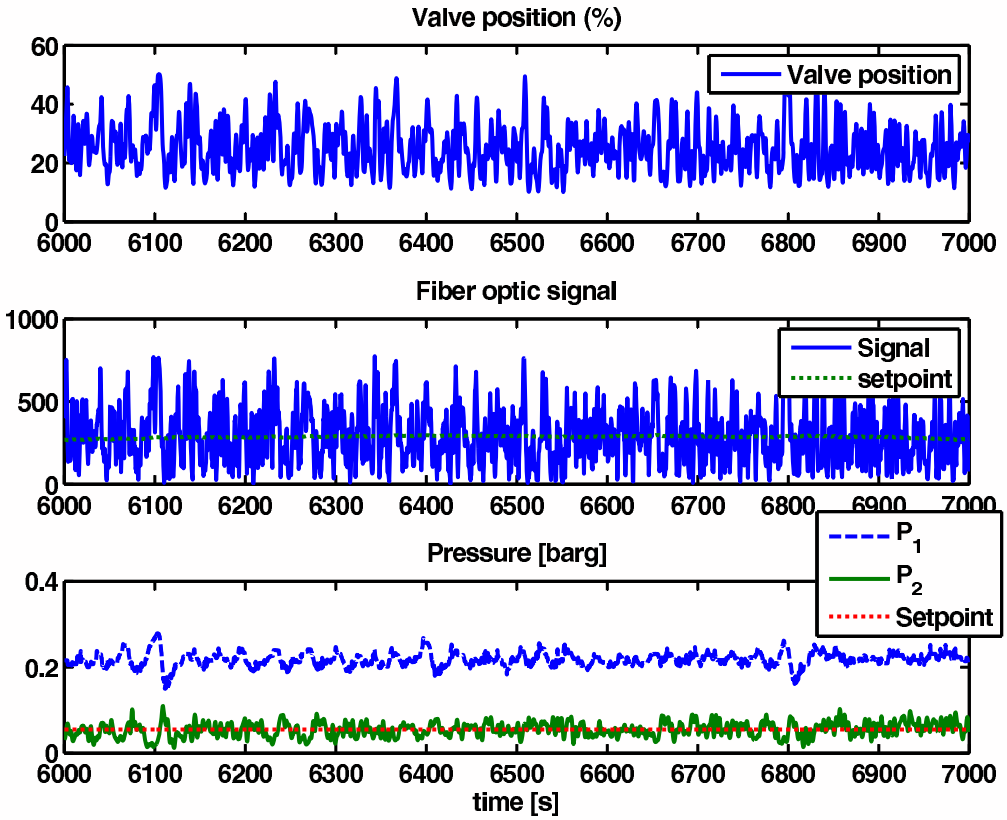

Figure A.13: Control quality when setpoint outer loop is 0.055%

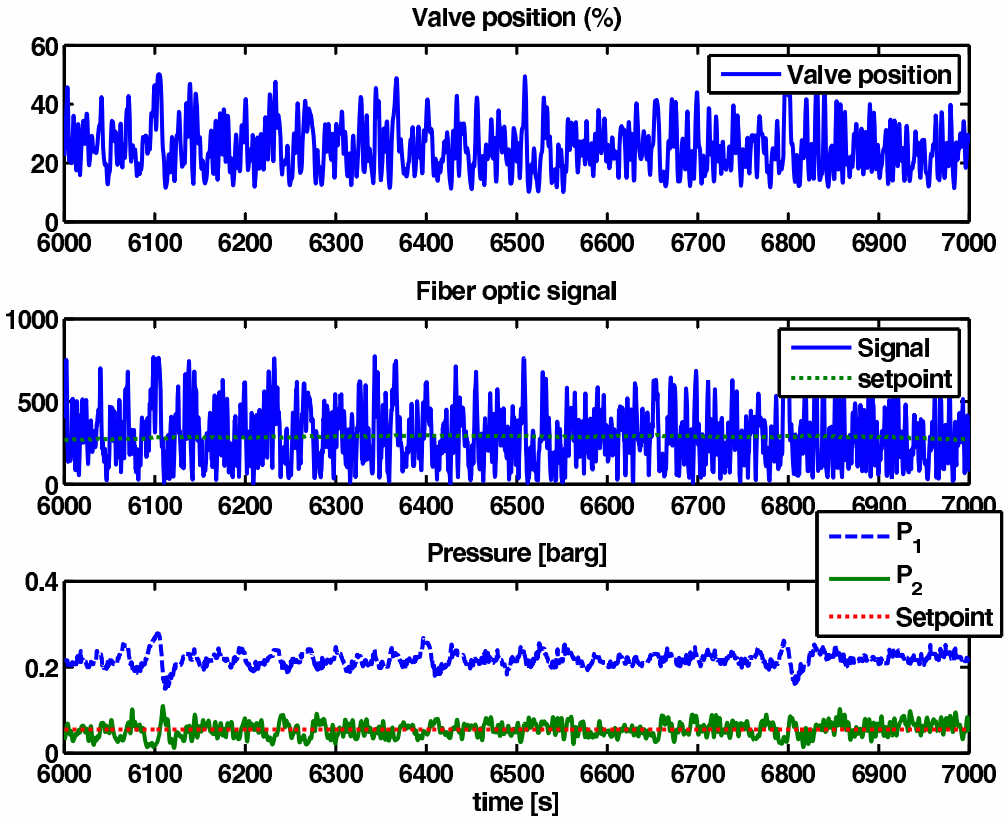

Figure A.14: Control quality when setpoint outer loop is 0.052%

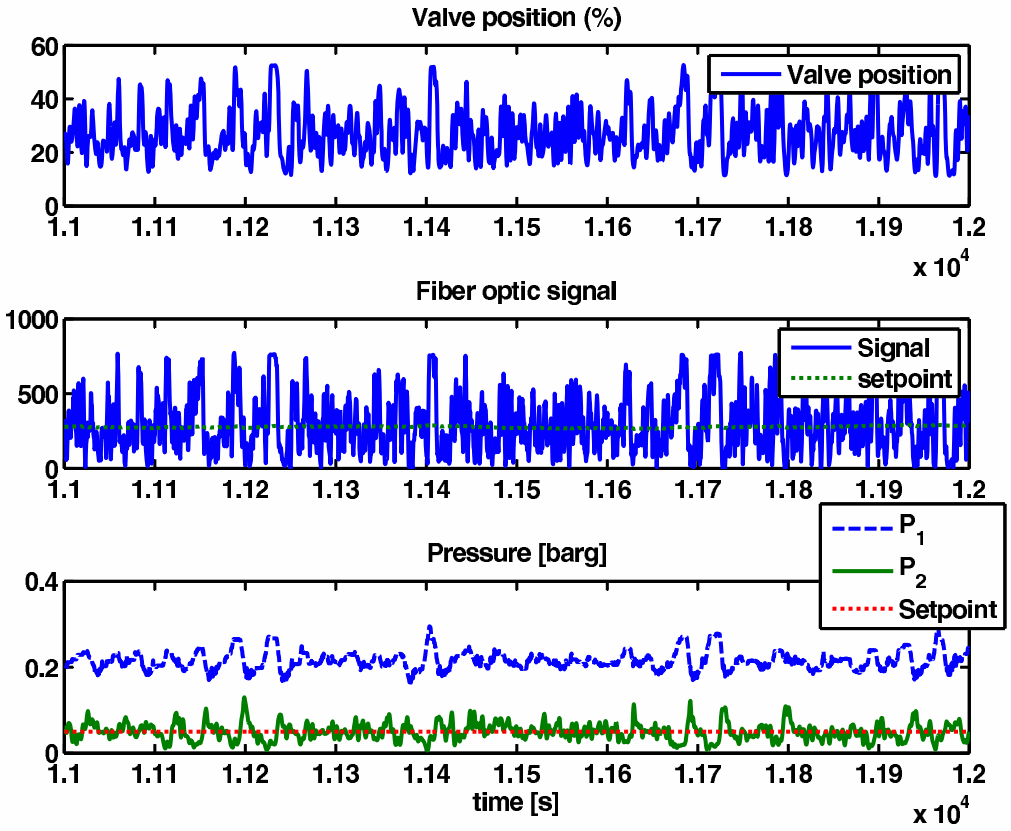

Figure A.15: Control quality when setpoint outer loop is 0.050%

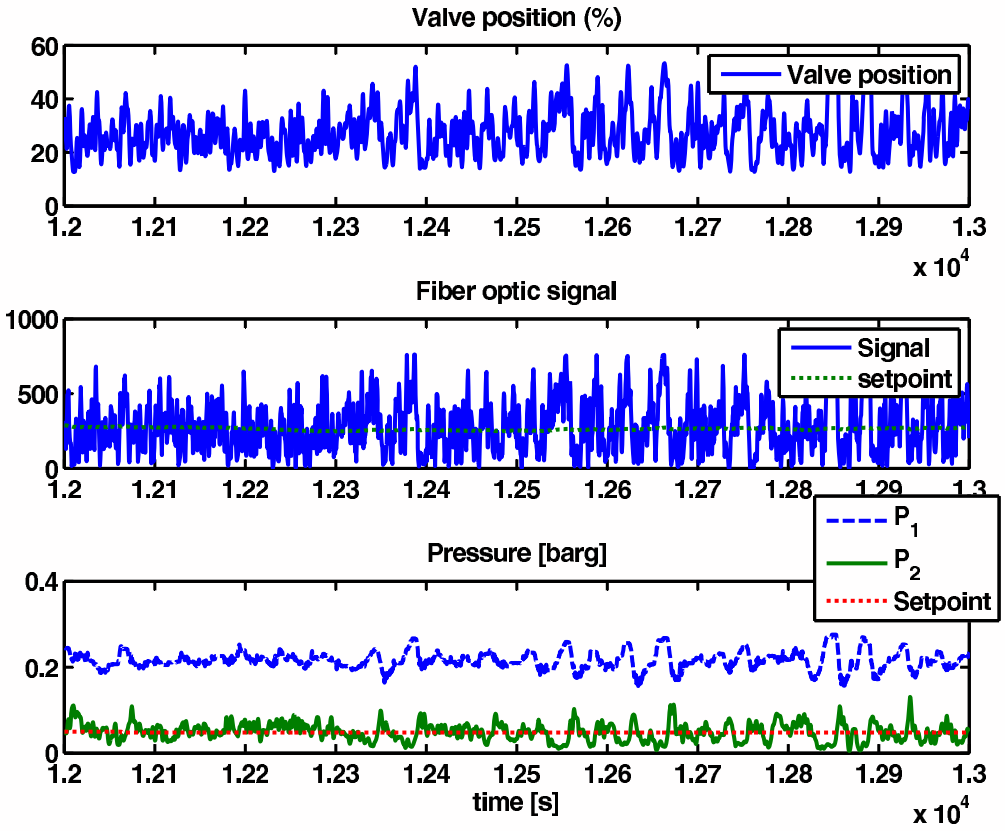

Figure A.16: Control quality when setpoint outer loop is 0.048%

Appendix B

Experimental data medium-scale loop

Plots showing the experimental data of the six cascade controllers presented in Section 3, are presented in Figure B.1. The average values from these experiments are presented in Table 3.4 (Section 3).

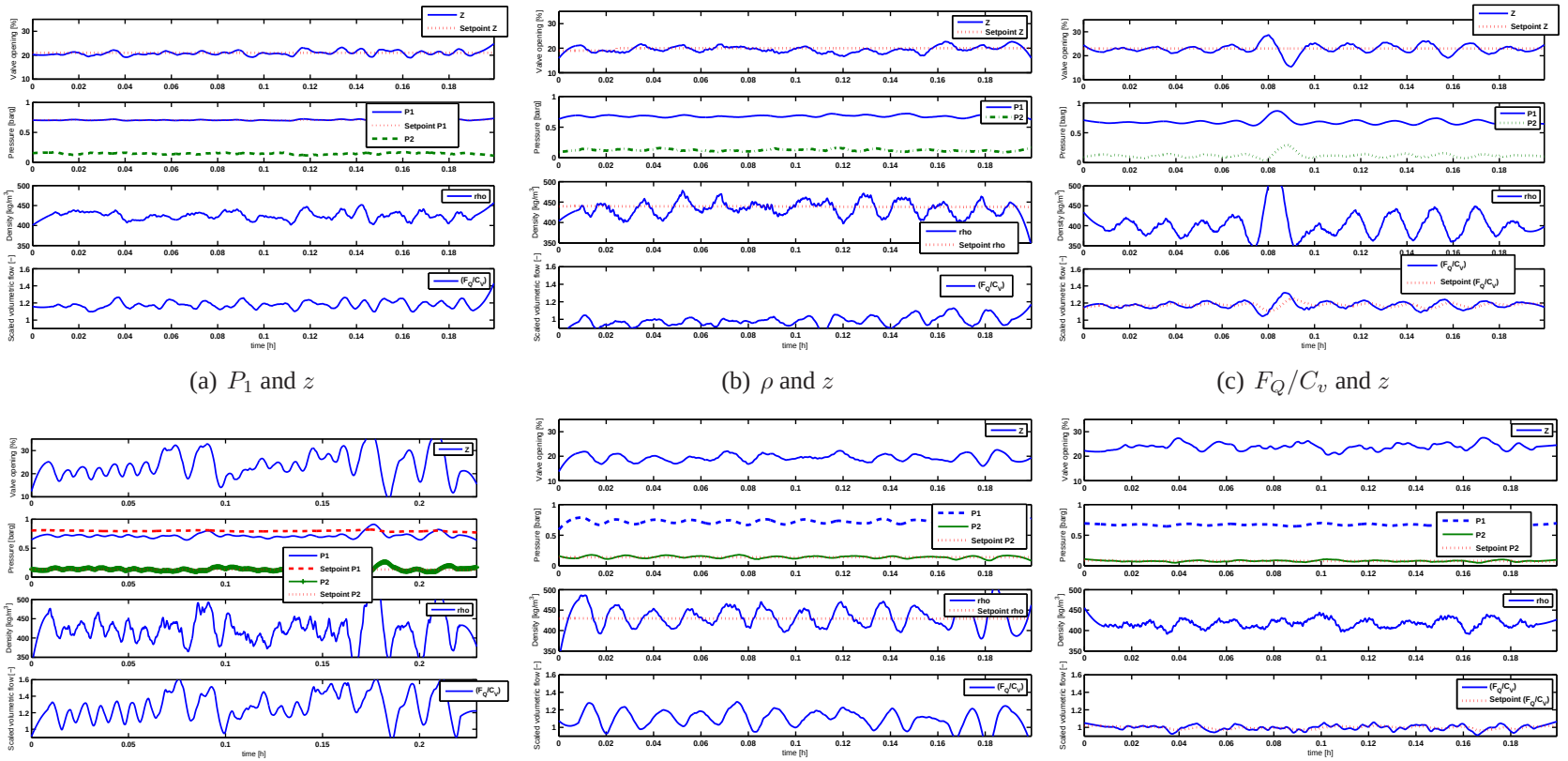

(a) P_1 and z (b) ρ and z (c) F_Q/C_v and z

(d) P_1 and P_2 (e) ρ and P_2 (f) F_Q/C_v and P_2

Figure B.1: Experimental results using six different combinations of measurements, last 12 min before instability

Appendix C

Papers published and for publication

European Symposium on Computer Aided Process Engineering – 15
L. Puigjaner and A. Espuña (Editors)

Anti-slug control experiments on a small-scale two-phase loop

Heidi Sivertsen and Sigurd Skogestad*

Department of Chemical Engineering,
Norwegian University of Science and Technology (NTNU),
N-7491 Trondheim, Norway

Abstract

Anti-slug control applied to two-phase flow provides a very challenging and important application for feedback control. It is important because it allows for operation that would otherwise be impossible, and challenging because of the presence of both RHP-poles and RHP-zeros.
To conduct experiments on pipeline-riser anti-slug control, a small-scale slug-loop has been build. The loop has been modeled and analyzed using a simplified model by Storkaas. The results from this analysis and experimental results using a PI-controller is presented in this paper.

Keywords: feedback control, riser slugging, controllability analysis

1. Introduction

Some of the problems in the offshore oil industry that have received increasingly interest in the last years are related to multiphase flow. In multiphase flow different flow regimes can develop, depending on parameters such as flow rates, fluid properties and pipeline geometry.
Slug flow is a flow regime which can cause a lot of problems for the production facilities. The slug flow is characterized by alternating bulks of gas and oil, and can be further divided into hydrodynamic and terrain induced slugging. Hydrodynamic slugs are caused by velocity differences between the phases and occur in near horizontal pipelines. These slugs are usually short and appear frequently. Terrain induced flow however, can contain a lot of liquid and therefore induce large pressure variations in the system. This flow is induced by low points in the pipeline geometry.
When the low-point is realized by a downsloping pipe terminating in a riser, we get what is known as riser slugging. Because of the large and abrupt fluctuations in pipe pressure and gas and liquid flow rates at the outlet, these slugs cause huge problems for the processing equipment. Unwanted variations in the separator level give rise to poor separation and possible overfilling. The pressure fluctuations wear and tear on the equipment and can sometimes result in unplanned process shutdowns.

* e-mail: skoge@chemeng.ntnu.no; phone: +47-7359-4154; fax: +47-7359-4080

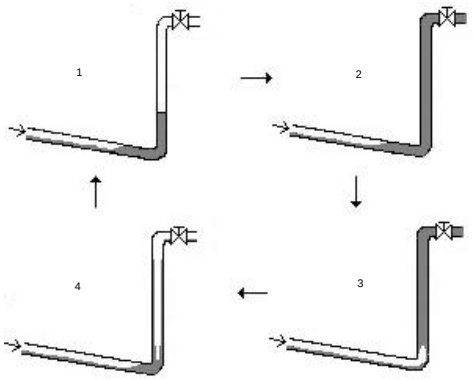

Figure 1. Illustration of the cyclic behavior (slug flow) in pipeline-riser systems

The behavior of pipeline-riser slug flow is illustrated in Figure 1. Liquid accumulates in the lowpoint of the riser, blocking the gas (1). As more gas and liquid enters the system, the pressure will increase and the riser will be filled with liquid (2). After a while the amount of gas that is blocked will be large enough to blow the liquid out of the riser (3). After the blow-out, a new liquid slug will start to form in the lowpoint (4).

Several solutions for eliminating or reducing these problems have been proposed (Sarica and Tengesdal, 2000), but they usually come at a price. Choking the valve at the top of the riser is one example of this. The slugging will disappear, but the increased pressure drop over the valve will lead to a lower production rate.

Stabilizing the flow using active control has been proposed earlier and also tested out both on experimental rigs (Hedne and Linga, 1990) and on offshore installations (Havre et al., 2000) and (Courbot, 1996). It has been proved that it is possibly to stabilize the flow at a pressure drop that would lead to slug flow if left uncontrolled. However, there is still a lot that can be done on deciding which measurements and control configuration gives the best results. Some measurements, like the inlet pressure, can even be hard to implement and maintain.

A small-scale loop (the Miniloop) was build in order to test out and analyze different control strategies in a cheap and easy way. The loop is very simple with a flow consisting of only two phases, air and water. We still get the same slugging phenomenon as expiri-enced offshore, with pressure fluctuations and varying flow rates. This makes it possible to screen different ideas before testing them on larger and more expensive experimental rigs and a lot of money can be saved.

2. Experimental setup

To test different control configurations, a small-scale two-phase flow loop with a pipeline-riser arrangement was build. The flow consists of water and air, which are mixed at the inlet of the system. Both the pipeline and the riser was made of a 20mm diameter trans-parent rubber hose, which makes it easy to change the shape of the system. A schematic diagram of the test facilities is shown in Figure 2.

From the mixing point the flow goes trough the low-point at the bottom of the riser and depending on different conditions, slug flow may occur. At the top of the riser there is a separator, which leads the water to a reservoir. From there the water is pumped back into the system through the mixing point. The air is being let out through a small hole at the

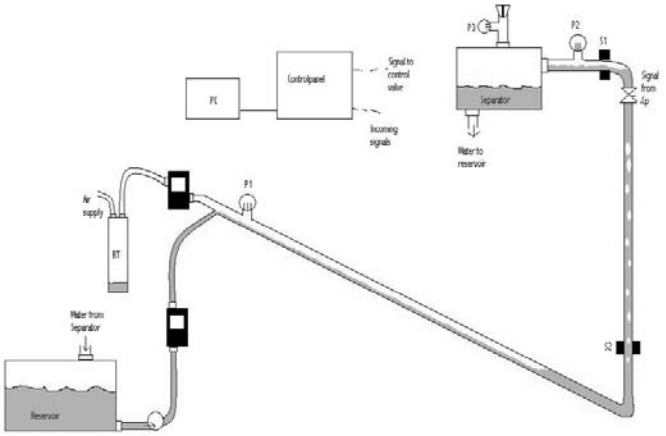

Figure 2. Experimental setup

top of the separator.

For slugging to appear there must be enough air in the system to blow the water out of the 1,5 meter long riser. This requires a certain amount of volume, which is accounted for by a buffer tank (BT) between the air supply and the inlet. The volume of the gas can be changed by partially filling this tank with water.

The flow rates of gas (Qair) and water (Qw) determines whether we will have slug flow in open loop operation or not. These flow rates are being measured upstream the inlet. Typically flow rates during an experiment are 1 l/min for the gas and 3 l/min for the water.

So far there are three pressure sensors located at different places in the loop. One is located at the inlet (P1) while the two others are topside measurements, located at the top of the riser (P2) and at top of the separator (P3). The latter is used for measuring the flow of air out of the separator.

Fiber optic sensors (S1, S2) give a signal depending on the amount of water in the hose where they are located. They can easily be mowed around to measure the holdup at different locations in the loop.

A control valve is placed at the top of the riser. A signal from the control panel sets the opening percentage of the valve.

The control panel converts the analog signals from the sensors into digital signals. These signals are then sent to a computer. The signals are continuously displayed and treated using Labview software. Depending on the control configuration, some of the measurements are used by the controller to determine the opening percentage for the control valve.

3. Controllability Analysis

Storkaas et al. (2003) have developed a simplified macro-scale model to describe the behavior of pipeline-riser slugging. The model has three states; the holdup of gas in the feed section (m_{G1}), the holdup of gas in the riser (m_{G2}), and the holdup of liquid (m_L). Using this model we are able to predict the variation of system properties such as pressure, densities and phase fractions.

In order for the model to fit the MiniLoop, it needs to be tuned. To do this we compare the bifurcation diagrams for the model and the Miniloop, plotted in Figure 3. The upper lines shows the maximum pressure at a particular valve opening and the lower line shows the

minimum pressure. The two lines meet at around 20% valve opening. This is the point with the highest valve opening which gives stable operation when no control is applied. When Storkaas' model is properly tuned, the bifurcation point from the model will match the one from the experimental data. The dashed line in the middle shows the unstable steady-state solution, which is the desired operating line with closed-loop operation.

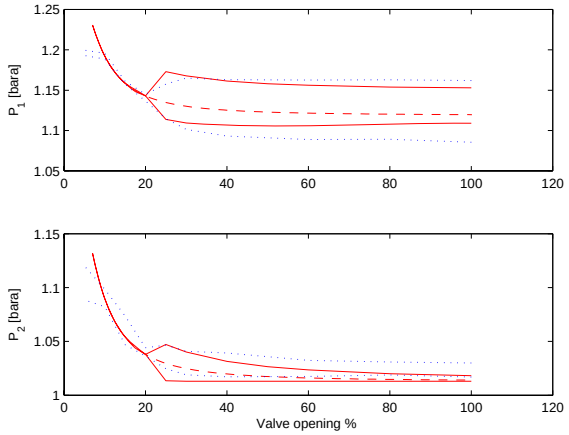

Figure 3. Bifurcation diagrams from experimental data (dotted line) and Storkaas' model (solid line)

When the model is tuned it can be used to perform a controllability analysis on the system. This way we can predict which measurements are suitable for control, thus avoiding slug flow. The analysis shows that the system consists of the poles given in Table 1.

Table 1. Poles of the system for valve openings z=0.12 and z=0.25

z	
0.12	0.25
-20.3411	-35.2145
-0.0197 $\pm$ 0.1301i	0.0071 $\pm$ 0.1732i

Since all poles of the system are in the LHP when using a valve opening of 12%, this valve opening results in stable flow in the pipeline. However, when the valve opening is set to 25% we get a pair of RHP poles leading to riser slugging. This could also be predicted from the bifurcation diagram in Figure 3.
To stabilize the flow we have available several measurements. Four of these are topside measurements; pressure P_2, density ρ, volume flow F_q and mass flow F_w. The fifth measurement is the inlet pressure, P_1. The zeros of the system using different measurements are given in Table 2.

Table 2. Zeros of the system using different measurements at valve opening z=0.25

P_1	P_2	ρ	F_q	F_w
-1.285	46.984	0.092	-3.958	-65.587
	0.212	-0.0547	-0.369 $\pm$ 0.192i	-0.007 $\pm$ 0.076i

It is well known that stabilization (shifting of poles from RHP to LHP) is fundamentally difficult if the plant has a RHP-zero close to the RHP-poles. From this, we expect no

particular problems using P_1 as the measurement. Also, F_q and F_w could be used for *stabilization*, but we note that the steady-state gain is close to zero (due to zeros close to the origin), so good control *performance* can not be expected. On the other hand, it seems difficult to use ρ or P_2 for stabilization because of presence of RHP-zeros.
From the controllability analysis we therefore can draw the conclusion that when using only one measurement for control, the inlet pressure P_1 is the only suitable choice.

4. Experimental results

The analysis showed that using the inlet pressure P_1 was the only possibility when using only one measurement for control. Based on this, a PI-controller was used to control the system using this measurement.
The MiniLoop was first run open loop for two minutes, with a valve opening of 30%. This is well inside the unstable area, as the bifurcation diagram shows. The result is the pressure oscillations plotted in Figure 4, which illustrates how the pressure and valve opening varies with time. Both experimental and simulated values using the simplified model are plotted.
When the controller is activated after two minutes, the control valve starts working. The flow is almost immediately stabilized, even though the average valve opening is still within the unstable area. It remains that way until the controller is turned of again after 8 min. When the controller is turned off, the pressure starts oscillating again.

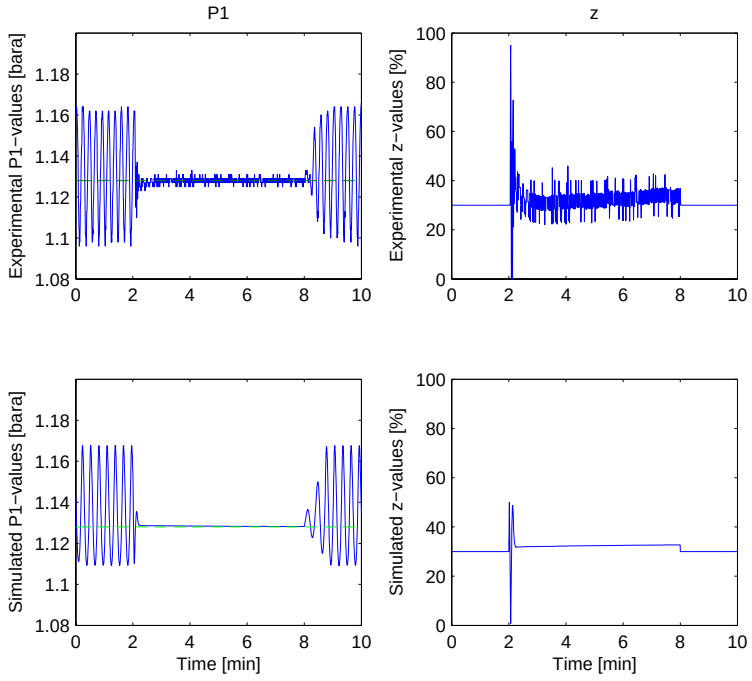

Figure 4. Experimental and simulated results using a PI-controller

From Figure 4 we see that the controller efficiently stabilizes the flow, confirming the results from the analysis. However, this measurement can be difficult to use in offshore installations because of its location.

Using other control configurations or measurements other than the ones analyzed in this paper might be the solution if there are only topside measurements available. The plan is to test out different ways to do this in the near future. The first possibility that will be explored, is using a cascade configuration involving the topside pressure P_2 and one of the flow measurements F_w or F_q. Storkaas and Skogestad (2003) have proved theoretically that this works for another case of riser slugging.

5. Conclusion

From the controllability analysis it was found that using the bottom hole pressure was the only measurement of the five measurements analyzed, that could be used for controlling the system. The experiments confirmed that the model used for the analysis was good, and that using this measurement we where able to control the flow without problems.
We are, however, looking for other ways to control the flow because of the problems related to down hole measurements. When using some of the other measurements analyzed, we must use combinations of measurements in order to avoid the problems related to the zeros introduced.

References

Courbot, A. (1996). Prevention of Severe Slugging in the Dunbar 16“ Multiphase Pipeline. Offshore Technology Conference, May 6-9, Houston, Texas.

Havre, K., Stornes, K. and Stray, H. (2000). Taming Slug Flow in Pipelines. *ABB review*, 4:pp. 55–63.

Hedne, P. and Linga, H. (1990). Supression of Terrein Slugging with Automatic and Manual Riser Choking. *Advances in Gas-Liquid Flows*, pp. 453–469.

Sarica, C. and Tengesdal, J. (2000). A new teqnique to eliminating severe slugging in pipeline/riser systems. SPE Annual Technical Conference and Exibition, Dallas, Texas. SPE 63185.

Storkaas, E. and Skogestad, S. (2003). Cascade control of Unstable Systems with Application to Stabilization of Slug Flow.

Storkaas, E., Skogestad, S. and Godhavn, J. (2003). A low-dimentional model of severe slugging for controller design and analysis. In *Proc. of MultiPhase ’03, San Remo, Italy, 11-13 June 2003*.

CASCADE CONTROL EXPERIMENTS OF RISER SLUG FLOW USING TOPSIDE MEASUREMENTS

Heidi Sivertsen * **Sigurd Skogestad** *,[1]

* *Department of Chemical Engineering, Norwegian University of Science and Technology, Trondheim, Norway*

Abstract: Anti-slug control applied to two-phase flow provides a very challenging and important application for feedback control. It is important because it allows for operation that would otherwise be impossible, and challenging because of the presence of both RHP-poles and RHP-zeros.
To conduct experiments on pipeline-riser anti-slug control, a small-scale slug-loop has been build. The loop has been modelled and analyzed using the simplified riser-slug model by Storkaas. The aim has been to find ways to control the flow using only topside measurements, as subsea measurements can be unavailable offshore. The results from this analysis and experimental results using a cascade controller are presented in this paper.

Keywords: Cascade control, unstable, poles, feedback control, controllability analysis

1. INTRODUCTION

Riser slugging is a flow regime that can develop in multiphase production systems offshore. It is characterized by alternating bulks of liquid and gas caused by a low-point in the pipeline topography. This low-point is realized by a downsloping pipe terminating in a riser.

This flow regime can cause large and abrupt fluctuations in pipe pressure and gas and liquid flow rates at the outlet. Some of the problems associated with this flow are wear and tear on equipment and poor separation.

The behavior of pipeline-riser slug flow is illustrated in Figure 1. Liquid accumulates in the lowpoint of the riser, blocking the gas (1). As more gas and liquid enters the system, the pressure will increase and the riser will be filled with liquid (2). After a while the amount of gas that is blocked will be large enough to blow the liquid out of the riser (3). After the blow-out, a new liquid slug will start to form in the low-point (4).

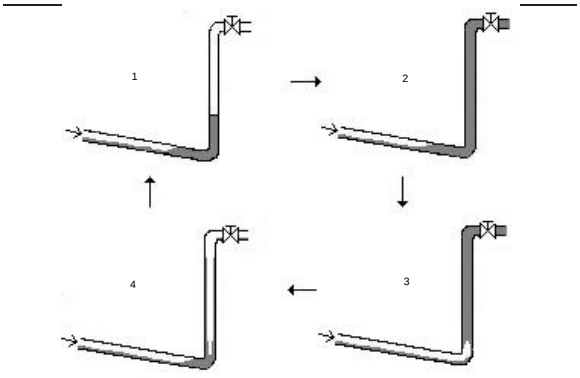

Fig. 1. Illustration of the cyclic behavior (slug flow) in pipeline-riser systems

Recently, anti-slug control has proven to successfully stabilize the flow at a pressure drop that would lead to slug flow if left uncontrolled. This has been done both in experiments (Hedne and Linga, 1990) and on offshore production facilities (Havre *et al.*, 2000) and (Godhavn *et al.*, 2005*a*).

[1] Author to whom correspondence should be adressed: skoge@chemeng.ntnu.no

The above applications use subsea measurements, which are expensive to install and maintain and are sometimes unavailable. For this reason ways to control the flow using only topside measurements are sought.

A small-scale experiment (the Miniloop) has been build to test different control strategies. Use of a simple PI-controller with a subsea pressure measurement gave good results as expected from a controllability analysis of the system (Sivertsen and Skogestad, 2005). This analysis also indicated large problems using a single topside measurement for control.

In this paper, we consider combinations of topside measurements that might be able to stabilize the flow. One example of this is a cascade control configuration, where two topside measurements are combined.

2. EXPERIMENTAL SETUP

To test different control configurations, a small-scale two-phase flow loop with a pipeline-riser arrangement was build. The flow consists of water and air, which are mixed at the inlet of the system. Both the pipeline and the riser was made of a 20mm diameter transparent rubber hose, which makes it easy to change the shape of the system. A schematic diagram of the test facilities is shown in Figure 2.

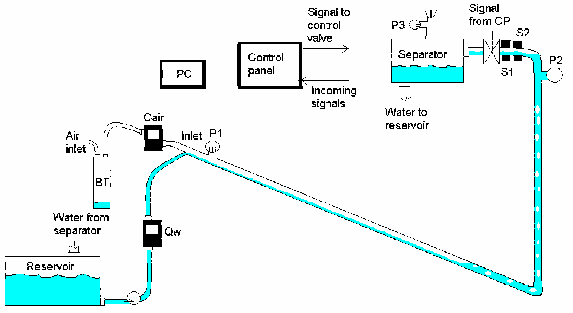

Fig. 2. Experimental setup

From the mixing point the flow goes trough the low-point at the bottom of the riser and depending on different conditions, slug flow may occur. At the top of the riser there is a separator, which leads the water to a reservoir. From there the water is pumped back into the system through the mixing point. The air is being let out through a small hole at the top of the separator.

For slugging to appear there must be enough air in the system to blow the water out of the 1,5 meter long riser. This requires a certain amount of volume, which is accounted for by a buffer tank (BT) between the air supply and the inlet. The volume of the gas can be changed by partially filling this tank with water.

The flow rates of gas (Qair) and water (Qw) determines whether we will have slug flow in open loop operation or not. These flow rates are measured at the inlet. Typically flow rates during an experiment are 1 l/min ($1.4 * 10^{-3}$ kg/min) for the gas and 3 l/min (3 kg/min) for the water.

A pressure sensor is located at the inlet (P1), and there are two pressure sensors located topside. One is placed at the top of the riser (P2) and one at top of the separator (P3). The latter is used for measuring the flow of air out of the separator.

There are two fiber optic sensors (S1, S2). These give a signal depending on the amount of water in the pipe. They can easily be mowed around to measure the hold-up at different locations in the loop.

A control valve is placed at the top of the riser. A signal from the control panel sets the opening percentage of the valve.

The control panel converts the analog signals from the sensors into digital signals. These signals are then sent to a computer. The signals are continuously displayed and treated using Labview software. Depending on the control configuration, some of the measurements are used by the controller to determine the opening percentage for the control valve.

2.1 Flow estimates

From the values given by the fiber-optic slug sensors the relative amount of water and air through the choke is found, which makes it possible to calculate the density of the mixture. The topside pressure sensor gives us the pressure drop over the control valve. Given pressure drop and density it is then possible to calculate the mass and volume flow through the choke, using a basic flow equation for volume flow (1).

$$Q = C * z * \sqrt{\Delta P / \rho} \tag{1}$$

The measurements from the fiber optic slug sensors needed some filtering because of spikes caused by reflections off the light on the water/air interface (Figure 3). Since these measurements where crucial for the flow estimates, the question was whether or not they had to be filtered too much for them to be used for control.

3. CONTROLLABILITY ANALYSIS

Storkaas *et al.* (2003) have developed a simplified model to describe the behavior of pipeline-riser slugging. The model is well suited for controller design and analysis. It consists of three states; the holdup of

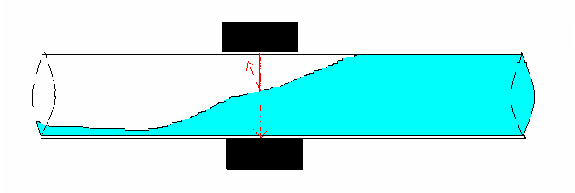

Fig. 3. Reflection of light on water surface

gas in the feed section (m_{G1}), the holdup of gas in the riser (m_{G2}), and the holdup of liquid (m_L). The model is illustrated by Figure 4. Using this model we are able to predict the variation of system properties such as pressure, densities and phase fractions.

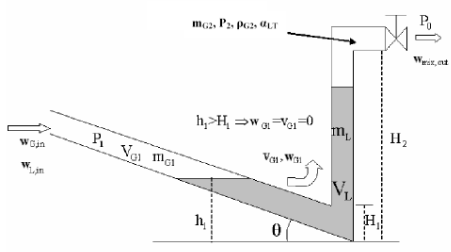

Fig. 4. Storkaas' pipeline-riser slug model

In order for the model to fit the MiniLoop, it needs to be tuned. To do this we compare the bifurcation diagrams of the model and the Miniloop. These diagrams are plotted in Figure 5. The upper lines shows the maximum pressure at a particular valve opening and the lower line shows the minimum pressure. The two lines meet at around 20% valve opening. This is the point with the highest valve opening which gives stable operation when no control is applied. When Storkaas' model is properly tuned, the bifurcation point from the model will match the one from the experimental data. The dotted line in the middle shows the unstable steady-state solution. This is the desired operating line with closed-loop operation. Details about the tuned model are given by (Storkaas, 2005).

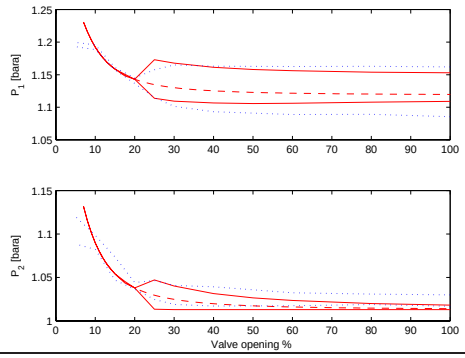

Fig. 5. Bifurcation diagrams from experimental data (dotted line) and Storkaas' model (solid line)

The tuned model can be used to perform a controllability analysis. This way we can predict which measurements are suitable for control, thus avoiding slug flow. The computed poles of the process at the valve position $Z = 0.12$ and $Z = 0.25$ are given in Table 1.

Table 1. Poles of the system

Valve opening Z	
0.12	0.25
-20.3411	-35.2145
-0.0197 $\pm$ 0.1301i	0.0071 $\pm$ 0.1732i

A valve opening of 12% results in only LHP poles, so running open loop with this valve opening will lead to stable flow in the pipeline. However, when the valve opening is set to 25% a pair of RHP poles indicates an unstable system.

This means that riser slugging will occur when the system is run open loop with this valve opening. These results could also be predicted from the bifurcation diagram in Figure 5, where we see that the system goes unstable for valve openings larger than 20%.

To stabilize the flow the measured topside pressure, P_2, and the estimated topside density ρ, volume flow F_q and mass flow F_w are available. The upstream pressure measurement P_1 is also available.

Unstable poles need feedback for stabilization, and place a lower bound on the bandwidth of the feedback system. It is well known that stabilization (shifting of poles from RHP to LHP) is fundamentally difficult if the plant has a RHP-zero close to a RHP-pole p. Skogestad and Postlethwaite (1996) derives the approximate *lower* bandwidth limit $w_c > 1.15|p|$ for imaginary RHP poles of magnitude $|p|$. For a real RHP zero z they derive an *upper* bandwidth limit $w_c < z/2$. From the 25% valve opening we see that all RHP zeros need to be larger than approximately 0.4 to be able to stabilize the system.

To find suitable measurements for control, the open-loop zeros for the system need to be inspected. They are given in Table 2.

Table 2. Open loop zeros of the system for different measurement alternatives

P_1	P_2	ρ	F_q	F_w
-1.285	46.984	0.092	-3.958	-65.587
	0.212	-0.0547	-0.369 $\pm$ 0.192i	-0.007 $\pm$ 0.076i

Because of the bandwidth limitations it seems evident that measurements ρ or P_2 cannot be used for stabilization. Measurement P_1 does not have any RHP zeros, so no particular problems using this measurement are to be expected. Also F_q and F_w could be used for *stabilization*. However the zeros close to the origin indicates a steady-state gain close to zero, so good control *performance* cannot be expected. The steady-state gain for F_q and F_w are found to be 0.4545 and 0.0015 respectively. Using these measurements we may be able to stabilize the system, but we cannot

affect its steady-state behavior and the system will "drift".

From the controllability analysis we can draw the conclusion that when using only a single measurement for control, the inlet pressure P_1 is the only suitable choice.

However, in many cases only topside measurements are available, and even though none of the topside measurements can be used as a single measurement, there is still the possibility that combinations of these measurements can stabilize the flow. The reason is that systems with extra outputs generally have no zeros, except when the same RHP-zero appears in all outputs. Table 2 shows that this is not the case here.

One possibility is to use a cascade control configuration with the flow measurements F_q or F_w in the inner loop and P_2 as measurement for the outer loop. The outer loop will then take care of the low-frequency performance in the system, while the flow measurement are used only for stabilization.

4. EXPERIMENTAL RESULTS

4.1 PI-controller

The above analysis showed that the inlet pressure, P_1, was the only suitable choice when using a single measurement for control. Experiments on the lab confirm that a PI-controller (Figure 6) using this measurement stabilizes the flow. The controller has a setpoint of $1.128bara$, gain $K = -2.5bara^{-1}$ and integral time $\tau_i = 10s$.

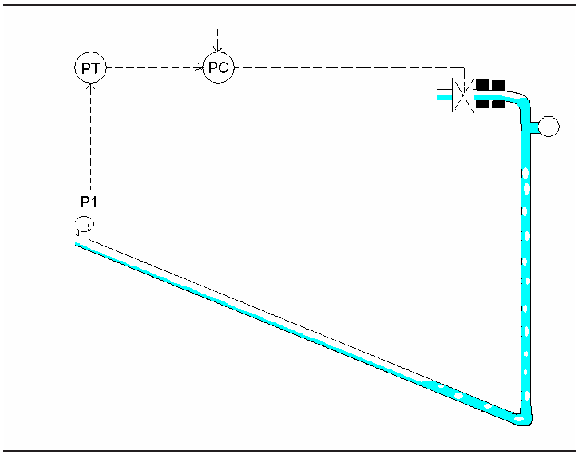

Fig. 6. PI control using measurement P_1

Figure 7 shows how the flow is stabilized after starting from open loop with a valve opening of 30%. It remains stable for the 6 minutes the controller is active. The simulated values using Storkaas' model are shown in the lower plot.

We see that the controller efficiently stabilizes the flow, confirming the results from the controllability analysis. However, this measurement can be unavailable in offshore installations because of its subsea location.

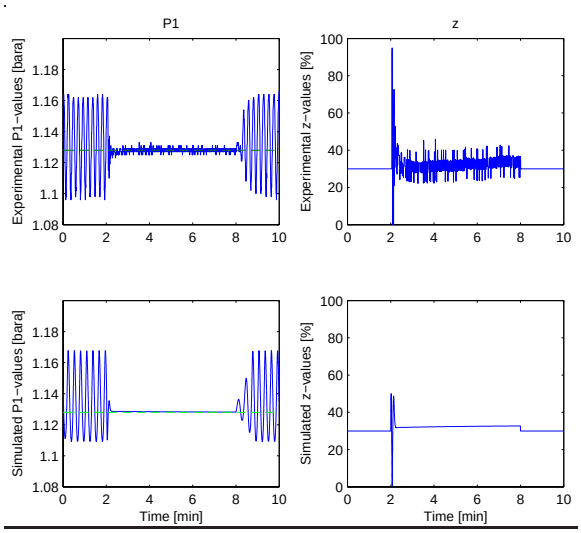

Fig. 7. Experimental (upper plots) and simulated (lower plots) results using a PI-controller

4.2 Cascade controller

To avoid the need for subsea measuremens, a cascade configuration using the topside pressure, P_2, in the outer loop and the mass flow, F_w, in the inner loop has been investigated. The control configuration is illustrated in Figure 8.

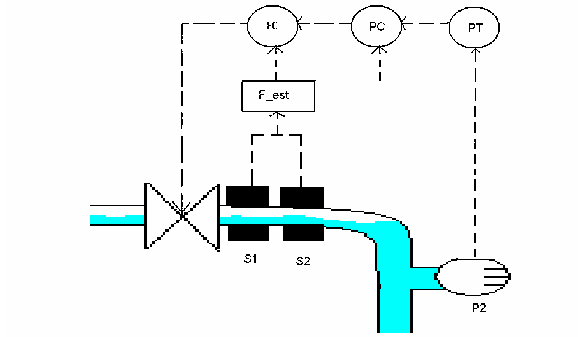

Fig. 8. Cascade control using measurements P_2 and F_w

Storkaas and Skogestad (2003) have proved theoretically that this works for another case of riser slugging and it has also been shown that it is possible to stabilize the flow this way on larger test facilities (Godhavn *et al.*, 2005*b*). However, so far we have not been able to verify this experimentally with the Miniloop. On the other hand simulations of the Miniloop confirme that this *should* be possible, as Figure 9 shows. The tuning parameters for the PI-controller in the outer loop are $K = -0.05bara^{-1}$ and $\tau_i = 30s$. The setpoint is $1.030bara$. The inner loop consisted of a P-controller with gain $K = 10s/kg$.

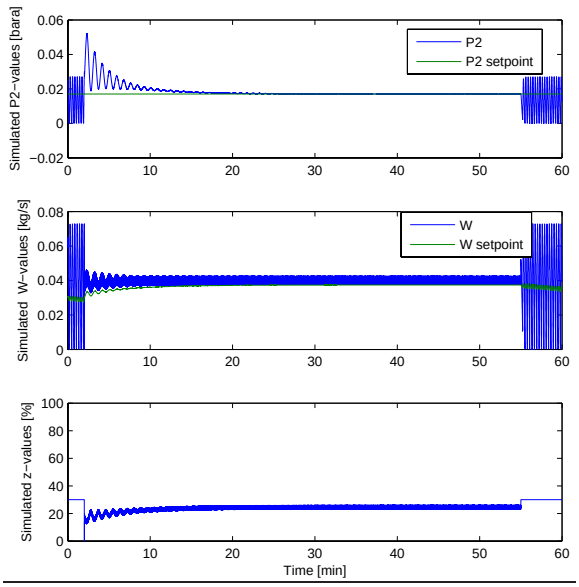

Fig. 9. Simulated values using a cascade controller

We see it takes the controller much more time to stabilize the flow than it did with the PI-controller which stabilized the flow almost immediately. Storkaas (2005) shows that this is due to unstable (RHP) zeros for the model as seen from the outer loop, when the inner loop is closed. These instable zeros will limit the bandwith of the system, and the controller based on only topside measurements are therefore slower than control systems based on upstream pressure measurements.

As mentioned, the controller did not work as well in the lab as it did for the simulations. The flow measurement was estimated from the signals given by the fiber-optic slug sensors, and it turned out that they had to be filtered to such an extent that they could not be used to stabilize the system at the lab.

4.3 Multivariable controller

It has earlier been shown that a MISO (Multiple Input - Single Output) $\mathcal{H}_\infty$ based on the same measurements as the cascade control configuration described above could give better performance when applied on riser-slugging than the cascade controller (Storkaas, 2005).

MISO controllers are more difficult to tune online than cascade controllers, and direct model-based controller design is usually needed. This can be done using Storkaas' simplified model in the case of the Miniloop. The method involves finding the controller K that minimizes the maximum singular value ($\mathcal{H}_\infty$ norm) of one or more weighted closed loop transfer functions and thereby maximizing robustness and, trough the weights, shaping the closed loop response.

5. CONCLUSION

From the controllability analysis it was found that using the inlet pressure was the only measurement that could be used as single measurement for anti-slug control. If only topside measurements where to be used, combinations of at least two of them was necessary.

A cascade controller was tested out, using the topside pressure and estimated mass flow as measurements. It was first tested in simulations using a simplified riser-slug model. The results showed that the cascade controller managed to stabilize the flow.

When trying the cascade controller in experiments on a small two-phase loop, the results where not so good. The reason for this was that the volume flow was estimated using hold up measurements that had to be heavily filtered.

If better measurements for the hold-up in the pipeline was available it could still be possible that the cascade configuration would give better results. Instruments based on capacitance would probably have been a better choice instead of the fiber optic slug sensors used in the experiments described in this paper. Also other, more robust, control configurations might handle the problem better than the cascade configuration. One example of such is the $\mathcal{H}_\infty$ controller which we plan to test in later experiments.

6. ACKNOWLEDGMENTS

The authors would like to thank former M.Sc. students Ingvald Baardsen and Morten Søndrol for assisting in building the Miniloop and performing experiments. Former Ph.D. student Espen Storkaas deserves thanks for help using his model. Also we would like to thank Statoil and the Norwegian Research Council for financial support.

REFERENCES

Godhavn, J.-M., S. Strand and G. Skofteland (2005*a*). Increased oil production by advanced control of receiving facilities. *IFAC'16, Prague, Czech Republic*.

Godhavn, J.M., M.P. Fard and P.H. Fuchs (2005*b*). New slug control strategies, tuning rules and experimental results. *Journal of Process Control* (15), 547–577.

Havre, K., K.O. Stornes and H. Stray (2000). Taming slug flow in pipelines. *ABB review* **4**, 55–63.

Hedne, P. and H. Linga (1990). Supression of terrein slugging with automatic and manual riser choking. *Advances in Gas-Liquid Flows* pp. 453–469.

Sivertsen, H. and S. Skogestad (2005). Anti-slug control experiments on a small scale two-phase loop. *ESCAPE'15, Barcelona, Spain*.

Skogestad, S. and I. Postlethwaite (1996). *Multivariable Feedback Control*. John Wiley & Sons.

Storkaas, E. (2005). Stabilizing control and controllability: Control solutions to avoid slug flow in pipeline-riser systems. PhD thesis. Norwegian University of Science and Technology.

Storkaas, E. and S. Skogestad (2003). Cascade control of unstable systems with application to stabilization of slug flow. *AdChem'03 Hong Kong*.

Storkaas, E., S. Skogestad and J.M. Godhavn (2003). A low-dimentional model of severe slugging for controller design and analysis. In: *Proc. of Multi-Phase '03, San Remo, Italy, 11-13 June 2003*.

Dynamic study of a subsea processing system

Heidi Sivertsen[1] John-Morten Godhavn[2] Audun Faanes[2]
Sigurd Skogestad[1] *

[1]Department of Chemical Engineering,
Norwegian University of Science and Technology, Trondheim, Norway
[2]R&D, Statoil ASA, Trondheim, Norway

Abstract

This paper describes the simulation setup applied in an introductory study in connection with implementation of subsea processing equipment at an already operating gas and oil field. The primary aim of the subsea processing equipment is to increase the oil recovery, but it is also considered as an important technological step forward. A subsea separation and boosting station is planned installed.
Several challenges need to be addressed before the implementation process, and simulations have therefore been performed to see how different types of control strategies can be introduced to overcome these challenges. The simulation model includes all the pipes and equipment from the wells to the topside first stage separators. The flow in the pipelines is modeled with the dynamic multiphase flow simulator OLGA 2000, whereas most of the processing equipment is modeled in Simulink. The focus of the paper is to demonstrate different ways of combining OLGA 2000 and Simulink, and how to divide the overall process model into sub-models in order to study local phenomena.

1 Introduction

Processing equipment may be installed at the sea bed in order to separate produced water from the production stream, inject the water into a reservoir, and possibly to increase the pressure in the production pipelines by compression or multiphase pumping.
Subsea processing enables production from low pressure reservoirs over long distances, and may increase the daily oil and gas production or even the total recovery from the reservoir. By injecting some of the produced water into a reservoir, the water emission from topside to sea is reduced, and subsea transportation pipelines are better exploited. Compression and pumping enable a lower wellhead pressure, and hence an increased production.
A general subsea production system with wells, manifold, subsea processing equipment, production pipelines and topside separators is shown in Figure 1.
Installation of subsea equipment leads to several challenges that need to be explored before the implementation. In the process of determining the control strategy and operation philosophy of the system, it is important to perform dynamic simulations that recapture the dynamical behavior adequately. Since the pressure, flow rates and composition of the flow vary with time, it is important to perform studies for several years throughout the life time of the field.
In the present paper, a simulation study applying different combinations of OLGA 2000 [10] provided by Scandpower Petroleum Technologies [11], and Simulink [9] is described. When combining these simulation tools, one needs to carefully consider which parts of the system to include in a simulation, and which assumptions can be made about the boundary conditions in each case.

2 Subsea processing equipment

Oil, gas and water are transported from the manifold connecting the different wells, to the subsea separator trough pipelines. From the subsea separator water is to be injected into a reservoir. Some water will be transported along with the oil and gas through the pipeline into each topside separator. A multiphase boosting pump is to be installed downstream the subsea sepa-

*Author to whom correspondence should be adressed: skoge@chemeng.ntnu.no

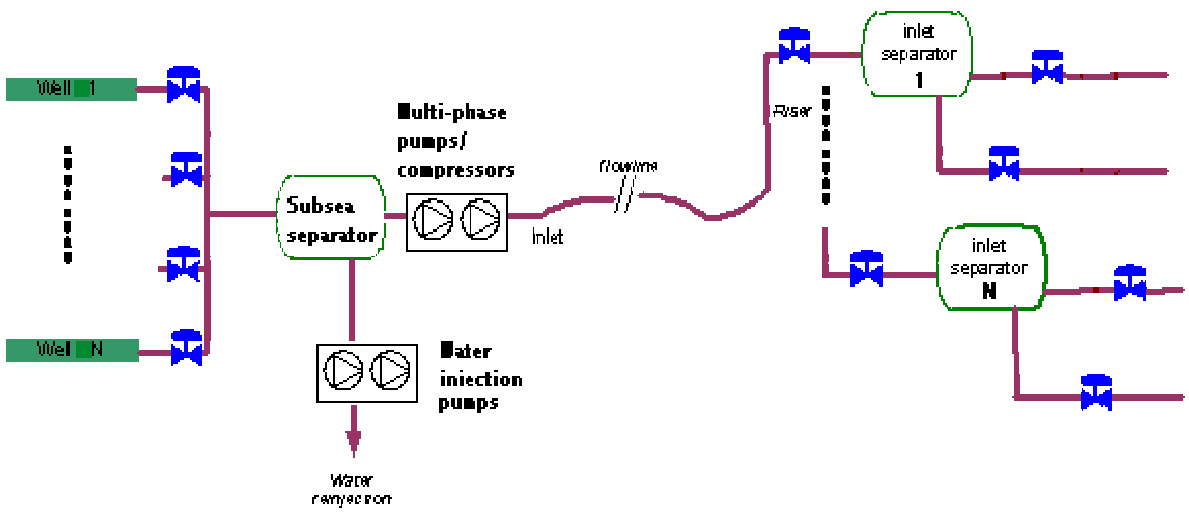

Figure 1: A production system including subsea processing equipment

rator to increase the pressure.

2.1 Subsea separator

The purpose of the subsea separator is to separate part of the water to be injected into a reservoir. The oil content in the injected flow shall be below a given limit.

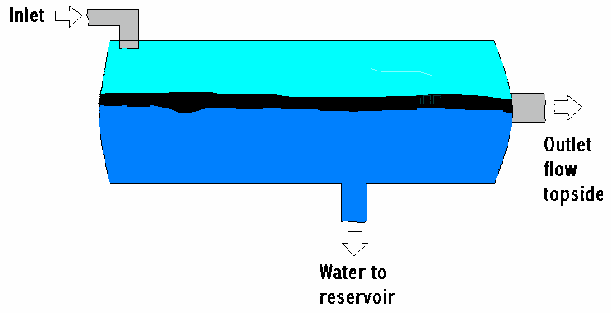

Figure 2: Subsea separator

The separator is simulated using a simple Simulink model. The inputs for the separator are the volumetric flow rates of gas, oil and water into the separator. Also the total volumetric flow to topside and the volumetric flow of water to the reservoir are used as input.

From the subsea separator model we get the subsea separator pressure, the gas density, the composition and density for the topside flow and also the water and oil levels in the separator.

2.2 Pumps

To transport the flow from the subsea separator to topside, a set of pumps or compressors able to handle multiphase flow can be used.

The flow rate to topside was used as input for the subsea separator model. This is also the flow rate that will be used as input to the OLGA model that represents the production pipelines for transporting the fluids to topside.

There is also a need for a set of water pumps to pump the water into the water reservoir. The water rate through the pump depends on the pressure difference between the reservoir and the subsea separator, and also the pump speed. The pump speed can be set either manually or by a controller. The inputs to the pump model are the pressures upstream and downstream the pump, and also the pump speed. The output is the mass flow of water injected into the reservoir.

2.3 Controllers

OLGA 2000 includes controllers. Simulink, however, gives the opportunity for more flexible choice of controllers and control structures. For this reason, the controllers where modeled in Simulink.

2.4 Chokes

There are subsea chokes for each well, which makes it possible to adjust the flow from each well independently.

At the top of each riser there are topside production

chokes. They make it possible to control the flow into each of the topside separators, and can be adjusted manually or by a controller.
The chokes are modeled in OLGA 2000. When they need to be adjusted during a simulation, the new choke openings can either be sent from Simulink to OLGA or they can be set directly as time series in OLGA.

2.5 Measurements

Several measurements are assumed available, monitoring pressure, density, flow rates and other values which are necessary for controlling the different parts of the system. Some of these are implemented in the OLGA 2000 simulations. During simulations, these values are sent from the OLGA model to the Simulink environment.

3 Simulation strategies

3.1 Integration of OLGA 2000 and Simulink

Using the OLGA - MATLAB toolbox it is possible to run OLGA simulations from a Simulink environment. The Simulink OLGA encapsulation enables the Simulink application to simulate multiphase flow in pipelines in OLGA 2000 together with additional process equipment. The communication between OLGA and Simulink is synchronous, which means that when the interface has sent a message to OLGA 2000, it waits until a response has been received before returning to Matlab.
From the OLGA block it is possible to get all the information about the flow and the equipment that is modeled in OLGA, into Simulink. In Simulink the information can be displayed and stored during the simulation. The values of the OLGA variables can this way be used for process equipment modeled in Simulink, such as controllers and separators. The outputs generated from the Simulink process equipment, such as separator pressure, are then sent back to OLGA and used as inputs for the OLGA calculations in the next time step.
Using OLGA 2000 to run all the simulations is also an option, as it is possible to include separators, controllers and other equipment in the models. There are, however, some advantages of combining OLGA 2000 with Simulink. Sometimes it is desired to use other models for process equipment than the ones used by OLGA, e.g. separators and controllers. It is particularly easy to implement these in Matlab/Simulink.

For the simulations performed during the study of our system, combinations of these methods have been used. To save computing time, and also to avoid some of the numerical problems that can occur during large simulations, parts of the system have been left out during some of the simulations. When doing this, it is important that the boundary conditions are well taken care of. Sometimes assuming constant values at the boundaries can be justified, but it is not always the case.
The calculations made by Simulink requires a very small percentage of the simulation time compared to the OLGA calculations. When sending inputs to OLGA, such as changes in boundary conditions or flow rates, the OLGA simulation time might increase. If these inputs are not essential for the results, it might be an idea to keep some of these inputs constant to reduce the time of the simulation.
Figure 3 shows the different ways to divide the system in our case. The wells and the pipelines into the subsea separators are modeled in OLGA, while the subsea separator and pumps are modeled in Simulink. The pipelines from the multiphase pump to topside are modeled in OLGA, and the topside separators are modeled in Simulink. All the controllers have also been modeled in Simulink.

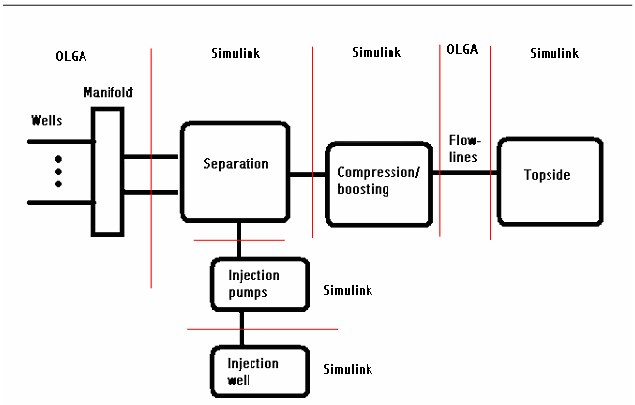

Figure 3: The subsystems of a general subsea processing system

To see how different parts of the total system can be run separately, some of the simulations that have been made will be presented. These simulations were performed during an early stage of the decision process on how to run the subsea system, so not all of this equipment or control structures will be used later on. However, they are included to show some of the considerations that where made when combining OLGA and Simulink.

3.2 Sequential simulations

One obvious possible way of doing the simulations, would be to run the different parts simulated in OLGA 2000 and Simulink separately. Then the time series obtained from one part could be used as input to a downstream simulation. The advantage of using such a method is that the simulations would in many cases require less time, and the programming would also be easier. The disadvantage is that this method does not capture the interactions between the different parts of the system, which can change the way the system behaves significantly. For example, the flow rates from one unit can be applied as input to the downstream unit. The sequential simulation will be appropriate if these flow rates are independent of the downstream pressure.

In [5] OLGA 2000 simulations were run first with a controller implemented in Simulink. The resulting outflow from OLGA was later used as varying inflow into an advanced topside simulator (ASSET from Kongsberg Maritime [8]) to see how the topside facilities would handle the flow variations.

3.3 Integrated simulation of wells and subsea separator

The wells and subsea separator simulations are important for studying the separator states during periods with varying well rates and pressure. Figure 4 shows a possible configuration in Simulink. Values for the flow rates of oil, water and gas are sent from the OLGA block to Simulink along with the pressure at the manifold. The flow rates are sent to the model of the subsea separator, while the inlet pressure is needed for the controller. The separator pressure is used by both the controller and as boundary condition for the OLGA block. The openings for the subsea chokes, set by Simulink, are also inputs for the OLGA block. In the case variations in separator pressure can be neglected by the OLGA model, computational speed can be increased by running the simulations with a constant downstream pressure input to the OLGA block.

The downstream equipment is not included in the simulations. When discarding the downstream equipment, assumptions have to be made about the boundary conditions. In these simulations we have assumed a constant pressure downstream the multiphase pump. This assumption was based on the fact that this pressure, as will be showed later, will most likely be controlled using other controllers, and not allowed to vary very much.

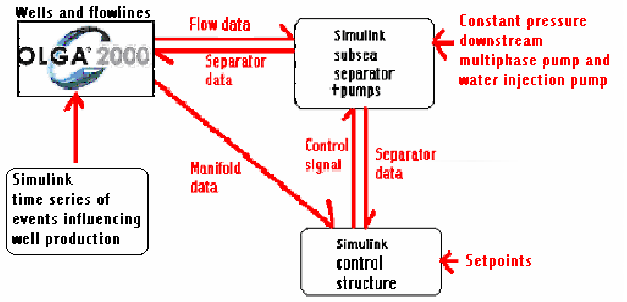

Figure 4: Simulation of wells and subsea separator

One example of a simulation that uses this set-up is presented in Section 4.1.

3.4 Integrated simulation of subsea separator, flowlines and topside separator

Simulations that include all equipment from the subsea separator to the topside separators can be used to see how changes in the subsea separator conditions influence the topside facilities. The simulation includes the subsea separator, the multiphase pump, the water injection pump, the pipelines to topside and the topside separators. Figure 5 shows how this was done in Simulink. Constant flow of oil, gas and water into the subsea separator was assumed. The reason why the wells were not included in the simulations, is that including them would lead to a very long simulation time. One example of such a simulation is given in Section 4.2.

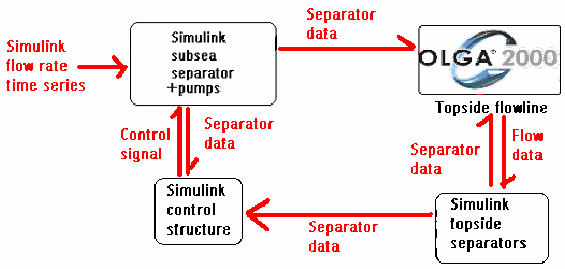

Figure 5: Simulation of subsea separator and topside pipelines

The pressure difference over the subsea chokes located downstream each well is quite large, so minor downstream pressure variations will not influence the flow rates very much. This pressure is not expected to differ dramatically, since the pressure in the subsea separator is held constant using controllers. Assuming constant flow rates into the separator is therefore justified.

It is also assumed that the equipment located downstream the topside separators are able to handle the flow rates from each separator. These flow rates are determined by controllers designed to keep the separator levels and pressure constant.
The flowrates of oil, gas and water out of the subsea separator are inputs to the OLGA block simulating the topside pipelines. These are obtained from the subsea separator model. Outputs from the OLGA model are the flow rates trough the topside chokes and the inlet pressure downstream the multiphase pump. The flow rates are sent to the models for the topside separators while the inlet pressure is used by a slug controller not shown in the figure. From the subsea separator model we also get the water level and pressure, needed for the controller and the model for the water injection pump.

3.5 Flowline simulations

Figure 6 shows the Simulink model for the topside pipeline, topside choke and controllers. This configuration has been used for testing a slug controller (see Section 4.3). From the OLGA block the inlet pressure of the pipeline is sent as input to the Simulink model of the controller. The controller calculates new topside choke openings that are sent as inputs back to the OLGA model.

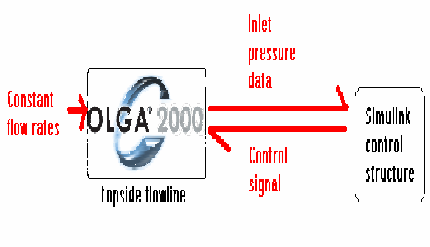

Figure 6: Slug control simulation setup

In this simulation it is assumed constant flow rates of oil, water and gas from the multiphase pump. In this way, the effect of pressure variations at the inlet of the pipelines on the flow rates upstream will not be modeled. When the slug controller is active this pressure will be fairly constant during normal operation.

4 Case study

4.1 Integrated simulation of wells and subsea separator: Well test

During a well test, one well after the other is shut down in order to calculate the flow rate from each individual well (deduction principle for subsea tie-ins). When a well is shut down, the pressure drop in the pipeline will decrease due to the reduced flow rate in the pipes, and the other wells will produce more. Normally the separator pressure is controlled, but during well testing it is the pressure at the *manifold* that is important to keep constant. There actually is a need for the subsea separator pressure to increase during a well test.
There are several ways to do this. Using a cascade control configuration is one possibility. The outer loop controls the manifold pressure where the set-point is the initial pressure before the well test. The inner loop controls the subsea pressure. This way the set-point for the subsea separator pressure will automatically increase for every well that is shut down. The control configuration illustrated in Figure 7. The simulation set-up from Section 3.3 have been used.

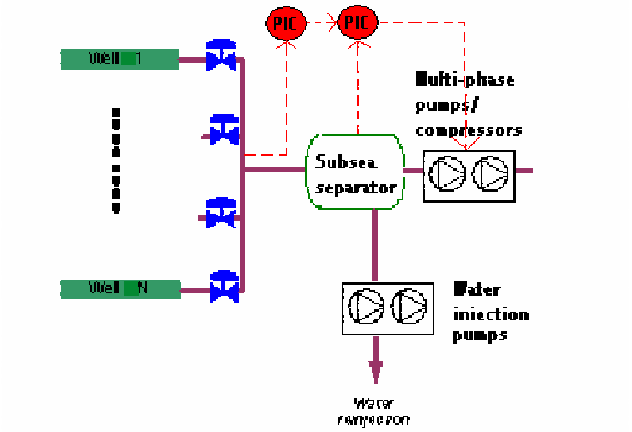

Figure 7: Well testing using cascade configuration

Using the cascade controller for the well test, it was possible to bring the manifold pressure back to its original value. Figure 8 shows the results when four of the wells are shut down one after another. The plot at the bottom shows how the subsea separator pressure increases to counteract the effect of the reduced pressure loss in the pipelines upstream the separator.
The results from the simulations show how long it takes for the manifold pressure to retain its initial value after a well is shut down. This information can be used to predict the duration of a well test.

4.2 Integrated simulation of subsea separator, flowlines and topside separator: Control of the water rate to top

By changing the water level in the subsea separator it is possible to control the water rate that is transported

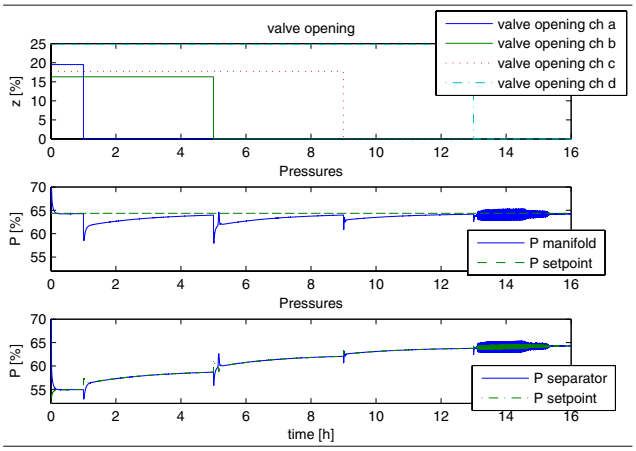

Figure 8: Well test results

to the platform. An increased water level will lead to increased water rate topside. A cascade configuration using the water rate out of the topside separator in the outer loop and the water level in the inner loop was used to handle this (Figure 9). The sub-models are combines as described in Section 3.4.

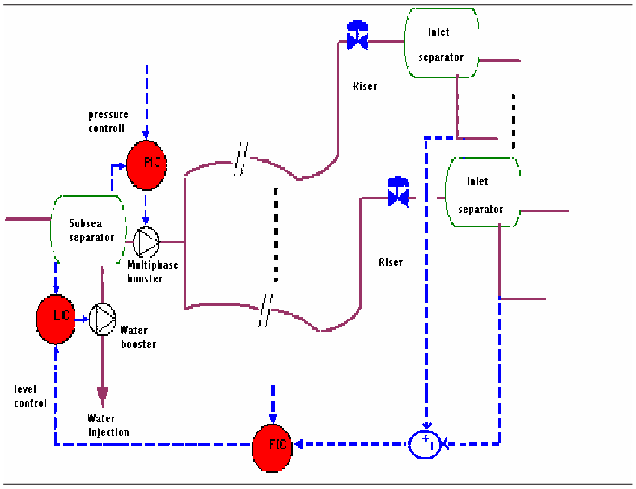

Figure 9: Cascade controller for subsea separator water level and water rate topside

Figure 10 shows what happens when the inlet flow rates to the subsea separator are reduced by 50% after 1 hour. The set-point for the water level controller in the inner loop is increased when to little water is transported topside. This way more of the water is brought topside, while less is pumped into the water reservoir.

4.3 Flowline simulations: Slug control

Riser slugging is a well known problem offshore, [1], [2], [3], [4], where alternating bulks of liquid and gas enters the receiving facilities and causes problems due to pressure and separator level oscillations. The results

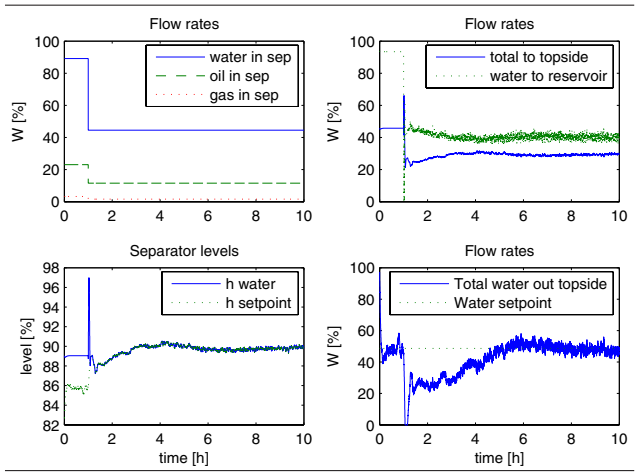

Figure 10: Results using a cascade controller to control subsea separator water level and water rate topside

are poor separation and wear on the equipment.
A simple PI controller using the inlet pressure downstream the multiphase pump and a control choke at the top of the riser has proven to be effective at other installations. This is illustrated in Figure 11. Section 3.5 describes the combination of the sub-models.

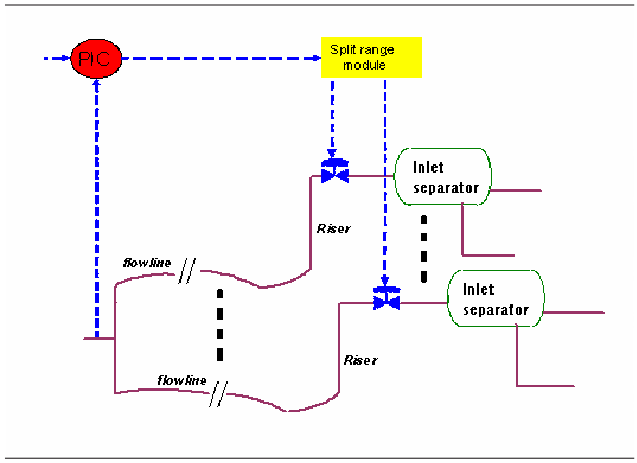

Figure 11: Slug control

Results from a simulation using the slug controller are shown in Figure 12. During the first 4 hours the controller is inactive, resulting in slugging and the pressure variations shown in the upper plot.
When the controller starts working, the pressure stabilizes at the desired set-point.

5 Discussion

This paper has shown some examples of the considerations that had to be made during the simulation study of a subsea station where a combination of OLGA 2000 and Simulink simulators have been used. The

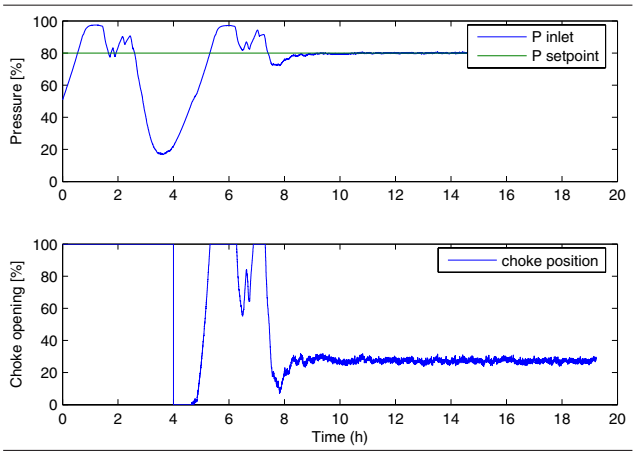

Figure 12: Slug control results

study has been performed to study different control strategies, and several options have been investigated. The simulations have been performed at a very early stage of the process, before the final decisions about equipment and operation have been made. Because of this, simplified models of the pipelines and equipment was used. Also the controllers have not been fine-tuned to get the best results at this stage. The results from this study might therefore differ from the final results. But the simulations can be been used as a tool to see which options are possible for control, and this way used as a basis for later studies.

There are also other dynamic process simulators that are commercially available and may be combined with OLGA 2000 for pipeline simulations.

D-SPICE is a dynamic simulator provided by Fantoft Process Technologies [7]. The simulator contains a module, the OLGA 2000 Interface (OLGAIF), that can be used to run an OLGA simulation as an integrated part of a D-SPICE model. Similar possibilities exists also for ASSET from Kongsberg Maritime [8] and HYSYS from Aspentech [6].

6 Conclusion

Using a combination of OLGA 2000 and Simulink simulator tools, it has been possible to study and plan for the implementation of a subsea station planned to increase the oil and gas productivity of an offshore field.

Because of the early stage at which these simulations have been performed, the final models for all the equipment were still not available at the time of the simulations. However, it was still important to capture the interactions between the different subsystems.

Depending on the problem at hand, local sub-models have been combined in different ways to save simulation time without introducing too large errors due to simplifications. Doing so requires a careful consideration of all assumptions for the boundary conditions.

References

[1] A. Courbot. Prevention of severe slugging in the dunbar 16" multiphase pipeline. *Offshore Technology Conference, May 6-9, Houston, Texas*, 1996.

[2] K. Havre, K. O. Stornes, and H. Stray. Taming slug flow in pipelines. *ABB review*, 4(4):55–63, 2000.

[3] P. Hedne and H. Linga. Supression of terrain slugging with automatic and manual riser choking. *Advances in Gas-Liquid Flows*, pages 453–469, 1990.

[4] G. Skofteland and J.M. Godhavn. Suppression of slugs in multiphase flow lines by active use of topside choke - field experience and experimental results. In *Proc. of MultiPhase '03, San Remo, Italy, 11-13 June 2003*, 2003.

[5] E. Storkaas and J.M. Godhavn. Extended slug control for pipeline-riser systems. *Multiphase production technology '05, Barcelona, Spain*, May 2005.

[6] `www.aspentech.com`.

[7] `www.fantoft.com`.

[8] `www.km.kongsberg.com`.

[9] `www.mathworks.com`.

[10] `www.olga2000.com`.

[11] `www.scandpowerpt.com`.

ADCHEM 2006

International Symposium on Advanced Control of Chemical Processes
Gramado, Brazil – April 2-5, 2006

CONTROL SOLUTIONS FOR SUBSEA PROCESSING AND MULTIPHASE TRANSPORT

Heidi Sivertsen * **John-Morten Godhavn** ** **Audun Faanes** **
Sigurd Skogestad *,[1]

* *Department of Chemical Engineering, Norwegian University of Science and Technology, Trondheim, Norway*
** *R&D, Statoil ASA, Trondheim, Norway*

Abstract: To increase the oil production for the Tordis subsea oilfield located at the Norwegian Continental Shelf, a subsea separation and boosting station will be installed. Most of the water will be injected into a subsea reservoir instead of being transported up to the platform. Several challenges conserning process control need to be addressed before the implementation process, and dynamic simulations have therefore been performed in order to develop and test different control strategies to deal with these challenges. The results from some of these simulations will be presented in this paper.

Keywords: Process control, control system design, PI controllers, cascade control, pipelines

1. INTRODUCTION

The Tordis field operated by Statoil has proved to be even more productive than anticipated when production began in 1994 (Godhavn *et al.*, 2005). To increase production and total recovery for the field in the last years of production, processing equipment is planned installed at the sea bed. This in order to separate produced water from the production stream, inject this water into a reservoir, and increase the production rate.

Subsea processing enables production from low-pressure reservoirs over long distances, and may increase the daily oil and gas production or even the total recovery from the reservoir. By injecting produced water into a reservoir, the water emission from topside to sea can be reduced, and the subsea transportation pipelines are better exploited. Compression and pumping enable a lower wellhead pressure, and hence an increased production.

However, the installation of new subsea equipment leads to several new challenges, also related to process control. There can be several ways to solve these problems, so the first question that needed answering was; which solutions are feasible and which one will solve the problems the best.

Having control of the subsea separator pressure and liquid levels are important as it determines the flow rates and compositions for the entire system. In Section 3, some solutions to achieve control of the separator will be presented. These control solutions are then expanded to achieve other benefits, such as faster well tests and control of the water rate that is transported with the oil and gas to the platform.

Under certain conditions a flow regime called riser slugging can develop in the pipelines, which is undesirable because it can introduce large pressure oscillations in the system. In the end of Section 3 it will be shown that this problem can be solved using feedback control.

[1] Author to whom correspondence should be adressed: skoge@chemeng.ntnu.no

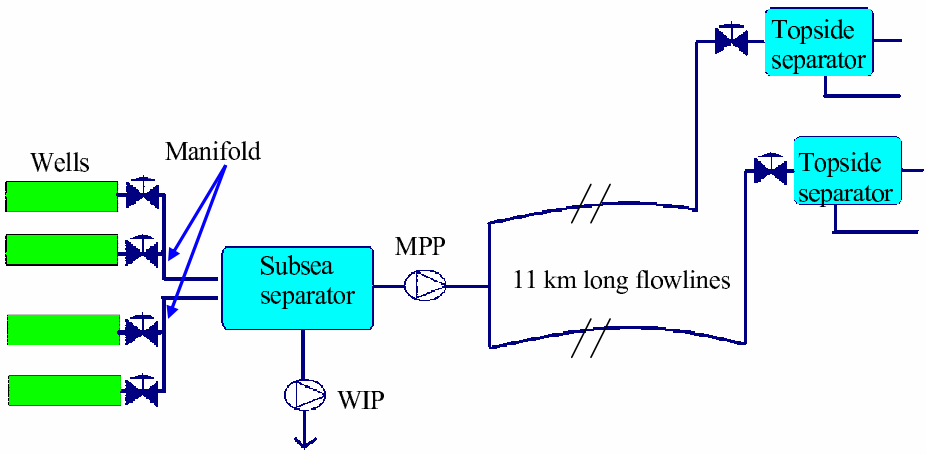

Fig. 1. Subsea processing equipment

The control solutions presented in this paper are illustrated with dynamic simulations including all equipment from the wells to the two topside receiving separators at the Gullfaks C platform (Figure 1). It is important to notice that these simulations were performed at a very early stage in the process of determining how to run the process, where the aim was to find feasible control solutions and not to find optimal control parameters. The controllers have therefore not been fine-tuned and simplified models for the equipment and pipelines have been used. This is also the reason why the absolute values for the different variables have been left out in this paper.

To simulate flow in the pipelines, OLGA 2000 dynamic multiphase simulator (`www.olga2000.com`), provided by Scandpower Petroleum Technologies (`www.scandpowerpt.com`) has been used. Most of the process equipment is simulated using Simulink. The OLGA - MATLAB toolbox enables the Simulink application to simulate multiphase flow in pipelines in OLGA together with additional process equipment and controllers modeled in Simulink.

2. SUBSEA PROCESSING EQUIPMENT

Oil, gas and water are transported from the manifold to the subsea separator through two pipelines. From the separator some of the water is to be injected into a disposal reservoir. The remaining water will be transported along with the oil and gas through two pipelines into each topside separator at the Gullfaks C platform. A multiphase boosting pump will be installed downstream the separator.

2.1 Wells

There will be a total of eight wells producing oil, water and gas to the Gullfaks C platform. The flows from the wells are merged at the manifold. Two short pipelines, each receiving the production from four wells, transport the fluid to the subsea separator.

2.2 Pipelines

To simulate the pipelines between the wells, the subsea separator and the topside separators, OLGA 2000 have been used. OLGA 2000 is a commercial available dynamic multiphase flow simulator. In our study OLGA has been run from Simulink. From OLGA, it is possible to get all the information about the flow and the equipment that is modeled in OLGA, into Simulink.

2.3 Subsea Separator

The subsea separator is illustrated in Figure 2. In the separator the water, oil and gas will separate due to gravity. The water, which is heaviest, will sink to the bottom. Most of the water is to be injected into a disposal reservoir through an outlet in the bottom of the separator. It is important that no oil enters this reservoir. The rest of the water is transported to the platform along with the gas and oil.

The thickness of the water layer and the oil layer is determined by the inlet and outlet flow rates. The multiphase pump and the water pump speed will therefore influence the thickness of these layers. The rest of the separator is filled with gas.

The separator is simulated using a simple Simulink model. It computes the separator pressure, density and composition for the flow to topside and the water and oil levels in the separator. It is assumed that the pressure is independent of gravity, that is: the pressure at the bottom is the same as in the gas layer at the top of the separator. The composition of the flow going to the platform is determined by the thickness of the water and oil layer. If the level of the water is below the outlet leading topside, no water will

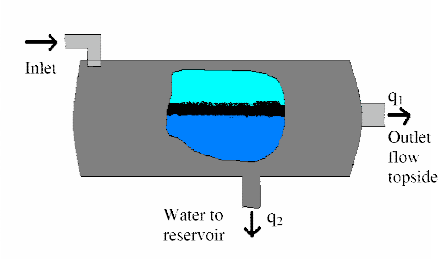

Fig. 2. Subsea separator

be transported topside. The same goes for the oil level, which depends both on the oil and water layer thickness. As already mentioned, the flow rate will be determined by the multiphase pump speed and the pressure in the separator and the pipelines.

2.4 Pumps

Multiphase pump To be able to operate the subsea separator at a low pressure despite the friction loss caused by the 11 km long pipelines to the Gullfaks C platform, pumps or compressors can be installed.

The plan is to install a multiphase boosting pump downstream the subsea separator. In this way it is possible to control the separator pressure by adjusting the pump speed and thereby the flow rate to topside, q_1.

Water pump There is also a need for a water pump to pump the water into the disposal reservoir, holding a higher pressure than the subsea separator.

The water rate through the water pump, q_2, depends on the pressure difference between the reservoir and the subsea separator, and also the pump speed. Pump speed and pressure drop over the *multiphase* pump will in the same way determine the topside production rate, but composition and density of the flow will also influence these flow rates.

2.5 Chokes

There are chokes for each of the eight wells, which make it possible to adjust the flow from each well independently. These chokes can be used for well tests, where one well after another is shut down.

At the top of each riser there are topside production chokes. They make it possible to control the flow into each of the topside separators, and can be adjusted manually or by a controller.

2.6 Measurements

Several measurements will be available, monitoring pressure, density, flow rates and other values which are necessary for controlling the different parts of the system. Measurements used directly for control are the manifold pressure, the subsea separator pressure and water level, pressure drop and density over topside production chokes, water rate out of topside separators and the pressure downstream the multiphase subsea pump. The pressure drop and density across the topside chokes are used to calculate the flow rate through the topside chokes as there are no flow measurements available.

3. CONTROL STRATEGIES

Several dynamic simulations were performed to test different control strategies for controlling the system, and some of these will be presented here. The results will be used in the design of the control system and this way serve as a basis for further studies. The solutions presented here might therefore not be the ones implemented in the end.

3.1 Control of subsea separator pressure and levels

3.1.1. Decentralized PI control of subsea separator pressure and water level To keep the oil contents in the injected water below a given limit, it is important to control the separator water level. By increasing the flow rate of the water injected into the reservoir, the water level will decrease. The flow rate through the water injection pump depends on the pressure difference across the pump and the pump speed. The speed of the pump can be set by a controller.

It is also important to control the separator pressure as this pressure will affect the wells and their production. The separator pressure can be controlled by changing the total flow rate to topside, which again is influenced by the speed of the multiphase pump. During the simulations this flow rate was set by the controller directly. The reason for this is that there was no model of the multiphase pump available at the time of the simulations.

Even though there are quite strong interactions between the level and pressure control, as will be shown, simple PI controllers were used to see how well the separator could be controlled. This is illustrated in Figure 3.

Figure 4 shows the results for a simulation where the input rates of water, gas and oil are reduced by 50% after 30 min. The pressure drops as the flow rates are reduced, but after about 15 min the pressure is back to normal due to the controller action.

What might seem surprising is that the water and liquid level start to increase at the time the inlet rates are reduced, before they decrease and end up at lower levels than they initially had. The reason for this is that the separator pressure and water level affect each other. When the separator pressure decreases due to

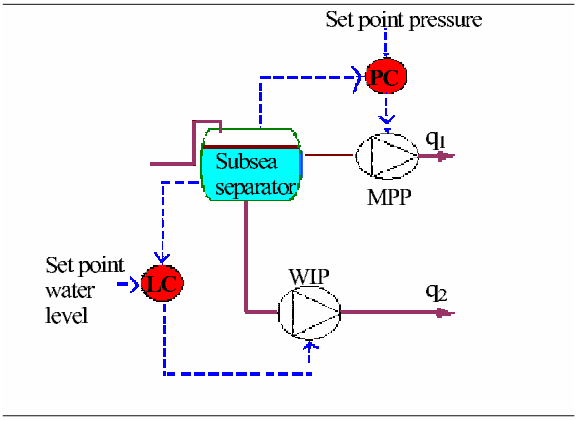

Fig. 3. PI control of subsea separator pressure and water level

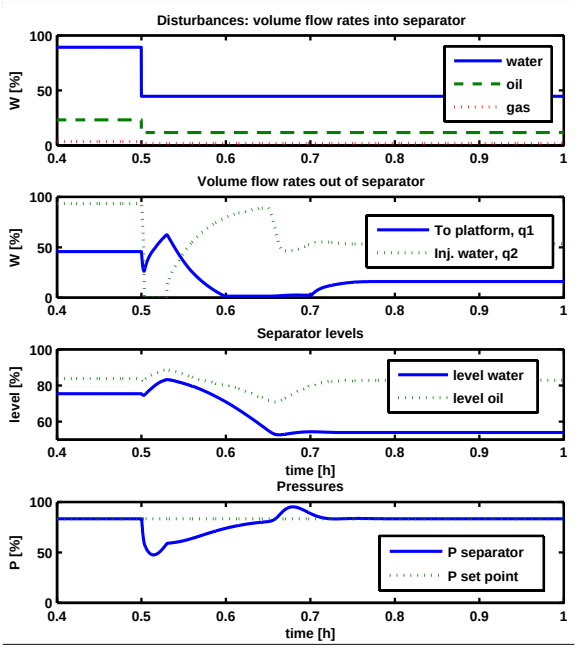

Fig. 4. Results using PI controllers to control subsea separator pressure and water level

the reduced inlet flow rates, it makes it harder for the water pump to inject water into the reservoir. Because of this, the water rate injected to the reservoir, q_2, temporarily goes down to zero, explaining the increase in levels.

In practice, a zero flow rate will cause problems for the water pump, but better tuning of the controller or other control configurations will remove this problem. Another way of avoiding this problem could be to use some other control configuration, e.g. a cascade controller where the inner loop controls the flow rate through the water pump and the outer loop controls the water level in the separator.

3.1.2. Cascade control : Control of water rate to topside At the Gullfaks C platform, the water that is transported to topside along with the gas and oil needs to be taken care of. There are limits to the amount of water the downstream process equipment can handle, and having control of this water rate can be an advantage.

By changing the water level in the subsea separator it is possible to control the water rate that is transported to the Gullfaks C platform. Figure 5 shows one way of doing this. It is an extension of the control structure presented in 3.1.1. An increased water level will lead to increased water rate topside (see Figure 2). A cascade configuration using the water rate out of the topside separator, q_3, in a slow outer loop and the water level in the inner loop, was developed to handle this.

Figure 6 shows the results from a simulation where the inlet flow rates are reduced by 50% after 1h. The set-point for the water level controller is increased when too little water is transported topside due to reduced inlet rates.

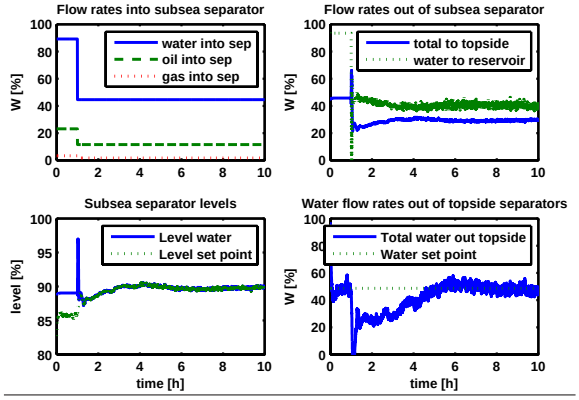

Fig. 6. Results using a cascade controller to control subsea separator water level and water rate topside

We see that after about 5 hours the water flow rate is back at its set-point, even though the flow rates into the subsea separator have been reduced substantially.

3.2 Well head pressure control

During a well test, one well after the other is shut down in order to determine the production rate from each individual well (deduction principle for tie-ins). Performing well tests is costly, as the production is reduced for the time the well test lasts. Being able to reduce the duration of a test, has therefore a large economic potential. Using active control might reduce the time needed to perform a well test.

However, when a well is shut down, the pressure drop in the pipeline will decrease due to the reduced flow rate in the pipe. This way the other wells will produce more, leading to a wrong estimate of the production from the well that is closed. Therefore, during well testing, the pressure at the *manifold* is kept constant rather than the subsea separator pressure which is normally controlled (Figure 3). There actually is a need for the subsea separator pressure to increase

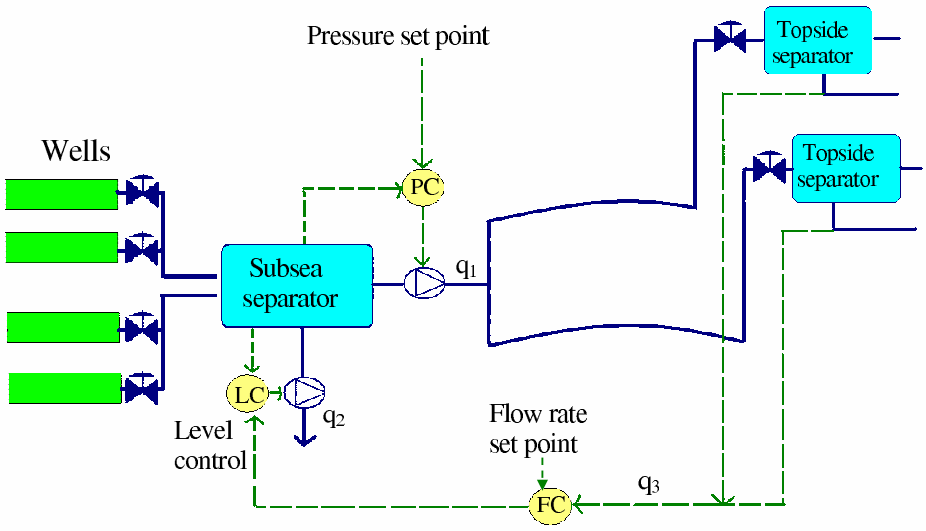

Fig. 5. Cascade controller for subsea separator water level and water rate topside

during a well test. The alternative would be to reduce the well choke openings accordingly.

There are several ways to do this. Using a cascade control configuration is one possibility. The outer loop controls the manifold pressure where the set-point is the initial pressure before the well test. The inner loop controls the subsea separator pressure. This way the set-point for the subsea separator pressure will automatically increase for every well that is shut down. The cascade control configuration is illustrated in Figure 7.

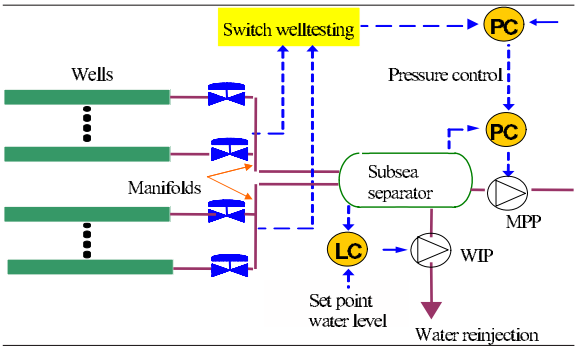

Fig. 7. Welltest using cascade configuration

Using the cascade controller for the well test, it was possible to bring the manifold pressure back to its original value. Figure 8 shows the results when three of the wells are shut down one after another. The plot at the bottom shows how the subsea separator pressure increases to counteract the effect of the reduced pressure loss in the pipelines upstream the separator.

Another way of controlling the manifold pressure is to estimate how much the manifold pressure will drop when a well is shut down, and then increase the set-point for the subsea separator pressure accordingly. This way the simple pressure PI controller described in Section 3.1.1 can be used, as long as steps in the set-point are introduced. It is important to find good estimates of how much the separator pressure need

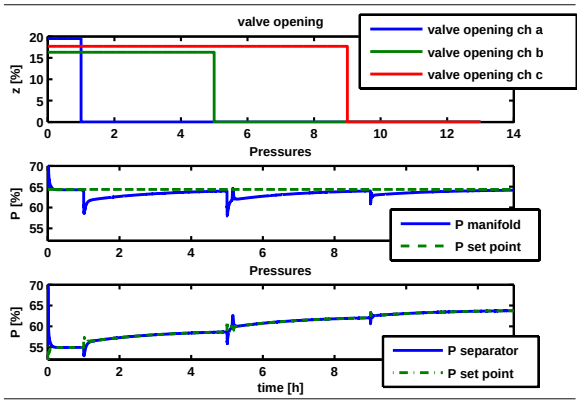

Fig. 8. Welltest results

to increase in order to use this method. Results from simulations show that it is possible to reduce the time before the manifold pressure reaches its initial value to less than 15 min. This is illustrated in Figure 9.

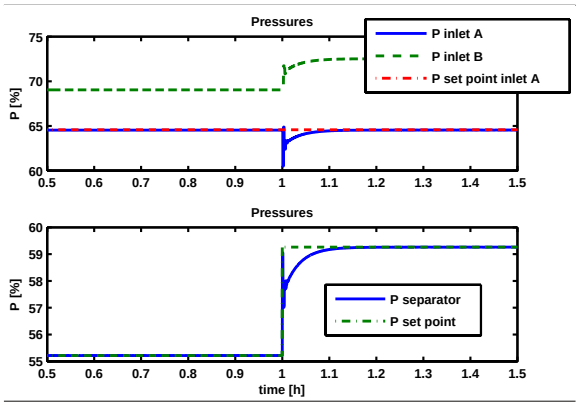

Fig. 9. Welltest results using a PI controller with setpoint changes

It is important to find a good estimate of how much the pressure drops at the manifold when a well is shut-in, in order to use this solution.

The results from the simulations show how long it takes for the manifold pressure to retain its initial

value after a well is shut down. This information can be used to predict the duration of a well test.

3.3 Slugging

Riser slugging is a well known problem offshore, where alternating bulks of liquid and gas enter the receiving facilities and cause problems due to pressure and separator level oscillations. The results are poor separation and wear on the equipment.

There are several ways to deal with the problem, but using active control has in the last years been the preferred way to avoid riser slugging, (Courbot, 1996), (Havre *et al.*, 2000), (Hedne and Linga, 1990), (Skofteland and Godhavn, 2003). Today a combination of active slug control and model predictive control (MPC) is used at Gullfaks C (Godhavn *et al.*, 2005).

A simple PI controller using the pressure upstream the flow-line ending in the riser and a control valve at the top of the riser has proved to be effective. This pressure oscillates heavily during slugging, due to the changing composition in the riser. Keeping this pressure stable forces the flow into another flow regime. In (Storkaas, 2005) control theory proves that using this measurement one is able to stabilize the flow and also to achieve good performance. This control configuration is illustrated in Figure 10.

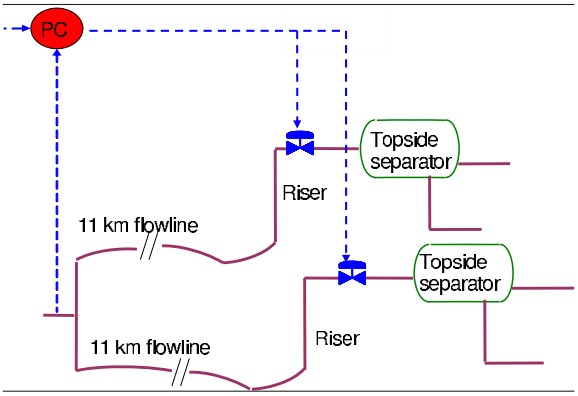

Fig. 10. Slug control applied to Tordis

Results from a simulation with the slug controller are shown in Figure 11. During the first 4 hours the controller is inactive, resulting in slugging in the pipeline and the pressure variations shown in the upper plot. When the controller starts working, the pressure stabilizes at the desired set-point.

4. CONCLUSIONS

The implementation of new subsea processing equipment to improve the productivity for a subsea oilfield is expected to introduce several new challenges regarding operation and process control that need to be addressed before the start-up. This paper presents some results from dynamic simulations performed in

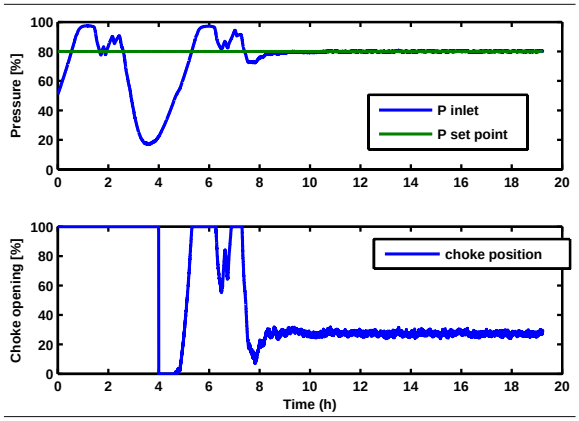

Fig. 11. Slug control results

order to investigate how the use of automatic control might deal with these challenges. For the different scenarios presented here, automatic control shows good results.

The simulations have been performed at a very early stage, before the final decisions about equipment and operation have been made. Because of this, simplified models of the pipelines and equipment were used. Also, the controllers have not been fine-tuned to get the best results at this stage. The results from this study will therefore differ from the final results. The simulations can, however, be used as a basis for later studies.

Examples of what better suited controllers can accomplish are; decreasing the time of well tests (Figure 8) and removing the effect that leads to the topside choke saturating in the first 4 hours of slug control (Figure 11).

REFERENCES

Courbot, A. (1996). Prevention of severe slugging in the dunbar 16" multiphase pipeline. *Offshore Technology Conference, May 6-9, Houston, Texas*.

Godhavn, J.-M., S. Strand and G. Skofteland (2005). Increased oil production by advanced control of receiving facilities. *IFAC'16, Prague, Czech Republic*.

Havre, K., K. O. Stornes and H. Stray (2000). Taming slug flow in pipelines. *ABB review* **4**(4), 55–63.

Hedne, P. and H. Linga (1990). Supression of terrain slugging with automatic and manual riser choking. *Advances in Gas-Liquid Flows* pp. 453–469.

Skofteland, G. and J.M. Godhavn (2003). Suppression of slugs in multiphase flow lines by active use of topside choke - field experience and experimental results. In: *Proc. of MultiPhase '03, San Remo, Italy, 11-13 June 2003.*

Storkaas, E. (2005). Stabilizing control and controllability: Control solutions to avoid slug flow in pipeline-riser systems. PhD thesis. Norwegian University of Science and Technology.

SMALL SCALE EXPERIMENTS ON STABILIZING RISER SLUG FLOW

Heidi Sivertsen * **Sigurd Skogestad** *,[1]

* *Department of Chemical Engineering, Norwegian University of Science and Technology, Trondheim, Norway*

Keywords: Process control, multihase flow, dynamic simulation, petroleum, riser slugging, controllability analysis

This paper is the first of two papers describing control experiments on different scale slug lab rigs. This first paper describes the study and results from a small-scale lab rig, build to test different riser slug control strategies without the huge costs involved in larger scale experiments. Earlier experiments on this small-scale rig have shown that it is possible to stabilize the flow using a PI-controller with a pressure measurement located upstream the riser base as measurement (Sivertsen and Skogestad (2005)). The aim now was to control the flow using only topside measurements and to compare these results with results found when using upstream measurements.

A controllability analysis was performed in order to screen the different measurement candidates using a model developed by Storkaas et al. (2003). The analysis showed that it should be possible to control the flow using only topside measurements. The results from this analysis were then used as a background for the experiments performed in the lab.

The experimental results were successful. They showed that it was possible to control the flow far better then predicted from the analysis and the results were in fact comparable with the results obtained when using a pressure measurement upstream the riser (subsea measurement).

1. INTRODUCTION

The behavior of multiphase flow in pipelines is of great concern in the offshore oil and gas industry, and a lot of time and effort have been spent studying this phenomena. The reason for this is that by doing relatively small changes in operating conditions, it is possible to change the flow behavior in the pipelines drastically. This has a huge influence on important factors such as productivity, maintenance and safety. Figure 1 shows different flow regimes that can develop in an upward pipeline.

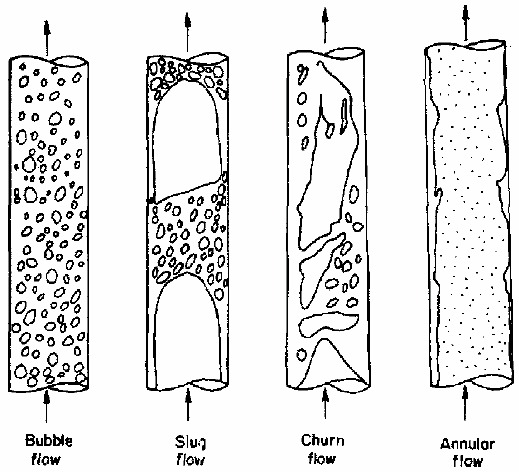

Fig. 1. Vertical horizontal flow map of Taitel et al. (1980)

Some operating conditions lead to an undesirable flow regime that may cause severe problems for the receiving facilities due to varying flow rates and pressure in the system. This usually happens in the end of the life cycle of a well, when flow rates are lower than the system was designed for. The rate and pressure variations are caused by a flow regime called slug flow.

[1] Author to whom correspondence should be adressed: skoge@chemeng.ntnu.no

It is characterized by alternating bulks of liquid and gas in the pipeline.

Being able to avoid slug flow in the pipeline is of great economic interest. For this reason it is important to be able to predict the flow regime before production starts, so that the problems can be taken care of as soon as they arise. Traditionally flow maps as the one in Figure 2 have been produced as a tool to predict the flow regime that will develop in a pipeline (Taitel and Dukler (1976), Barnea (1987), Hewitt and Roberts (1969)). These maps show that the flow regime in a pipeline is highly dependent on the incoming superficial flow rates of gas (u_{GS}) and oil (u_{LS}).

Even though the system is designed to avoid such problems in the earlier years of production, the production rate is changed during the production lifetime and problems can arise later on. Note however that these flow maps represent the ”natural” flow regimes, observed when no feedback control is applied.

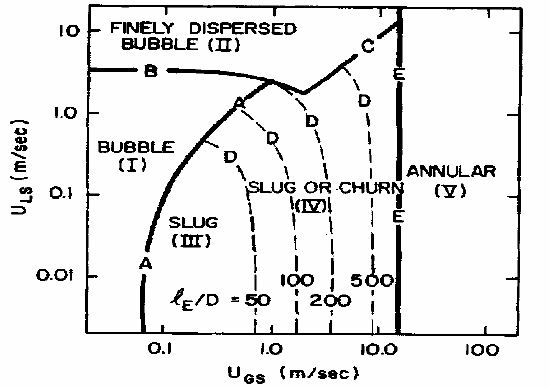

Fig. 2. Flow pattern map for 25 mm diameter vertical tubes, air-water system (Taitel et al. (1980))

There exist different types of slugs, depending on how they are formed. They can be caused by hydrodynamical effects or terrain effects. The slugs can also be formed due to transient effects related to pigging, start-up and blow-down and changes in pressure or flow rates.

Hydrodynamic slugs are formed by liquid waves growing in the pipeline until the height of the waves is sufficient to completely fill the pipe. These slugs can melt together to form even larger slugs and occur over a wide range of flow conditions.

Terrain slugging is caused by low-points in the pipeline topography, causing the liquid to block the gas until the pressure in the compressed gas is large enough to overcome the hydrostatic head of the liquid. A long liquid slug is then pushed in front of the expanding gas upstream. One example of such a low-point is a subsea line with downwards inclination ending in a vertical riser to a platform. In some cases the entire riser can be filled with liquid until the pressure in the gas is large enough to overcome the hydrostatic pressure of the liquid-filled riser. Under such conditions a cyclic operation (limit cycle) is obtained. It is considered to consist of four steps (Schmidt et al. (1980), Taitel (1986)). These steps are illustrated in Figure 3. Liquid accumulates in the low point of the riser, blocking the gas (1). As more gas and liquid enters the system, the pressure will increase and the riser will be filled with liquid (2). After a while the amount of gas that is blocked will be large enough to blow the liquid out of the riser (3). After the blow-out, a new liquid slug will start to form in the low-point (4).

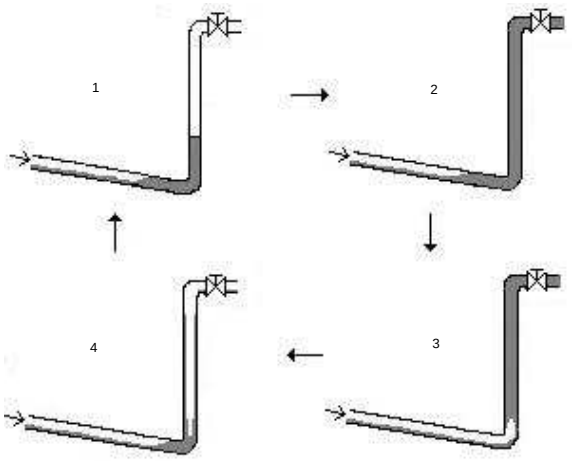

Fig. 3. Illustration of the cyclic behaviour (slug flow) in pipeline-riser systems

Terrain induced slugs can become hundreds of meters long, whereas hydrodynamic slugs are relatively shorter. This is also the reason why terrain slugging is often referred to as severe slugging.

Slug flow has a negative impact on the receiving facilities during offshore oil and gas production due to the large fluctuations in flow rates and pressure. Frequent problems are unwanted flaring and reduced operating capacity. The fluctuating pressure also leads to a lot of strain on other parts of the system, such as valves and bends. The burden on the topside separators and compressors can in some cases become so large that it leads to damages and plant shutdown, representing huge costs for the producing company. Being able to remove slugging has a great economic potential and this is why lot of work and money has been spent on finding solutions to the problem.

It is possible to avoid or handle the slugs by changing the design of the system. Examples of this are; changing the pipeline topology, increasing the size of the separator, adding a slug catcher or installing gas lift. However, the implementation of this new equipment usually costs a lot of money. Another option is changing the operating conditions by choking the topside valve. Also this comes with a drawback; the increased pressure in the pipeline leads to a reduced production rate and can lower the total recovery of the field that is being exploited.

In the last years there have been several studies on active control as a tool to ”stabilize” the flow and thereby avoiding the slug flow regime. Mathematically, the objective is to stabilize a flow region which otherwise would be unstable. A simple analogue is stabilization of a bicycle which would be unstable without control. Schmidt et al. (1979) was the first to successfully apply an automatic control system on a pipeline-riser system with a topside choke as actuator. Hedne and Linga (1990) showed that it was possible to control the flow using a PI controller and pressure sensors measuring the pressure difference over the riser. Lately different control strategies have also been implemented on production systems offshore with great success (Hollenberg et al. (1995), Courbot (1996), Havre et al. (2000), Skofteland and Godhavn (2003)).

Active control changes the boundaries of the flow map presented in Figure 2, so that it is possible to avoid the slug flow regime in an area where slug flow is predicted. This way it is possible to operate with the same average flow rates as before, but without the huge oscillations in flow rates and pressure. The advantages with using active control are large; it is much cheaper than implementing new equipment and it also removes the slug flow all together thereby removing the strain on the system. This way a lot of money can also be saved on maintenance. Also, it is possible to produce with larger flow rates than what would be possible by manually choking the topside valve.

Subsea measurements are usually included in the control structures that have been reported in the literature so far. Pressure measurements at the bottom of the riser or further upstream are examples of such measurements. When dealing with riser slugging, subsea measurements have proved to effectively stabilize the flow. When no subsea measurements are available, we will see that the task gets far more challenging.

Since subsea measurements are less reliable and much more costly to implement and maintain than measurements located topside, it is interesting to see if it is possible to control the flow using only topside measurements. Is it also possible to combine topside measurements in a way that improve the performance? And are the results comparable to the results obtained when using a controller based on subsea measurements?

Earlier studies on using only topside measurements are found in Godhavn et al. (2005) where experiments where performed on a larger rig and the flow was controlled using combinations of pressure and density measurements. Similar experiments as the ones described in this paper was later performed on a medium-scale lab rig to investigate the effect the scale of the lab rig has on the quality of the controllers. These experiments are described in Sivertsen et al. (2008).

2. CASE DESCRIPTION

2.1 Experimental setup

To test different control configurations, a small-scale two-phase flow loop with a pipeline-riser arrangement was build at the Department of Chemical Engineering at NTNU, Trondheim (Bårdsen (2003)). The flow consists of water and air, mixed together at the inlet of the system. Both the pipeline and the riser was made of a 20mm diameter transparent rubber hose, which makes it easy to change the shape of the pipeline system. A schematic diagram of the test facilities is shown in Figure 4.

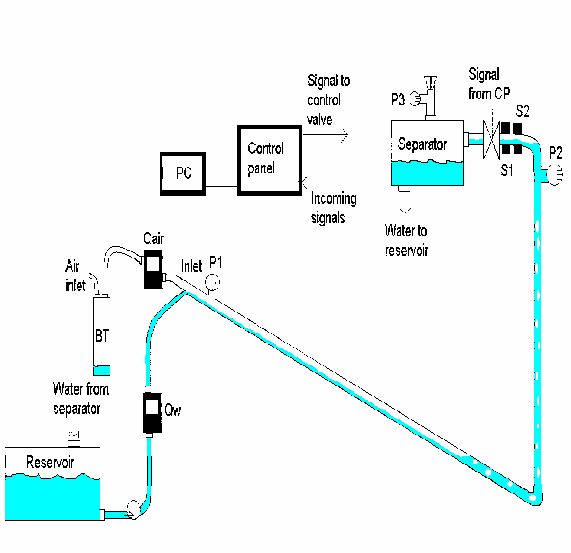

Fig. 4. Experimental setup

From the inlet, which is the mixing point for the air and water, the flow is transported trough a 3m long curved pipeline to the low-point at the bottom of the riser. Depending on different conditions such as water and air flow rates, slug flow may occur. At the top of the riser there is an acryl tank which serves as a separator, leading the water to a reservoir while the air is let out through an open hole in the top. The separator is thus holding atmospheric pressure.

From the reservoir the water is pumped back into the system through the mixing point using a Grundfos UPS 25-120 180 pump with a lifting capacity of 12m. It is possible to adjust the power of the pump, thereby changing the pressure dependency of the inlet flow rate of the water. The pressure dependency during the experiments is discussed in Section 2.3, where periodic disturbances in the inlet flow rate of gas from the air supply system are also described.

For slugging to appear there must be enough air in the system to blow the water out of the 2.7m long riser. This requires a certain amount of volume, which is accounted for by a 15 l acryl buffer tank (BT) between the air supply and the inlet. The volume of the gas can be changed by partially filling this tank with water.

The inlet flow rates of gas (Q_{air}) and water (Q_w) determine whether we will have slug flow in open loop operation or not. The gas flow rate is measured at the inlet using a 2-10 l/min mass flow sensor from Cole-Parmer. The water flow rate was measured using a 2-60 l/min flow transmitter from Gem. Typically inlet flow rates during an experiment are 5 l/min both for the gas and water.

Pressure sensors MPX5100DP from Motorola are located at the inlet (P_1) and topside (P_2). They measure the pressure difference between the atmospheric pressure and the pipeline pressure in the range 0-1 bar. Typically average values for the pressure during the experiments are approximately 0.2 barg at the inlet and 0.05 barg just upstream the topside control valve.

Two fiber optic sensors (S_1, S_2) from Omron are placed just upstream the control valve in order to measure the water content in the pipeline. Water in the pipeline will attenuate the laser beam and weaken the signal send to the control panel. The measurements from the fiber optic slug sensors needed some filtering because of spikes caused by reflections of the laser beam on the water/air interface (Figure 5). When correctly calibrated, the fiber optic sensors give a signal proportional to the amount of water the laser beam travels through in the pipeline and can be used to calculate the density ρ in the pipeline.

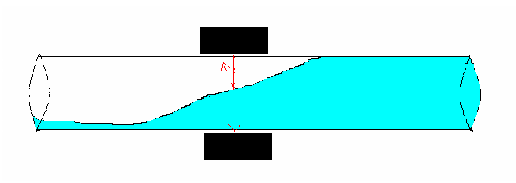

Fig. 5. Reflection of light on water surface

A pneumatic operated Gemü 554 angle seat globe valve with 20 mm inner diameter is installed at the top of the riser. A signal from the control panel sets the choke opening percentage of the valve. The valve responds well within a second to the incoming signal.

The control panel, consisting of Fieldpoint modules from National Instruments, converts the analog signals from the sensors into digital signals. The digital signals are then sent to a computer where they are continuously displayed and treated using Labview software. Depending on the control configuration, some of the measurements are used by the controller to set the choke opening for the control valve.

2.2 Labview software

Labview from National Instruments was chosen as tool for acquiring, storing, displaying and analyzing the data from the different sensors. Also the valve opening of the topside valve was set from this program. The controllers was made using Labview PID controllers with features like integrator anti-windup and bumpless controller output for PID gain changes.

Also Labviews PID Control Input Filter has been used to filter the noisy fiber optic signals. This is a fifth-order low-pass FIR (Finite Impulse Response) filter and the filter cut-off frequency is designed to be 1/10 of the sample frequency of the input value.

2.3 Disturbances

Two of the largest sources of disturbances during the experiments were the variations in the air and water inlet flow rates. The left plots in Figure 6 show how the air inlet rate Q_a is fluctuating with a period of approximately 200s between 5.5 and 5.9 l/min when the valve is 10% open and the flow is stable. These 200s fluctuations are caused by the on-off controller used for the pressurized air facility at the laboratory. The fluctuations in water rate Q_w are however quite small for this valve opening.

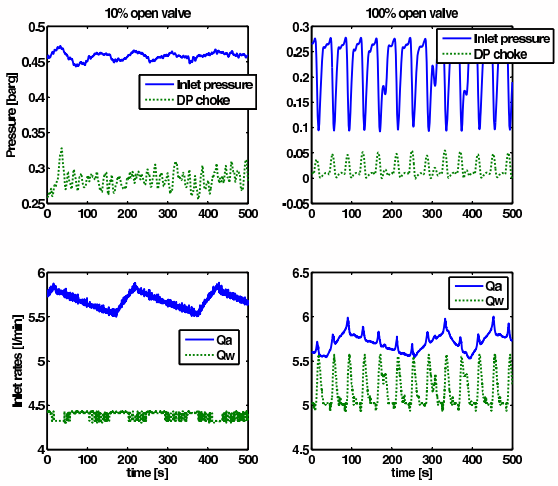

Fig. 6. Disturbances in the inlet water flow rate (Qw) and air inlet rate (Qa)

When the topside valve is fully open and the inlet pressure (P_1) starts to oscillate due to slug flow in the pipeline, larger fluctuations in the water flow was observed. The capacity of the water pump is pressure dependent, and oscillations in the inlet pressure cause the water rate to fluctuate between approximately 4.9 and 5.6 l/min as is seen from the right plots in Figure 6. The pressure oscillations also lead to oscillations in the air inlet flow rate, which come in addition to the 200s periodic fluctuations.

3. CONTROLLABILITY ANALYSIS AND SIMULATIONS

In order to have a starting point for the lab experiments, an analysis of the system has been performed. The analysis reveals some of the control limitations

that can be expected using different measurements for control. Closed-loop simulations using these measurements are also performed.

3.1 Theoretical background

Given the feedback control structure shown in Figure 7 the measured output y is found by

$$y = G(s)u + G_d(s)d \tag{1}$$

Here u is the manipulated input, d is the disturbance to the system and n is measurement noise. G and G_d are the plant and disturbance models.

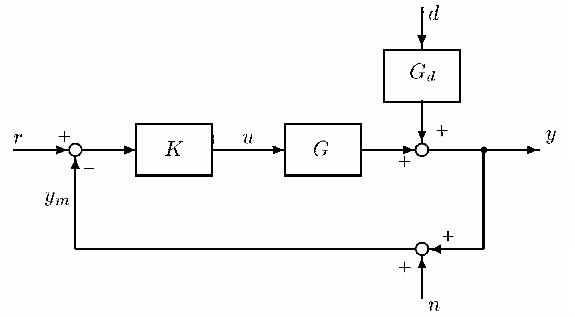

Fig. 7. One degree-of-freedom negative feedback control structure (Skogestad and Postlethwaite (1996))

The location of RHP (Right Half Plane) poles and zeros in $G(s)$ impose bounds on the bandwidth of the system. These bounds can render it impossible to control the system when the RHP-poles and -zeros are located close to each other. Skogestad and Postlethwaite (1996) show that a pair of pure complex RHP-poles places a lower bound on the bandwidth of the closed loop system:

$$w_c > 1.15|p| \tag{2}$$

whereas a real RHP zeros imposes an *upper* bound

$$w_c < |z|/2 \tag{3}$$

For an imaginary RHP-zero the bound is

$$w_c < 0.86|z| \tag{4}$$

When comparing Equation (2) with (3) and (4) it is easy to see that if the RHP-zeros and -poles are located close to each other, bandwidth problems can occur. The closed-loop system can also be expressed as

$$y = Tr + SG_d d - Tn \tag{5}$$

where $T = (I+L)^{-1}L$, $S = (I+L)^{-1}$ and $L = GK$. L is the loop transfer function, whereas S is called the classical sensitivity function and gives the sensitivity reduction introduced by the feedback loop. The input signal is

$$u = KSr - KSG_d d - KSn \tag{6}$$

and the control error $e = y - r$ is

$$e = -Sr + Sg_d d - Tn \tag{7}$$

From these equations it is obvious that the magnitude for transfer functions S, T, SG, KS, KSG_d and SG_d give valuable information about the effect u, d and n have on the system. In order to keep the input usage u and control error e small, these closed-loop transfer functions also need to be small. There are however some limitations for how small the peak values of these transfer functions can be. The locations of the RHP-zeros and -poles influence these bounds significantly.

Minimum peaks on S and T

Skogestad and Postlethwaite (1996) shows that for each RHP-zero z of $G(s)$ the sensitivity function must satisfy

$$||S||_\infty \geq \prod_{i=1}^{N_p} \frac{|z + p_i|}{|z - p_i|} \tag{8}$$

for closed-loop stability. Here $||S||_\infty$ denotes the maximum frequency response of S. This bound is tight for the case with a single RHP-zero and no time delay. Chen (2000) shows that the same bound is tight for T.

Minimum peaks on SG and SG_d

The transfer function SG is required to be small for robustness against pole uncertainty. Similar, SG_d needs to be small in order to reduce the effect of the input disturbances on the control error signal e. In Skogestad and Postlethwaite (1996) the following bounds are found for SG and SG_d

$$||SG||_\infty \geq |G_{ms}(z)| \prod_{i=1}^{N_p} \frac{|z + p_i|}{|z - p_i|} \tag{9}$$

$$||SG_d||_\infty \geq |G_{d,ms}(z)| \prod_{i=1}^{N_p} \frac{|z + p_i|}{|z - p_i|} \tag{10}$$

These bounds are valid for each RHP-zero of the system. Here G_{ms} and $G_{d,ms}$ are the "minimum, stable version" of G and G_d with RHP poles and zeros mirrored into the LHP.

Minimum peaks on KS and KSG_d

The peak on the transfer function KS needs to be small to avoid large input signals in response to noise

and disturbances, which could result in saturation. Havre and Skogestad (2002) derives the following bound on KS

$$||KS||_\infty \geq |G_s^{-1}(p)| \tag{11}$$

which is tight for plants with a single real RHP-pole p. Havre and Skogestad (2002) also finds

$$||KSG_d||_\infty \geq |G_s^{-1}(p)G_{d,ms}(p)| \tag{12}$$

When analyzing a plant, all of the closed-loop transfer functions should be considered.

3.2 Modelling

Storkaas et al. (2003) have developed a simplified model to describe the behavior of pipeline-riser slugging. One of the advantages of the model is that it is well suited for controller design and analysis. It consists of three states; the holdup of gas in the feed section (m_{G1}), the holdup of gas in the riser (m_{G2}), and the holdup of liquid (m_L). The model is illustrated by Figure 8.

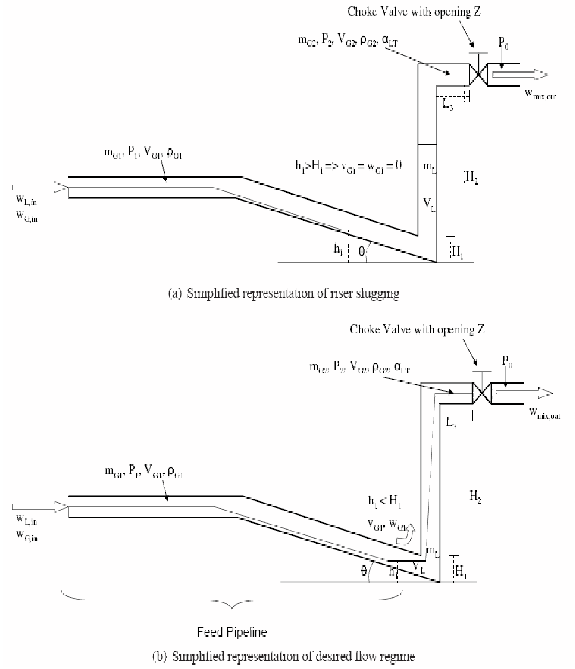

Fig. 8. Storkaas' pipeline-riser slug model (Storkaas et al. (2003))

Using this model we are able to predict the variation of system properties such as pressures, densities and phase fractions and analyze the system around desired operation points. After entering the geometrical and flow data for the lab rig, the model was tuned as described in Storkaas et al. (2003) to fit the open loop behavior of the lab rig. The model data and tuning parameters are presented in Table 1.

A bifurcation diagram of the system is plotted in Figure 9. It was found by open-loop simulations at different valve openings and gives information about the valve opening for which the system goes unstable. Also the amplitude of the pressure oscillations for the inlet and topside pressure (P_1 and P_2) at each valve opening can be seen from the plot.

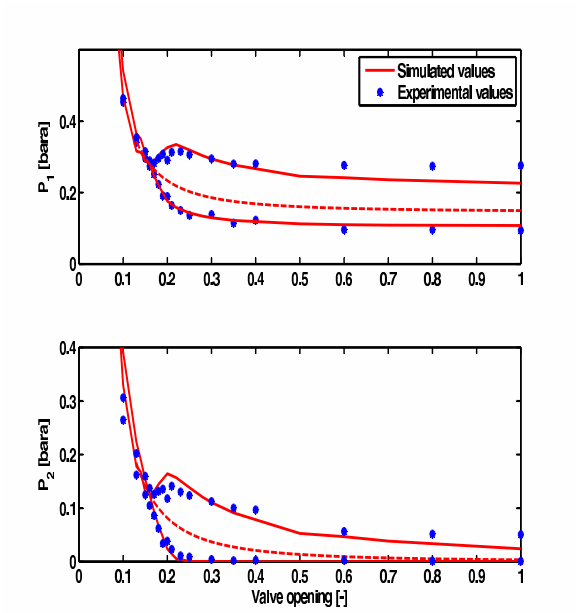

Fig. 9. Bifurcation plot showing the open loop behavior of the system

The upper line in the bifurcation plots shows the maximum pressure at a particular valve opening and the lower line shows the minimum pressure. The two lines meet at around 16% valve opening. This is the point with the highest valve opening which gives stable operation when no control is applied for this particular system. When Storkaas' model is properly tuned, the bifurcation point from the model will match the one from the experimental data. From the bifurcation diagram in Figure 9 it is seen that the tuned model values fit the results from the lab quite well. The dotted line in the middle shows the unstable steady-state solution. This is the desired operating line with closed-loop operation.

Figure 10 shows some of the simulations performed in order to find the bifurcation diagram. The plots show that the frequency predicted by the model is approximately 50% higher than the frequency of the slugs in the lab. In Figure 11 a root-locus diagram of the system is plotted. This plot shows how the poles cross into the RHP as the valve opening reaches 16% from below. This also confirms the results plotted in the bifurcation diagram in Figure 9.

3.3 Analysis

The model can now be used to explore different measurement alternatives for controlling the flow. The lab

Table 1. Model data parameters

Parameter	Symbol	Value
Inlet flow rate gas $[kg/s]$	$w_{G,in}$	$1.145 * 10^{-4}$
Inlet flow rate water $[kg/s]$	$w_{L,in}$	0.090
Valve opening at bifurctionpoint [-]	z	0.16
Inlet pressure at bifurcationpoint $[barg]$	$P_{1,stasj}$	0.28
Topside pressure at bifurcationpoint $[barg]$	$P_{2,stasj}$	0.125
Separator pressure $[barg]$	P_0	0
Liquid level upstream low point at bifurcationpoint $[m]$	$h_{1,stasj}$	$9.75 * 10^{-3}$
Upstream gas volume $[m^3]$	V_{G1}	$6.1 * 10^{-3}$
Feed pipe inclination $[rad]$	θ	$1 * 10^{-3}$
Riser height $[m]$	H_2	2.7
Length of horizontal top section $[m]$	L_3	0.2
Pipe radius $[m]$	r	0.01
Exponent in friction expression [-]	n	16
Choke valve constant $[m^{-2}]$	K_1	$2.23 * 10^{-4}$
Internal gas flow constant [-]	K_2	0.193
Friction parameter $[s^2/m^2]$	K_3	$3.4 * 10^3$

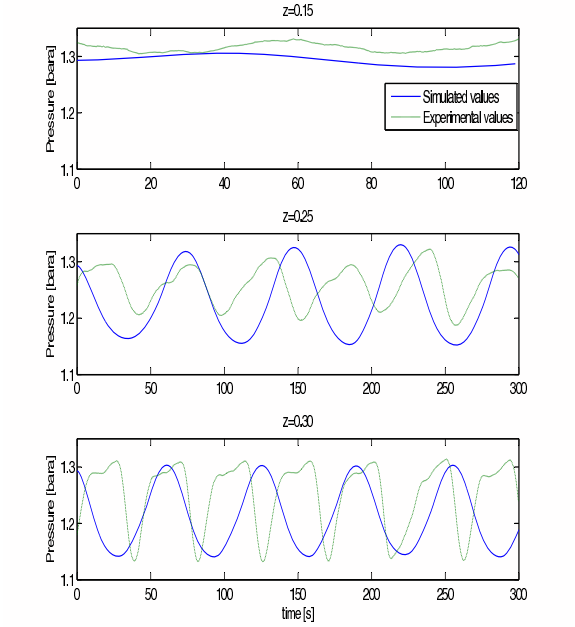

Fig. 10. Open-loop behavior of inlet pressure P_1 for valve openings 15, 25 and 30%

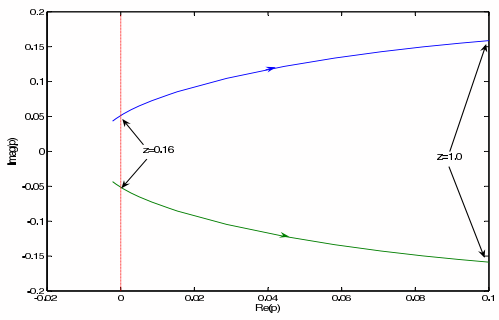

Fig. 11. Root-locus plot showing the trajectories of the RHP open-loop poles when the valve opening varies from 0 (closed) to 1 (fully open)

rig has four sensors as described in Section 2. There are two pressure sensors; one located at the inlet (P_1) and one located topside upstream the control valve (P_2). Also two fiber optic water hold-up measurements are located upstream the control valve. Using these measurements it is possible to estimate the density (ρ) and flow rates (F_Q, F_W) through the control valve. Figure 12 shows the different measurement candidates.

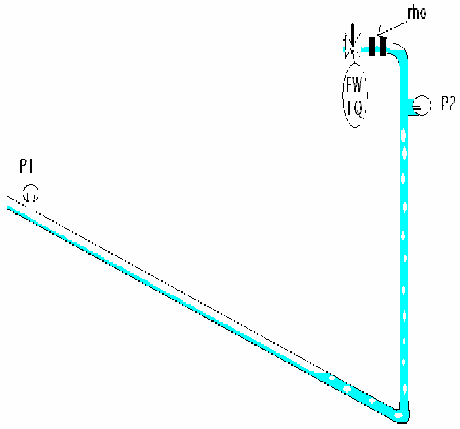

Fig. 12. Measurement candidates for control

In Section 3.1 it was shown how the locations of the RHP poles and zeros had a big influence on the controllability of the system. By scaling the system and calculating the sensitivity peaks it is possible to get a picture of how well a controller, using one of these measurements, can perform. The only two measurements of the ones considered in this paper which introduces RHP-zeros into the system, are the topside density ρ and pressure P_2.

The location of the pair of complex RHP-zeros introduced by P_2 does not cause any concern, as they are much larger and located to the right of the RHP-poles in the complex plane. The real RHP-zero introduced by ρ, however, seems to be more worrying as it is located to the right of the RHP-poles.

The process model G and disturbance model G_d were found from a linearization of Storkaas' model around two operation points. The model was then scaled as described in Skogestad and Postlethwaite (1996). The process variables were scaled with respect to the largest allowed control error and the disturbances were scaled with the largest variations in the inlet flow rates in the lab. The disturbances were assumed to be frequency independent. The input was scaled with the maximum allowed positive deviation in valve opening since the process gaing is smaller for large valve openings. For measurements y = $[P_1; P_2; \rho; F_W; F_Q]$ the scaling matrix is De = diag[0.1 0.05 100 0.01 $1e^{-5}$ 0.1]. The scaling matrix for the outputs is Dd = diag [$1e^{-5}$ $1e^{-2}$]. This represents approximately 10% change in the inlet flow rates from the nominal values of $1.145e^{-4}$ kg/s (5.73 l/min)for gas and $90{*}e^{-}3$ kg/s (5.4 l/min) for water. The input is scaled Du = $1 - z_{nom}$ where z_{nom} is the nominal valve opening.

Tables 2 and 3 presents the controllability data found. The location of the RHP poles and zeros are presented for valve openings 25 and 30 %, as well as stationary gain and lower bounds on the closed-loop transfer functions described in Section 3.1. The pole location is independent of the input and output (measurement), but the zeros may move. From the bifurcation plot in Figure 9 it is seen that both of these valve openings are inside the unstable area. This can also be seen from the RHP location of the poles.

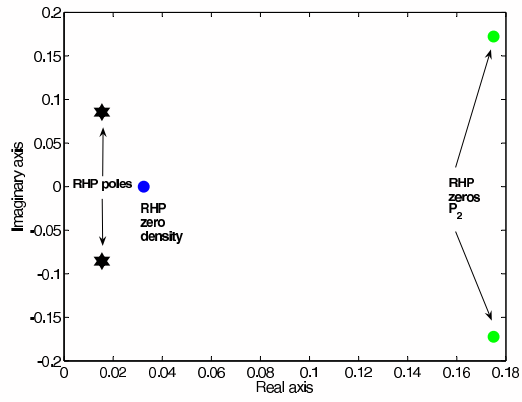

Fig. 13. Plot-zero map for valve opening 30%

The only two measurements of the ones considered in this paper which introduces RHP-zeros into the system, are the topside density ρ and pressure P_2. In Figure 13 the RHP poles and relevant RHP zeros are plotted together. The RHP zeros are in both cases located quite close to the RHP poles, which results in the high peaks especially for sensitivity function SG but also for S. From this we can expect problems when trying to stabilize the flow using these measurements as single measurements.

The stationary gain found when using the volumetric flow rate F_W is approximately zero, which can cause a lot of problems with steady state control of the system. Also the stationary gain for the plant using density ρ as measurement has a low stationary gain. The model is however based on constant inlet flow rates. The stationary gain for F_W predicted by the model is 0, which means that it is not possible to control the steady-state behavior of the system and the system will drift. Usually the inlet rates are pressure dependent, and the zeros for measurements F_Q and F_W would be expected to be located further away from the origin than indicated by Tables 2 and 3.

When comparing $|KS|$ and $|KSG_d|$ for the two tables, it is obvious that the peak values for these transfer functions increase with valve opening for all the measurement candidates, indicating that controlling around an operating point with a larger valve opening increases the effect disturbances and noise have on the input usage.

Figure 14 and 15 shows the bode plots for the different plant models and disturbance models respectively. The models were found from a linearization of the model around valve opening 25%. For the volumetric flow rate measurement F_W the value of the disturbance model G_dW is higher than plant model GW for low frequencies. For acceptable control we require $|G(jw)| > |Gd(jw)| - 1$ for frequencies where $|G_d| > 1$ (Skogestad and Postlethwaite (1996)). In this case both $|G_dW|$ and $|G_W|$ are close to zero, which means problems can occur for this measurement.

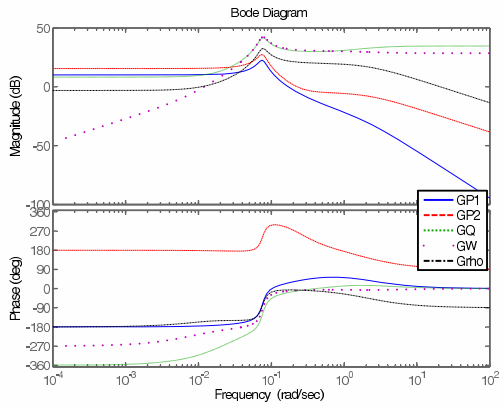

Fig. 14. Bode plots for the plant models using different measurements

3.4 Simulations

Closed-loop simulations were performed in order to investigate the effect of the limitations found in the analysis. The measurements were used as single measurements in a feedback loop with a PI-controller. Figure 16 shows this control structure using the inlet pressure P_1 as measurement.

Figure 17 compares the results using four different measurement candidates. The disturbances in inlet

Table 2. Control limitation data for valve opening 25%. Unstable poles at $p = 0.010 \pm 0.075i$.

Measurement	RHP zeros	Stationary gain	Minimum bounds				
		$\|G(0)\|$	$\|S\|$	$\|SG\|$	$\|KS\|$	$\|SG_d\|$	$\|KSG_d\|$
$P_1[bar]$	-	3.20	1.00	0.00	0.14	0.00	0.055
$P_2[bar]$	0.18±0.17i	5.97	1.13	1.59	0.091	0.085	0.055
$\rho[kg/m^3]$	0.032	0.70	1.20	4.62	0.048	0.31	0.056
$F_W[kg/s]$	-	0.00	1.00	0.00	0.015	1.00	0.055
$F_Q[m^3/s]$	-	2.59	1.00	0.00	0.015	0.00	0.055

Table 3. Control limitation data for valve opening 30%. Unstable poles at $p = 0.015 \pm 0.086i$

Measurement	RHP zeros	Stationary gain	Minimum bounds				
		$\|G(0)\|$	$\|S\|$	$\|SG\|$	$\|KS\|$	$\|SG_d\|$	$\|KSG_d\|$
$P_1[bar]$	-	1.85	1.00	0.00	0.34	0.00	0.086
$P_2[bar]$	0.18±0.17i	3.44	1.22	1.25	0.23	0.085	0.079
$\rho[kg/m^3]$	0.032	0.41	1.26	2.86	0.091	0.31	0.081
$F_W[kg/s]$	-	0.00	1.00	0.00	0.028	1.00	0.079
$F_Q[m^3/s]$	-	1.53	1.00	0.00	0.028	0.00	0.079

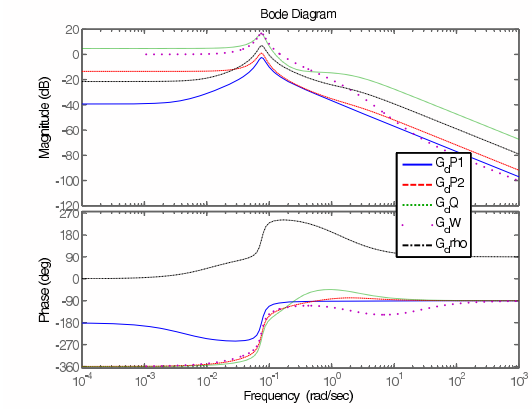

Fig. 15. Bode plots for the disturbance models using different measurements

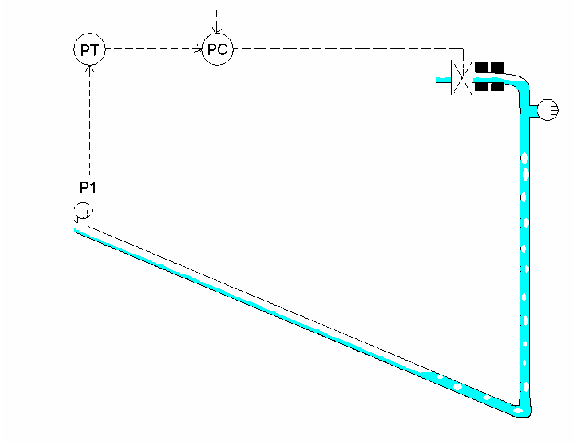

Fig. 16. Feedback control using PI controller with inlet pressure P_1 as measurement

flow rates for the gas and water, as described in Section 2.3, are also included in these simulations. The only measurement that is not included is the topside pressure P_2, as the corresponding controller was not able to stabilize the flow.

At first, the controller is turned off and the system is left open-loop with a valve opening of 20% for approximately 5-10 min. From the bifurcation diagram in Figure 9 it was shown that the system goes unstable for valve openings larger than 16%, as expected the pressure and flow rates start to oscillate due to the effects of slug flow.

When the controllers are activated, the control valve starts working as seen from the right plot in Figure 17. The aim of the simulation study is to see how far into the unstable region it is possible to control the flow with satisfactory performance. A larger valve opening gives higher production with a given pressure dependent source.

As expected the measurement giving the best result was inlet pressure P_1. The upper left plot shows how the controller quickly stabilizes at the desired set point. The average valve opening is 25 %, which is far into the unstable region. After about 70 min the set point for the pressure is decreased, and the valve opening is now larger than 30%. Still the performance of the controller is good.

The figure also shows the results from controlling the flow using the topside volumetric flow rate F_Q, mass flow rate F_W and the density ρ. Not surprisingly the density measurement was not very well suited, as was expected from the analysis in Section 3.3. It was possible to control the flow using this measurement, but not at an average valve opening larger than 17-18 % which is just inside the unstable area. The benefits of using control are therefore negligible.

The small oscillations seen in each plot has a period of 200 s and is caused by the periodic oscillations of the inlet air flow rate. The results using the topside pressure P_2 are not included in the figure. This is because it was not possible to stabilize the flow inside the unstable region using this measurement. Although the analysis suggested otherwise, the disturbances added in the simulations might have had a larger effect on this measurement than on the others.

Sometimes control configurations using combinations of measurements can improve the performance of a

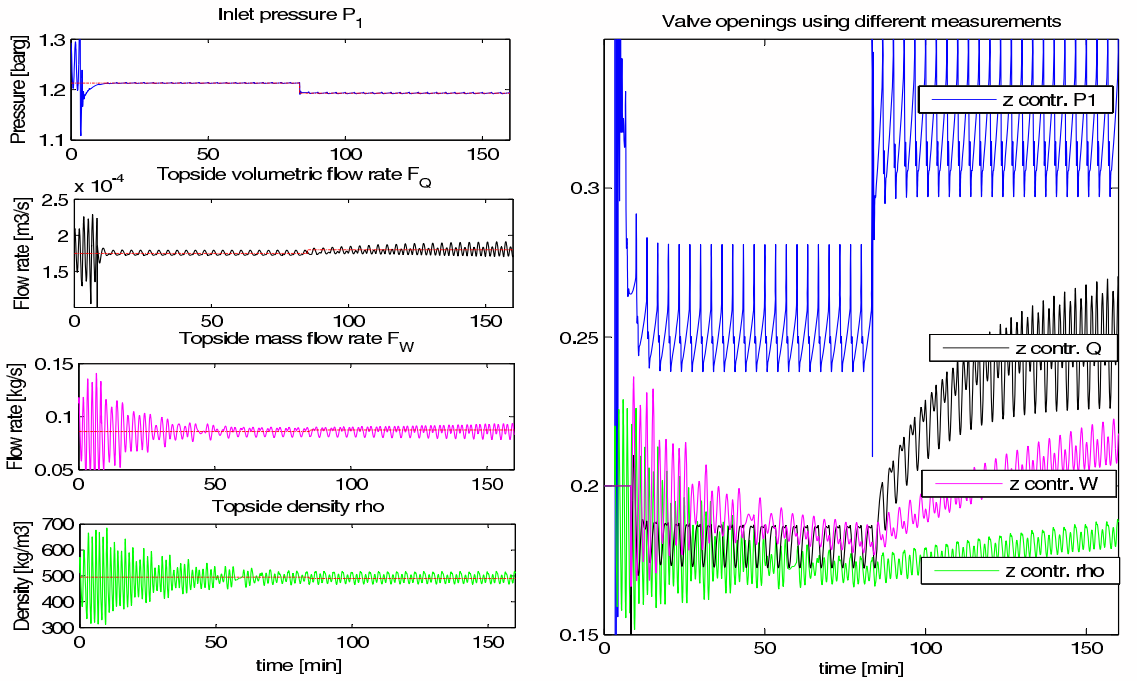

Fig. 17. Controlling the flow using PI controllers

controller when compared with controllers using single measurements. This is why cascade controllers using different combinations of the topside measurements have been applied to the system. Figure 18 shows an example of such a control configuration. The inner loop controls the topside density ρ, while the set point for this inner controller is set by an outer loop controlling the valve opening. This way drift due to the low stationary gain for ρ is avoided.

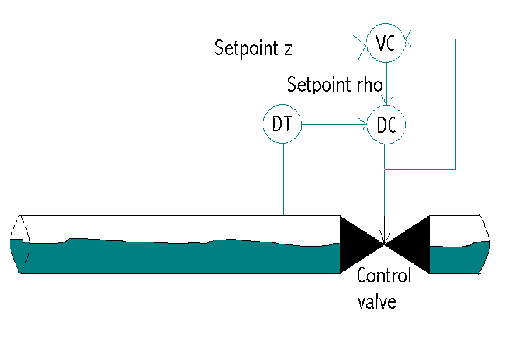

Fig. 18. Cascade controller using measurements density ρ and valve opening z

The results from simulations using this control structure are plotted in Figure 19. The set point for the outer loop controller, controlling the valve opening, is increased from 17% to 18% after approximately 170 min. The flow then quickly becomes unstable, even though the valve opening is just inside the unstable region. The results using this controller are approximately the same as when using the PI controller with density ρ. What is not revealed by Figure 17 however, is whether or not the controller will drift as the simulations is stopped before the controller has stabilized at the desired set point.

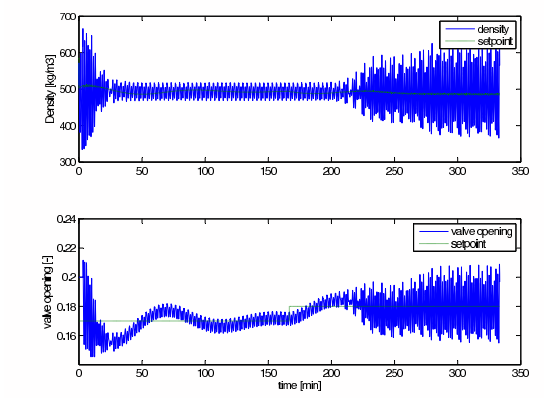

Fig. 19. Simulation results using density ρ and valve opening z as measured variables in a cascade control structure

Using the volumetric flow rate measurement, F_Q, in the inner loop instead would probably give better results as this measurement stabilizes the flow better than the density measurement ρ.

4. EXPERIMENTAL RESULTS

Even though the results from the analysis and simulations suggested that the topside volumetric or mass flow rates F_Q and F_W would be better measurements for control than the topside density ρ, an attempt was made on controlling the flow using the density as measurement in the inner loop. The density was found using the fiber optic signals.

The reason why flow measurements were not included in the experiments was because no direct measurements were available. One alternative would be to calculate the flow using a valve equation for two-phase flow and the topside pressure measurement P_2, fiber optic signals S_1 and S_2 and the valve opening z. However, two-phase flow valve equations are quite complicated, and it seemed easier first to use the measurements at hand.

Three different combinations of measurements were tested in a cascade control structure. One of the controllers uses the inlet pressure P_1 in the inner loop and the valve opening z in the outer loop. Even though P_1 is not a topside measurement, the results using this controller serve as a basis to compare the other two controllers with. The other two control structures use the topside density ρ in the inner loop, and had either the valve opening z (Figure 18) or the topside pressure P_2 as a measurement in the outer loop .

Figure 20 shows the experimental results using the three control systems. First the system was left open-loop with a valve opening of 25%. Since this is well inside the unstable area, the pressures and density in the system is oscillating. After about 100s the controllers are turned on, and in both three cases the controllers are able to control the flow. When the controllers are turned off after 500-600s, the flow quickly becomes unstable again. The thick lines indicated the set points for the different controllers. In plot a) and b) in Figure 20 the valve opening set point for the outer loop was 25% fully open, whereas for the experiment presented in plot c) the set point for the topside pressure P_2 in the outer loop was 0.056. Earlier experiments had shown that this lead to an average valve opening of about 25%.

From the analysis and simulations presented in Section 3, it is expected that the control structure with the inlet pressure P_1 in the inner loop would perform best, as this measurement was by far the best suited for controlling the flow as seen both from simulations and control limitations for each measurement candidate. Also, the density measurement at the laboratory is extremely noisy as the plots in Figure 20 show. Despite all this, looking at the experimental results the differences are less obvious. In fact, using the density ρ as the inner measurement works quite well, contradicting the results from the analysis in Section 3.

The main reason for adding the outer loop is to avoid drift in the inner loop caused by the low steady state gain shown in Tables 2 and 3. Since the results from the experiments using a cascade configuration by far outperform the results from the simulations, it was reason to question the values given by the model. This is why an attempt was made to see whether it was possible to control the flow using the density as *only* measurement for control. Figure 21 shows the results using this PI controller and the density measurement ρ.

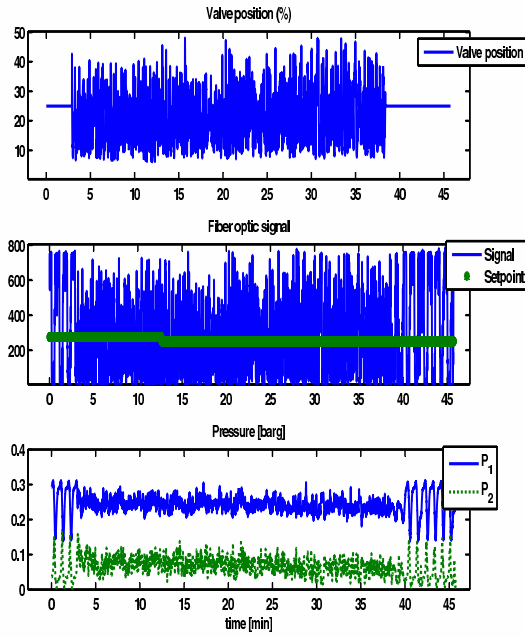

Fig. 21. Experimental results using a PI controller with density ρ as single measurement (no outer loop added)

Also now the controller manages to control the flow. The system does not seem to drift, which means that the steady state gain is not too small for stabilizing the flow in this case. Controlling the flow at a larger average valve opening led to reduced performance and the flow either became unstable or the controller did not manage to satisfactory keep the measurements at the desired set points (large fluctuations). As the analysis showed, the control task gets harder as the valve opening increases. This is due to the fact that the gain is reduced as the valve opening gets larger. By gradually increasing the average valve opening, either by increasing the set point for valve opening in the outer loop or, for case c), reducing the set point for the density, the effect of this increase in valve opening was found.

Some results are plotted in the Appendix, where it is seen that the effect of increasing the average valve opening from approximately 24% to 32%using P_1 as measurement leads to increasingly larger fluctuations around the set points. The same experiments were performed for using density ρ as measurement in the inner loop with a) z and b) P_2 in the outer loop. This made the system go unstable as the valve opening was gradually increasing. The average valve opening for which the system goes unstable using these controllers were approximately a) 26% and b) 29%.

5. DISCUSSION

When comparing different controllers, the tuning of the parameters has a high influence on the results.

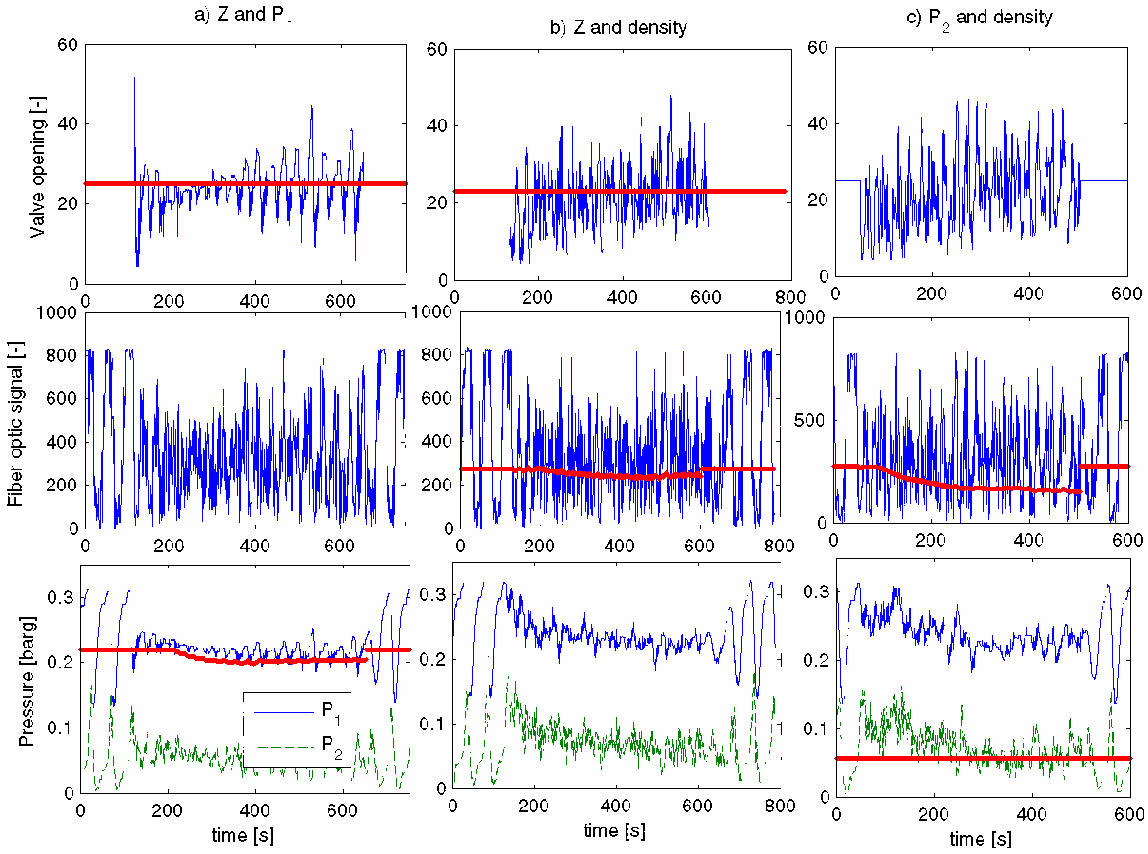

Fig. 20. Results from cascade control experiments at the lab at an approximately valve opening of 25%

None of the controllers described in this paper have been fine-tuned and the results might be improved further with some more work. This is why the maximum average valve opening for which the controllers stabilize the flow, presented in Section 4, might be increased with proper tuning. However, from the results it seems obvious that all three controllers perform well up to approximately 25% valve opening and that as the valve opening moves towards an average value of 30% the controller performance decreases for all the controllers.

It is important to note that the model used for the analysis is a very simplified model. It was used merely as a tool to see which problems might occur in the lab, and the underlying reasons for the problems. When comparing the experimental results with analysis and simulations using Storkaas' model prior to the experiments, it was clear that the experimental results were far better than the model predicted when using the density as measurement. On the other hand, the topside pressure P_2 could not be used for stabilization, in agreement with Storkaas' model.

An attempt was made to model the small-scale rig using multiphase simulator OLGA from Scandpower Petroleum Technologies. However, the simulations seemed to fail due to numerical errors, which could be caused by the small scale nature of the rig. Even though results using only a PI controller and a single topside density measurement seemed to work very well, without the expected steady state drift, there are other advantages in adding an outer loop. One example of such is that it may be more intuitive to understand what is going on with the plant when adjusting the set point for the valve opening rather than the set point for the topside density.

The experiments have been conducted on a small-scale rig with only 20mm inner diameter pipeline. Whether or not the results can be directly applied to larger test facilities was further investigated in Sivertsen et al. (2008). The results from these experiments showed that similar controllers as the ones described in this paper, also were successful when applied to a medium scale lab rig with a 10m high riser and 7.6 cm diameter pipelines.

6. CONCLUSION

This paper presents results from a small-scale riser laboratory rig where the aim was to control the flow using only topside measurements and thereby avoiding slug flow in the pipeline. The results were good in the sense that it was possible to control the flow with good performance far into the unstable region. In order to avoid the slug merely by choking the topside valve it would be necessary to operate with a valve opening of 15%, whereas here it was shown that it was possible to control the flow with an average valve opening of 25%, despite very noisy measurements. This makes

it possible to produce with a larger production rate and increase the total recovery from the producing oil field.

7. ACKNOWLEDGMENT

The authors would like thank former students who have been involved in the project and helped in building the lab rig; Ingvald Baardsen and Morten Sndrol. Also the staff at the Faculty of Natural Sciences and Technology has been great in helping with equipment and software problems. We would also like to thank StatoilHydro and the Norwegian Research Council for their financial support.

APPENDIX

Figures showing the behavior when increasing the setpoint, z_s for the outer loop using measurment P_1 in the inner loop:

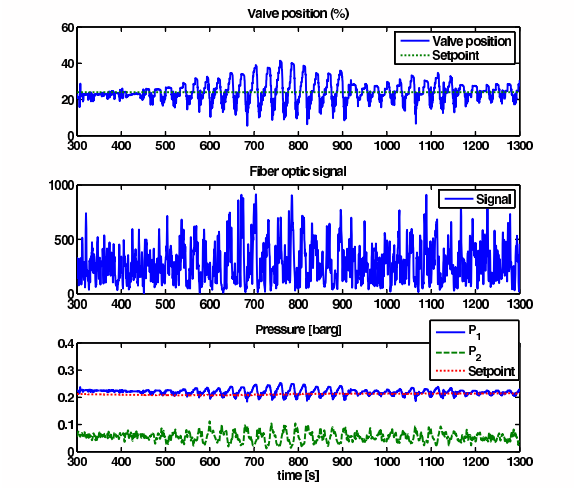

Fig. 22. Control quality when setpoint outer loop is 24%

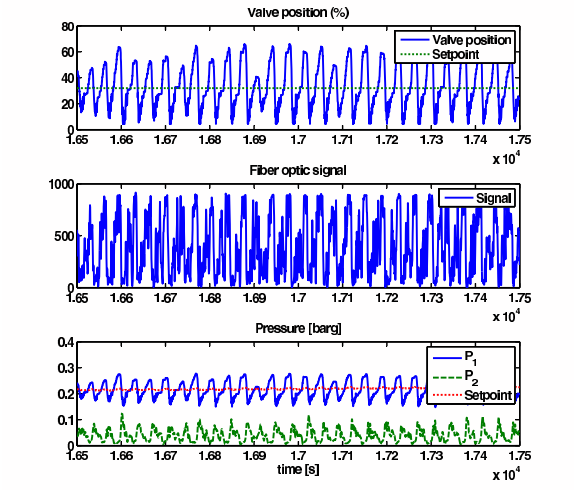

Fig. 23. Control quality when setpoint outer loop is 32%

REFERENCES

I. Bårdsen. Slug regulering i tofase strømning - eksperimentell verifikasjon. Project report, Norwegian University of Science and Technology, November 2003.

D. Barnea. A unified model for predicting flow pattern transitions for the whole range of pipe inclinations. *Int. J. Multiphase Flow*, 13:1–12, 1987.

J. Chen. Logarithmic integrals, interpolation bounds and performance limitations in MIMO feedback systems. *IEEE Transactions on Automatic Control*, AC-45(6):1098–1115, 2000.

A. Courbot. Prevention of severe slugging in the Dunbar 16" multiphase pipeline. *Offshore Technology Conference, May 6-9, Houston, Texas*, 1996.

J.M. Godhavn, M.P. Fard, and P.H. Fuchs. New slug control strategies, tuning rules and experimental results. *Journal of Process Control*, 15(15):547–577, 2005.

K. Havre and S. Skogestad. Achievable performance of multivariable systems with unstable zeros and poles. *International Journal of Control*, 74:1131–1139, 2002.

K. Havre, K. O. Stornes, and H. Stray. Taming slug flow in pipelines. *ABB review*, 4(4):55–63, 2000.

P. Hedne and H. Linga. Supression of terrain slugging with automatic and manual riser choking. *Advances in Gas-Liquid Flows*, pages 453–469, 1990.

G.F. Hewitt and D.N. Roberts. Studies of two-phase flow patterns by simultaneous x-ray and flash photography. Technical report, UKAEA Report AERE M-2159, 1969.

J.F. Hollenberg, S. de Wolf, and W.J. Meiring. A method to supress severe slugging in flow line riser systems. *Proc. 7th Int. Conf. on Multiphase Technology Conference*, 1995.

Z. Schmidt, J.P. Brill, and H. D. Beggs. Choking can eliminate severe pipeline slugging. *Oil & Gas Journal*, (12):230–238, Nov. 12 1979.

Z. Schmidt, J.P. Brill, and H.D. Beggs. Experimental study of severe slugging in a two-phase pipeline-riser system. *Soc. Pet. Eng. J.*, pages 407–414, 1980. SPE 8306.

H. Sivertsen and S. Skogestad. Anti-slug control experiments on a small scale two-phase loop. *ESCAPE'15, Barcelona, Spain*, 2005.

H. Sivertsen, V. Alstad, and S. Skogestad. Medium-scale experiments on stabilizing riser slug flow. To be published, 2008.

G. Skofteland and J.M. Godhavn. Suppression of slugs in multiphase flow lines by active use of topside choke - field experience and experimental results. *Multiphase '03, San Remo, Italy*, 2003.

S. Skogestad and I. Postlethwaite. *Multivariable feedback control*. John Wiley & sons, 1996.

E. Storkaas, S. Skogestad, and J.M. Godhavn. A low-dimentional model of severe slugging for controller design and analysis. *Multiphase '03, San Remo, Italy*, 2003.

Y. Taitel. Stability of severe slugging. *Int. J. Multiphase Flow*, 12(2):203–217, 1986.

Y. Taitel and A.E. Dukler. A model for predicting flow regime transitions in horizontal and near-horizontal gas-liquid flow. *AIChE Journal*, 22:47–55, 1976.

Y. Taitel, D. Barnea, and A.E. Dukler. Modeling flow pattern transitions for steady upward gas-liquid flow in vertical tubes. *AIChE Journal*, 26:345–354, 1980.

MEDIUM-SCALE EXPERIMENTS ON STABILIZING RISER SLUG FLOW

Heidi Sivertsen * **Vidar Alstad** ** **Sigurd Skogestad** *,[1]

* *Department of Chemical Engineering, Norwegian University of Science and Technology, Trondheim, Norway*
** *StatoilHydro Research Centre, Porsgrunn*

This is the second of two papers describing control experiments on different scale slug rigs. The first paper describes experiments performed on a small-scale lab rig build at NTNU's Department of Chemical Engineering. These experiments showed that despite noisy measurements, it is possible to stabilize the flow in the slug flow region using only topside measurements. The question to be answered in this paper is; do these results also apply for *larger* riser-systems?

In this paper, we look at some results obtained from a 10m high, 3" diameter *medium*-scale test rig located at StatoilHydro's Research Centre in Porsgrunn, Norway. Several cascade control structures are tested and compared; both with each other and the results obtained from the small-scale NTNU loop. The rig was also modelled and analysed using a simple three-state model. The new experiments were successful and confirmed the results achieved using the small-scale rig. This suggests that the small-scale lab loop can be used as a tool to predict possible useful control strategies for the riser slug problem.

1. INTRODUCTION

The behavior of multiphase flow in pipelines is of great concern in the offshore oil and gas industry, and a lot of time and effort have been spent studying this phenomena. The reason for this is that by doing relatively small changes in operating conditions, it is possible to change the flow behavior in the pipelines drastically. This has a huge influence on important factors such as productivity, maintenance and safety.

Slug flow is a flow regime that has a negative impact on the receiving facilities during offshore oil and gas production due to the large fluctuations in flow rates and pressure. Frequent problems are unwanted flaring and reduced operating capacity. The fluctuating pressure also leads to a lot of strain on other parts of the system, such as valves and bends. The burden on the topside separators and compressors can in some cases become so large that it leads to damages and plant shutdown, representing huge costs for the producing company. Being able to remove slugging has a great economic potential and this is why lot of work and money has been spent on finding solutions to the problem.

In the last years there have been several studies on active control as a tool to "stabilize" the flow and thereby avoiding the slug flow regime. Mathematically, the objective is to stabilize a flow region which otherwise would be unstable. A simple analogue is stabilization of a bicycle which would be unstable without control. Schmidt et al. (1979) was the first to successfully apply an automatic control system on a pipeline-riser system with a topside choke as actuator. Hedne and Linga (1990) showed that it was possible to control the flow using a PI controller and pressure sensors measuring the pressure difference over the riser. Lately different control strategies have also been implemented on production systems offshore with great success (Hollenberg et al. (1995), Courbot (1996), Havre et al. (2000), Skofteland and Godhavn (2003)).

Active control makes it possible to avoid the slug flow regime with conditions where slug flow is predicted. This way it is possible to operate with the same average flow rates as before, but without the huge oscillations in flow rates and pressure. The advantages with using active control are large; it is much cheaper

[1] Author to whom correspondence should be addressed: skoge@chemeng.ntnu.no

than implementing new equipment and it also removes the slug flow all together thereby removing the strain on the system. This way a lot of money can also be saved on maintenance. Also, it is possible to produce with larger flow rates than what would be possible by manually choking the topside valve.

Subsea measurements are usually included in the control structures that have been reported in the literature so far. Pressure measurements at the bottom of the riser or further upstream are examples of such measurements. When dealing with riser slugging, subsea measurements have proved to effectively stabilize the flow. When no subsea measurements are available, we will see that the task gets far more challenging.

Since subsea measurements are less reliable and much more costly to implement and maintain than measurements located topside, it is interesting to see if it is possible to control the flow using only topside measurements. Is it also possible to combine topside measurements in a way that improve the performance? And are the results comparable to the results obtained when using a controller based on subsea measurements?

Earlier studies on using only topside measurements are found in Godhavn et al. (2005) where experiments were performed on a larger rig and the flow was controlled using combinations of pressure and density measurements. Similar experiments as the ones described in this paper was later performed on a medium-scale lab rig to investigate the effect the scale of the lab rig has on the quality of the controllers. These experiments are described in Sivertsen and Skogestad (2008).

The medium-scale multiphase flow control rig at StatoilHydro Research Centre in Porsgrunn is built to simulate multiphase flow in an offshore well/pipeline and production unit. The facility is ideal for development and testing of new control solutions for anti-slug and separator control under realistic conditions. Figure 1 shows a photograph of the facility.

Fig. 1. A birds-view perspective of the medium-scale riser rig at StatoilHydro Research Centre in Porsgrunn

Several experiments were performed to test similar control configurations as was also tested on the NTNU small-scale lab rig. This was done in order to investigate whether different scales have an effect on the quality of the control structures. Having results from a larger rig could give an indication on whether the small-scale NTNU lab rig really was suitable as a tool for finding good control solutions to be used in larger scale facilities, such as a production platform.

The question was; could active control be used to stabilize the flow also for the medium-scale lab rig? In particular, it was interesting to see whether only topside measurements could be used to stabilize the flow, as was done on the small-scale lab rig described in Sivertsen and Skogestad (2008).

2. EXPERIMENTAL SETUP

During the experiments the flow consisted of water and air. The pipe diameter is 3" (7.6 cm) and the height of the riser is approximately 10 m. The inflow of gas and water was pressure dependent. Water inlet rate during the experiments was 7-8 m^3/h while the air inflow rate fluctuated between 8 to 11 m^3/h. Slugging occurred for valve openings larger than about 12%. Figure 2 show a schematic overview of the layout and available instrumentation.

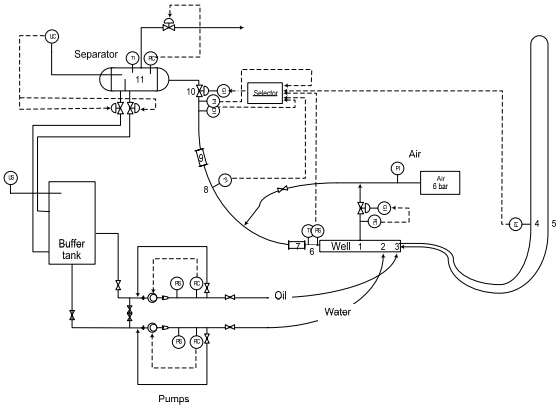

Fig. 2. Schematic overview of the layout and available instrumentation

The loop includes an approximately 4 m long section where gas, oil and water are introduced through different inlets. This "well section" consists of annulus and tubing, a 15.2 cm outer pipe and a 7.6 cm inner tubing with perforations.

The pipe section consist partly of flexible tubing, hence it is possibly to vary the geometry of the piping. This way the inclination of the riser and other parts of the pipe can be adjusted to achieve the desired geometry.

The pipeline geometry during the experiments was chosen to give terrain-induced slugging. A more detailed schematic of the geometry used in the experiments is shown in Figure 3. The numbers indicate the

location of feeding inlets and important instrumentation.

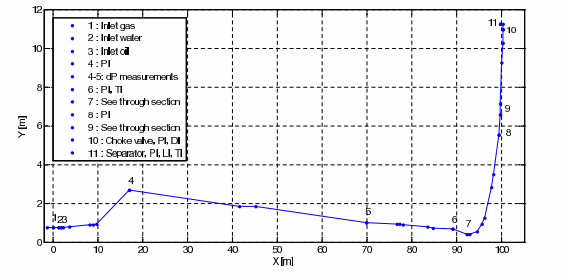

Fig. 3. Schematic of the geometry of the riser-system

The numbers 1, 2 and 3 indicate the air, water and oil inlets respectively. Downstream this section the pipeline is close to horizontal for about 10 m. An approximately 7 m, 35° inclined section then follows. A pressure measurement (P_1) is implemented at the end of this section (4). The next 60 m section has a 1.8° declination, followed by an approximately 20 m horizontal section with a pressure and temperature measurement at the end (6). A 10 m long vertical riser then follows a low point in the geometry (7). The low-point contains a see-trough section, which makes it possible to determine visually the flow regime in this section. At the top of the riser a production choke (10) and separator (11) are located. There is also a pressure measurement (8) and a see-through section (9) located half-way up the riser. Upstream the production choke a pressure measurement (P_2) and a gamma densiometer are implemented.

The water and oil outlets from the separator are returned to a large 10 m^3 buffer tank. The oil and water feed are pumped from this buffer tank back to the respective phase inlets in the well section using two displacement pumps. Before entering the well section, the feed flow rate and density of each phase are measured.

2.1 Gas feed

The compressed air is supplied from the local air supply net. The supplied air holds a pressure of approximately 7 bara. An automated control valve controls the feed flow rate of compressed air to the well section. The operating range of the control valve is 10-400 kg/h. During experiments the feed flow of air is normally in the range 15 to 50 kg/h.

The mass flow and the density of the compressed air are measured using a Coriolis type mass flow meter.

2.2 Water feed

A displacement pump controls the feed flow rate of water. The power is either set directly by the operator or given as output from a feedback controller using the volumetric flow rate as measurement. The pressure and single-phase flow rates are measured downstream the pumps, using a differential pressure volumetric flow meter (Pivot tube) for the air and a Coriolis type mass flow for the water.

2.3 Separator

The three-phase separator located at the top of the riser has a volume of approximately 1.5 m^3. A 53 cm high weir plate separates the oil and water outlets. The separator is equipped with a pressure measurement and measurements of the oil and water levels. No oil was added to the flow during the experiments presented in this paper.

2.4 Control choke valve

The control choke valve is a vertically positioned valve located at the top of the riser. The valve is equipped with a Profibus-PA Positioner, which returns the actual valve position to the control system.

2.4.1. Choke valve characteristics Several flow experiments had been performed in order to find the single- and two-phase (water/air) valve characteristics:

$$Q = \overbrace{C_v f(z)}^{K(z)} \sqrt{\frac{\Delta P}{\rho}} \tag{1}$$

C_v is the valve constant and $f(z)$ is the characteristics of the valve. ΔP is the pressure drop across the valve and ρ is the density of the fluid. For valve openings less than 50% and 60% for single-phase and two-phase flow respectively, the characteristics were found to be close to linear. Thus, Equation (1) can be written

$$Q/C_v = z\sqrt{\frac{\Delta P}{\rho}} \tag{2}$$

Values for Q/C_v can be calculated from given values for valve opening z, measured pressure drop across the valve ΔP and measured density ρ.

2.5 Instrumentation

A number of automatic control valves are installed. This includes the production choke valve, the valves controlling gas, water and oil outlet from the separator and the feed flow of air to the well section. These valves can be operated either in manual mode or in automatic mode where valve openings are given as output from PID feedback controllers. The rig is controlled from a control room located close to the rig.

3. CONTROLLABILITY ANALYSIS

3.1 Modelling

In Sivertsen and Skogestad (2008) it was shown how an analysis of a model describing a *small*-scale lab-rig did reveal fundamental control limitations depending on which measurements that were used for control. This was found using a simplified model (Storkaas et al. (2003)). One of the advantages of this simple model is that it is well suited for controller design and analysis. It consists of three states; the holdup of gas in the feed section (m_{G1}) and in the riser (m_{G2}), and the holdup of liquid (m_L). The model is illustrated in Figure 4.

The same model was used to predict the behaviour for the medium-scale lab rig used in this study. Using this model the system was analysed in the same way as in Sivertsen and Skogestad (2008). Both open- and closed loop simulations were performed.

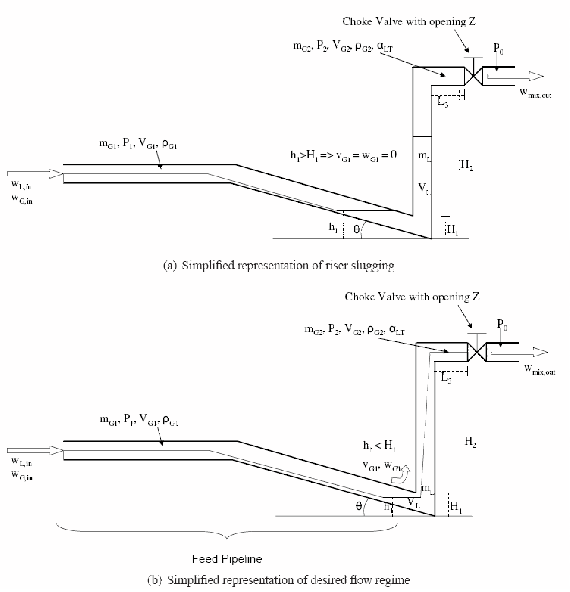

Fig. 4. Storkaas' pipeline-riser slug model (Storkaas et al. (2003))

After entering the geometrical and flow data for the lab rig, the model was tuned as described in Storkaas et al. (2003) to fit the open loop behaviour of the lab rig. The model data and tuning parameters are presented in Table 1. After inserting new system parameters and re-tuning the model, the open-loop data found using the model fitted the experimental results quite well as shown by the bifurcation plot in Figure 5.

The bifurcation diagram gives information about the valve opening for which the flow becomes unstable and shows the amplitude of the pressure oscillations for the inlet and topside pressures (P_1 and P_2). The upper lines in the bifurcation plot show the maximum pressure at a particular valve opening and the lower line shows the minimum pressure. The lines meet at the "bifurcation point" when the valve opening is approximately 12%. This is the point where transition to slug flow occurs naturally and this is the highest valve opening which gives "non-slug" behaviour in open-loop operation, without control. The dotted line in the middle shows the unstable "non-slug" solution predicted by the model. This is the desired operating line with closed-loop operation.

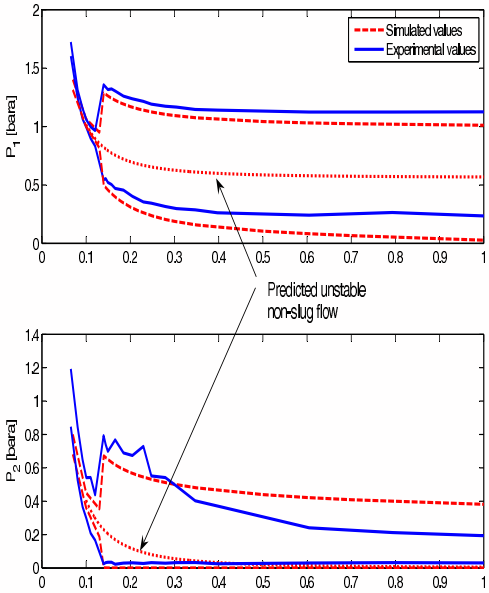

Fig. 5. Bifurcation plot for the medium scale rig: Pressures at inlet P_1 and topside P_2 as function of choke valve opening z

The bifurcation plot was obtained by open-loop simulations of the system at different valve openings. Some of these results are plotted in Figure 6 together with experimental results. The model fit the experimental data quite well, in terms of both amplitude and frequency of the oscillations. Note that a shift in time does not matter. The match between simulated and experimental results is especially very good for a valve opening of 14.9%.

In Figure 7 a root-locus diagram of the system is plotted. This shows how the poles, computed eigenvalues from the model, cross into the RHP as the valve opening reaches 12% from below. This confirms what was seen in the bifurcation diagram.

3.2 Analysis

The model can now be used to explore different measurement alternatives for controlling the flow. The following measurements were analysed in this study; inlet pressure P_1, pressure upstream production choke P_2, density ρ, mass flow rate F_W and volumetric flow rate F_Q through the topside choke. Figure 8 shows the different measurement candidates.

Table 1. Model data parameters

Parameter	Symbol	Value
Inlet flow rate gas $[kg/s]$	$w_{G,in}$	0.0075
Inlet flow rate water $[kg/s]$	$w_{L,in}$	1.644
Valve opening at bifurction point [-]	z	0.12
Inlet pressure at bifurcation point $[barg]$	$P_{1,stasj}$	0.9
Topside pressure at bifurcation point $[barg]$	$P_{2,stasj}$	0.3
Separator pressure $[barg]$	P_0	0
Liquid level upstream low point at bifurcation point $[m]$	$h_{1,stasj}$	0.05
Upstream gas volume $[m^3]$	V_{G1}	0.2654
Feed pipe inclination $[rad]$	θ	0.05
Riser height $[m]$	H_2	10
Length of horizontal top section $[m]$	L_3	0.1
Pipe radius $[m]$	r	0.0381
Exponent in friction expression [-]	n	2.15
Choke valve constant $[m^{-2}]$	K_1	0.0042
Internal gas flow constant [-]	K_2	1.83
Friction parameter $[s^2/m^2]$	K_3	72.37

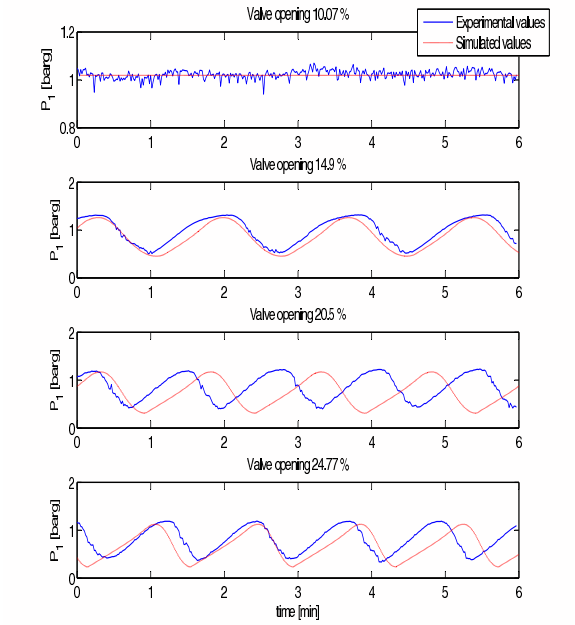

Fig. 6. Open loop data for valve openings 10, 15, 20 and 25%.

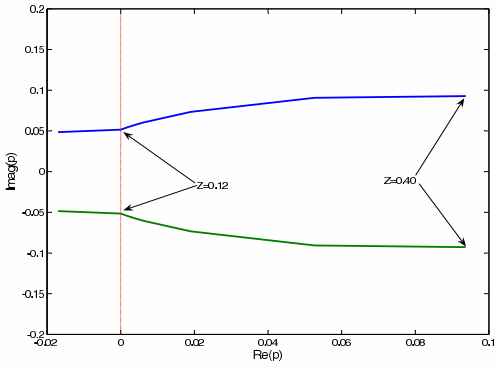

Fig. 7. Root-locus plot showing the trajectories of the RHP open-loop poles when the valve opening varies from 0 (closed) to 0.4

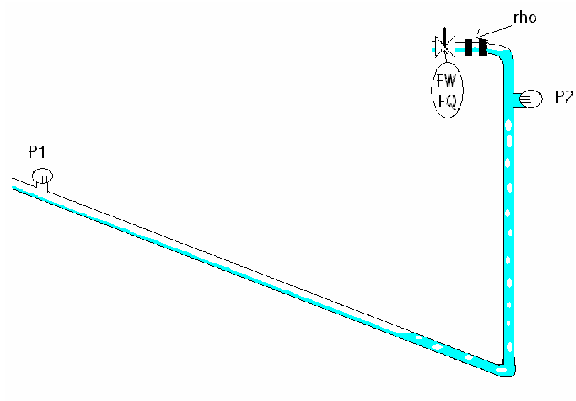

Fig. 8. Measurement candidates for control

In Sivertsen and Skogestad (2008) it was shown how the RHP poles and zeros and their locations compared to each other in the imaginary plane had a large influence on the controllability of the system. By scaling the system and calculating the sensitivity peaks, it is possible to get a picture of the challenges in terms of stabilizing the system.

The process model G and disturbance model G_d were found by linearizing Storkaas' model at two operation points (z = 0.15 and z = 0.2). The process variables were scaled with respect to the largest allowed control error and the disturbances were scaled with the largest variations in the inlet flow rates in the lab, as described in Skogestad and Postlethwaite (1996). The disturbances were assumed to be frequency independent. The input was scaled with the maximum allowed positive deviation in valve opening since the process gain is smaller for large valve openings. For measurements y=[P_1 P_2 ρ F_W F_Q] the scaling matrix is De=diag[0.1bar 0.1bar 50kg/m^3 0.2kg/s $1e{-}3$m^3/s]. The scaling matrix for the disturbances d=[m_G and m_L] is Dd= diag [$2e{-}$3kg/s 0.2kg/s]. The nominal values are 0.0075 kg/s for the gas and 1.64 kg/s for the water rate. The input is scaled $Du = 1 - z_{nom}$ where z_{nom} is the nominal valve opening.

Tables 2 and 3 summarize the results of the analysis. The locations of the RHP poles and zeros are pre-

sented for valve openings 15 and 20%, as well as stationary gain and lower bounds on the closed-loop transfer functions described Sivertsen and Skogestad (2008). The pole location is independent of the input and output (measurement), but the zeros may move. From the bifurcation plot in Figure 5, it is seen that both of these valve openings are inside the unstable area. This can also be seen from the RHP location of the poles.

The only two measurements of the ones considered in this paper which introduces RHP-zeros into the system, are the topside density ρ and pressure P_2. The RHP zeros are in both cases located quite close to the RHP poles, which results in the high peaks especially for sensitivity function SG but also for S. In Figure 9 the RHP poles and relevant RHP zeros are plotted together. This plot shows that we can expect problems when trying to stabilize the flow using these measurements as controlled variables.

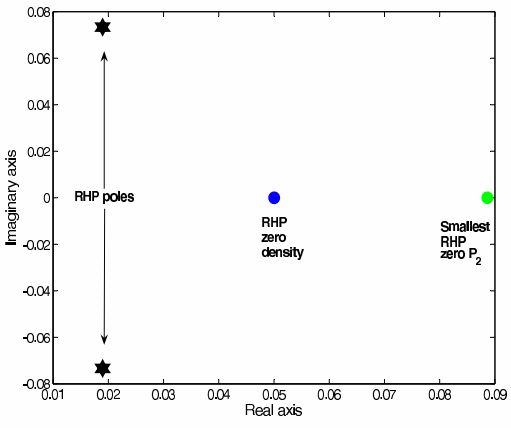

Fig. 9. Plot-zero map for valve opening 20%

The model is based on constant inlet flow rates. The stationary gain for F_W predicted by the model is 0, which means that it is not possible to control the steady-state behavior of the system and the system will drift. Usually the inlet rates are pressure dependent, and the zeros for measurements F_Q and F_W would be expected to be located further away from the origin than indicated by Tables 2 and 3.

Figure 10 and 11 shows the Bode plots for the different plant models and disturbance models respectively. The models were found from a linearization of the model around valve opening 15%. As in Sivertsen and Skogestad (2008) the Bode plots show that for the mass flow rate measurement F_W the low frequency value of the disturbance model $|G_dW|$ is higher than plant model $|GW|$. For acceptable control we require $|G(jw)| > |G_d(jw)| - 1$ for frequencies where $|G_d| > 1$ (Skogestad and Postlethwaite (1996)). In this case $|G_d(0)|$ is 1.01 and G_W is close to zero, which means problems can occur for this measurement.

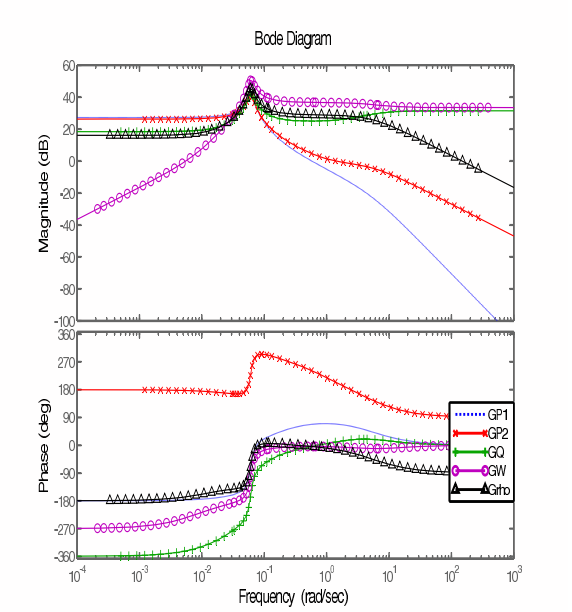

Fig. 10. Bode plots for the plant models using different measurements

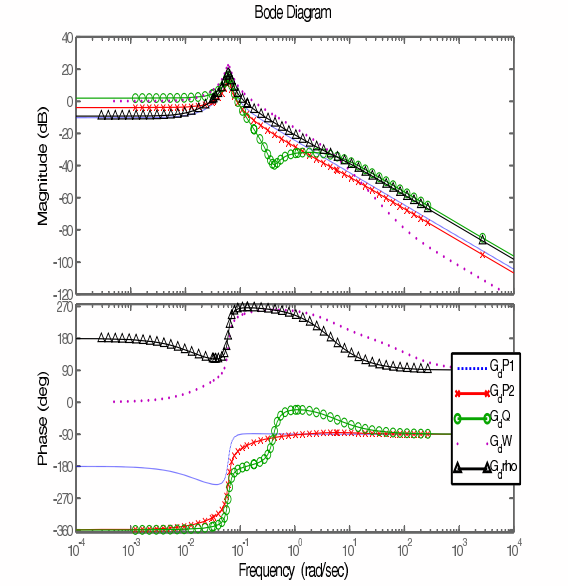

Fig. 11. Bode plots for the disturbance models using different measurements

3.3 Simulations

Closed-loop simulations were performed in order to investigate the effect of the limitations found in the analysis. The measurements were used as single measurements in a feedback loop with a PI-controller. Figure 12 shows this control structure using the inlet pressure P_1 as measurement.

Figure 13 compares the simulation results obtained using four different measurement candidates. Disturbances in inlet flow rates for the gas and water are not included in the simulations. The results can for this reason differ somewhat from the results obtained in Sivertsen and Skogestad (2008). Despite this, the

Table 2. Control limitation data for valve opening 15%. Unstable poles at $p = 0.0062 \pm 0.060i$.

Measurement	RHP zeros	Stationary gain	Minimum bounds				
		$\|G(0)\|$	$\|S\|$	$\|SG\|$	$\|KS\|$	$\|SG_d\|$	$\|KSG_d\|$
$P_1[bar]$	-	22.9	1.00	0.00	0.016	0.00	0.042
$P_2[bar]$	1.00, 0.09	20.5	1.21	15.6	0.017	0.54	0.040
$\rho[kg/m^3]$	0.051	33.1	1.22	33.4	0.011	1.02	0.042
$F_W[kg/s]$	-	0.00	1.00	0.00	0.006	0.00	0.042
$F_Q[m^3/s]$	-	8.3	1.00	0.00	0.013	1.02	0.040

Table 3. Control limitation data for valve opening 20%. Unstable poles at $p = 0.019 \pm 0.073i$

Measurement	RHP zeros	Stationary gain	Minimum bounds				
		$\|G(0)\|$	$\|S\|$	$\|SG\|$	$\|KS\|$	$\|SG_d\|$	$\|KSG_d\|$
$P_1[bar]$	-	10.1	1.00	0.00	0.082	0.00	0.090
$P_2[bar]$	1.08, 0.089	8.94	1.66	10.7	0.10	0.55	0.070
$\rho[kg/m^3]$	0.050	2.87	1.60	19.6	0.048	1.27	0.080
$F_W[kg/s]$	-	0.00	1.00	0.00	0.021	0.00	0.070
$F_Q[m^3/s]$	-	4.16	1.00	0.00	0.047	0.00	0.070

results were quite similar. Results using the topside pressure P_2 are not included in the plot, as the corresponding controller was not able to stabilize the flow.

At first, the controllers are turned off and the system is left open loop for approximately three and a half minute with a valve opening of 20%. From the bifurcation diagram in Figure 5 it was shown that the system goes unstable for valve openings larger than 12%. As expected the system oscillates due to the presence of slug flow.

When the controllers are activated the control valves start working as seen from the right plot in Figure 13. After about 80 minutes the set points are changed for all the controllers, bringing the flow further into the unstable region. The aim of the simulation study is to be able to control the flow with satisfactory performance as far into the unstable region as possible, which means with as high average valve opening as possible. Several simulations were performed, and the ones stabilizing the flow at the highest valve opening are presented in 13.

As in Sivertsen and Skogestad (2008), the controllers giving the best results were the ones using inlet pressure P_1 and volumetric flow rate F_Q as measurements. However, this time the flow controller F_Q outperformed the pressure controller, being able to stabilize the flow with an average valve opening of impressing 55%. Based on earlier knowledge of slug control and experimental results; these results are too good to be true, and might come from the fact that no disturbances in the inlet flow rates were added in the simulations this time.

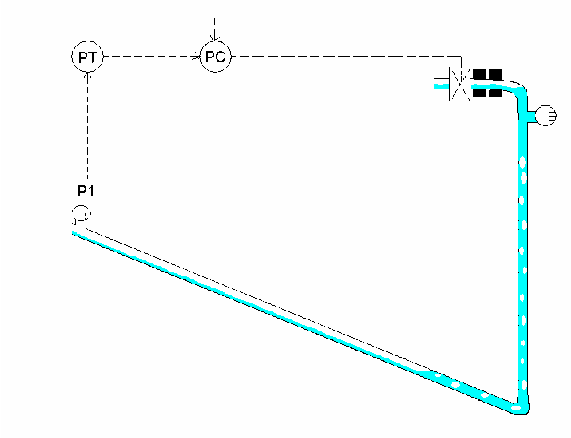

Fig. 12. Feedback control using PI controller with inlet pressure P_1 as measurement

The results using the density and mass flow controller were quite similar to those obtained for the small scale lab rig in Sivertsen and Skogestad (2008). It was possible to control the flow in the unstable region, but the controllers were slow and did not manage to stabilize the flow very far into the unstable region. The analysis in Section 3.2 indicates that these problems stems from the RHP zeros introduced when using these measurements.

4. EXPERIMENTAL RESULTS

The analysis in Section 3.2 showed that both the inlet pressure P_1 and the scaled topside volumetric flow rate F_Q were suitable for stabilizing the flow. The results using the topside density ρ were not as good as for P_1 and F_Q, but still it was possible to control the flow using also this measurement.

Figure 14 shows experimental results from an attempt to stabilize the flow using ρ as *single* measurement. Even though the controller stabilizes the flow initially, the flow eventually returns to the slug flow pattern. The fact that the flow is so quickly stabilized suggest that the density is better suited for control than the model predicts, in fact it stabilizes the flow at approximately 20% which is far better than the results found in the analysis. However, the controller seems to eventually drift from the desired set point causing the flow to become unstable.

Looking at Table 3 it is clear that except for the mass flow measurement F_W with zero steady-state gain,

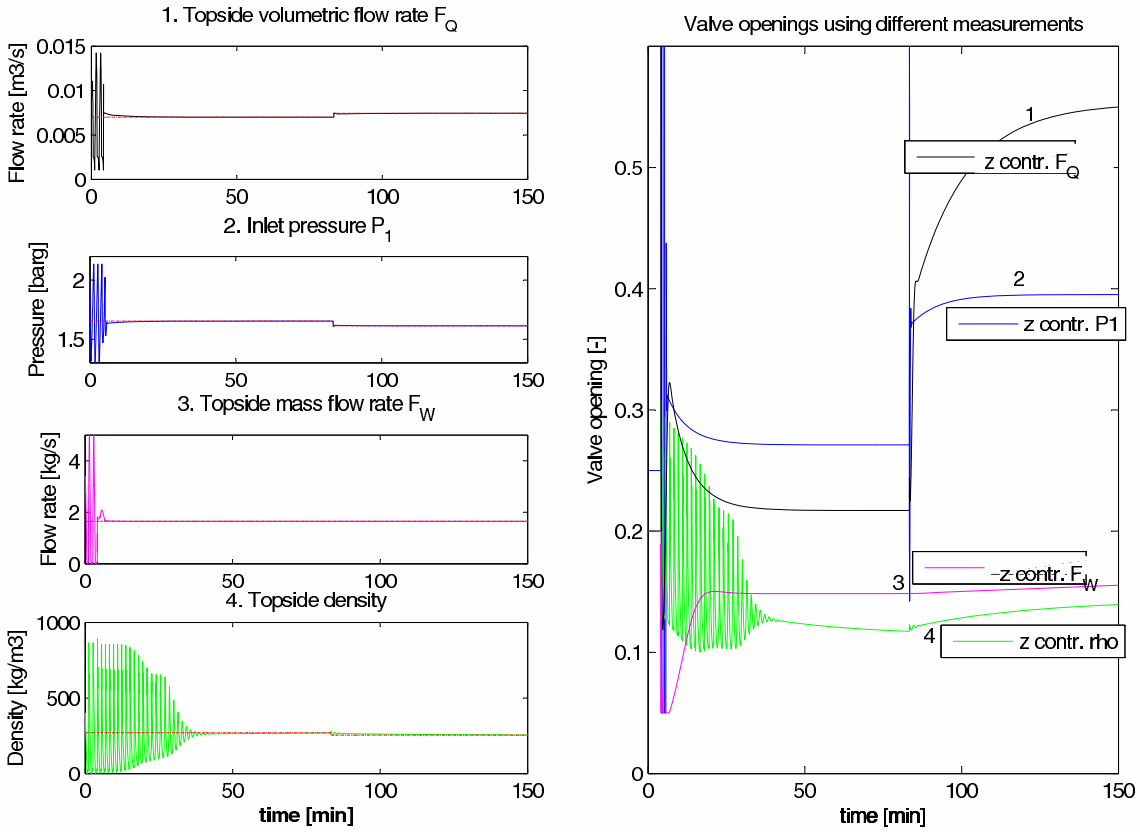

Fig. 13. Stabilizing slug flow using the choke valve (z); PI control with four alternative measurements

ρ is the measurement having the lowest steady-state gain at valve opening 20%. This explains why the controller does not seem to be able to keep the flow stable at the set point after the flow has been stabilized. Also for the volumetric flow rate measurement F_Q the steady-state gain is quite low for valve opening 20%, and we might expect the same problems using this measurement as the single measurement.

Control configurations using combinations of measurements can improve the performance of a controller when compared to controllers using single measurements. In order to avoid the drift problem, different cascade controllers were tested experimentally. Six cascade controllers with different measurement combinations were tested. The measurements were combined in a cascade control configuration, where the set point for the inner controller is adjusted by the outer loop to prevent the inner controller from drifting. This way ρ and F_Q can be used as measurement in an inner loop, even though the controller based solely on one of these measurements suffer from the drift problem. The volumetric flow measurement used during the experiments was scaled with respect to the choke valve constant C_v.

Topside measurements are often noisy, and so also in this case. For this reason the density measurement signal was filtered using a first-order low-pass filter with a time constant of $4s$.

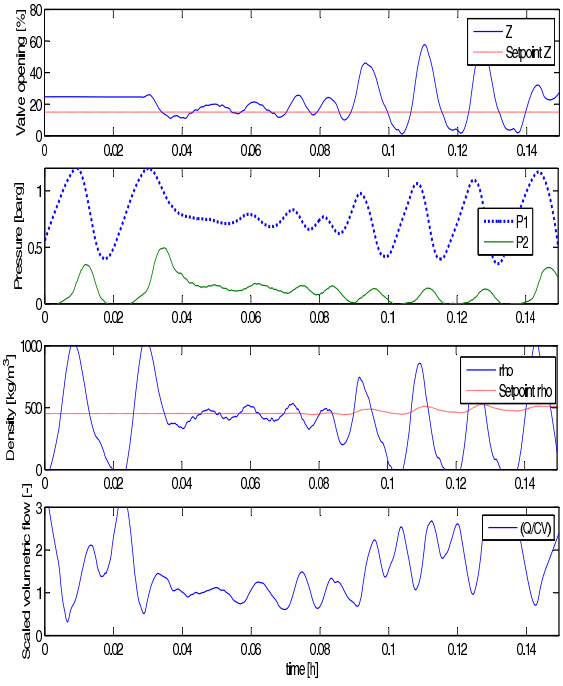

Fig. 14. Experimental results using a single measurement ρ in an attempt to stabilize the flow

Additional experiments were performed using the inlet pressure P_1 as measurement for the inner loop. Although P_1 is not a topside measurement, and often not available in many real subsea applications, it was included to serve as a comparison for the other

controllers. As outer measurements, the pressure drop across the control valve P_2 and topside choke valve opening z were used. This gives all together six combinations of measurements in the outer and inner loop; (a) z and P_1 (b) z and ρ (c) z and F_Q (d) P_2 and P_1 (e) P_2 and ρ (f) P_2 and F_Q.

Figure 15 shows a sketch of a cascade control structure for alterative (e) and Figures 16-18 shows the experimental results for all six alternatives. Plot (a) shows the results when valve opening z is used as outer loop measurement. In plot (b) the measured topside pressure P_2 is used.

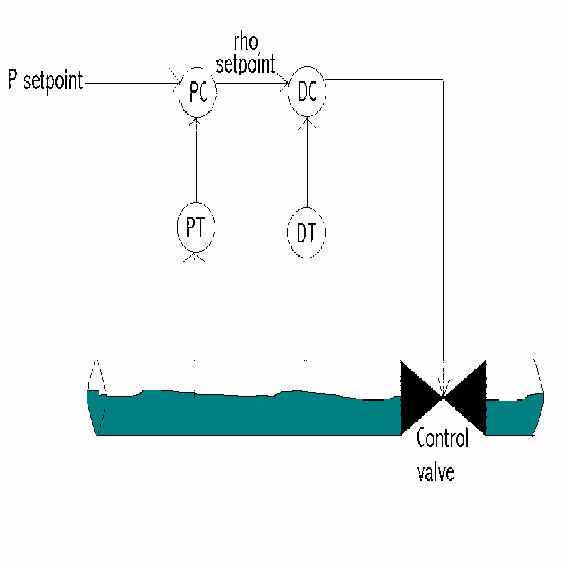

Fig. 15. Cascade control with measurements density ρ (inner loop) and pressure drop across topside valve P_2 (outer loop)

During the experiments, the operation is gradually moved further into the unstable region by changing the set point in the outer loop (increasing z_S and decreasing $P_{2,S}$). The valve opening for which the flow can no longer be stabilized gives a measure on the performance of each controller. Note that being able to increase the mean valve opening and at the same time keep the flow stable has large economic advantages. This is because producing at a higher valve opening implies less friction loss and increased production.

The results using all of the controllers were very good, and they all managed to stabilize the flow far into the unstable region. The upper plot in each of the subfigures shows how the valve opening is increased during the experiments.

Table 4 compare the average values the last 12 min before the controllers go unstable. As mentioned, the mean valve opening gives a good indication of the quality of the controller. See also Figure 19 in the Appendix which shows more detailed plots for all the controllers the last 12 minutes before instability.

Based on the results, we conclude that using P_2 in the outer loop and either P_1 or F_Q in the inner loop is the best choice with average maximum valve opening 23.8% and 23.9%, respectively. The third best choice is using z in the outer loop and F_Q in the inner loop (22.8%).

The controllers were not fine-tuned and the results might for this reason be influenced somewhat by the quality of the tuning. Still, the results showed that it was possible to stabilize the flow very well using only topside measurements and that these results are comparable to the results found when including subsea measurement P_1 as one of the measurements.

5. DISCUSSION

It is important to note that Storkaas' model used to analyze the system is a very simplified model, and it was used merely as a tool to see which problems might occur in the lab, and the underlying reasons for the problems. When comparing the experimental results with analysis and simulations using Storkaas' model prior to the experiments, it was clear that the experimental results were far better than the model predicted when using the density as measurement. The model is however not very detailed and it is merely used as a tool to understand the underlying dynamics of the problem. The pressure dependency of the inflow rates of gas and water was not included, and the effect of this dependency probably helps to stabilize the flow since the inlet rates are decreased as more water accumulates in the riser.

During the experiments the timing for when the controller is activated (where in the slug-cycle) was very important for the controller's ability to stabilize the flow. When the controller was activated just after the inlet pressure had peaked, the controller managed to stabilize the flow quite easily. If the controller was activated at some other time, usually the controller didn't manage to stabilize the flow at all.

Also, the tuning of the controllers has a big influence on the results. Even better results might be achieved with other types of controllers or better tuning. This is also why it is not possible to make a clear recommendation of which combination of measurements is best. The study does however show that all the combinations stabilize the flow quite well.

6. CONCLUSION

This paper has presented results from a medium-scale riser rig where the aim was to control the flow using only topside measurements. The results show that it was possible to stabilize the flow using different combinations of topside measurements. Table 4 shows the different controller results compared to each other. The best results were achieved with the scaled volumetric flow rate F_Q/C_v as the inner measurements, although this result may be dependent on the tuning

Table 4. Mean values just before instability using different cascade controllers, based on data plotted in Figure 19

Outer loop	z			P_2		
Inner loop	P_1	ρ	F_Q/C_v	P_1	ρ	F_Q/C_v
$P_1[barg]$	0.71	0.68	0.68	0.72	0.72	0.67
$P_2[barg]$	0.146	0.123	0.119	0.132	0.142	0.079
$\rho[kg/m^3]$	425	433	403	424	433	417
$Q/C_v[-]$	1.18	0.98	1.18	1.28	1.0943	0.997
$z[\%]$	20.9	19.5	22.8	23.8	19.3	23.9
$F_w[kg/h]$	7.24	7.55	7.6	7.54	7.60	7.55
$F_Q[m^3/h]$	7.53	10.07	9.2	8.17	8.56	11.05
$Figure$	19(a)	19(b)	19(c)	19(d)	19(e)	19(f)

of the controllers. All of the controllers managed to stabilize the flow well, increasing the maximum valve opening from 12% without control to more than 20% with control.

When comparing the results with similar experiments performed on a small-scale riser rig build at our department, Sivertsen and Skogestad (2008), the results using different control configurations are quite similar. This suggests that the small-scale riser rig might be suitable for testing different control strategies prior to more costly and time-consuming tests on larger rigs.

Appendix

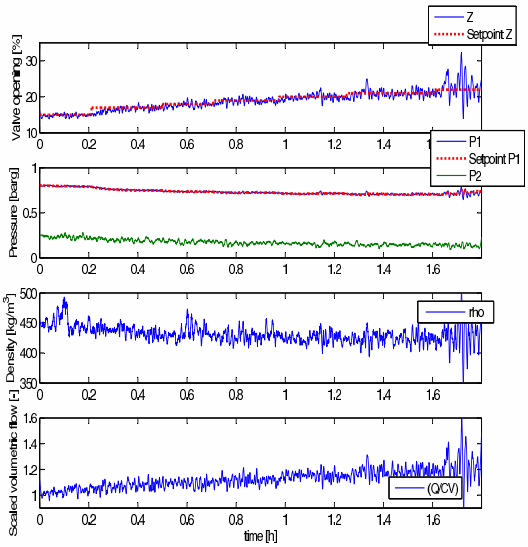

(a) z and P_1

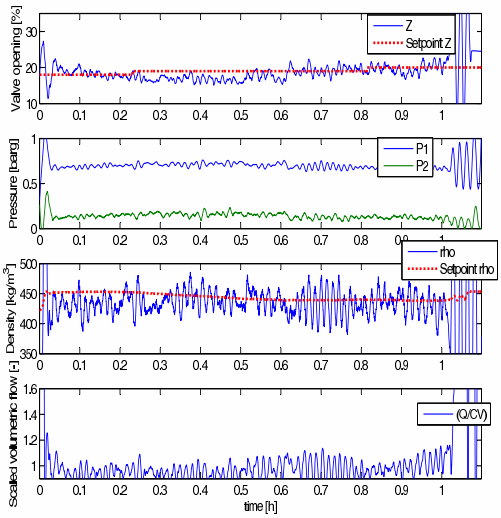

(a) z and ρ

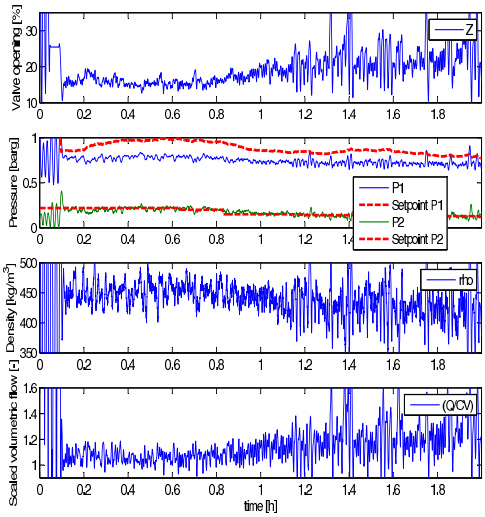

(b) P_2 and P_1

Fig. 16. Experimental results using P_1 in the inner loop and a) z and b) P_2 in the outer loop

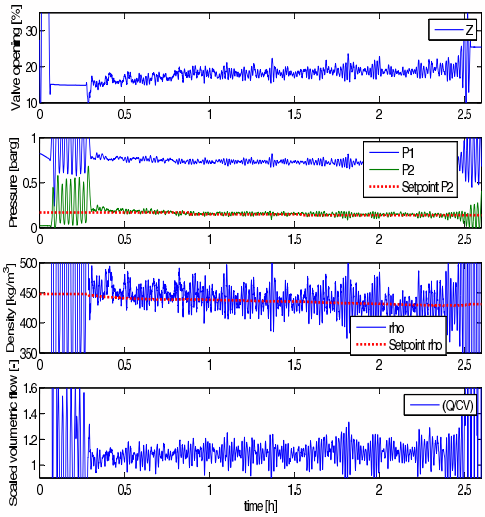

(b) P_2 and ρ

Fig. 17. Experimental results using ρ in the inner loop and a) z and b) P_2 in the outer loop

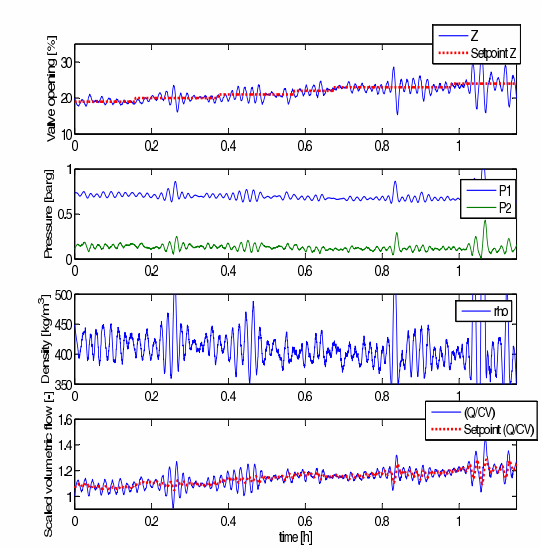

(a) z and F_Q

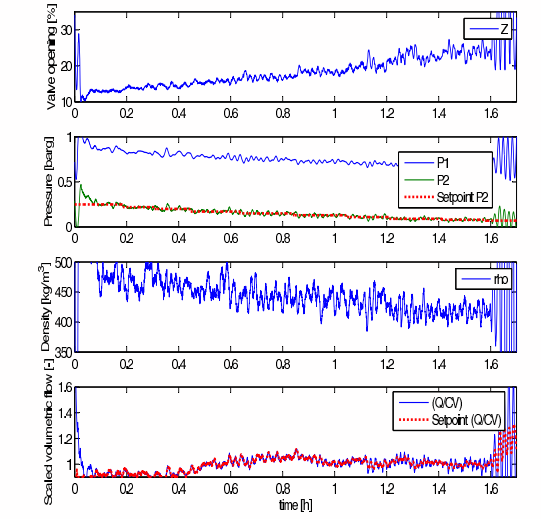

(b) P_2 and F_Q

Fig. 18. Experimental results using F_Q/C_v in the inner loop and a) z and b) P_2 in the outer loop

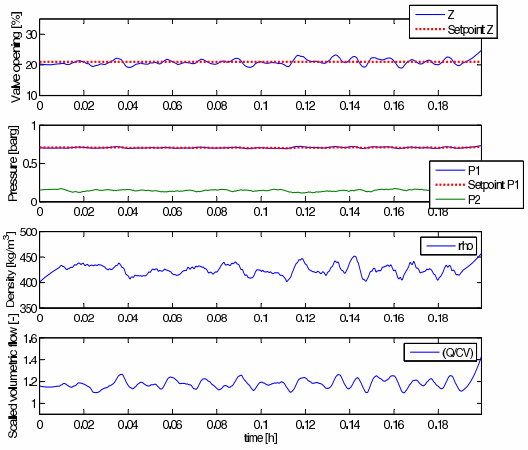

(a) P_1 and z

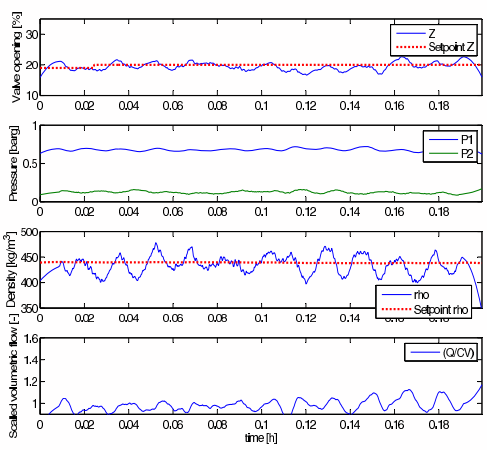

(b) ρ and z

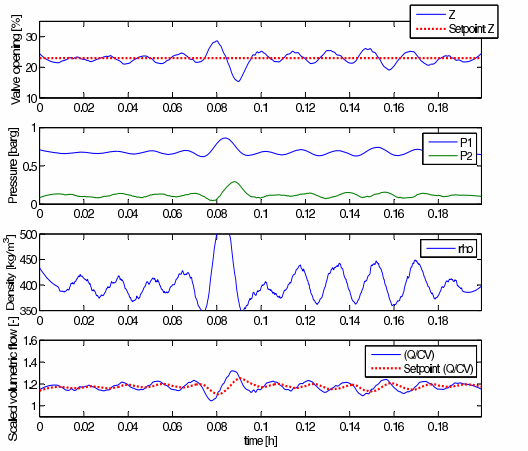

(c) F_Q and z

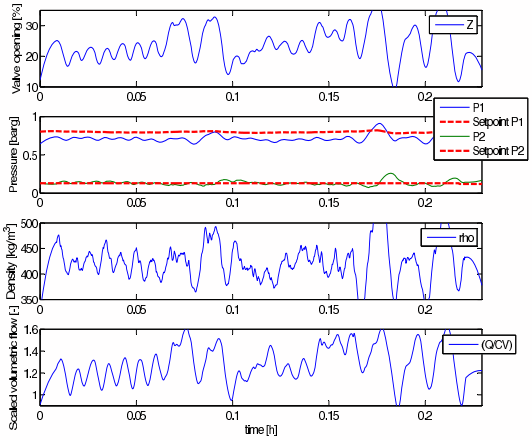

(d) P_1 and P_2

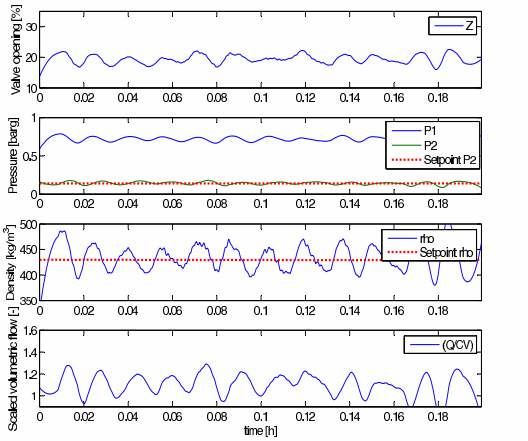

(e) ρ and P_2

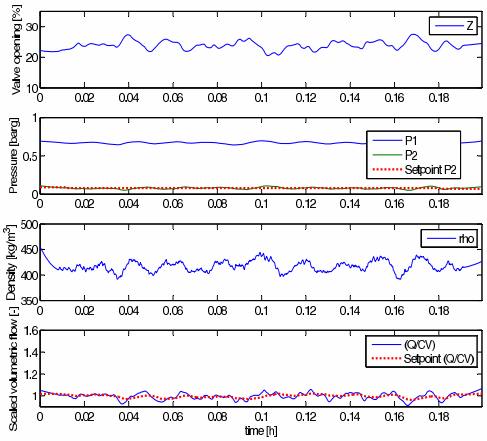

(f) F_Q and P_2

Fig. 19. Experimental results using six different combinations of measurements, last 12 min before instability

REFERENCES

A. Courbot. Prevention of severe slugging in the Dunbar 16" multiphase pipeline. *Offshore Technology Conference, May 6-9, Houston, Texas*, 1996.

J.M. Godhavn, M.P. Fard, and P.H. Fuchs. New slug control strategies, tuning rules and experimental results. *Journal of Process Control*, 15(15):547–577, 2005.

K. Havre, K. O. Stornes, and H. Stray. Taming slug flow in pipelines. *ABB review*, 4(4):55–63, 2000.

J.F. Hollenberg, S. de Wolf, and W.J. Meiring. A method to supress severe slugging in flow line riser systems. *Proc. 7th Int. Conf. on Multiphase Technology Conference*, 1995.

Z. Schmidt, J.P. Brill, and H. D. Beggs. Choking can eliminate severe pipeline slugging. *Oil & Gas Journal*, (12):230–238, Nov. 12 1979.

H. Sivertsen and S. Skogestad. Small-scale experiments on stabilizing riser slug flow. To be published, 2008.

G. Skofteland and J.M. Godhavn. Suppression of slugs in multiphase flow lines by active use of topside choke - field experience and experimental results. *Multiphase '03, San Remo, Italy*, 2003.

S. Skogestad and I. Postlethwaite. *Multivariable feedback control*. John Wiley & sons, 1996.

E. Storkaas, S. Skogestad, and J.M. Godhavn. A low-dimentional model of severe slugging for controller design and analysis. *Multiphase '03, San Remo, Italy*, 2003.